Imperial College London

The effects of type I interferons (IFN-Is) on immune cell metabolism

Lunnathaya Tapeng

[redacted]

A Thesis Submitted in Requirement for the Degree of Doctor of Philosophy (PhD) and Diploma of Imperial College London

Department of Immunology and Inflammation
Faculty of Medicine, Imperial College London

Professor Marina Botto
Associate Professor Jacques Behmoaras
Doctor Norzawani Binti Buang

Declaration of originality

I declare that this thesis is my original work. Where included, the work of others is acknowledged in the text.

Lunnathaya Tapeng

Copyright declaration

Acknowledgements

Firstly, I would like to express my deepest gratitude to my supervisors Professor Marina Botto, Associate Professor Jacques Behmoaras and Dr Norzawani Binti Buang for their valuable advice, patience, and guidance throughout my project.

I am also greatly grateful towards Dr Heidi Ling, Dr Ming Yang and Professor Christian Frezza and all the staff at the Centre for Inflammatory Disease (CID) for their undivided help and kindness during my project.

I sincerely thank my family and my friends for their constant support and words of encouragement during times of difficulty.

Finally, I would like to thank the Development and Promotion of Science and Technology Talents Project scholarship (Royal Government of Thailand) for funding me to study at Imperial College London.

Abstract

Systemic lupus erythematosus (SLE) is a chronic autoimmune disease characterised by the formation of immune complexes that, when deposited in tissues, can cause damage. Type I interferons (IFN-Is) are thought to be a major driver of SLE pathogenesis, but the underlying mechanism(s) remains elusive. Emerging literature has shown that PBMCs and $CD4^+$ T cells from SLE patients display an abnormal metabolic status that can lead to aberrant T cell activation and impaired cell death pathways, causing further immune dysregulation. However, the link between the metabolic changes observed in the immune cells of SLE patients and the IFN-I signature remains unclear.

Preliminary findings from my host laboratory using RNA-sequencing analysis of $CD8^+$ T cells from SLE patients showed a potential link between the IFN-I signature and an abnormal $CD8^+$ T cell metabolism. These preliminary data and the knowledge gap in the literature inspired me to investigate the effects of chronic IFN-I exposure on mitochondrial metabolism and functions of $CD8^+$ T cells and macrophages, two key immune cells in lupus pathogenesis. To achieve this, I treated PBMCs, $CD8^+$ T cells and macrophages from healthy donors with IFN-α for several days and performed transcriptomic, metabolic and functional analyses. Using these experimental conditions, I found that in $CD8^+$ T cells only the combination of IFN-α and TCR stimulation triggered the same abnormal mitochondrial features (e.g increased mitochondrial mass and activity and reduced spare respiratory capacity) seen in SLE patients with a high IFN-I signature. Further functional analyses also revealed that the combination of chronic IFN-I exposure and TCR activation led to an increased cell death upon antigen rechallenge.

On the other hand, in macrophages chronic IFN-I exposure induced a striking metabolic reprogramming characterised by increased NAD consumption and activation of tryptophan pathways. Furthermore, chronic IFN-I exposure promoted a unique pro-inflammatory phenotype with increased CD38, CD80 and IL-6 expression and induced cell death in response to TLR4 stimulation but no to other TLR triggers. These IFN-I-induced changes in macrophages were mediated by CD38, a NAD-consuming enzyme, possibly via activation of the tryptophan pathway. Inhibition of CD38 or deficiency of tryptophan was able to rectify the IFN-I-mediated pro-inflammatory phenotype and the LPS-induced cell death.

Taken together, the data suggest that chronic IFN-α exposure affects the mitochondrial metabolism in $CD8^+$ T cells and macrophages differently, leading to abnormal immune functions.

Table of contents

List of figures

Chapter 1

Chapter 2

Chapter 3

Chapter 4

Chapter 5

Chapter 6

List of tables

Chapter 1

Chapter 2

Abbreviations

2-DG	2-deoxyglucose
3-HAA	3-hydroxyanthranilic acid
3-HAO	3-hydroxyanthranilic acid oxygenase
3-HK	3-hydroxykynurenine
8-OHdG	8-hydroxy-2′-deoxyguanosine
ACMS	α-amino-β-carboxymuconate ε-semialdehyde
ACR	American College of Rheumatology
ADP	Adenosine diphosphate
ADPR	Adenosine diphosphate ribose
AhR	Aryl hydrocarbon receptor
AMPK	Adenosine Monophosphate-Activated Protein Kinase
ATP	Adenosine triphosphate
BAFF	B cell-activating factor
BCR	B cell receptor
BMDM	Bone marrow-derived macrophages
BSA	Bovine serum albumin
Btk	Bruton’s tyrosine kinase
c-Myc	Cellular myelocytomatosis oncogene
cADPR	Cyclic adenosine diphosphate ribose
CD	Cluster of differentiation
CD40L	CD40 ligand
cDNA	Complementary DNA
CFSE	Carboxyfluorescein succinimide ester
CoA	Co-enzyme A
COX	Cyclooxygenase
CpG	Cytidine-phosphate-guanosine
cROS	Cellular reactive oxygen species
DAMPs	Damage-associated molecular patterns
DCs	Dendritic cells
DEGs	Differential expression genes
DMA	Differential metabolomic analysis
dsDNA	Double-stranded DNA

EBV	Epstein-Barr virus
ECAR	Extracellular acidification rate
ETC	Electron transport chain
EULAR	European League Against Rheumatism
FACs	Flow cytometry
$FADH_2$	Flavin adenine dinucleotide
FAO	Fatty acid oxidation
FBS	Fetal bovine serum
FC	Fold change
FCCP	Fluorocarbonylcyanide phenylhydrazone
FcγR	Fc gamma receptor
FDA	Food and Drug Administration
GASs	Gamma-activated sequences
GLUT	Glucose transporter
GSH	Glutathione
GWAS	Genome-wide association studies
GZMB	Granzyme B
H^+	Hydrogen ions
HBSS	Hank's balanced salt solution
HC	Healthy controls
HIF	hypoxia-inducible factor
HMDM	human monocyte-derived macrophages
ICOS-1	Inducible co-stimulator-1
ICs	Immune complexes
IDO	Indoleamine 2,3-dioxygenase
IFN-I	Type I interferon
IFNAR	IFN-α/β receptor
Ig	Immunoglobulin
IGF	insulin-like growth factor
IL	interleukin
iNOS	inducible nitric oxide synthase
IRF	IFN regulatory factor
ISGF	IFN-stimulated gene factor
ISGs	IFN-stimulated genes

ISRE	IFN-stimulated response elements
JAK	Janus kinase
JAK-STAT	Janus kinase signal transducer and transcription activator
KEGG	Kyoto Encyclopedia of Genes and Genomes
KMO	Kynurenine 3-monooxygenase
Kyn	Kynurenine
KYNU	Kynureninase
LC-MS	Liquid chromatography–mass spectrometry
LPS	Lipopolysaccharide
LXR	Liver X receptor-alpha
M-CSF	Macrophage colony-stimulating factor
M1	Pro-inflammatory macrophages
M2	Anti-inflammatory macrophages
MDA5	Melanoma Differentiation-Associated protein 5
mDCs	Myeloid dendritic cells
MDM	Monocyte-derived macrophages
MFI	Mean fluorescent intensity
MHC	Major histocompatibility complex
MMP	Mitochondrial membrane potential
mROS	Mitochondrial reactive oxygen species
Mtb	Mycobacterium tuberculosis
mtDNA	mitochondrial DNA
MTDR	MitoTracker Deep Red
MTG	MitoTracker Green
mTOR	Mammalian target of rapamycin
mTOR	Mammalian target of rapamycin complex
NA	Nicotinic acid
NAAD	Nicotinic acid adenine dinucleotide
NAADP	Nicotinic acid adenine dinucleotide phosphate
NAD	Nicotinamide adenine dinucleotide
NADH	A reduced form of nicotinamide adenine dinucleotide
NADS	Nicotinamide adenine dinucleotide synthetase
NAM	Nicotinamide
NAMN	Nicotinamide mononucleotide

NAMPT	Nicotinamide phosphoribosyltransferase
NAPRT	Nicotinic acid phosphoribosyltransferase
NETs	Neutrophil extracellular traps
NF-κB	Nuclear factor kappa B
NK	Natural killer
NMN	Nicotinamide mononucleotide
NMNAT	Nicotinamide mononucleotide adenylyltransferases
NO	Nitric oxide
NOS	Nitric oxide synthase
NR	Nicotinamide riboside
NRF	Nuclear factor erythroid-related factor
OCR	Oxygen consumption rate
OD	Optical density
OX40L	OX40 ligand
OXPHOS	Oxidative phosphorylation
PARPs	Poly-adenosine ribose polymerase
PBMCs	Peripheral blood mononuclear cells
PBS	Phosphate-buffered saline
PCA	Principal component analysis
PD-1	Programmed death ligand 1
pDCs	Plasmacytoid dendritic cells
PI	Propidium iodide
PP2A	Protein phosphatase 2A
qPCR	Quantitative polymerase chain reaction
QPRT	Quinolinate phosphoribosyltransferase
R848	Resiquimod
RIG	Retinoic acid-inducible gene
RNA-seq	RNA sequencing
RNase L	Ribonuclease L
RNP	Ribonucleoprotein
ROS	Reactive oxygen species
SARM1	Sterile alpha and TIR motif containing 1
SASP	Senescence-associated secretory phenotype
SEM	Standard error of the mean

SIRT	Sirtuins
SLAMF4	Signalling lymphocytic activation molecule family member 4
SLE	Systemic lupus erythematosus
SOCS	Suppressors of cytokine signalling
SOD	Superoxide dismutase
SRC	Spare respiratory capacity
STAT	Signal transducers and activators of transcription
TCA	Tricarboxylic acid
TCM	T cell complete medium
TCR	T cell receptor
TDO	Tryptophan 2,3-dioxygenase
Tfh	T follicle helper cells
TGF	Transforming growth factor
Th	T helper
TIC	Total ion count
TLR	Toll-like receptor
TMRM	Tetramethylrhodamine methyl ester perchlorate
TNF	Tumor necrosis factor
Treg	Regulatory T cells
Trp	Tryptophan
TYK2	Tyrosine kinase 2
UV	Ultraviolet light

Chapter 1: Introduction

1. Systemic lupus erythematosus (SLE)

1.1. Epidemiology, aetiology and clinical manifestations

SLE is a chronic multisystem autoimmune disease characterised by the generation of autoantibodies against self-antigens, deposition of immune complexes (ICs) in tissue and inflammation in several organs. This disease affects women of child-bearing age 9-10 times more than men[1]. This sex bias in SLE is probably caused by epigenetically altered X-linked immune gene expressions, particularly in B cells[2-4]. SLE patients are diagnosed according to the European League Against Rheumatism (EULAR) and the American College of Rheumatology (ACR) criteria (**Table 1.1**)[5]. The clinical features of SLE are diverse, ranging from mild, such as the characteristic malar rash, to life-threatening conditions affecting the kidney (glomerulonephritis) and central nervous system. Moreover, it has been recently reported that patients with SLE had a 1.8-fold increased mortality rate compared with the general population[6].

The main causes of SLE development remain greatly elusive. However, multiple genetic risk factors and environmental triggers have been implicated. Studies in twins have shown that identical twins or monozygotic twins have a higher rate of SLE concordance than dizygotic twins (>20%)[7-9]. Multiple survey studies have also revealed that 10-12% of SLE patients had first or second-degree relatives affected by lupus and other autoimmune diseases, compared to <1% of healthy subjects[9,10]. Besides, genome-wide association studies (GWAS) have identified a handful of genes that are associated with SLE development. Some of these genes are found to control the immune response such as type I interferon (IFN-I) production and Toll-like receptor (TLR) 7 and 9 signalling[11]. These reports support the concept of a complex genetic predisposition in SLE. Apart from genetic factors, the environment can also contribute to triggering the disease. The environmental factors include ultraviolet light (UV), sex hormones, drugs, smoking, trace elements (such as cadmium) and virus infections[12,13]. These factors may trigger or exacerbate the disease by promoting apoptosis, DNA damage, lymphocyte activation, inflammatory cytokine production and

molecular mimicry. For instance, Epstein-Barr virus (EBV) can elicit the production of antibodies which can cross-react with self-antigens leading to SLE development[14].

The complex nature of SLE makes the treatment of SLE challenging. To date, there is still no cure for lupus and the ultimate goal is clinical remission, preferably without the requirement for continuous immunosuppressive treatment or glucocorticoid medication[15]. Drugs are mainly used to control abnormal immune/inflammatory responses and are not specific, causing many adverse reactions[16]. More recently biological therapies targeting specific immune molecules have been shown to be effective[17,18]. The first biological drug approved by the USA Food and Drug Administration (FDA) was belimumab which is a monoclonal antibody targeting B cell-activating factor (BAFF)[17,18], an important factor for B cell survival and maturation. SLE patients treated with Belimumab demonstrated a better improvement in clinical manifestations and a reduction in disease relapsing compared to those treated with a placebo[17,18]. However, more than 40% of the SLE patients in the clinical trials unsuccessfully responded to BAFF neutralisation[17], reflecting that B cells may not be the only contributor to disease activity. Due to the complex and heterogeneous nature of SLE, further investigations are required to deepen our understanding of its pathogenesis and to develop effective new treatments.

Table 1.1. Classical criteria for SLE from EULAR and ACR[5]

Entry criterion

Antinuclear antibodies (ANA) at a titer of ≥1:80 on HEp-2 cells or an equivalent positive test (ever)

↓

If absent, do not classify as SLE
If present, apply additive criteria

↓

Additive criteria

Do not count a criterion if there is a more likely explanation than SLE.
Occurrence of a criterion on at least one occasion is sufficient.
SLE classification requires at least one clinical criterion and ≥10 points.
Criteria need not occur simultaneously.
Within each domain, only the highest weighted criterion is counted toward the total score§.

Clinical domains and criteria	Weight	Immunology domains and criteria	Weight
Constitutional		***Antiphospholipid antibodies***	
Fever	2	Anti-cardiolipin antibodies OR	
Hematologic		Anti-β2GP1 antibodies OR	
Leukopenia	3	Lupus anticoagulant	2
Thrombocytopenia	4	***Complement proteins***	
Autoimmune hemolysis	4	Low C3 OR low C4	3
Neuropsychiatric		Low C3 AND low C4	4
Delirium	2	***SLE-specific antibodies***	
Psychosis	3	Anti-dsDNA antibody* OR	
Seizure	5	Anti-Smith antibody	6
Mucocutaneous			
Non-scarring alopecia	2		
Oral ulcers	2		
Subacute cutaneous OR discoid lupus	4		
Acute cutaneous lupus	6		
Serosal			
Pleural or pericardial effusion	5		
Acute pericarditis	6		
Musculoskeletal			
Joint involvement	6		
Renal			
Proteinuria >0.5g/24h	4		
Renal biopsy Class II or V lupus nephritis	8		
Renal biopsy Class III or IV lupus nephritis	10		

Total score:

↓

Classify as Systemic Lupus Erythematosus with a score of 10 or more if entry criterion fulfilled.

1.2. SLE pathogenesis

1.2.1. Source of autoantigens

One of the serological hallmarks of SLE is the production of immunoglobulin G (IgG) antibodies against nuclear antigens which target nucleosomes including double-stranded DNA (dsDNA), chromatin and ribonucleoprotein (RNP)[19]. These antibodies are triggered by the availability of self-antigens. Dysregulation of apoptosis, and/or the defective clearance pathways have been proposed as a possible source for the excessive self-antigen generation as apoptotic cells express on the surface self-antigens[20].

Several studies have demonstrated an increased rate of apoptosis in lymphocytes and peripheral blood mononuclear cells (PBMCs) of SLE patients[21-24]. Besides, macrophages from SLE patients have been reported to have an impaired ability to engulf dying cells[25]. Without efficient clearance, the accumulated apoptotic cells may undergo secondary necrosis and cellular components are released[26]. These cellular components include nucleosomes, and other damage-associated molecular patterns (DAMPs) such as uric acid, IL-1α, Adenosine triphosphate (ATP) and mitochondrial content[26]. Circulating nucleosomes can be detected in the sera of healthy subjects and SLE patients[27]. These nucleosomes can induce inflammatory cytokine production from innate immune cells and can be modified to appear like foreign antigens. For instance, nucleosomes may be altered by the acetylation and methylation of histones[28] and the production of autoantibodies specific for the modified histones has been demonstrated in SLE patients and lupus-prone mice[29,30]. Following the release of cellular components, these nucleosomes may be taken up by antigen-presenting cells such as dendritic cells (DCs). DCs subsequently process and present these self-antigens to autoreactive $CD4^+$ T cells, resulting in autoreactive B cell activation, autoantibody production and IC accumulation.

The binding of autoantibodies to self-antigens forming ICs can be pathogenic[31] and may result in tissue deposition and systemic inflammation. For example, ICs can deposit to the mesangial matrix and basement membranes of the glomeruli and trigger complement activation and inflammation in the kidney, also known as glomerulonephritis[32]. Moreover, ICs containing RNP can prime neutrophils to undergo

NETosis, a distinctive form of cell death whereby the cells release web-like structures called neutrophil extracellular traps (NETs)[33]. NETs contain decondensed chromatin and granular proteins which can capture and destroy pathogens such as bacteria. Interestingly, NETs can bind to anti-dsDNA antibodies and deposit in the kidney, causing tissue damage by recruiting additional immune cells to the inflammatory site[34].

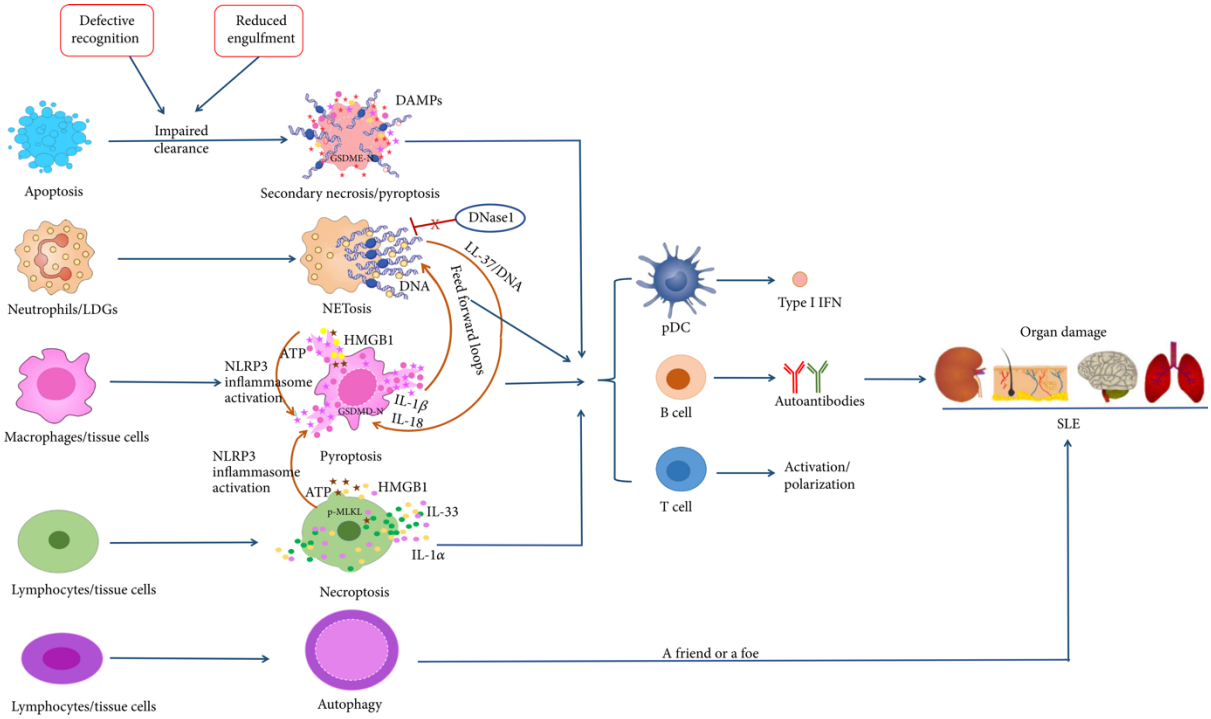

Figure 1.1. Source of autoantigens contributing to SLE pathogenesis. In SLE, dysregulation of programmed cell death pathways, including apoptosis, NETosis, pyroptosis, and necroptosis, together with the defective clearance pathways can lead to the release of DAMPs, amplification of inflammatory and immune responses, autoantigen generation, and tissue damage. This figure is taken from Yang *et al.*[35]

1.2.2. Innate immune cell response

SLE pathogenesis involves numerous immune abnormalities in both innate and adaptive immune responses. Innate immune cells have recently been identified as a key player in disease progression. For example, neutrophils from SLE patients have been found to be overly activated and involved in vascular diseases[36,37]. These activated neutrophils tend to undergo NETosis and release NETs. As described above, NETs contain decondensed chromatin and other proteins which are considered to be self-antigens. Failure to remove NETs may increase the presentation of self-

antigens. These excessive NETs can also cause thrombosis and endothelial damage in lupus[35]. Interestingly, two papers have reported that in SLE patients' mitochondrial DNA in an oxidised form is released during NET formation[33,38]. This oxidised mitochondrial DNA can activate plasmacytoid DCs leading to the production of IFN-Is and the induction of $CD4^+$ memory T cells which can assist autoantibody production by B cells[37].

Mononuclear phagocytes which include macrophages and DCs have been implicated in the SLE pathogenesis in terms of initiation and progression of the disease. It is commonly known that macrophages participate in inflammation and the regulation of adaptive immune response. The major functions of these cells are phagocytosis, antigen presentation and cytokine secretory functions[33]. The initiation role of macrophages has been reported by studies demonstrating that SLE macrophages have defects in the ability to phagocytose apoptotic cells[25,39]. This inefficient clearance ability of macrophages results in prolonged self-antigen exposure to the adaptive immune cells and may initiate the autoimmune response. In addition, the activation, polarisation and secretory functions of macrophages are abnormal in SLE patients and lupus-prone mice[40]. SLE monocytes tend to display an inflammatory profile[41] and tissue-infiltrating macrophages have been reported to elicit local inflammation resulting in tissue destruction[42].

DCs are known to be the initiators of immunity and tolerance induction by processing and presenting antigens to T cells[43]. DCs can be divided into two main groups: the myeloid DCs (mDCs) and the plasmacytoid DCs (pDCs). mDCs are the professional antigen-presenting cells which are essential to elicit the adaptive immune response. When encountering antigens, mDCs are converted from antigen-capturing cells towards antigen-presenting cells during the process called maturation. After that, they migrate to the secondary lymphoid organ and present antigens in an immunogenic manner to T cells. These mature mDCs have an increased major histocompatibility complex (MHC) molecule and co-stimulatory molecule (CD86 and CD40) expression. They also secrete pro-inflammatory cytokines and chemokines including IL-6 and TNF-α[44]. The secreted cytokine and molecules expressed on the surface of mDCs (e.g OX40 ligand (OX40L) or ICOS-1 (inducible co-stimulator-1)) can dictate T cell polarisation including T helper (Th) 1, Th2, and Th17 cells, or regulatory T cells

(Treg)[45]. The overactivation of mDC has been linked to SLE development[46]. For example, during a disease flare, elevated CD80/CD86 expression was observed on mDC[47]. pDCs have been extensively implicated in SLE due to their high IFN-I-producing ability. ICs containing apoptotic materials can stimulate the endosomal TLR9 of pDCs leading to immune dysregulation and high production of IFN-Is, mainly IFN-α[48,49]. Additionally, circulating proteins in SLE patient blood can act as an endogenous inducer of IFN-Is by pDCs.

1.2.3. Adaptive immune cell response

B cells are intrinsically essential in autoimmune diseases on account of their ability to produce autoantibodies and present self-antigens to T cells. B cell dysfunction has been reported to be pivotal in lupus pathogenesis. Abnormalities in SLE B cells include an excessive B cell receptor (BCR) response and an increased number of memory B cells which are characterised by a lower activation threshold that allows autoreactive production of autoantibodies targeting nucleosomes is the main feature of SLE. These autoantibodies can be detected within the majority of SLE patients (more than 90%) and are correlated with disease severity, especially the anti-dsDNA antibodies[50].

T cells are increasingly being recognised to play a critical role in the development of SLE. Historically, the balance of Th1/Th2 was thought to be a major contributor to SLE pathogenesis[51,52]. However, accumulating studies have recently elucidated the complicated roles of different subtypes of T cells in the pathogenesis of this autoimmune disease. Abnormal T cell signalling together with aberrant cytokine production have been described in SLE patients[53]. The expression levels of the CD3ζ chain, which is a component of T cell receptor (TCR), are found to be lower in T cells from SLE patients and this leads to the rewiring of the TCR complex[54-56]. At the transcription level, the expression of the CD3ζ chain can be controlled by the serine/threonine protein phosphatase 2A (PP2A). SLE T cells exhibit an increase in PP2A activity, contributing to the abnormal TCR signalling and T cell function[57]. $CD4^+$ T cells help B cells in their maturation, differentiation and proliferation[58]. The interaction between CD40 expressed on the B cell surface and CD40 ligand (CD40L) expressed on $CD4^+$ T cells augment B cell activation by providing co-stimulatory signals[59]. The overexpression of CD40L presents in SLE patients can promote B cell

activation and autoantibody production[59,60]. Consistent with the observation in lupus patients, in lupus-prone mice an increased number of activated T cells displaying aberrant signalling have been found[61,62]. These activated $CD4^+$ T cells also show increased proliferation and IL-2 production following low-affinity antigen stimulation[63]. Considering $CD4^+$ T cells subtypes, effector and memory T cells have been found to be increased in lupus patients and this may be the result of these cells being resistant to activation-induced cell death via the activation of phosphatidylinositol 3-kinase (PI3K)/AKT/mammalian target of rapamycin (mTOR) signalling[64]. Furthermore, an imbalance among the Th1/Th2/Th17 and Treg has been shown to correlate with SLE disease severity[65].

$CD8^+$ T cells can directly kill other cells by releasing IFN-γ and cytotoxic granules such as perforin and granzymes B (GZMB) and thus play an important role in controlling infection, cancer and autoimmunity[66]. However, the functions of these cells in SLE are still yet to be fully grasped. There is evidence that $CD8^+$ T cells can play both protective and deleterious roles in the pathogenesis of SLE and other autoimmune diseases through activities such as suppression or cytotoxicity[67], supporting the idea that these cells may function differently during the different stages of the disease. Several studies have shown reduced cytotoxic function in the $CD8^+$ T cells from SLE patients which may lead to an increased risk of viral infection and could trigger an autoimmune response[68]. The increased conversion of lupus $CD8^+$ T cells into double-negative T cells and/or programmed death ligand 1 (PD-1) expression has been proposed to cause a reduction in cytotoxicity against viruses[69]. For example, lupus $CD8^+$ T cells with a reduction of signalling lymphocytic activation molecule family member 4 (SLAMF4), which is a checkpoint regulator related to the conversion of CD8+ into double negative T cells, have a compromised ability to deal with infections[70].

Data collected from studies in SLE patients have correlated $CD8^+$ T cells with SLE progression. For example, the frequency of circulating cytolytic $CD8^+$ effector T cells is elevated when compares to health controls[71]. Urinary $CD8^+$ T cell counts are also increased during the disease flare-up[72]. Infiltrating $CD8^+$ T cells were also reported in the kidney of patients with active lupus nephritis and could subsequently promote local inflammation[73]. Furthermore, tissue injury in SLE could be directly amplified by $CD8^+$ T cells[74]. The pathogenic roles of $CD8^+$ T cells have also been explored. Research

has shown that the proteolytic activity of GZB mediated by $CD8^+$ T cells could generate unique autoantigen fragments and thus increase autoantigen loads[71]. Following the induction of lupus (the bm12 model[75]), the depletion of $CD8^+$ T cells restrained the autoimmune response in C1q-deficient mice (C1qa-/-), reflecting that $CD8^+$ T cells could enhance the disease progression[76]. A transcriptional signature study suggested that $CD8^+$ T cell exhaustion could be used for the prediction of a good prognosis in autoimmune diseases including lupus[77]. $CD8^+$ T cell exhaustion is typically characterised by the reduction of T-cell function. This often occurs after chronic viral infection, as a result of antigen persistence[78]. This exhaustion seemed to facilitate the peripheral tolerance, which normally suppresses self-reactive T and B cells, thus prevents the disease deteriorating[77]. Interestingly, a recent study has identified a new subset of $CD8^+$ T cells named $CXCR5^+PD1^+$ T follicle helper cells (Tfh) [79]. These cells are located within the germinal centre and have a similar function to $CD4^+$ T follicular helper cells. The function of these $CD8^+$ Tfh cells has been found to control the germinal B cell response and facilitate B cells to produce autoantibody. Therefore, this new subset of $CD8^+$ T cells is likely to contribute to the breakdown of B cell tolerance and the induction of autoimmunity[79].

2. Type I interferons (IFN-Is)

IFN-Is have been known to be potent mediators in antiviral responses since 1957[80]. Recently, these pleiotropic cytokines are also found to be crucial in immunoregulation[81]. Imbalance regulation in IFN-I signalling or production can cause significant pathological processes[82]. Research has shown that exogenous IFN-I treatment can improve the clinical outcomes of patients with chronic viral infection (such as hepatitis) and cancer[83-85]. On the other hand, IFN-I neutralisation has been prosed as a potential treatment of autoimmune diseases[86-88]. These reports reflect the centrality of IFN-Is in the immune response.

In humans, IFN-Is are composed of IFN-α, IFN-β, IFN-ε, IFN-κ, and IFN-ω subtypes. IFN-α and IFN-β are the major subtypes of IFN-Is in immunity. 13 distinct genes encode IFN-α, whereas IFN-β is encoded from a single gene[89]. Both subtypes bind to a common heterodimeric IFN-α/β receptor (IFNAR), which is composed of IFNAR1 and IFNAR2 transmembrane receptor subunits with different affinities. This receptor

is expressed on many cell types, suggesting that most cell types can be affected by IFN-Is[89].

2.1. Regulation of IFN-I response

IFN-Is can be produced by many cell types (such as lymphocytes, pDCs, macrophages and endothelial cells) in response to endogenous viral elements. The viral RNA can be recognised by retinoic acid-inducible gene I (RIG-I)-like receptors including RIG-I and Melanoma Differentiation-Associated protein 5 (MDA5)[90]. Nevertheless, the most potent IFN-I producers are pDCs owing to their high production rate (up to 1000-fold more than other cell types) upon TLR7 and 9 activations by single-stranded RNA and CpG-rich DNA, respectively[91,92]. At the molecular level, this cytokine can promote significant changes in transcriptional regulation and can activate large cytokine gene networks[93,94]. In response to IFNAR engagement, the canonical pathway of IFN-I signalling is induced by activating tyrosine kinase 2 (TYK2) and Janus kinase 1 (JAK1), which bind to IFNAR1 and IFNAR2 respectively. Activated JAK1 and TYK2 then phosphorylate the signal transducers and activators of transcription (STAT) 1 and 2 resulting in the induction of STAT1-STAT2 dimerisation which then translocates into the nucleus and involves IFN regulatory factor (IRF) 9 to form an IFN-stimulated gene factor 3 (ISGF3) complex. This complex subsequently binds to the promoter region of IFN-stimulated genes (ISGs) leading to the expression of over 300 ISGs (**Fig.1.2)**. Therefore, IFN-I signalling serves as a gateway to the activation of selected genes contributing to different cellular functions including antiviral response, inflammation, immunomodulation and apoptosis[95,96]. Apart from the canonical pathway, IFN-Is can also initiate the phosphorylation of STAT3, STAT4, STAT5 and STAT6, which may then form homodimerisation or heterodimerisation[97].

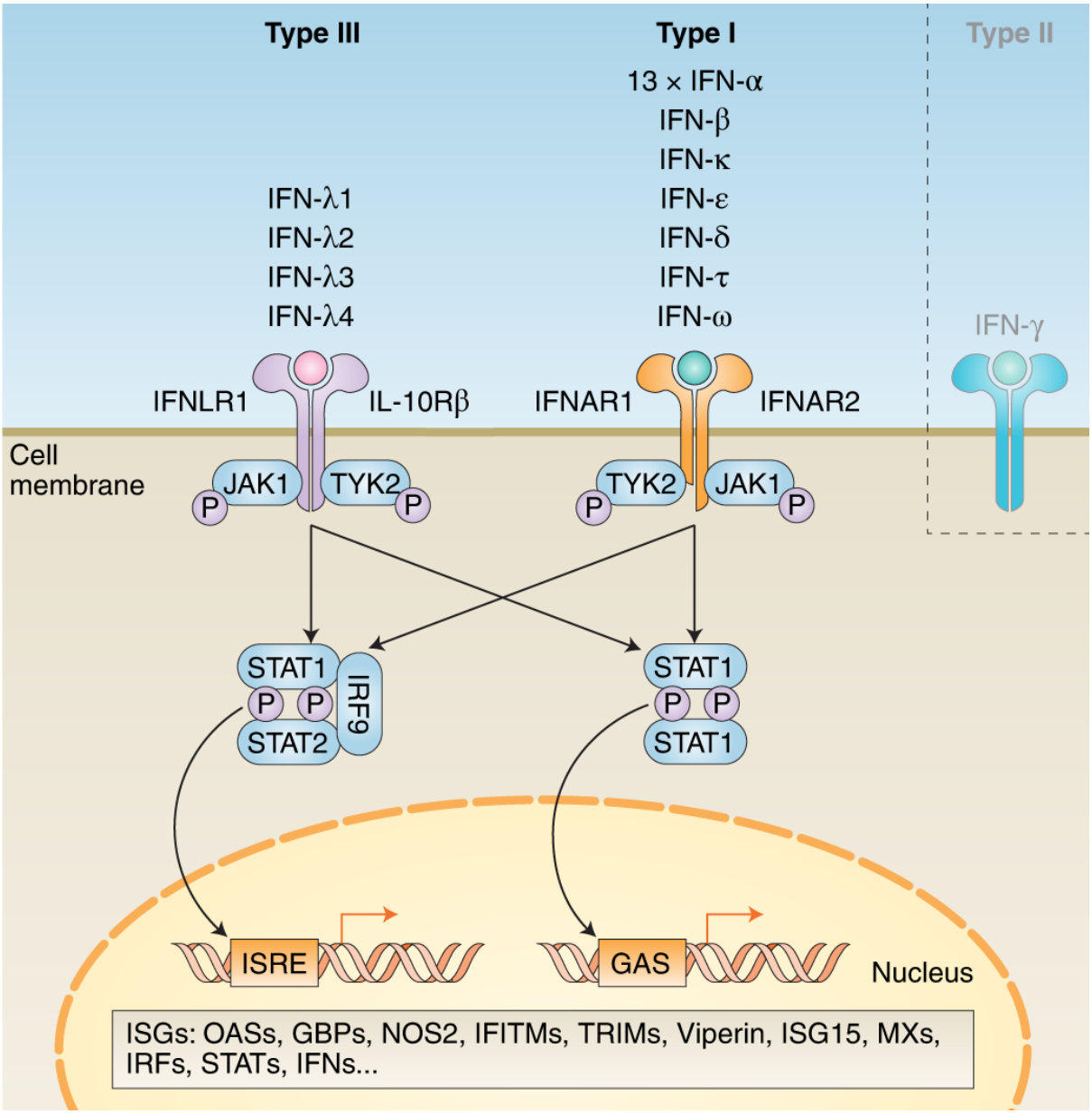

Figure 1.2. IFN-I signalling cascade. IFN-Is bind to IFNAR1/IFNAR2 receptor complex and activate the Janus kinase signal transducer and transcription activator (JAK-STAT) pathway. These STATs can then bind to IFN-stimulated response elements (ISREs) or gamma-activated sequences (GASs) on the promoters of ISGs leading to the transcription of ISGs. This figure is taken from Mesev *et al.* [98]

2.2. IFN-Is and immune responses

Accumulating evidence suggests that IFN-Is can regulate both innate and adaptive immune responses by acting differently on various immune cell types as shown in **figure 1.3**[99]. Research has shown that mice without IFNAR1 were severely susceptible to viral infection[100], highlighting the significance of early IFN-I induction to subdue viral replication. T cell activation is partly required to effectively elicit viral defence mechanisms. IFN-I signalling has been found to play a role in T cell proliferation and early cytotoxic function of $CD8^+$ T cells[101]. IFN-Is can enhance T cell priming by activating DCs leading to an increase in surface expression of co-stimulatory receptors (such as CD80, CD86, CD40) and MHC-II and thus increasing the antigen presentation capacity of DCs to T cells[11,102,103]. In addition, IFN-Is can also promote natural killer (NK) cell activation and recruitment by chemokine secretion and STAT1-dependent IFN-γ production[104,105]. In contrast, during persistent viral infection, IFN-Is have a pathogenic role by inducing immune suppression, lymphoid tissue disorganisation and $CD4^+$ T cell dysfunction[106]. IFN-Is are also reported to be responsible for impaired viral clearance and effector cell functions[107,108]. Studies revealed that continuous IFN-I activation could reduce T cell response by enhancing the generation of anti-inflammatory cytokines such as IL-10 and the expression of PD-1 in macrophages and DCs[109,110]. Continuous IFN-I expression can also directly subdue the effector activity of NK cells[31].

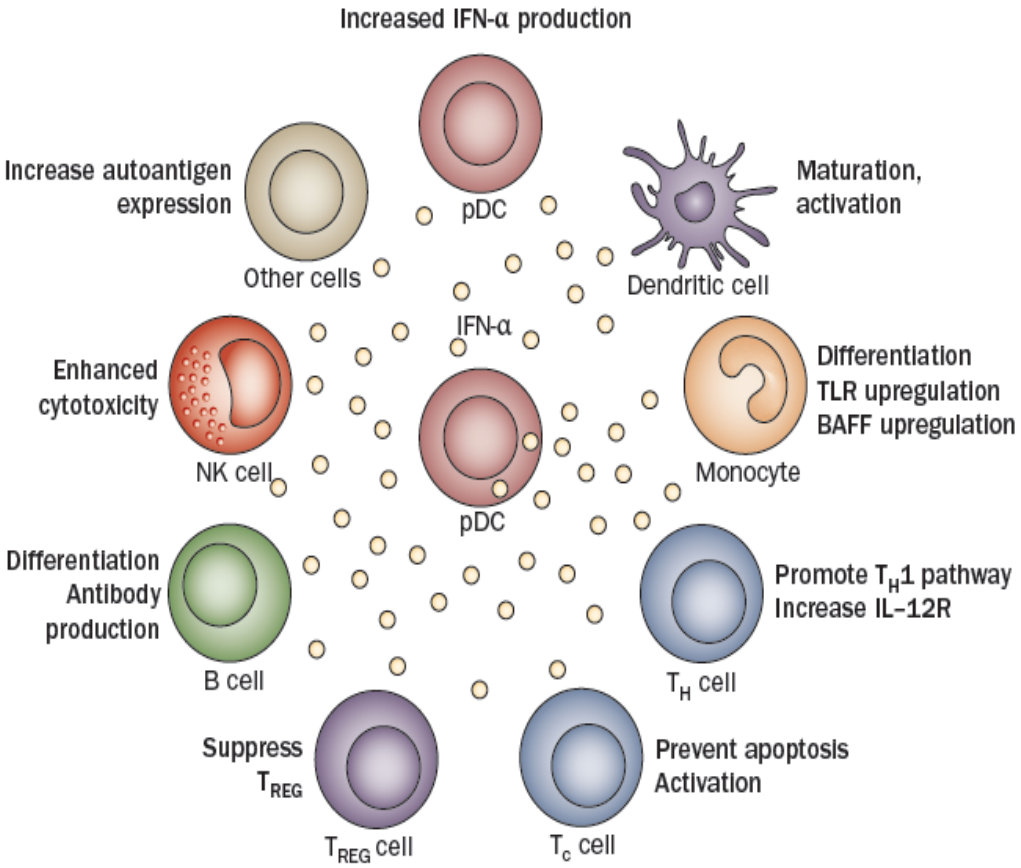

Figure 1.3. The role of IFN-I on immune cell response. pDCs is a major producer of IFN-Is which have various effects on different immune cell types. This figure is taken from Rönnblom *et al*.[111]

2.3. IFN-I signatures in SLE

In 1979, the association between IFN and SLE disease was first discovered by Hook and colleagues whereby they detected elevated IFN levels in the serum of SLE patients[112] and this IFN was later identified as IFN-Is[113]. Interestingly, patients with malignant carcinoid tumours who were treated with IFN-α exhibited SLE-like symptoms with the production of autoantibodies against their nuclear antigens, indicating that IFN-Is may be sufficient to breach the self-tolerance and contribute to SLE[114,115]. Subsequently, numerous studies have shown that blood and tissue from SLE patients have an increased expression of ISGs, known as “IFN signature”. GWAS studies of PBMCs have revealed that 50-75% of adult lupus patients, as well as 90% of children with SLE, have an increased IFN-I signature[1,116-119]. Research using epigenetic analyses from hypomethylated genome sites has also established that

various expressed genes are associated with IFN-I signalling[120,121]. IFN-I signature is usually thought to correlate with disease activity in several conditions including infection, cancer and autoimmune disease[86,122-125]. However, it remains controversial whether the IFN signature correlates with disease severity in SLE. In cross-sectional studies, IFN-I levels in the serum of SLE patients were found to be associated with flare rates[126], whereas analysis of longitudinal gene expression signatures displayed no positive correlation between IFN signature and disease activity whereby ISG expression remained stable over time[127]. A study using refined cluster analysis demonstrated that IFN signature in lupus patients is more complex than estimated and can be divided into different gene module subgroups[128]. Interestingly, research conducted by using modular repertoire analysis has elucidated that blood-IFN signatures in adult SLE are not specific to IFN-Is but also linked to IFN-γ[128]. Therefore, it is essential to note that complex IFN signatures observed in SLE patients may be associated with other types of IFNs, although IFN-Is appear to be the most important[129].

As previously described, ISGs induced by IFN-Is can encode important proteins related to antiviral defence mechanisms and cellular function regulation[130,131]. Nevertheless, the exact biological functions of these genes remain elusive. A handful of ISGs such as IRF5 can promote IFN-I production, whereas some can reduce IFN-I response through the cytokine signalling suppressor (SOCS) family[131]. Moreover, the expression of different ISGs seems to depend on the cell types, the types of IFN-inducing stimuli and pathophysiological circumstances[132].

The IFN signature stimuli in SLE are dynamic and complex. There are at least four plausible causes. The first possible factor is the interferogenic ICs which consist of autoantibody and self-antigen complexes as well as the DNA and RNA-containing materials which are released during NETosis. These complexes can be endocytosed via Fc gamma receptor (FcγR) IIα on pDCs and serve as endogenous IFN inducers by activating pDCs via the TLR 7 or TLR9 signalling pathway[133]. Secondly, genetic variations within the IFN-I signalling pathway can affect IFN-α production[134]. For instance, research conducted within diverse ethnic groups demonstrated that IRF5, which is a lupus susceptibility gene, was highly expressed in SLE patients and has a consistent relationship with IFN-α activity[135,136]. The third cause is the defect in the

modulation of pDC activation. Generally, IFN-I production is strictly controlled to normal homeostatic level after viral clearance[131]. Defective negative feedback signals in pDCs, which have been shown in SLE[131], can contribute to the chronic stimulation of these cells by the endogenous nucleic acids. For example, the lack of sufficient complement protein C1q, which has been reported to suppress pDC stimulation, can contribute to prolonged IFN-α production in SLE[137,138]. The final reason behind the increased IFN signature is the activation of IFN-I-producing cells. Even though many observations indicate that pDCs are responsible for the ongoing IFN production in SLE, recent lines of evidence have suggested that other cell types may also be implicated. For example, monocytes could generate IFN signature, especially in the pristane-induced murine lupus model whereby cells transfected with a small non-coding Y RNA or stimulated with IC were subsequently able to produce IFN-α and IFN-β mRNA transcripts[139]. Microarray and single cell RNA sequencing studies have reported IFN signature in other myeloid cells that are not pDcs such as monocytes and macrophages in tissues and in PBMCs from SLE patients[140-142]. Importantly, recent data have emphasised the role of non-hematopoietic cellular sources. Psarras and colleagues have found a significant enrichment of an interferon signature in the skin of patients with preclinical manifestations[143]. In this report, keratinocytes isolated from a skin biopsy of SLE patients and autoantibody-positive healthy individuals highly express IFN-κ compared to healthy controls[143].

Several mouse and human studies are suggesting that IFN-Is can contribute to SLE progression through numerous mechanisms. For example, conditional upregulation of IFN-Is was adequate to promote SLE in autoimmune-resistant C57BL/6 strain[144]. This discovery has been consistent with other spontaneous lupus models, including BXSB, NZW/NWB F1 mice, whereby IFN-Is are essential for disease development. It is well known that IFN-Is can increase self-antigen production by promoting apoptosis and enhancing NETs formation[145]. Furthermore, IFN-Is can induce monocyte differentiation into activated DCs and increase the self-antigen-presenting capacity of these cells to T cells[11]. Regarding adaptive immune response, IFN-Is can promote B cell survival by inducing the expression of BAFF and can support B cell differentiation and class-switch recombination enhancing autoantibody production[146]. IFN-Is also directly affect both $CD4^+$ and $CD8^+$ T cells. IFN-Is are found to induce human naive $CD4^+$ T cells to differentiate into IFN-γ–secreting Th1-like T cells that promote B cell

class switching[147,148] and support the development of T follicle helper cells in lymph nodes[149]. Furthermore, IFN-Is have effects on $CD8^+$ T cells with paradoxical consequences. Evidence has revealed that these cytokines can facilitate the generation of effector and memory $CD8^+$ T cells *in vivo*[150]. However, prolonged exposure to IFN-Is promotes $CD8^+$ T cell exhaustion and impaired immune response[108]

In July 2021, the US FDA has approved the use of a drug that inhibits the activity of all IFN-Is for the treatment of SLE including lupus nephritis[151]. Anifrolumab is a fully human IgG1κ monoclonal antibody that binds to IFNAR1 with high specificity and affinity. Anifrolumab (intravenous or subcutaneous) is currently being evaluated for SLE treatment in many countries[151]. Collectively, these studies based on genetic and gene expression data and positive phase III clinical trials of IFN-I-blocking therapy highlight the importance of chronic IFN-I signalling in SLE pathogenesis.

3. Cell metabolism

3.1. Main metabolic pathways

It is known that metabolic constituents play an important role in dictating the effector functions of immune cells[152]. For instance, T cell survival, differentiation and effector functions are reliant on the generation of cellular energy in the form of adenosine triphosphate[4]. Macrophages exist in a variety of environments. Therefore, to promptly respond to pathogenic or tissue damage signals, they have developed the ability to use energy under normoxic and hypoxic conditions as well as in the presence of varying concentrations of glucose or other nutrients[153].

It is also widely acknowledged that mitochondria play a fundamental role in energy production by the coupling of nutrient oxidation (e.g. glycolysis) and oxidative phosphorylation (OXPHOS). Cellular metabolism involves a variety of metabolic processes depending on the availability of nutrients such as glucose, glutamine and fatty acids (**Fig.1.4**). Glucose can be utilised through glycolysis and OXPHOS. Glycolysis, which occurs in the cytoplasm, converts glucose into pyruvate and can generate ATP and a reduced form of nicotinamide adenine dinucleotide (NADH) which acts as an electron carrier. Furthermore, glycolysis is critical for the generation of

intermediate products of other metabolic processes such as the pentose phosphate pathway. Pyruvate derived from glucose can be either converted to lactate (in the cytoplasm) or transported to mitochondria and then converted into acetyl coenzyme A (CoA). This novel product can be alternatively generated from the metabolism of fatty acids in a process called fatty acid oxidation (FAO). Acetyl CoA is then oxidised into ATP and CO_2 to fuel the tricarboxylic acid (TCA) cycle, also known as the Krebs cycle. Glutamine is also involved in the TCA cycle, being converted to TCA cycle machinery such as α-ketoglutarate. The oxidisation of acetyl-CoA in this TCA cycle leads to the production of NADH and hydroquinone form of flavin adenine dinucleotide ($FADH_2$).

OXPHOS refers to the metabolic process which produces ATP via acetyl-CoA oxidation and the transfer of electrons to the electron transport chain (ETC) by NADH and $FADH_2$[74]. ETC is a series of organic molecules and protein complexes located on the inner mitochondrial membrane[154] as shown in **figure 1.4**. NADH and $FADH_2$ donate their electrons to electron acceptors which are the ETC complex I and II respectively and lead to a series of redox reactions. Ultimately, this reaction forms an electrochemical proton gradient by pumping hydrogen ions (H^+) across the inner mitochondrial membrane which results in the production of ATP via the ETC complex V (ATP synthase). The transfer of electrons through the chain and proton pumping into the mitochondrial intermembrane space maintains the mitochondrial membrane potential (MMP), which is an important factor for mitochondrial function[155]. Since the MMP can facilitate the production of ATP[156], the imbalance between MMP and insufficient ATP production can cause more electron leakage. This leakage leads to the reduction of oxygen to form superoxide. Subsequently, superoxide is promptly dismutased to hydrogen peroxide by two dismutases (superoxide dismutase 1 and 2 (SOD1, SOD2)). The superoxide and hydrogen peroxide generated by this process is called mitochondrial reactive oxygen species (mROS)[157]. This elevated intracellular ROS is referred to as oxidative stress which can consequently cause damage to lipids, proteins and DNA[158].

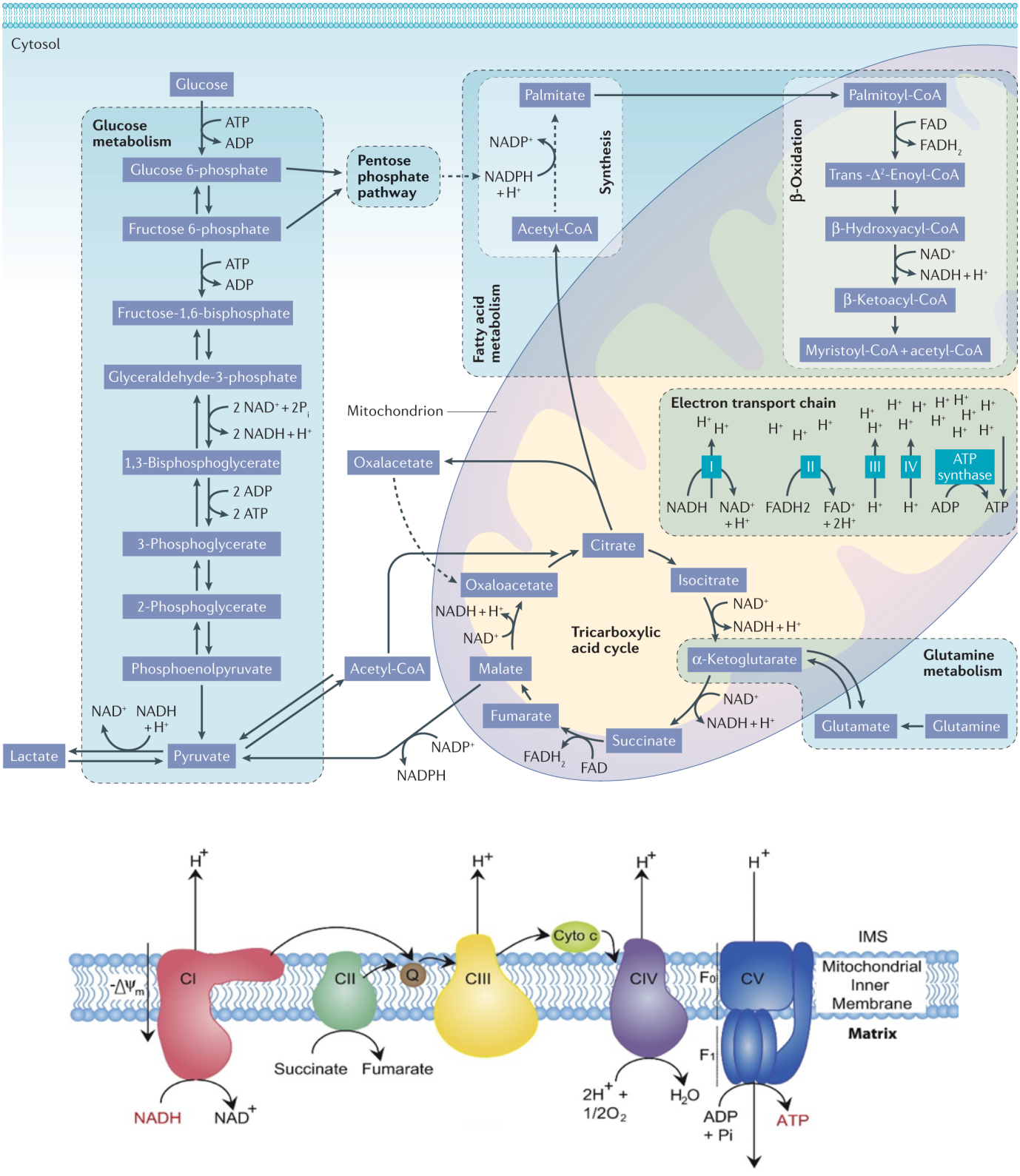

Figure 1.4. Main pathways of cell metabolism including glycolysis, TCA cycle, fatty acid metabolism and electron transport chain (ETC). This figure is taken from Basso *et al.* and Osellame *et al.*[159,160]

3.2. Metabolism of immune cells

3.2.1 T cell metabolism

T cell subsets have been found to be crucial in the development of SLE. The functions of each T cell subset are shaped by the activity of different metabolic pathways demanding the availability of certain nutrients and intracellular enzymes[161]. Different subsets of T cells utilise distinct metabolic pathways to dominate ATP generation. For instance, naïve T cells, exiting from the thymus to migrate to peripheral sites, are in a quiescent state and are metabolically inactive which only necessitates basic energy for persistence and survival. Thus, these T cells predominantly rely on highly energy-favourable OXPHOS[162].

TCR and co-stimulatory signalling enable the metabolic reprogramming of naïve T cells. After engaging with the cognate antigen through TCR, naïve T cells become activated and initiate an exceptionally high rate of clonal expansion. Therefore, activated T cells undergo a metabolic shift toward rapid aerobic glycolysis and glutaminolysis to meet their higher metabolic demands and to generate intracellular components including lipids, amino acids, nucleotides and other carbohydrates through the pentose phosphate pathway. Furthermore, they also increase their mitochondrial mass for energy supply via a process called mitochondrial biogenesis[161]. The stimulation of TCR also leads to the rapid upregulation of glucose transporter Glut1 via PI3K-Akt signalling, resulting in elevated glucose uptake and metabolism, and the upregulation of hypoxia-inducible factor (HIF)-1α and cellular myelocytomatosis oncogene (c-Myc)[163]. The engagement of TCR can also activate mTOR pathway, the sensor system regulating cellular growth and energy utilisation. This process skews the lineage specification of T cells[164,165] and involves two distinct protein complexes: the mTORC1 complex and the mTORC2 complex. These complexes enable many signalling pathways by leading a metabolic reprogramming of the cells and shifting from FAO towards glycolysis and glutaminolysis[166,167].

Following the antigen activation, most effector T cell populations undergo activation-induced apoptosis, while some differentiate into memory T cells. Memory T cells adopt a metabolic profile similar to that of naïve T cells since they no longer need a high metabolic demand to proliferate but require a quiescent oxidative metabolism to

maintain long-term survival. Nevertheless, memory T cells have been found to have increased lipid oxidation activity and decreased glycolytic flux, leading to elevated mitochondrial mass and more spare respiratory capacity (SRC) compared to naïve or effector T cell populations[168]. The increase in mitochondrial mass and SRC of memory T cells facilitates quick mitochondrial ATP production upon TCR signalling, reflecting the energetic benefit of these cells in response to repeated antigen exposure[169].

3.2.2. Macrophage metabolism

Macrophages play a crucial role in maintaining tissue homeostasis and protecting against infections. These cells are characterized by their ability to phagocytose and digest microorganisms and cellular debris, as well as their capacity to produce a variety of cytokines and chemokines that help coordinate immune responses. The wide range of macrophage functions is due to their heterogeneity and flexibility, as these cells are highly specialised in sensing the milieu and changing their features accordingly through a process defined as polarisation[170].

Although it is obvious that macrophage phenotypes are difficult to classify and should be viewed as plastic and adaptive, they can be simplified into two extremes. Macrophages are categorised into a pro-inflammatory (M1)[171,172] or an anti-inflammatory (M2) phenotype[173,174] based on unique gene expression patterns that result in the accumulation of various markers on the cellular surface, the production of specific cytokines, and metabolic alterations[170].

Pro-inflammatory macrophages are capable of initiating and maintaining inflammatory responses by secreting pro-inflammatory cytokines such as IL-6, IL-12, TNF-α and IL-1β to kill pathogens. They are also characterised by the expression of CD80, CD86, MHC-II receptor, cyclooxygenase 2 (COX-2), and inducible nitric oxide synthase (iNOS)[175]. These cells can also activate endothelial cells, recruit other immune cells into damaged tissue and present antigens to T cells to elicit adaptive immune responses[170]. These pro-inflammatory macrophages can be induced by microbial products like lipopolysaccharide [176] and other TLR ligands, or by cytokines released by Th1 cells like IFN-γ. On the other hand, anti-inflammatory macrophages produce anti-inflammatory cytokines such as IL-10 and TGF-β that facilitate the resolution of inflammation. In addition, they are crucial for wound healing and tissue repair. M2

macrophages produce pro-fibrotic factors such as insulin-like growth factor 1 (IGF-1) leading to inducing collagen deposition and regulating tissue integrity[177]. Furthermore, their increased arginase activity promotes tissue remodelling and wound healing by increasing polyamine and collagen synthesis[177]. These anti-inflammatory macrophages can be induced by IL-4 or IL-13 which are cytokines secreted by innate and adaptive immune cells including mast cells and Th2 cells[173,174]. They are found to express CD206, CD163 and CD36 surface markers. Distinct macrophage profiles have been reported in the literature according to the activation trigger as detailed in **table 1.2**[178].

These various subtypes of macrophages highlight the plasticity of the cells to adapt and respond promptly as a first-line defender of the immune system. Given these unique features, macrophages play an essential role in the initiation, maintenance and resolution of inflammation.

Table 1.2. A classification of the different phenotypes of macrophages[178]

Polarization	Stimuli	Released cytokines	Surface markers	Metabolic enzymes	Transcription factors	Functions
M1	LPS + IFN-γ	TNF-α, IL-1β, IL-6, IL-12, IL-23	CD80, CD86, CIITA, MHC-II	iNOS, PFKFB3, PKM2, ACOD1	NF-κB (p65), STAT1, STAT3, IRF-4, HIF1α, AP1	Bacterial killing, tumor resistance, Th1 response
M2a	IL-4/IL-13	IL-10, TGF-β	CD206, CD36, IL1Ra, CD163	ARG1, CARKL	STAT6, GATA3, SOCS1, PPARγ	Anti-inflammatory response, tissue remodeling, wound healing
M2b	IC, TLR ligands/IL-1Ra	IL-10, IL-1β, IL-6, TNF- α	CD86, MHC II	ARG1, CARKL	STAT3, IRF4, NF-κB (p50)	Tumor progression, immunoregulation, Th2 response
M2c	Glucocorticoids/IL-10	IL-10, TGF- β	CD163, TLR1, TLR8	ARG1, GS	STAT3, STAT6, IRF4, NF-κB (p50)	Phagocytosis of apoptotic bodies, tissue remodeling, immunosuppresion
M2d (TAM)	TLR ligands + A2R/IL-6	IL-10, VEGF	CD206, CD204, CD163	ARG1, IDO	STAT1, IRF3, NF-κB (p50)	Angiogenesis, tumor progression

A2R, adenosine receptor 2; ACOD1, aconitate decarboxylase 1; AP-1, Activator proten 1; ARG1, Arginase 1; CARKL, carbohydrate kinase- like; IC, immunocomplexes; IDO, indoleamine dioxygenase; iNOS, inducible Nitric Oxide Synthase; GATA3, GATA binding protein 3; GS, glutamine synthetase; HIF1α, Hypoxia-inducible factor 1-alpha; IFN-γ, Interferon gamma; IL-, interleukin; IRF, interferon regulatory factor; MHC-II, major histocompatibility complex class 2; NF-κB, nuclear factor kappa-light-chain-enhancer of activated B cells; PPARγ, Peroxisome proliferator-activated receptor gamma; SOCS1, Suppressor of cytokine signaling 1; STAT, Signal transducer and activator of transcription; TNF-α, Tumor necrosis factor alpha; TGF-β, transforming growth factor beta; TLR, toll like receptor; VEGF, Vascular endothelial growth factor.

To support their diverse functional roles, macrophages exhibit high metabolic activity. They rely on a range of metabolic pathways to generate ATP depending on the stimuli in the microenvironment. In pro-inflammatory macrophages, an increase in glycolysis accompanied by decreased oxygen consumption was reported first in 1970[179]. Several studies have later confirmed that M1 macrophages primarily use glycolysis and the pentose phosphate pathway as a source of ATP generation[180-182]. Their OXPHOS activity and FAO are also diminished[181]. The TCA cycle leads to the accumulation of

metabolites with innate immune functions such as itaconate and succinate[170]. In addition, succinate leads to HIF1 stabilisation. HIF1α controls the expression of genes encoding for glycolytic enzymes, the glucose transporter GLUT1, as well as inflammatory mediators[183-185]. Therefore, the stabilisation of HIF1 induced by the accumulation of succinate then sustains M1 macrophage glycolytic metabolism. In contrast, anti-inflammatory macrophages are more reliant on OXPHOS to generate ATP. Their TCA cycle is intact and supplies substrates for the ETC. The role of glycolysis in M2 macrophages is still controversial. Some studies demonstrated that blocking glycolysis by 2-deoxyglucose (2-DG), a glycolysis inhibitor may inhibit M2 differentiation[186,187]. However, recent research suggests that glycolysis is not necessary for M2 differentiation as long as OXPHOS is still functioning[188]. These cells can sustain OXPHOS in the absence of glucose by using glutamine instead[188]. In addition, M2 macrophages have an enhanced gene expression for fatty acid uptake, transport, and oxidation, as well as increased fatty acid uptake in culture[189]. Fatty acid oxidation is crucial for supporting their OXPHOS activity. Another distinct metabolic profile in M2 macrophages is the arginine metabolism[190]. In M1 macrophages, induction of nitric oxide synthase 2 (NOS2) metabolises arginine to nitric oxide (NO) and citrulline. NO can then be metabolised to reactive nitrogen species, while citrulline may be salvaged for NO synthesis. In contrast, M2 macrophages highly express the enzyme arginase which can hydrolyse arginine to ornithine and urea instead. Ornithine can be used as a substrate for downstream pathways of polyamine and proline syntheses[190]. The metabolic differences between these two traditional types of macrophages can influence the ability of these cells to generate ROS. ROS have been shown to affect various processes in macrophages, including bacterial killing, phagocytosis, and polarisation[170]. Recent research has shown that M2 macrophages generate fewer ROS and extracellular hydrogen peroxide compared to the M1 macrophages[191]. In summary, macrophage metabolism is a complex and dynamic process that is essential for orchestrating their multiple innate functions. The regulation of macrophage metabolism can be influenced by a range of factors, including nutrient availability and cytokine signalling pathways.

3.3. NAD metabolism

Nicotinamide adenine dinucleotide (NAD+) is a vital coenzyme that helps transfer hydrogen atoms during various metabolic processes including glycolysis, the TCA cycle, ETC and FAO. NAD+ was initially identified in 1906 as a component capable of increasing the rate of yeast fermentation[192]. Years later, NAD+ was discovered to be necessary for hydrogen transport in redox reactions[193]. The coenzyme is found in two forms: NAD+ and NADH. NAD+ acts as an oxidizing agent which accepts electrons from other molecules and becomes reduced, forming NADH. NADH can then be used as a reducing agent to donate electrons to produce ATP in the mitochondria through OXPHOS, as well as for the generation of ROS in the cytoplasm and mitochondria.

In addition to acting as a co-enzyme in energy metabolism, NAD+ is also important for other cellular processes. The most notable one is being a co-substrate of non-redox enzymes that add or remove chemical groups from proteins in post-translational modifications. For example, NAD+ can serve as an adenosine diphosphate (ADP)-ribose (ADPR) donor for NAD-consuming enzymes including CD38, sirtuins, poly-ADPR polymerase (PARPs) and Sterile alpha and TIR motif containing 1 (SARM1)[194]. These NAD-consuming enzymes have distinct roles in normal conditions. For example, CD38 is an NAD+ glycohydrolase that utilises NAD+ to generate calcium-releasing second messengers such as ADPR (primary product), nicotinic acid adenine dinucleotide phosphate (NAADP) and cyclic-ADPR (cADPR). Sirtuins (SIRT) 1-7 are NAD-dependent deacetylases present in the nucleus, cytoplasm, and mitochondria. SIRT1 is the most studied sirtuin that can be found in the nucleus and cytoplasm of the cells. These enzymes have several functions in gene modulation, bioenergetic regulation, cell survival, DNA repair, inflammation, and circadian rhythm control[195,196]. PARPs are DNA-damage sensors and play an important role in the initial chromatin organisation and DNA repair pathway[197]. PARP1 accounts for the largest amount of PARP activity in eukaryotic cells and acts as the key NAD+-consuming enzyme in the nucleus[198].

To respond to the high and dynamic NAD^+ cellular demand for both redox and non-redox processes, mammalian cells can obtain NAD^+ from three independent biosynthetic pathways as shown in **figure 1.5 and 1.6**. NAD+ can be synthesised from

dietary amino acid tryptophan through the *de novo* synthesis pathway or from dietary nicotinic acid (NA) through the Preiss-Handler pathway or NAD+ can be recycled from the NAD+ salvage pathway.

The *de novo* NAD synthesis pathway or the kynurenine pathway utilises tryptophan which enters the cell through the transporters SLC7A5 and SLC36A4 to produce NAD+. This pathway is initiated by rate-limiting enzymes either indoleamine 2,3-dioxygenase isozyme (IDO) for immune cells such as monocytes/macrophages or tryptophan 2,3-dioxygenase (TDO) for liver cells. The enzyme IDO-1 is found in many immune cells including mononuclear phagocytes. While little is known about IDO-2, it is believed to be expressed more selectively in particular tissues such as the liver, kidney, and brain[199]. Within the cell, IDO or TDO enzyme converts tryptophan into N-formylkynurenine. This N-formylkynurenine is then metabolised into L-kynurenine, which is further transformed to 3-hydroxykynurenine (3-HK) by kynurenine 3-monooxygenase (KMO) and to 3-hydroxyanthranilic acid (3-HAA) by kynureninase (KYNU). Following this, 3-hydroxyanthranilic acid oxygenase (3-HAO) enzyme then converts 3-HAA to α-amino-β-carboxymuconate ε-semialdehyde (ACMS). This ACMS can be condensed into quinolinic acid spontaneously. The quinolinic acid is then metabolized by quinolinate phosphoribosyltransferase (QPRT) enzyme to generate nicotinamide mononucleotide (NAMN) where it intersects the Preiss-Handler pathway[200].

The Preiss-Handler pathway begins with the import of NA via SLC5A8 or SLC22A13 transporters. Within the cell, NA is converted to NAMN by the enzyme nicotinic acid phosphoribosyltransferase (NAPRT). Following this, the group of enzyme nicotinamide mononucleotide adenylyltransferases (NMNATs) transform NAMN into nicotinic acid adenine dinucleotide (NAAD). The last step is completed by NAD+ synthetase (NADS) which converts NAAD into NAD+[200].

Rather than being generated through these two pathways, most NAD^+ is recycled from the nicotinamide (NAM) produced as a by-product of NAD-consuming enzymes in the NAD+ salvage pathway to maintain the cellular NAD^+ levels. Initially, this pathway recycles NAM into nicotinamide mononucleotide (NMN) using the nicotinamide phosphoribosyltransferase (NAMPT) enzyme. NMN is used as a substrate to generate NAD+ by the different NMNATs (NMNAT1, NMNAT2 and NMNAT3) depending on the location of the process. The extracellular NMN can be alternatively dephosphorylated

by CD73 to nicotinamide riboside (NR) and these NMN and NR can be later transported into the cell with their transporters[200].

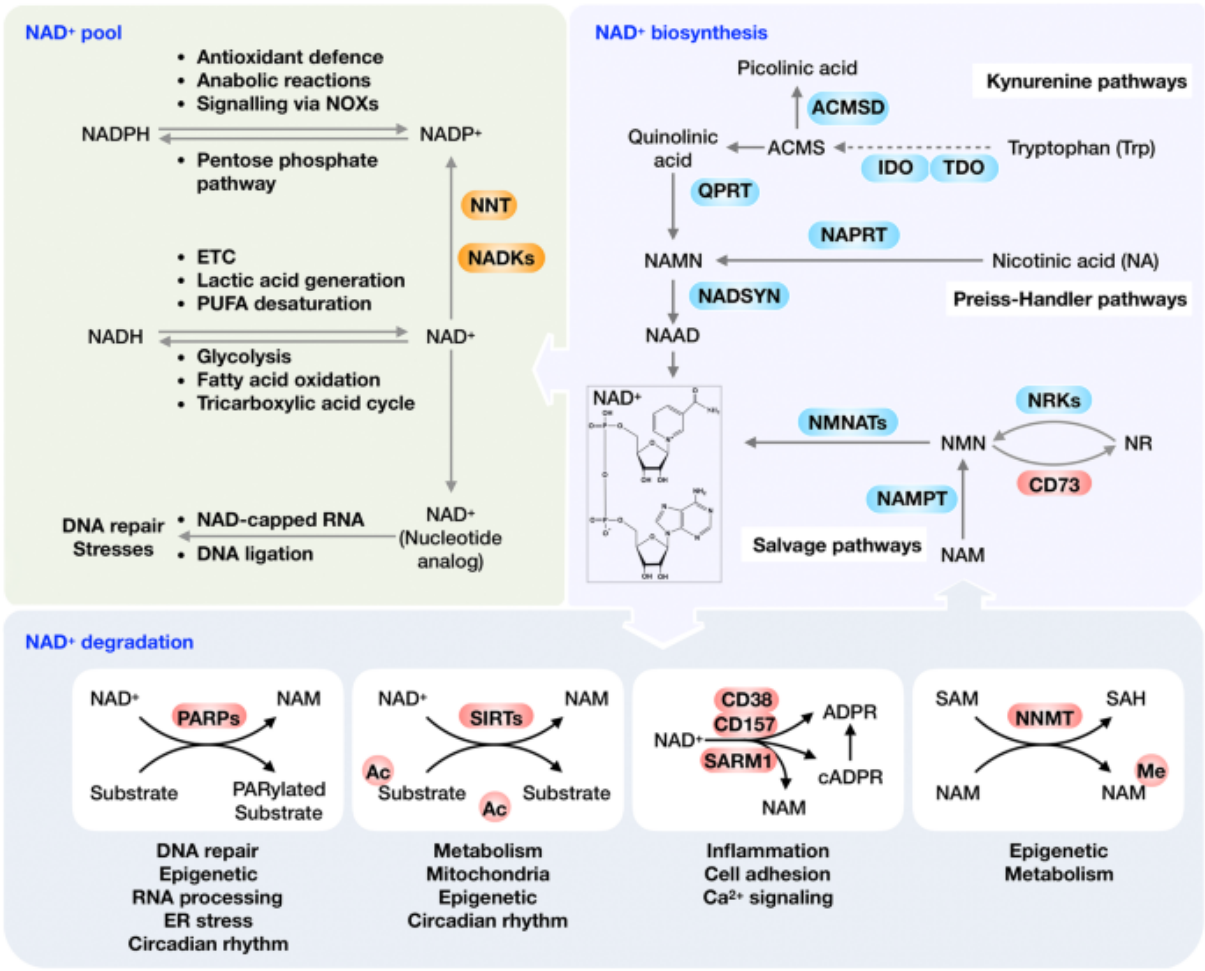

Figure 1.5. Overview of the NAD+ metabolism and its physiological function. NAD+ is rapidly used for both redox and non-redox reactions and can be degraded by several NAD-consuming enzymes for different purposes. Mammalian cells can either synthesise or recycle NAD+ by three different pathways. This figure is taken from Xie *et al.*[194]

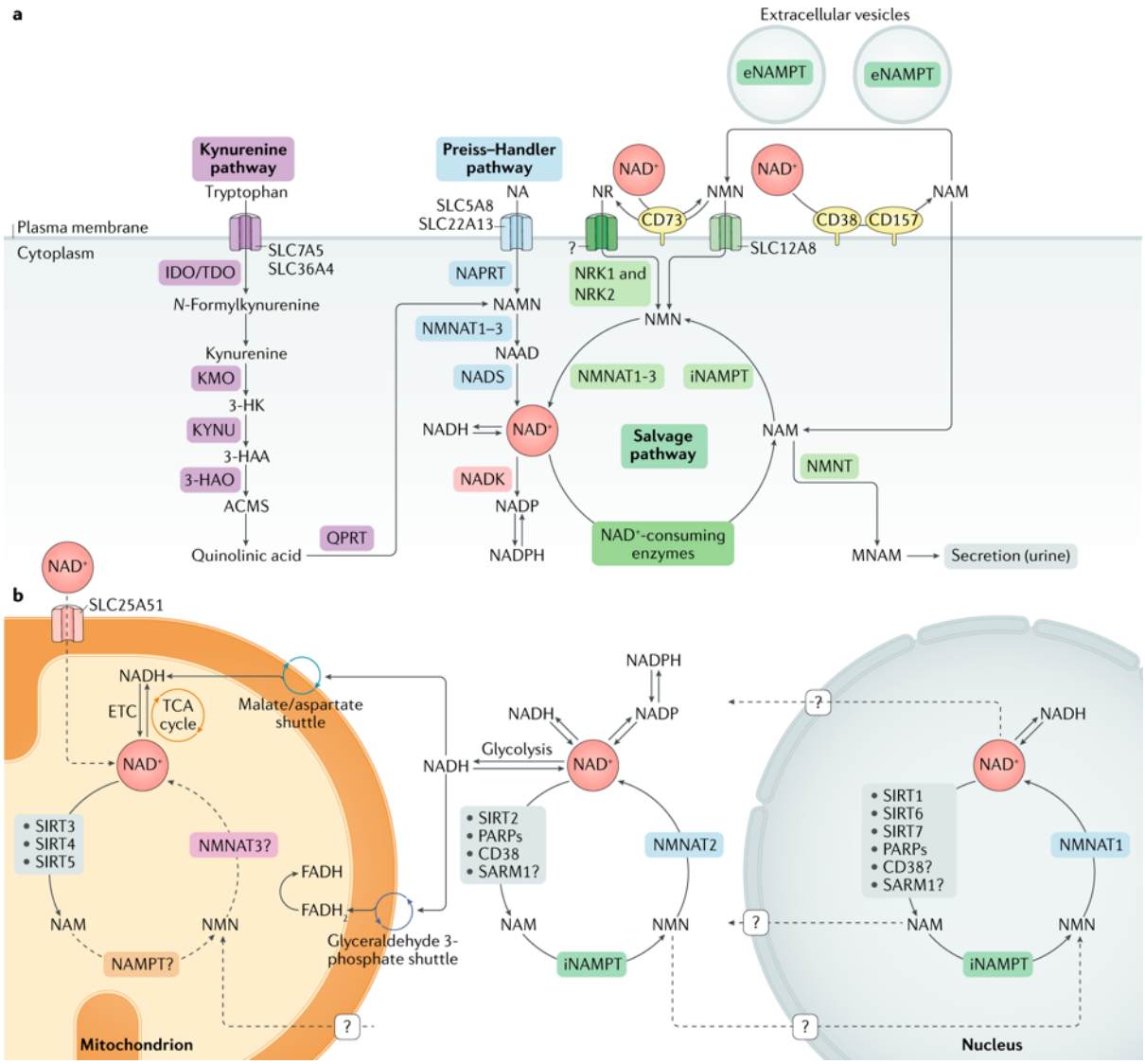

Figure 1.6 Details of NAD+ synthesis pathways and NAD+ metabolism in different subcellular compartments. NAD metabolism happens in various cites in the cells depending on involved enzymes. This figure is taken from Covarrubias *et al.*[200]

3.3.1.NAD-consuming enzyme CD38

CD38 is a multifunctional enzyme expressed on various immune cells including T cells, B cells, neutrophils, and macrophages that has a variety of roles including the metabolism of adenosine, the regulation of calcium signalling, and the production of ROS[201]. CD38 has been identified as a key modulator of NAD+ metabolism in the context of aging and cancer biology[202]. CD38 can also modulate infection-driven

inflammatory processes ranging from cell recruitment to the generation of adaptive immunological responses[203,204].

Structurally, CD38 is a single chain glycoprotein that is abundantly found on the cell surface with its catalytic site facing toward the extracellular environment in a type II orientation[205-207], but it can also be found in intracellular compartments such as the endoplasmic reticulum, nuclear membrane, and mitochondrial membrane[205,208,209] (**Fig.1.7**). Although CD38 is present inside the cells, the majority of CD38 activity is extracellular. Approximately 90% of CD38 functions as an ecto-NADase (NAD+ glycohydrolase), catabolizing NAD+ resulting in the synthesis of NAM and ADPR[206]. CD38 can also act as ecto-NMNase by metabolising extracellular NAD precursors, NAM and NR before they are delivered to the cell for NAD+ biosynthesis[210]. These functions of type II membrane-bound CD38 sustain NAD+ homeostasis by controlling NAD+ level and NAD+ synthesis precursors in the extracellular environment[202]. Another role of CD38 is to act as a second messenger enzyme for the synthesis of cADPR. CD38 is a relatively inefficient cyclase, requiring roughly 100 molecules of NAD+ to be degraded to create one molecule of cADPR[211]. It is likely that the production of cADPR could be a by-product of the NAD+ glycohydrolase activity of CD38[202].

CD38 can act as a regulator of NAD+ during inflammation. It has been studied extensively in an inflammaging context. Inflammaging indicates a process of inflammatory responses mediated by cytokines and triggered by DNA and protein damage coupled with a decreased ability for cell repair in aging individuals[212,213]. During the aging process, a reduction of NAD+ is observed in several cell types and tissue types. This NAD+ decline has been implicated in the pathogenesis of age-related conditions[202]. One of the possible causes of this age-related NAD decline could be the decrease in NAD+ synthesis. The expression of NAMPT, a rate-limiting NAD+ synthesis enzyme in the NAD salvage pathway, is reduced in some aging tissues[214,215], demonstrating a reduced capacity to synthesize intracellular NAD+ via salvage pathway synthesis and a dependency on importing of external NAD+ precursors NMN and NR[202]. Another cause could be the increased expression of NAD-consuming enzymes such as the PARPs and CD38[216,217]. Like in many tissues, CD38 is highly expressed in macrophages during aging. During aging, the activation of CD38 may boost nuclear factor kappa B (NF-κB) signal transduction which is one of the key

signalling pathways related to the emergence of senescence-associated secretory phenotype (SASP)[218] and pro-inflammatory genes[219].

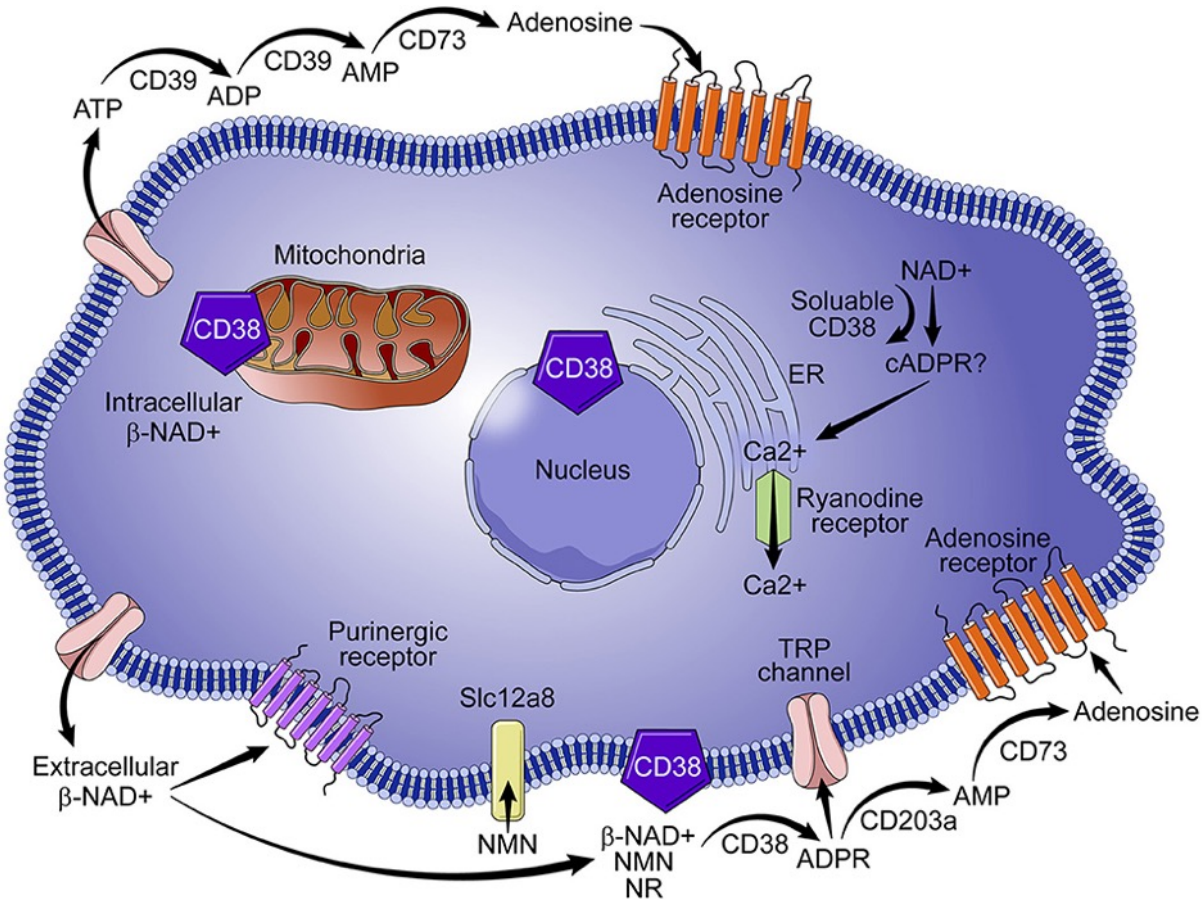

Figure 1.7. The localisation of CD38 and its role in NAD+ metabolism. CD38 is an enzyme that converts nicotinamide nucleotides (NAD+ and NMN) to ADPR and cADPR, resulting in calcium transport. It is found both within and outside of the cell membrane. However, the vast majority of CD38 activity is extracellular, resulting in NAD+ precursor degradation. This figure is taken from Hogan *et al.*[202]

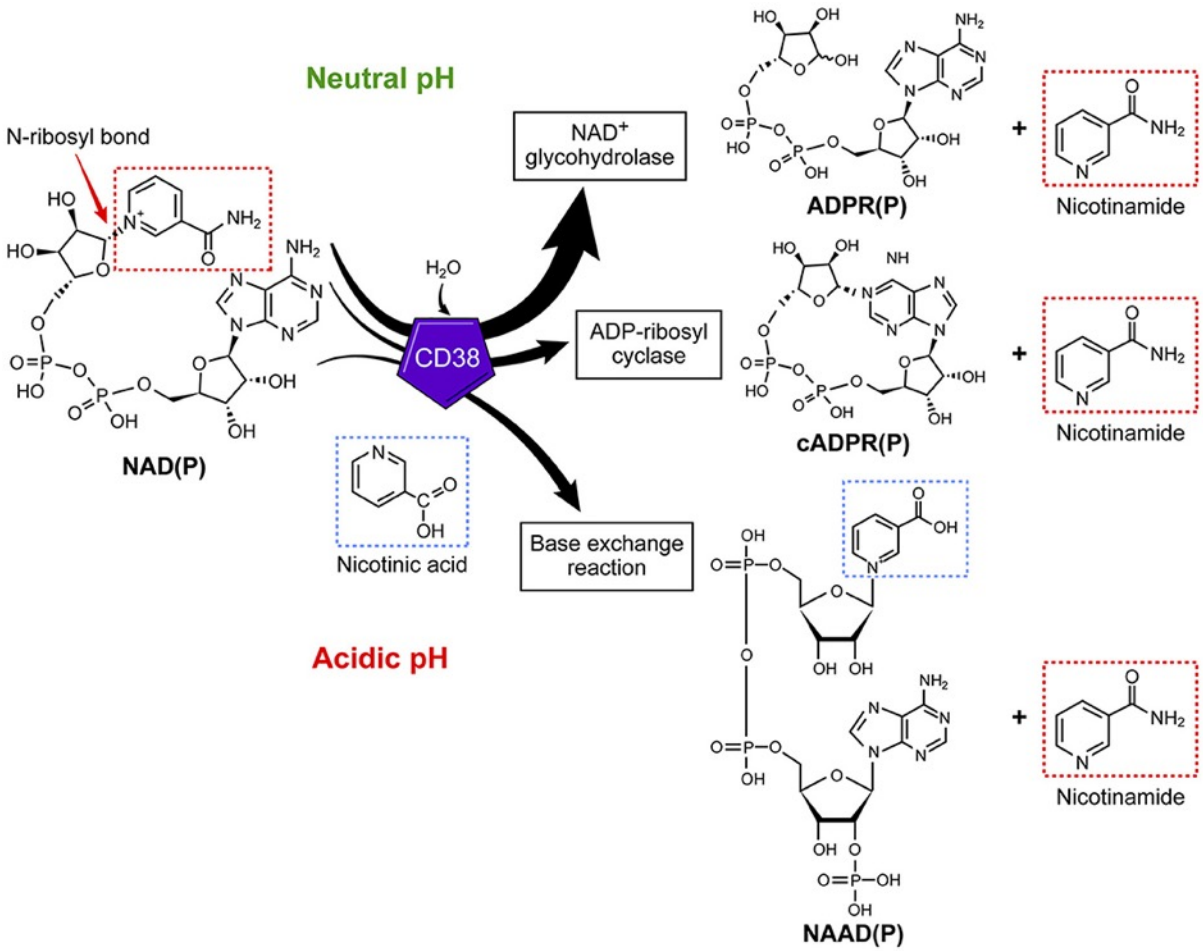

Figure 1.8. The multi-functions of CD38 enzyme utilising NAD+ as a substrate. CD38 acts mainly as an NAD+ glycohydrolase, degrading nicotinamide nucleotides. CD38 also has ineffective ADP-ribosyl cyclase activity and facilitates a base-exchange of vitamin B3 bases in the presence of surplus nicotinamide. This figure is taken from Hogan *et al.*[202]

CD38 has recently been reported as a potential new marker for macrophages. Jablonski and their colleagues discovered that the expression of CD38 is dramatically increased in pro-inflammatory macrophages, whereas its expression is reduced in anti-inflammatory macrophages in mouse models[220]. Furthermore, Amici *et al*. reported that CD38 can be used as a marker of inflammatory monocytes and macrophages in humans[203]. They also showed that inhibition of CD38 (both pharmacologically and genetically) significantly decreased the production of inflammatory cytokines including IL-6 and IL-12p40 in human macrophages[203].

Several studies have highlighted the effects of CD38 on the proliferation, polarisation and functions of macrophages. LPS is one of the inducers of pro-inflammatory

macrophages and LPS has the ability to increase the expression of CD38 in a time and dose-dependent manner[221]. This LPS-induced CD38 gene expression is due to the activation of JAK-STAT pathway[221]. Inhibiting or knocking out CD38 suppresses LPS-induced pro-inflammatory polarisation and decreases NF-κB signal activation. CD38 has been shown to reduce the probability of macrophage infection by regulating the nuclear receptor liver X receptor-alpha (LXR) pathway[222]. CD38 can also limit the growth of intracellular bacteria such as *Haemophilus aegypti* and *Haemophilus influenzae*. These bacteria cannot generate NAD therefore they are dependent on the uptake of NAD+ and NAD+ precursors to maintain their metabolism and growth. The ability of CD38 in degrading extracellular NAD+ in the environment triggers the metabolic shutdown of these pathogens hence limiting the development of infection[202,223].

4. Mitochondrial metabolism and IFN-Is

Several lines of evidence indicate that cytokine signalling can also regulate mitochondria metabolism, oxidative stress, and mitochondria dynamics[224]. While the antiviral response of IFNs have been associated with the activation of lipid metabolism including the synthesis of fatty acid and cholesterol[225], emerging studies have observed that IFN-Is can also modulate mitochondrial functions in various cell types but the results are not always consistent[225].

IFN-Is have been discovered to enhance mitochondrial metabolism including glycolytic activity and OXPHOS. With regard to glycolysis, a study in mouse embryonic fibroblasts revealed that IFN-β could upregulate the expression of glucose transporter type 4 (GLUT4) leading to an increase in glucose uptake and ATP generation[226]. This augmented glycolysis is mediated via PI3K/AKT signalling which can also contribute to the reduced activation of the AMP-activated protein kinase (AMPK). AMPK is an essential kinase known to facilitate FAO and memory T cell development[227]. Furthermore, *in vitro* experiment of mouse fibroblast demonstrated that when this IFNβ-induced glycolysis was inhibited by 2-DG, the replication of coxsackievirus B3 was enhanced[226], suggesting that increased glycolysis probably facilitate the acquisition of an antiviral state. Similarly, the stimulation of TLR3 with poly(I:C) promoted glycolytic activity in *ex vivo* splenic $CD11c^{+}MHCII^{+}$ DCs[228]. This increase

was found to depend on IFNAR1, confirming the effects of IFN-Is in this context. Furthermore, in macrophages to increase the glycolysis-induced lactate production IFN-I signalling molecules including TYK2 and IFNAR1 are required[229]. In addition, IFN-Is can promote mitochondrial function by increasing OXPHOS activity. For example, in pDCs, autocrine IFN-I signalling following TLR9 activation could increase FAO and OXPHOS, which subsequently increased the oxygen consumption rate (OCR)[230]. The same study also showed that IFN-Is could promote OXPHOS in murine memory $CD8^+$ T cells, but not effector $CD8^+$ T cells[230].

In contrast, several studies have reported that IFN-Is may impair mitochondrial functions. IFN-Is have been found to increase mROS accumulation and induce mitochondrial apoptotic pathways in hematopoietic cells[231]. Similarly, monocytes treated with IFN-α have been found to increase mROS levels and reduce ATP levels, suggesting that IFN-α may promote oxidative stress through altering OXPHOS[232]. In human B cell lines IFN-Is treatment reduced the expression of mitochondrial genes, ETC activity and promoted antiproliferation[233-235]. Similar results were also observed in H9 cells whereby IFN-α treatment suppressed the expression of mitochondrial-derived genes by promoting 2-5A synthetase/ ribonuclease L (RNase L) antiviral pathway in which the RNaseL can degrade mitochondria-derived RNA[236]. Taken together, the aforementioned studies indicate that IFN-I signalling is implicated in metabolic modulation, but the downstream effects are diverse and depend on the cell types.

5. Metabolic changes in SLE

So far, the evidence of cellular metabolic abnormalities in SLE patients has primarily been observed in PBMCs and $CD4^+$ T cells. These metabolic changes possibly contribute to abnormal T cell activation and impaired cell-death signal processes, resulting in immune dysregulation and autoantibody production in SLE[237]. In serum and PBMCs from SLE patients, the levels of glutathione (GSH), a non-enzymatic antioxidant, were reduced when compared to healthy individuals. Accordingly, their PBMCs displayed diminished ATP generation, mitochondrial hyperpolarisation, and excessive ROS production[238]. Studies in $CD4^+$ T cells from lupus patients showed that these cells produce elevated levels of nitric oxide and have defects in mitophagy[239].

These changes can contribute to an increase in mitochondrial biogenesis, mitochondrial mass, MMP and mitochondrial OCR, indicating mitochondrial dysfunction[239]. Interestingly, regardless of their ETC hyperactivity, SLE $CD4^+$ T cells still produced a minimal level of ATP leading to an excessive release of mROS, an indicator of oxidative stress[238]. In addition, oxidative stress can be an important contributor to SLE pathogenesis through the oxidative modification of the self-antigens[238]. Consistent with this, higher levels of 8-hydroxy-2′-deoxyguanosine (8-OHdG), the oxidative DNA damage marker, were found in SLE patient samples and they correlated positively with SLE disease activity[240].

An immunological consequence of oxidative stress is the activation of mTOR signalling, leading to the differentiation of specific types of T cells including Th1 and Th17 cell lineages[164,165]. Enhanced mTORC1 complex activity was observed in double-negative T cells from lupus patients[164], as well as in $CD4^+$ T cells from SLE patients[241] and lupus mouse models[165,242]. This hyperactive mTOR signalling can promote glycolysis and hampers autophagy, alterations that support mitochondrial dysfunction. Indeed, inhibition of mTORC1 activity by the treatment of metformin, which promotes AMPK activation, alleviates SLE disease progression in a mouse model[243].

Since T cells from lupus-prone mice and SLE patients have a chronically active status, their mitochondria tend to be hyperpolarised towards increased glycolysis and OXPHOS activity[238,244]. The increased glycolytic activity was also reported in $CD4^+$ T cells from SLE patients and this was considered a compensatory mechanism for the ATP depletion[245]. As a result of these observations, a combination of metformin and 2-DG, two metabolic regulators that inhibit mitochondrial and glucose metabolism, respectively, were tried and shown to reduce IFN-γ production from $CD4^+$ T cells *in vitro*, to reverse disease biomarker expression and improve disease severity in B6.Sle1.Sle2.Sle3 mice and NZB/W F1 mice[165,246].

The connection of abnormal mitochondrial metabolism in SLE and monocytes has been reported. Gkirtzimanaki and their colleagues suggested that SLE monocytes exhibited dysregulated mitochondrial metabolism and impaired autophagy leading to mitochondrial DNA (mtDNA) accumulation[232]. Furthermore, this event was linked to IFN-I stimulation[232]. A more recent study in macrophages has shown that the

macrophage glycolytic switch upon IgG stimulation enhanced kidney inflammation in lupus nephritis[247]. However, there has been little consideration of how macrophage metabolic reprogramming plays a role in SLE pathogenesis and how chronic IFN-I affects macrophage metabolism.

Overall, based on the literature, the direct link between the metabolic changes in SLE and IFN signature has not been thoroughly investigated and thus it remains unclear whether and how IFN-Is are responsible for metabolic reprogramming observed in SLE.

6. Preliminary data

My host laboratory has recently reported that, in the context of C1q deficiency, an exaggerated $CD8^+$ T cell response, due to an aberrant mitochondrial metabolism, contributes to disease severity in a murine lupus model[201]. Furthermore, using RNA sequencing analysis of peripheral blood $CD8^+$ T cells, they found that the expression of mitochondrial-derived genes involved in OXPHOS was significantly downregulated in $CD8^+$ T cells from lupus patients with high ISG expression compared to the patients with no IFN signature (**Fig.1.9**)[248], suggesting a possible link between mitochondrial changes and IFN-I exposure. They also observed that $CD8^+$ T but not $CD4^+$ T cells, from the IFN-high SLE patients showed an increase in mitochondrial mass and activity assessed by flow cytometry using MitoTracker Green (MTG) and MitoTracker Deep Red (MTDR) staining, respectively. Nonetheless, these $CD8^+$ T cells exhibited lower spare respiratory capacity (SRC), the reserve cell capacity to generate energy via OXPHOS in response to increased metabolic demand, compared to the cells of IFN-negative SLE patients and healthy controls (HC) (**Fig.1.10**)[248], suggesting a reduced bioenergetic capacity to maintain survival under stress. These findings highlighted a potential association between IFN-Is and the mitochondrial metabolism of $CD8^+$ T cells in lupus. However, the immunological consequences of these metabolic changes have not been explored.

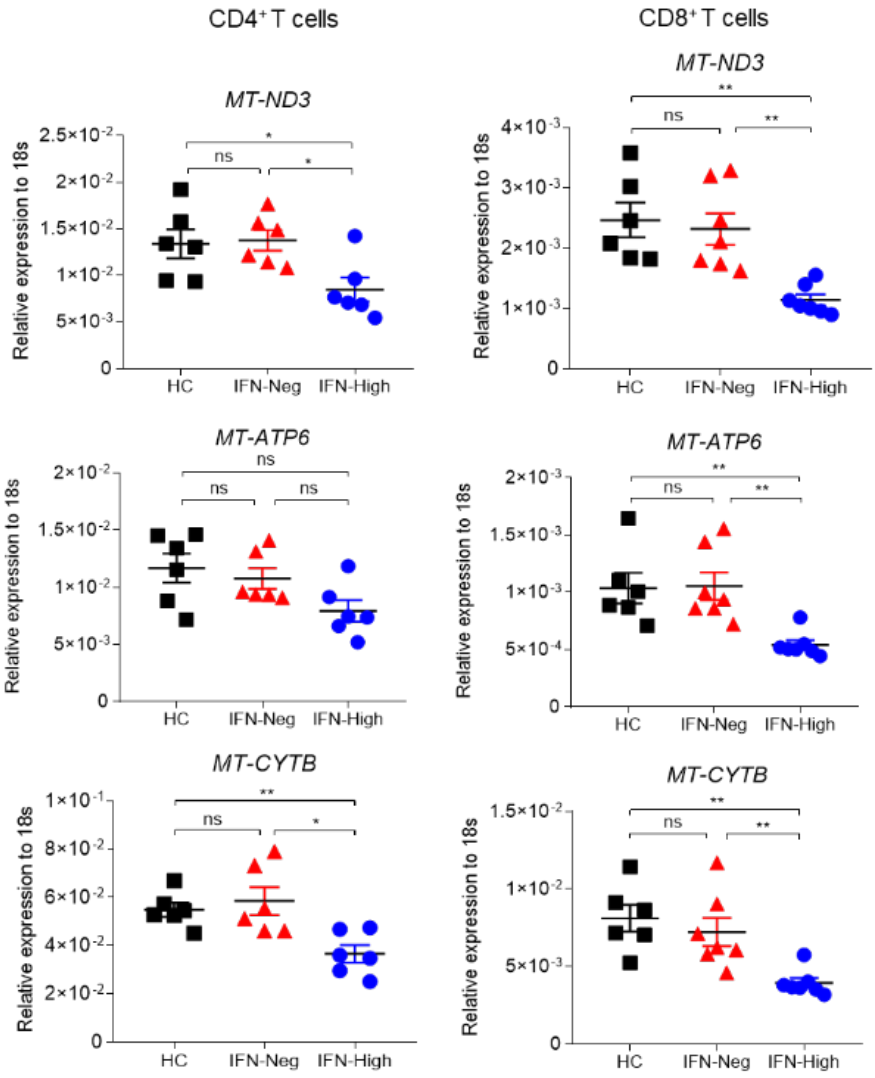

Figure 1.9. Mitochondria-derived gene expression analysis between IFN negative and IFN high SLE groups. qPCR analysis of mitochondrial-encoded OXPHOS genes in $CD4^+$ and $CD8^+$ T cells. Data presented as mean ± standard error of the mean. Each symbol represents one individual. (HC n=6 IFN-Low n=6 IFN-High n= 6). HC: healthy controls ns: not significant * $p < 0.05$, ** $p < 0.01$, *** $p < 0.001$. One-way ANOVA. This figure is published by Buang *et al.*[248]

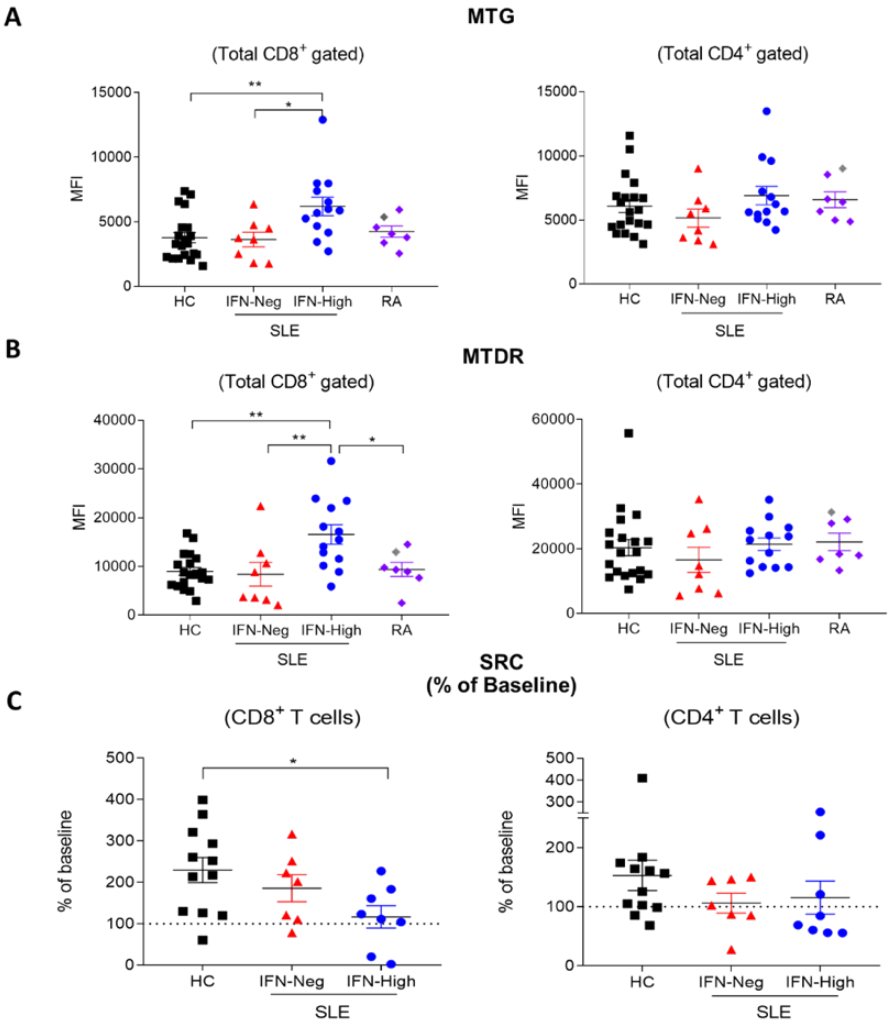

Figure 1.10. Mitochondrial phenotype of CD4⁺ and CD8⁺ T cells from IFN negative and IFN high SLE groups. (**A**). Mitochondrial mass was assessed by the mean fluorescence intensity (MFI) of MitoTracker Green (MTG). (**B**). Mitochondrial activity was accessed by MitoTracker Deep Red (MTDR) MFI. (**C**). SRC was measured using extracellular flux assay. Data presented as mean ± S.E.M. Each symbol represents one individual. (HC n=11-20 IFN-Neg n=7-8 IFN-High n= 8-14 RA n=4-7) HC: healthy controls RA: rheumatoid arthritis ns: not significant * $p < 0.05$, ** $p < 0.01$. One-way ANOVA. This figure is published by Buang *et al.*[248]

7. Hypothesis and aims

Literature has shown that hallmarks of SLE include enhanced IFN-I signalling, abnormal T cell activation and inability to remove apoptotic cells by macrophages[249]. Abnormal metabolism has been described in SLE, mostly in PBMCs and CD4+ T cells; less is known about other immune cell types including macrophages. Furthermore, the link between the IFN signature and aberrant metabolism in the context of SLE has not been demonstrated. Therefore, investigating how chronic IFN-I affects mitochondrial metabolism and functions of T cells and macrophages would further our understanding of SLE pathogenesis.

Based on the preliminary data and the current literature, I hypothesised that chronic exposure to IFN-I can cause metabolic changes in $CD8^+$ T cells and macrophages and these may result in abnormal cell death and abnormal immune responses.

Specifically, my study aims to:

1. Create SLE-like $CD8^+$ T cells *in vitro* by stimulating $CD8^+$ T cells from healthy donors with IFN-Is and assess whether the metabolic defects observed in the $CD8^+$ T cells from lupus patients are due to chronic exposure to IFN-Is.

2. Explore the effects of chronic IFN-I exposure on $CD8^+$ T cell phenotypes and functions

3. Investigate the effects of chronic IFN-I exposure on macrophages

Chapter 2: Materials and methods

2.1. Cell isolation and purification

2.1.1. Isolation of peripheral blood mononuclear cells (PBMCs)

Healthy leukocyte cones were purchased from NHS Blood and Transplant. Blood was diluted with phosphate-buffered saline (PBS) with the addition of 2% fetal bovine serum (FBS) (Pan Biotech). 25 ml of diluted blood was then layered on top of 15 ml of Lymphoprep solution in a 50 ml falcon tube. PBMCs were obtained by density gradient centrifugation at 800g for 20 minutes at room temperature without break. Following this, PBMCs were collected from the interface and washed twice with PBS 2%FBS. PBMCs were used immediately or processed further to obtain $CD8^+$ T cells, macrophages, or cryopreserved in 10% Dimethyl sulfoxide (Sigma-Aldrich) with 90% FBS.

2.1.2. Isolation of $CD8^+$ T cells

$CD8^+$ T cells were purified from PBMCs by negative selection using a human $CD8^+$ T Cell Isolation Kit (Myltenyi Biotec) according to the manufacturer's protocol. Following this, cells were centrifuged down and resuspended in T cell complete medium (TCM) composed of RPMI 1640, 10% FBS, 2% 1M HEPES buffer solution, 1% L-glutamine with penicillin-streptomycin, 1% MEM non-essential amino acids solution, 0.1% 50 mM β-mercaptoethanol (all purchased from Gibco) and 2% of 100 mM Sodium pyruvate solution (Sigma-Aldrich). The total number of cells was counted by trypan blue staining with hematocytometer. The average purity as assessed by flow cytometry was more than 85%.

2.1.3. Differentiation of human monocyte-derived macrophages (HMDMs)

PBMCs were suspended in RPMI 1640 medium, and monocytes were separated through an adherence process for 1 hour at 37°C in a humidified atmosphere containing 5% CO_2. The adhered PBMC monolayer was washed twice with Hank's balanced salt solution (HBSS) (Gibco). The monocytes were differentiated into monocyte-derived macrophages (MDMs) over 4 days. This was achieved by incubating the monocytes in a macrophage medium (consisting of RPMI 1640 medium containing 100 ng/ml macrophage colony-stimulating factor (M-CSF) (PeproTech))

supplemented with 20% FBS. The average purity as assessed by flow cytometry was more than 90%.

To collect the cells for further analysis, cell dissociation buffer (enzyme-free) (Gibco) was added to the cell culture and incubate for 15 minutes at 37°C in a humidified atmosphere containing 5% CO_2. After the cells were visibly detached, the macrophage medium was added. Cells were then spined down at 1500 rpm for 5 minutes before being resuspended in a complete medium for further analysis.

2.2. Cell culture

2.2.1. PBMCs and $CD8^+$ T cells

2.2.1.1. Chronic IFN-I treatment

PBMCs (5.0 x 10^5 cells per well) or isolated $CD8^+$ T cells (2.0 x 10^5 cells per well) from healthy buffy coats were plated into U-bottom 96-well plates. Cells were cultured in TCM containing 10U/ml of recombinant human IL-2 (PeproTech). Cells were then subjected to treatment with 1000U/ml (or other doses as indicated) of Human IFN-alpha A/D [BglII] (R&D System) or left untreated. As shown, cells were either not treated or treated with Dynabeads Human T-Activator CD3/CD28 (Gibco) with the bead-to-cell ratio 1:4. After that, cells were incubated for 2 or 7 days at 37°C in a humidified atmosphere containing 5% CO_2. On the third day, half of the media was disposed of and replaced with newly prepared TCM with 10U/ml IL-2 and the appropriate concentration of IFN-I.

2.2.1.2. CD3/CD28 restimulation

At day 7, CD3/CD28 beads were removed from the PBMC culture and cells were allowed to rest overnight in preparation for the re-stimulation. In the following step, $CD8^+$ T cells were sorted using BD FACS Aria II Cell Sorter (BD Biosciences). The purified $CD8^+$ T cells were then replated at a density of 2.0 x 10^5 cells per well. Cells were activated once more with the Dynabeads Human T-Activator CD3/CD28 (beads to cell ratio as indicated) for 4 or 24 hours.

For further analysis, the beads were removed by placing a tube containing cell suspension on a magnet for 2 minutes to separate the beads from the cells. These cells were then further analysed for flow cytometry analysis, gene expression analysis and metabolic analysis.

2.2.2. HMDMs

2.2.2.1. Chronic IFN-I treatment

HMDMs were plated at the density of 5.0 x 10^5 cells per well in 12-well plates with macrophage medium supplemented with 10%FBS. Cells were subsequently treated with 1000U/ml of Human IFN-alpha A/D [BglII] or left untreated for 3 days. HMDMs and supernatant were collected and used for flow cytometry analysis, gene expression analysis, metabolic analysis, and functional analysis.

2.2.2.2. TLR-restimulation

After 3 days of culture, cells were washed once with HBSS. Cells were cultured in a macrophage medium supplemented with 10%FBS. Following that, the final concentration of 1 ng/ml of LPS (*Escherichia coli* serotype O111:B4) (Sigma-Aldrich) or 100ng/ml of R848 (InvivoGen) or 7.5μg/ml of CpG (ODN2395) (InvivoGen) or 10μg/ml of Poly I:C (InvivoGen) was added into the cell culture for 3 or 8 hours. These cells were then further analysed for their cell viability using flow cytometry.

2.2.2.3. CD38 inhibition experiment

HMDMs were plated at the density of 5.0 x 10^5 cells per well in 12-well plates with macrophage medium supplemented with 10%FBS. To identify an optimal dose for 78c treatment, cells were first treated with 1000U/ml of Human IFN-alpha A/D [BglII] with different concentrations of 78c (10, 20 and 50μM) or left untreated for 3 days. Cell viability and polarization markers were later assessed via flow cytometry.

After identifying the optimal dose, cells were subsequently treated with 1000U/ml of Human IFN-alpha A/D [BglII] or a combination of 1000U/ml of Human IFN-alpha A/D [BglII] and 20μM of 78c or left untreated for 3 days. HMDMs and supernatant were collected and used for flow cytometry analysis, gene expression analysis, metabolic analysis and functional analysis.

2.2.2.4. Tryptophan-deficiency experiment

HMDMs were plated at the density of 5.0 x 10^5 cells per well in 12-well plates. Cells were cultured with macrophage medium or tryptophan-free RPMI1640 medium supplemented with 100ng/ml M-CSF. FBS was excluded from all medium in this experiment since 10% of FBS contains around 1μM of tryptophan. Cells were

subsequently treated with 1000U/ml of Human IFN-alpha A/D [BglII] or left untreated for 3 days. HMDMs and supernatant were then collected for further analysis.

2.4. Flow cytometry analysis

All samples were acquired on an LSRFortessa flow cytometer (BD Biosciences), and data were analysed with FlowJo software, version 10 (Tree Star Inc, USA).

2.3.1. Surface staining

Cells were washed with PBS and incubated with Live/dead aqua fluorescent reactive dye (Invitrogen) diluted 1/100 in PBS for 10 minutes at room temperature. Following a PBS wash, cells were incubated at 4°C for 30 minutes with TruStain Fc Receptor Blocking Solution (Biolegend) and antibody combinations (listed in **Table 2.1**) diluted in FACs buffer composed of PBS, 2mM EDTA (Gibco), 0.1% bovine serum albumin (BSA) (Gibco), and 0.09% sodium azide (Sigma-Aldrich). After being washed with FACs buffer, cells were resuspended in either 1x CellFIX (BD Biosciences) or PBS.

Table 2.1. Lists of surface monoclonal antibodies

Antibody specificity	Fluorochrome	Clone	Distributor	Dilution in PBS (µl)
CD107a	FITC	eBioH4A3	eBioscience	1
CD14	BV711	M5E2	Biolegend	0.5
CD16	PE-Cy7	3G8	Biolegend	0.5
	APC	3G8	Biolegend	0.5
CD163	APC	GHI/61	Biolegend	1
CD206	APC	19.2	Biolegend	1
CD25	APC	BC96	eBioscience	0.5
CD3	BV421	SK7	eBioscience	0.5
	APC-Cy7	SK7	Biolegend	0.5
	PE-Cy7	UCHT1	Biolegend	2
CD38	FITC	HIT2	eBioscience	1
	PE-Cy7	HIT2	eBioscience	0.5
CD4	APC	SK3	eBioscience	1
	FITC	SK3	eBioscience	2
	BV421	A161A1	Biolegend	1
CD69	PE	FN50	Biolegend	0.5
CD8	PE	SK1	Biolegend	1.5
	APC	SK1	Biolegend	1
	BV711	RPA-18	Biolegend	1
CD80	PE	2D10	Biolegend	1
CD86	FITC	BU63	Biolegend	1
HLA-DR	BV421	L243	Biolegend	0.5

2.3.2. Intracellular staining

Cells were stained for surface markers as previously described. After 30 minutes of incubation at 4°C, cells were washed with FACs buffer.

For the staining of cytoplasmic proteins such as cytokines, cells were then resuspended in fixation/permeabilization solution (BD Biosciences) and incubated at 4°C for 20 minutes. Cells were washed with 1X of BD Perm/Wash™ buffer (BD Biosciences). Anti-cytokine antibodies or anti-mouse IgG1 isotypes (listed in **Table 2.2**) were incubated with cells at 4°C for 30 minutes. After washing with BD Perm/Wash™ buffer, cells were resuspended in FACs buffer.

For the staining of nuclear protein Ki-67, Foxp3/Transcription Factor Staining Buffer Set (eBioscience) was used according to the manufacture's protocol. In brief, cells were Foxp3 fixation/permeabilization buffer at RT in the dark for 30 minutes. Next, cells were washed twice with permeabilization buffer. Ki-67 antibody was incubated with cells at RT in the dark for 30 minutes. After washing with permeabilization buffer, cells were resuspended in FACs buffer.

Table 2.2. Listed of antibodies used for intracellular staining.

Antigen specificity	Fluorochrome	Clone	Company	Dilution in the buffer
IFN-γ	PE-Cy7	B27	Biolegend	1/10
Granzyme B	PE	QA161762	Biolegend	1/40
TNF-α	A488	MP6-XT22	Biolegend	1/10
Ki-67	PE-Cy7	SolA15	Biolegend	1/20

2.3.3. Mitochondrial staining

Mitochondrial-specific fluorescent probes (listed in **Table 2.3**) were added to each well to detect the changes in mitochondrial phenotypes. The cells were then incubated for 30 minutes at 37°C in a humidified atmosphere containing 5% CO_2 before harvesting for flow cytometry analysis.

Table 2.3. Lists of mitochondrial probes

Mitochondrial probes	Distributor	Working concentration
MitoTracker Green (MTG)	Life Technologies	50 nM
MitoTracker Deep Red (MTDR)	Life Technologies	10 nM
Tetramethylrhodamine methyl ester perchlorate (TMRM)	Life Technologies	25 nM
MitoSOX red	Life Technologies	3 μM
CellROX Deep Red	Life Technologies	2.5 μM

2.4. Gene expression analysis

2.4.1. RNA extraction

Total RNA was extracted using RNeasy Mini kits (Qiagen) according to the manufacturer's instructions. In a nutshell, cells were lysed with RTL buffer with the addition of 1% of β-mercaptoethanol. The same volume of 70% ethanol was then added to provide ideal binding conditions. Following this, the cell lysate was transferred to the RNeasy MinElute spin column which has a silica membrane that specifically binds to RNA. RNase-free DNase I enzyme from the RNase-free DNase Kit (Qiagen) was then added directly onto the column to digest genomic DNA in samples. The spin column was washed twice to remove contaminants and dried by centrifugation. Finally, total RNA was eluted into an RNase-free tube with RNase-free water. The quality and concentration of total RNA were analysed using NanoDrop 1000 spectrophotometer (Thermo Fisher Scientific). All RNA samples had an A260/A280 ratio of 1.9-2 and were stored at -80°C freezer.

2.4.2. Complementary DNA (cDNA) synthesis

RNA from each sample was reverse transcribed to cDNA using iScript cDNA synthesis kit (Bio-Rad), consisting of iScript Reverse Transcriptase, 5X iScript reaction mix, and Nuclease-free water. Nuclease-free water was added to reach a total volume of 20 μl for each sample. The reaction was set up as shown in **Table 2.4**. The PCR reaction

was conducted at 25°C for 5 minutes, then 42°C for 30 minutes and 85°C for 5 minutes, followed by being held at 4°C. cDNA was then diluted with Nuclease-free water to acquire a final concentration of 2.5 ng/µl.

Table 2.4. cDNA synthesis set-up

Reagents	Volume per reaction (µl)
5x iScript reaction mix	4
iScript reverse transcriptase	1
Nuclease-free water	15-x
RNA template	x
Total volume	20

2.4.3. Real-time quantitative PCR (qPCR)

Real-time qPCR reactions were performed using Power SYBR^{TM} Green Master Mix (Applied Biosystems). The master mixes were prepared as shown in **Table 2.5.** The specific forward and reverse primers for each gene are presented in **Table 2.6.**

2 µl of cDNA from each condition and 8 µl of master mixes were added onto an optimal 384 well plate (Life Technologies). The ViiA 7 system (Life Technologies) was used to quantify gene expression, and relative gene expression was estimated by normalising to the housekeeping genes HPRT or 18s and using the $2^{-\Delta\Delta Ct}$ method

Table 2.5. qPCR reaction mix

Reagents	Company	Volume (µl)
SYBR® Green PCR Master Mix	Life Technologies	5
Forward Primer (4µM)	Sigma-Aldrich	1
Reverse Primer (4µM)	Sigma-Aldrich	1
RNase-free water	Qiagen	1

Table 2.6. Lists of primers

Genes	Primer Sequence	
HPRT	Forward	5'-TGAGGATTTGGAAAGGGTGT
	Reverse	5'-AATCCAGCAGGTCAGCAAAG
18s	Forward	5'-CCGCAGCTAGGAATAATGGA
	Reverse	5'-ACCTCCGACTTTCGTTCTTG
CMPK2	Forward	5'-TGACCTTATCCTGCTGCTCA
	Reverse	5'-CGTCTGCAGGACCTTTTCTC
HERC5	Forward	5'-TCATTCTCCACCCCAAGAAG
	Reverse	5'-CATCTGGACCAGTTTGCTGA
ESPTI	Forward	5'-CCAGACAGAAGTGCCTGTCA
	Reverse	5'-TCTGGTGGATTTTGGCTCTT
Mt-CYTB	Forward	5'-TATCCGCCATCCCATACATT
	Reverse	5'-TTTTATCGGAATGGAGGTG
Mt-ATP6	Forward	5'-GCCCTAGCCCACTTCTTACC
	Reverse	5'-GTGGCGCTTCCAATTAGGTG
Mt-ND1	Forward	5'-CTACTACAACCCTTCGCTGAC
	Reverse	5'-GGATTGAGTAAACGGCTAGGC
Mt-ND3	Forward	5'-TGCGGCTTCGACCCTATATC
	Reverse	5'-GCCAGACTTAGGGCTAGGAT
CD38	Forward	5'-TCAGCCACTAATGAAGTTGGGA
	Reverse	5'-CTGGACCTGTGTGAACTGATGG
SIRT1	Forward	5'-GCGATTGGGTACCGAGATAA
	Reverse	5'-GTTCGAGGATCTGTGCCAAT
PARP1	Forward	5'-GAAGCTGGAGGAGTGACAGG
	Reverse	5'-TCAATCATGCCTAGCTGTGG

NAMPT	Forward	5’-TGGTGGAGGTTTGCTACAGA
	Reverse	5’-TCCTTTTCCTTCCTCCAGTG
IDO1	Forward	5’-TTGCTCTGCCAAATCCACAG
	Reverse	5’-TGGTGATGCATCCCAGAACT
KYNU	Forward	5’-GGGGTCTGTGGATTCCGAAT
	Reverse	5’-CTGGTTTCTTGGTTGCTGCT
QPRT	Forward	5’-GGCTGGTGATGGTGAAGGAT
	Reverse	5’-GCTCCTCTGGCTTGAAGTTG
HKII	Forward	5’-CCCTGCCACCAGACTAAACT
	Reverse	5’-TGGACTTGAATCCCTTGGTC
GAPDH	Forward	5’-AGGGCTGCTTTTAACTCTGGT
	Reverse	5’-CCCCACTTGATTTTGGAGGGA
LDH	Forward	5’-GCAGATTTGGCAGAGAGTATAATG
	Reverse	5’-GACATCATCCTTTATTCCGTAAAGAC
PDH	Forward	5’-CCTAACTGGCATGCATCACC
	Reverse	5’-GAGGCGCTCATGATCAACAG
PDK1	Forward	5’-CAAGACCTCGTGTTGAGACCT
	Reverse	5’-ACGTGATATGGGCAATCCAT
IL-1β	Forward	5’-ACAGATGAAGTGCTCCTTCCA
	Reverse	5’-GTCGGAGATTCGTAGCTGGAT
TNF-α	Forward	5’-AGCCTCTTCTCCTTCCTGATCGTG
	Reverse	5’-GGCTGATTAGAGAGAGGTCCCTGG

2.4.4. RNA-sequencing (RNA-seq)

RNA-seq library preparation and next generation sequencing were performed by Imperial BRC Genomics Facility. In brief, total RNA was extracted as previously described in **2.4.1**. mRNA was isolated from 500 ng of total RNA using oligo dT beads. After fragmentation, the samples were converted to double stranded DNA and ligated to Illumina adapters. The second strand cDNA was then degraded by the UNG enzyme providing directional information to the library. For each pool of libraries, Tapestation was used to assess fragment distribution and presence of artefacts. Sequencing was performed using a HiSeq4000 platform for 1 lane (75 bp paired end reads). Data processing, alignment and visualisation were kindly performed by Dr Norzawani Buang. Briefly, more than 25 million paired end reads were achieved for all samples. Quality filtering and adapter removal were performed using Trimmomatic (v.0.36). The reads quality was checked using FastQC (v.0.11.2) before and after trimming. Reads were aligned to the human genome using STAR (v.2.6.0) package. Mapping quality, read distribution, gene body coverage, GC content, and rRNA contamination, were checked using picard (v.2.6.0) software. Gene level read counts of processed reads were then computed using HTseq (v.2.0.0) package. Differential gene expression analysis between groups was performed using DESeq2 (v.1.14.1) package. To visualise the similarities between samples, PCA and hierarchical clustering were performed using pcaExplorer (v.2.6.0) and pheatmap (v.1.0.10) packages, respectively. Volcano plots of differentially expressed genes were generated using ggplot2 (v.3.0.0) package. Gene set enrichment analysis was done using clusterProfiler (v.4.6.0) and plotted using enrichplot (v.1.18.3) packages. Significantly enriched pathways were defined as pathways with adjusted p-value less than 0.05. All raw RNA-seq data processing steps were performed in Cx1 high-performance cluster computing environment, Imperial College London. Further analyses were conducted in R/Bioconductor environment (v.3.4.4).

2.5. Metabolic analysis

2.5.1. Extracellular flux assay (Seahorse assay)

The mitochondrial metabolism of $CD8^+$ T cells and macrophages was assessed using XF Cell Mito Stress Kit (Agilent Technologies) according to the manufacture's protocols.

Briefly, at day 7 of the PBMC culture, $CD8^+$ T cells were sorted using BD FACS Aria II Cell Sorter with more than 95% purity. These cells were resuspended in Seahorse medium which consisted of Seahorse XF RPMI medium (Agilent Technologies), 2mM L-Glutamine (Gibco), 1mM pyruvate (Gibco) and 25mM glucose (Sigma-Aldrich). Sorted $CD8^+$ T cells at the density of $3.0x10^5$ cells/well were subsequently seeded onto an XF96 plate (Agilent Technologies) that had been pre-coated with 22.4μg/ml of Cell-Tak Cell and Tissue Adhesive (Corning).

For macrophages, after 3 days of culture, macrophages at the density of $4x10^4$ cells/well were resuspended in RPMI 1640 medium supplemented with M-CSF and 10%FBS and were plated in a XF96 plate overnight. The medium then was replaced with the Seahorse medium.

Oxygen consumption rate (OCR) and extracellular acidification rate (ECAR) values were assessed under basal conditions and in response to 1μM oligomycin, 2μM fluorocarbonylcyanide phenylhydrazone (FCCP), 1μM antimycin A + 1μM rotenone using the Seahorse XFe96 Extracellular Flux Analyzer (**Fig.2.1**) The measurements were conducted three to four times in a 3-0-3-minutes mix-wait-measure cycle. All tests were performed in triplicate or quadruplicate. Metabolic parameters were calculated following the publication from Gubser *et al*.[250].

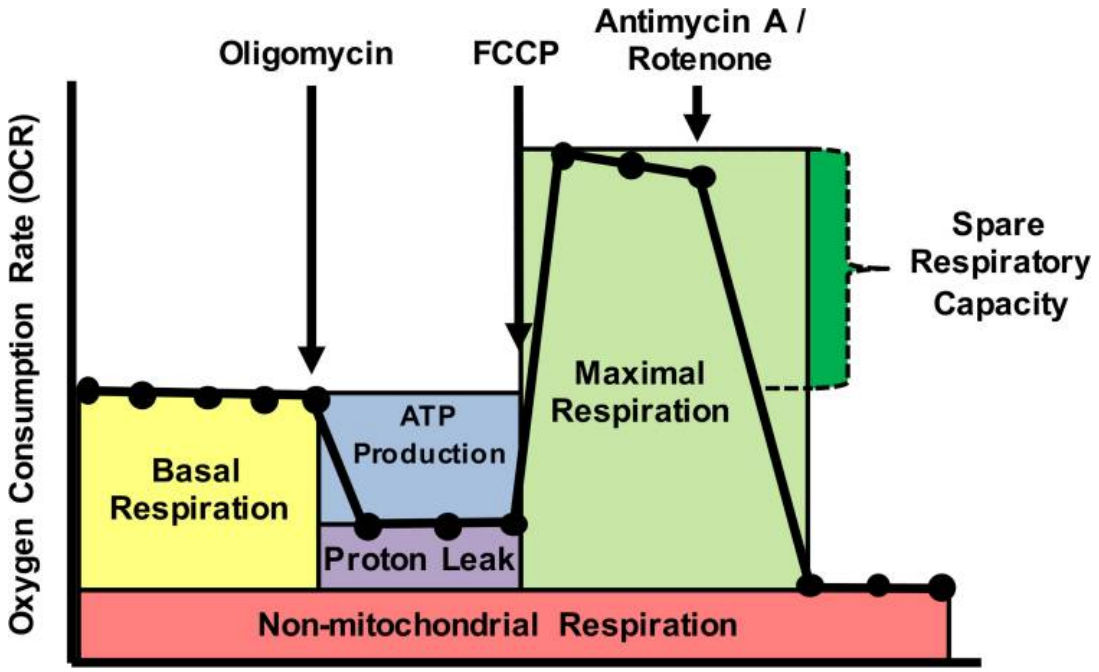

Figure 2.1. Schematic of oxygen consumption from extracellular flux analysis. This figure is taken from Nicholas *et al*.[251]

2.5.2. NAD and NADH assay

2.0 x 10^6 HMDMs were lysed and intracellular levels of NAD, NADH and the ratio of NAD and NADH were quantified using NAD/NADH Assay Kit (colorimetric - ab65348) (Abcam) according to the manufacturer's protocol. The Multiskan™ FC Microplate Photometer (Thermo Fisher Scientific) was used to measure the emitted light at the optical density (OD) 450nm. All OD450nm values were corrected to the blank controls.

2.5.3. Lactate assay

The levels of extracellular lactate were measured from the supernatant of the macrophage culture using the L-Lactate Assay Kit (colorimetric - ab65330) (Abcam) as directed by the manufacturer. All samples were diluted in PBS at a 1:100 ratio. The Multiskan™ FC Microplate Photometer (Thermo Fisher Scientific) was used to measure the amount of light emitted at OD 450nm. All OD450nm values were corrected to the blank controls.

2.5.4. Global metabolomic profiling (Intracellular metabolites)

2.5.4.1. Sample preparation

After 3 days of culture, $1x10^6$ HMDMs in a well of 6-well plate were washed twice with PBS. The plate was placed on dry ice and 200 μl of metabolite extraction solution composing of 50% LC-MS grade methanol (Thermo Fisher Scientific), 30% LC-MS grade acetonitrile (Thermo Fisher Scientific), 20% ultrapure water (Invitrogen) and 5 μM of valine-d8 (CK isotopes) was added into each well. Cells were incubated on dry ice for 20 minutes to break cell membranes. Following this, cells were scraped off the plate using cell scraper (Greiner) and transferred into pre-chilled Eppendorf tubes. The cell extraction suspension was then vortexed and incubated for 15 minutes at 4°C. After that, the suspension was centrifuged at 13000 rpm, 4°C for 20 minutes. 80% of the supernatant was then collected into autosampler vials (Merck life science). A pooled sample was also prepared by combining 10 μl of each sample into one autosampler vial to use as a control. Samples were then shipped on dry ice to the CECAD Research Centre, University of Cologne, Germany for LC-MS analysis.

2.5.4.2. Liquid chromatography–mass spectrometry (LC–MS)

Data acquisition, processing and analysis was kindly performed by Dr Ming Yang. Briefly, chromatographic separation of metabolites was conducted using a Millipore Sequant ZIC-pHILIC analytical column equipped with a guard column (both 5 mm particle size) with a binary solvent system. Metabolites were quantified by Vanquish Horizon UHPLC coupled to an Orbitrap Exploris 240 mass spectrometer (Thermo Fisher Scientific) through a heated electrospray ionization source. Metabolite identification was analysed in the Compound Discoverer software (v.3.2). The generated metabolite list was then employed for further processing in the Tracefinder software (v.5.0) in which extracted ion chromatographs for all compounds were examined and manually integrated if necessary. After that, the peak area for each detected metabolite was normalized against the total ion count (TIC) of that sample to rectify any discrepancies brought by sample processing and equipment analysis. The raw and normalized ion intensities of metabolites were then provided and used for further analysis.

2.6. Cell viability assay

PBMCs or HMDMs from healthy controls were first stained for surface marker staining for gating purposes. After being washed twice with PBS, the cells were then stained for Annexin V and propidium iodide (PI) using the FITC-Annexin V Apoptosis Detection Kit (BD Biosciences) following the manufacturer´s protocol. Briefly, $2.5x10^5$ to $5x10^5$ cells were resuspended in annexin V binding buffer and 5 µl of FITC-annexin was added to the cell suspension. Cells were then incubated for 15 minutes in the dark at the room temperature. Following this, 250 µl of binding buffer and 1 µl of PI were added and cells were analysed by flow cytometry using BD LSRFortessa.

For CD3/CD28 re-stimulation experiments, on day 6, CD3/CD28 beads were removed from the PBMC culture, and the cells were rested overnight. After that, cells were resuspended in PBS at a concentration of 10×10^6 cells/ml and incubated for 5 minutes at 37^{o}C with 1 µM CFSE (Carboxyfluorescein succinimide ester) (Invitrogen) to detect proliferating cells. Cells were subsequently washed 3 times in ice-cold TCM to quench the labelling reaction. Cells were then re-plated at 2.0×10^5 cells per well and re-stimulated for 3 days with Gibco Dynabeads Human T-Activator CD3/CD28 (at the beads to cell ratios of 1:4, 1:8, or 1:16, as indicated). Subsequently, cells were stained for annexin V and PI as previously described and analysed by flow cytometry.

2.7. Phagocytosis assay

The phagocytosis assay of fluorescent beads was assessed using the Phagocytosis Assay Kit (IgG FITC) (Cayman Chemical) following the manufacturer's instructions. Briefly, after 3 days of culture, $5x10^5$ HMDMs in 12-well plates were washed with HBSS. Cells were then incubated with fluorescent beads (1:250 dilution) for 30 minutes. Subsequently, cells were collected and stained for surface markers. Phagocytosis of fluorescent beads was then measured by flow cytometry.

2.8. Cytokine assays

The supernatant from PBMC, CD8+ T cell or macrophage cell culture was collected. IFN-γ, TNF-α, Granzyme B and IL-6 cytokines in the supernatant were measured using commercial ELISA kits (Invitrogen) according to the manufacturer’s protocols.

2.9. Statistical analysis

Data from RNA-sequencing and metabolomic profiling were kindly analysed by Dr Norzawani Buang and Dr Ming Yang using standard tests as previously demonstrated. The rest of the data were analysed using GraphPad Prism version 9.5.0 (GraphPad Software, Inc. USA). One-way ANOVA or Kruskal-Wallis test or Paired samples Wilcoxon test were used to calculate significant differences between multiple or two treatments. Only differences with p values less than 0.05 were considered statistically significant.

Chapter 3:
The effects of IFN-I on CD8$^+$ T cells

3.1. Introduction

Studies in human and mouse models have established that IFN-Is play a pivotal role in the pathogenesis of SLE, although the underlying processes are still poorly defined. In addition, mitochondrial abnormalities, such as mitochondrial enlargement and hyperpolarisation, have been identified in T cells from SLE patients. These mitochondrial perturbations can result in abnormal T-cell activation and defective cell death pathways, causing immunological dysregulation. However, the link between IFN-I exposure and mitochondrial defects remains elusive.

The laboratory of my supervisors generated preliminary data showing a possible connection between IFN-I signature and mitochondrial metabolism in CD8$^+$ T cells from lupus patients[248]. Using RNA-sequencing analysis of CD8$^+$ T cells from SLE patients, they found downregulation of mitochondria-derived gene expression in patients with IFN-I signature. Mitochondrial phenotypic and functional analyses also showed increased mitochondrial mass, activity and lower SRC in CD8$^+$ T cells from IFN-high SLE patients. Based on the literature and preliminary observations, I hypothesised that chronic IFN-I exposure could trigger mitochondrial changes in SLE CD8$^+$ T cells, which could lead to abnormal cell death and detrimental immunological responses. As a result, the purpose of this chapter is to examine the biological effects of IFN-induced mitochondrial changes in CD8$^+$ T cells.

However, studying CD8$^+$ T cell metabolism directly from SLE patients has some limitations. One of them was that *ex vivo* CD8$^+$ T cells from patients lose their IFN-I signature after being cultured for 2 days. This made it difficult to investigate the long-term effect of IFN-I exposure on the functions of CD8$^+$ T cells. Therefore, in this chapter, I aimed to first establish an *in vitro* setup that would allow me to further investigate how persistent IFN-I exposure affects CD8$^+$ T cell metabolism, phenotypes, and functions.

3.2. Results

Identification of the optimal IFN-I concentration recapitulating IFN signature seen in SLE patients

To experimentally establish the mitochondrial alterations observed in lupus patients, I cultured PBMCs from healthy donors with different concentrations of IFN-α to first identify the optimal condition. PBMCs were treated with 10, 100 or 1000 U/ml IFN-α for 7 days and supplemented with 10U/ml of IL-2 to maintain cell viability in all conditions throughout this project. To examine the appropriate dose of IFN-α, I assessed the gene expression levels of *ESPTI (Epithelial stromal interaction1)*, *HERC5 (HECT And RLD Domain Containing E3 Ubiquitin Protein Ligase 5)* and *CMPK (Cytidine/Uridine Monophosphate Kinase 1)* which are the ISGs commonly used to analyse the IFN score in lupus patients[252] and compared them with the levels identified in IFN-negative and IFN-high SLE patients. The results shown in **figure 3.1A** indicate that 1000U/ml of IFN-α enhanced all ISG expression to the level seen in IFN-high SLE patients. This result was verified with two more donors (**Fig.3.1B**). Consequently, 1000U/ml of IFN-α was selected to use as an optimal concentration in all the following experiments to mimic chronic IFN-I exposure observed in SLE patients.

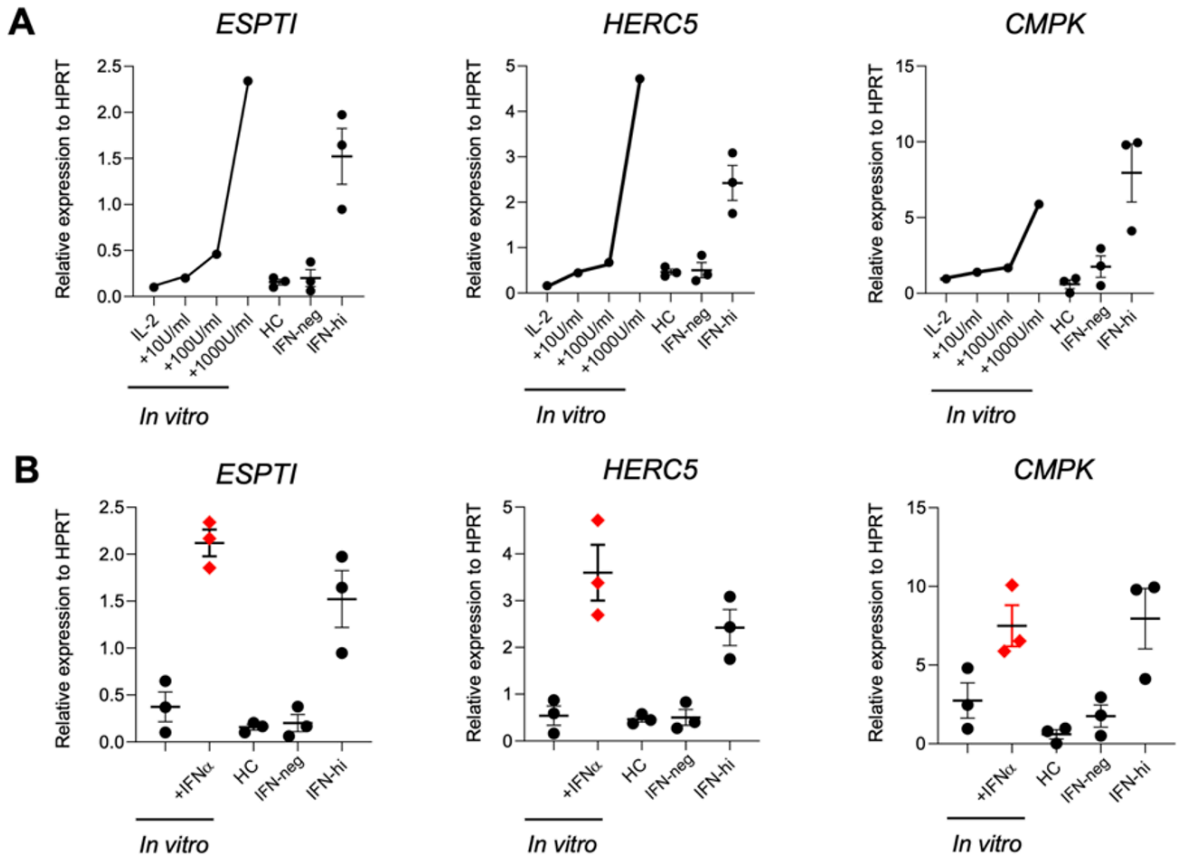

Figure 3.1. Dose effect of IFN-α on ISGs and comparison with SLE samples. PBMCs from a healthy donor were treated with varying concentrations of IFN-α for 7 days. qPCR was then performed. (**A**) Relative expression level of ISGs in IFN-α treated PBMCs compared to PBMCs from IFN-high, IFN-neg SLE patients and healthy controls (HC). (**B**) Relative expression levels of ISGs from 3 donors pooled from 2 separate experiments. Data presented as mean ± S.E.M.

Effects of chronic IFN-I treatment on mitochondria of CD8$^+$ T cells in PBMC culture

To study the impacts of chronic IFN-α exposure on CD8$^+$ T cell mitochondria, I cultured healthy PBMCs with and without 1000U/ml of IFN-α for 7 days and stained the cells with the following mitochondrial specific probes to assess the mitochondrial mass, activity, membrane potential (MMP) and ROS production by flow cytometry. These specific probes included; i) MitoTracker Green dye (MTG), which accumulates in the mitochondria independently of MMP, to detect the mitochondrial mass; ii) MitoTracker Deep Red dye (MTDR), which was particularly taken up by active mitochondria, to measure mitochondrial activity; iii) Tetramethylrhodamine, methyl ester (TMRM),

which electrophoretically accumulates in active mitochondria, to assess mitochondrial membrane potential (MMP); iv) CellROX green dye to determine cellular ROS (cROS) production; v) MitoSOX red dye, which is only oxidised by superoxide in mitochondria, to measure mitochondrial ROS (mROS) production.

The data were analysed from a gated $CD3^+CD8^+$ cell population. The Mean Fluorescence Intensity (MFI) of MTG, MTDR, TMRM and CellROX green together with the percentage of cells expressing MitoSox red dye is illustrated in **figure 3.2**. I found that the MFI of MTG staining was unaffected by IFN-α, indicating no difference in mitochondrial mass upon the treatment (**Fig.3.2A**). On the other hand, there was a significant increase in MFI of MTDR staining following prolonged IFN-α treatment, suggesting enhanced mitochondrial activity (**Fig.3.2B**). The MMP of these cells was then assessed as it can reflect mitochondrial function. Alterations in polarisation can be representative of defective cell stress. Nonetheless, no difference in the MFI of TMRM was observed in the IFN-α treated conditions (**Fig. 3.2C**).

It is known that dysfunctional ETC produces excessive mROS, suggestive of oxidative stress. I then assessed mROS, a by-product of ETC. The data revealed that the basal mROS expression was variable across subjects ranging from less than 1% to 40% of cells expressing high mROS (**Fig.3.2E**). Regarding the effect of IFN-α treatment, I found that there was a consistent reduction in the percentage of high mROS-expressing cells in the IFN-α-treated condition compared to the untreated group (**Fig.3.2E**). This IFN-I-mediated mROS reduction prompted me to determine cROS generation as cROS in T cells is predominantly produced from the mitochondria. The intensity of CellRox green staining was not significantly affected by the IFN-α treatment, showing that IFN-α did not change cROS production in $CD8^+$ T cells (**Fig.3.2D**).

Collectively, these results suggested that 7-day-IFN-I treatment was able to induce changes in $CD8^+$ T cell mitochondria by increasing mitochondrial activity and reducing mROS production.

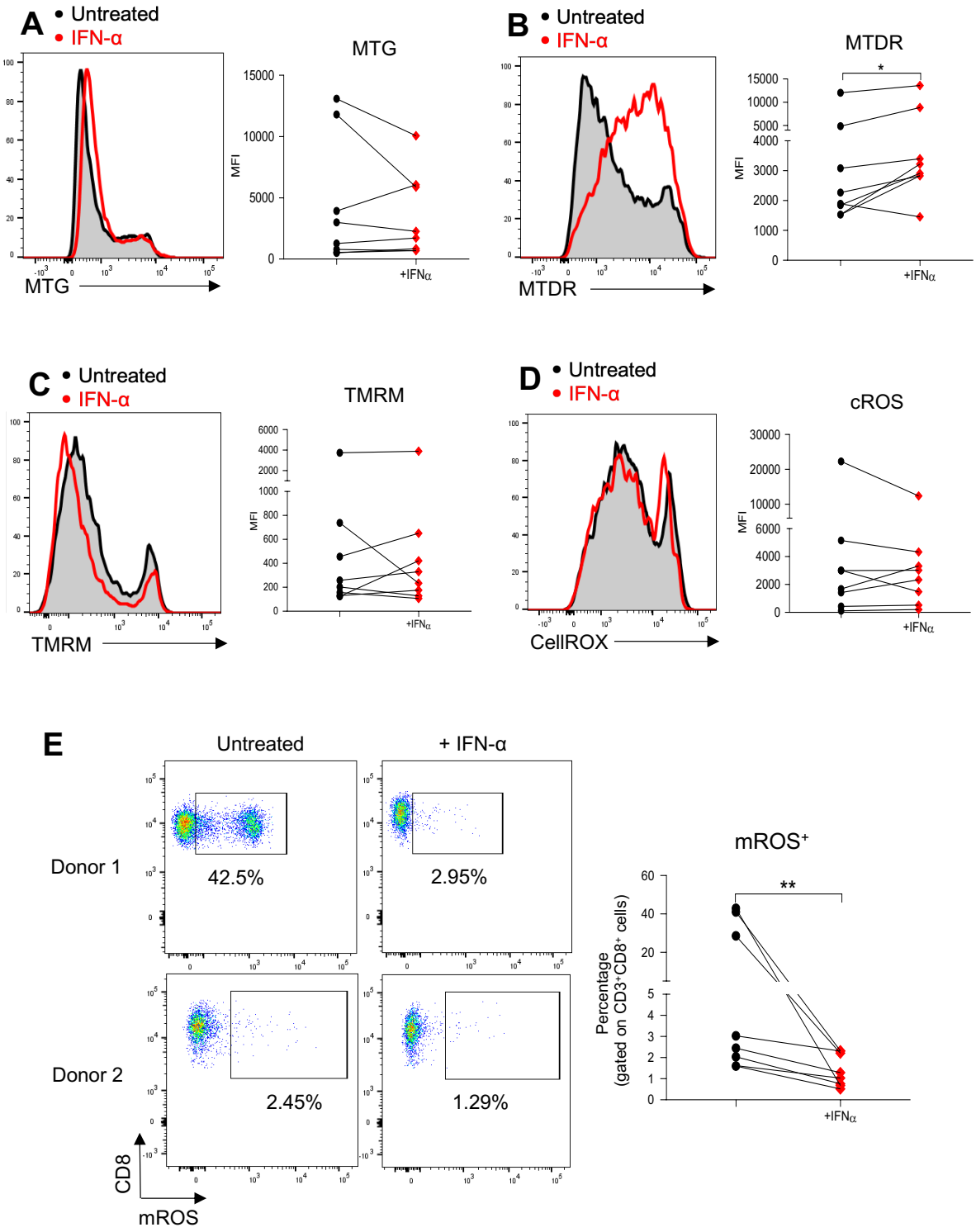

Figure 3.2. Phenotype of CD8⁺ T cell mitochondria after chronic IFN-α.
Human PBMCs treated with 1000U/ml of IFN-α or medium alone for 7 days were stained with (**A**) MTG, (**B**) MTDR, (**C**) TMRM, (**D**) CellROX Green, and (**E**) MitoSOX Red. (**A-D**) Representative histograms and (**E**) representative flow cytometry plots of mROS⁺ population (left panels). Gating was performed on CD3⁺CD8⁺ cells. (**A-D**) Summary graphs of MFI and (**E**) percentage of mROS expressing cells are shown (right panels). Each dot represents one donor. Data presented as mean ± S.E.M. * p<0.05, ** p<0.01. Wilcoxon test.

Effects of chronic IFN-I treatment on mitochondria of CD3/CD28 activated CD8$^+$ T cells in PBMC culture

On top of chronic IFN-I exposure, CD8$^+$ T cells of SLE patients are persistently exposed to autoantigens resulting in TCR signalling activation. Evidence also shows that stimulation of TCR (CD3) and co-stimulatory receptors (CD28) leads to elevated mitochondrial activity and can influence T cell activation and differentiation[253]. Therefore, to mimic more closely the lupus conditions, I elected to investigate the impact on mitochondria of prolonged IFN-α exposure together with T-cell stimulation. I then activated PBMCs from healthy subjects with CD3/CD28 beads together with or without 1000U/ml of IFN-α for 7 days. The mitochondrial phenotypes of the CD8$^+$ T cells were then assessed. The data obtained from flow cytometry showed that chronic IFN-α treatment increased the MFI of the MTG (**Fig.3.3A**) and MTDR (**Fig.3.3B**) staining in the stimulated CD8$^+$ T cells, suggesting enhanced mitochondrial mass and activity, respectively. Like the observations in the unstimulated conditions, IFN-α treatment did not alter MMP (**Fig.3.3C**) and cROS levels (**Fig.3.3D**). Following chronic IFN-α treatment, a downward trend of mROS generation was observed in most individuals, albeit not statistically significant (**Fig.3.3E**).

In summary, the combination of prolonged IFN-α treatment and TCR stimulation changed the mitochondrial phenotypes of CD8$^+$ T cells by increasing mitochondrial mass and activity.

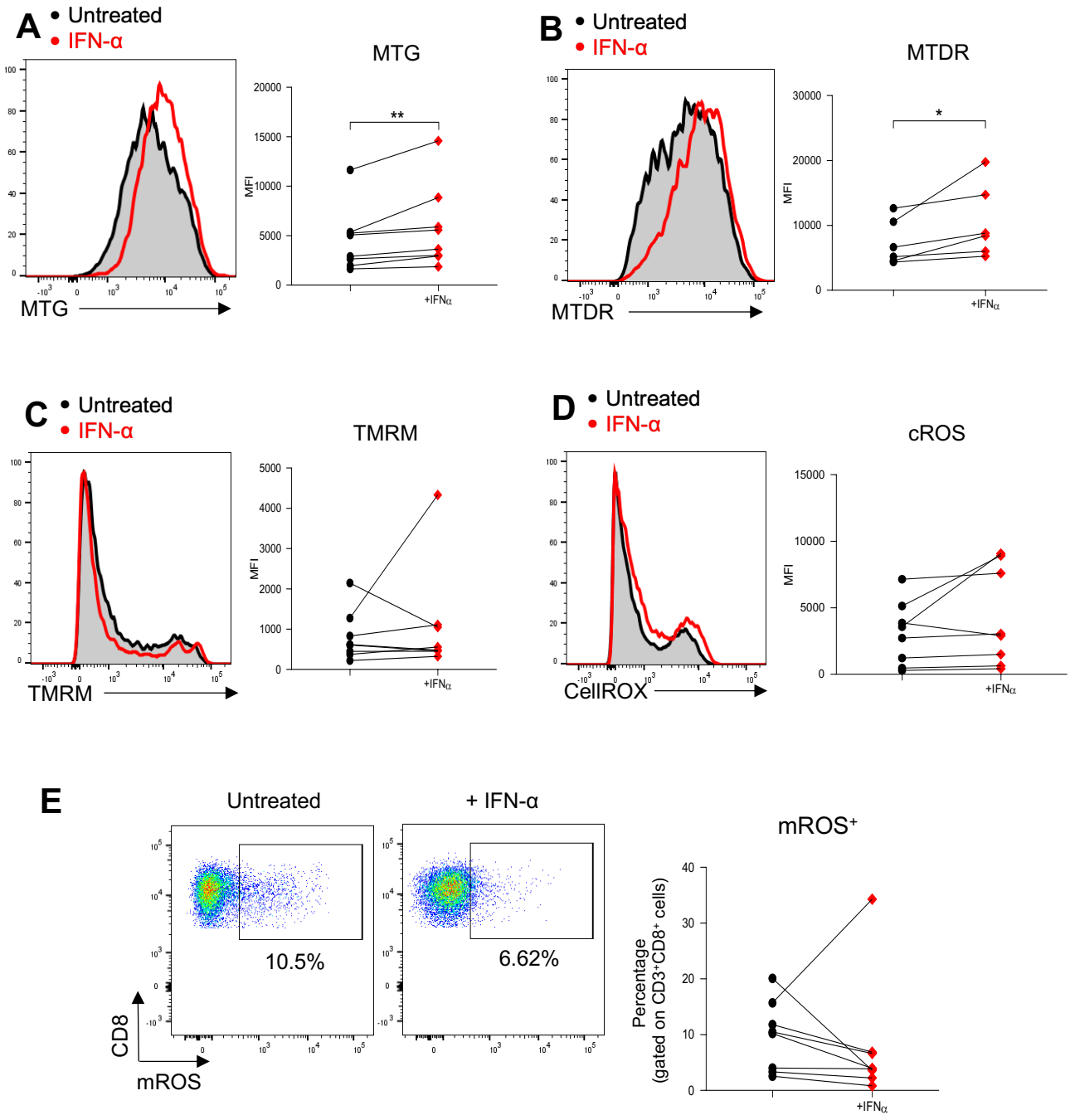

Figure 3.3. Phenotype of CD8⁺ T cell mitochondria after chronic IFN-α and CD3/CD28 stimulation. Human PBMCs treated with or without IFN-α and stimulated with CD3/CD28 beads for 7 days were stained with (**A**) MTG, (**B**) MTDR, (**C**) TMRM, (**D**) CellROX Green, and (**E**) MitoSOX Red. (**A-D**) Representative histograms and (**E**) representative flow cytometry plots of mROS⁺ population (left panels). Gating was performed on CD3⁺CD8⁺ cells. (**A-D**) Summary graphs of MFI and (**E**) percentage of mROS expressing cells are shown (right panels). Each dot represents one donor. Data presented as mean ± S.E.M. * p<0.05, ** p<0.01. Wilcoxon test.

Effects of chronic IFN-I treatment on mitochondrial functions of CD8$^+$ T cells in PBMC culture

These IFN-α-mediated changes in the mitochondrial phenotypes of CD8$^+$ T cells compelled me to explore mitochondrial functions. After culturing PBMCs with IFN-α for 7 days, I purified CD8$^+$ T cells using the cell-sorter. I then assessed their basal mitochondrial metabolic profile including mitochondrial respiration and glycolysis simultaneously using extracellular flux assay by Seahorse XFe96 Bioanalyser.

As illustrated in **figure 3.4A** and **3.4B**, this extracellular flux assay can track the oxygen consumption rate (OCR), which is an index of OXPHOS, and the extracellular acidification rate (ECAR), which is an index of glycolysis, at the basal state and in response to treatment with several mitochondrial inhibitors. I evaluated their OCR and ECAR following the serial injection of oligomycin (an inhibitor of ATP synthase), carbonyl cyanide-p-trifluoromethoxyphenyl-hydrazone or FCCP (a protonophoric uncoupler), and the combination of rotenone and antimycin A (ETC complex I and III inhibitors respectively). This serial administration enabled measurement of the basal OCR, maximum OCR, and spare respiratory capacity (SRC) that was calculated from the difference between the basal OCR and maximum OCR. SRC reflects the available mitochondrial capacity to produce extra energy upon increased metabolic demand.

As demonstrated in **figure 3.4**, chronic IFN-α treatment alone slightly increased basal OCR in CD8$^+$ T cells (**Fig.3.4A** and **3.4C**), but remarkably reduced basal ECAR compared to untreated cells (**Fig.3.4B** and **3.4G**). As a result, the ratio of OCR to ECAR was enhanced following the IFN-α treatment (**Fig.3.4H**), highlighting that prolonged IFN-α treatment decreased glycolysis and a triggered metabolic shift favouring OXPHOS in these unstimulated CD8$^+$ T cells. Nevertheless, no difference in the maximum OCR and SRC of these cells was detected (**Fig.3.4D-F**).

Research has shown that TCR activation promptly increases aerobic glycolysis. Consistent with this, basal ECAR was prominently enhanced in all CD3/CD28-stimulated conditions compared to those left unstimulated (**Fig.3.4G**). However, following chronic IFN-I treatment ECAR values remained unaffected (**Fig.3.4G**). This resulted in an elevated OCR/ECAR ratio in the IFN-α-treated samples (**Fig.3.4H**). Remarkably, prolonged IFN-α treatment reduced the percentage of SRC of stimulated

$CD8^+$ T cells (**Fig.3.4F**), reflecting the decreased mitochondrial ability to generate extra ATP upon increased energy demand.

The data from this mitochondrial functional assay revealed that persistent IFN-α treatment induced metabolic reprogramming in both unstimulated and TCR-stimulated $CD8^+$ T cells leading to enhanced OCR/ECAR ratio and decreased percentage of SRC. Of note, IFN-α treatment alone resulted mostly in the reduction of glycolysis, whereas the combination of TCR stimulation and chronic IFN-α treatment impacted mainly basal respiration.

Effects of chronic IFN-I treatment on mitochondria-encoded OXPHOS (MT-OXPHOS) gene expression

It is known that IFN-I affects mitochondrial functions at the transcriptomic level[25]. Therefore, I decided to investigate whether chronic IFN-α exposure affected mitochondria-derive gene expression. After 7 days of IFN-I treatment, mRNA was extracted from PBMCs. I next generated cDNA and employed qPCR to analyse the expression of OXPHOS-derived genes which are changed in IFN-high SLE patients we observed from the preliminary data. These genes included *MT-CYTB* (mitochondrially encoded cytochrome b), *MT-ND1* (mitochondrially encoded NADH dehydrogenase 1), *MT-ND3* (mitochondrially encoded NADH dehydrogenase 3) and *MT-ATP6* (mitochondrially encoded ATP synthase 6).

The relative expression of these genes to the 18S rRNA gene in both unstimulated and TCR-stimulated conditions is shown in **figure 3.5**. I found that chronic IFN-α treatment alone did not change the observed MT-OXPHOS gene expression compared to the untreated group (**Fig.3.5A**). In contrast, the combined IFN-α and TCR activation significantly decreased gene expression levels of *MT-CYTB* and *MT-ND3*. A downward trend was also detected with *MT-ATP6* even though it was not statistically significant (**Fig.3.5B**).

Altogether, the results from IFN-α treated PBMC experiments revealed that the combination of chronic IFN-α exposure and TCR stimulation possibly triggers changes in transcriptional and metabolic levels, comparable to the ones detected in $CD8^+$ T cells from IFN-high SLE patients[248]. Nevertheless, since I used PBMCs in all the experiments, the data may not reflect a direct effect of chronic IFN-α exposure on $CD8^+$ T cells.

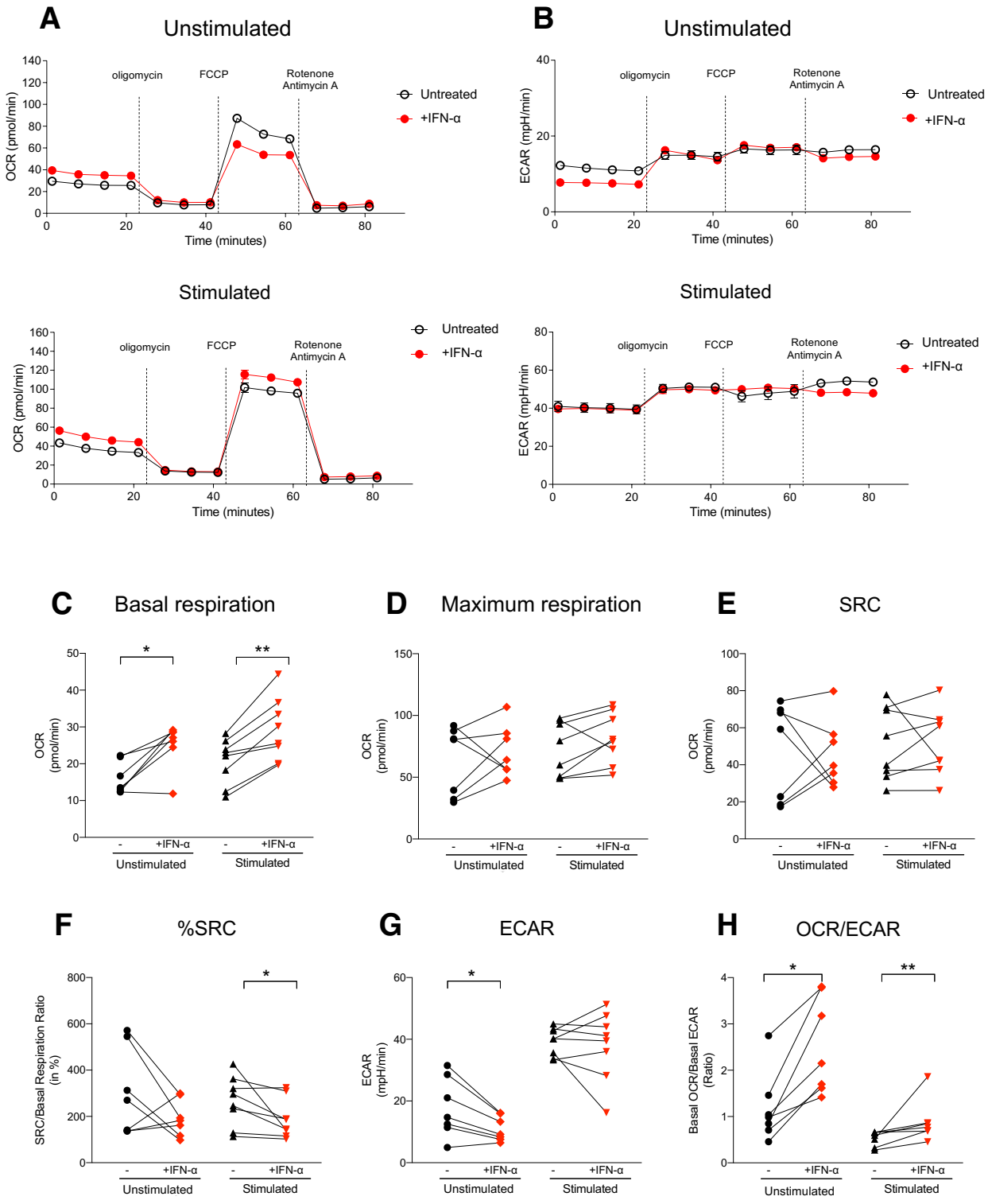

Figure 3.4. Extracellular flux analysis of CD8⁺ T cells
Unstimulated and CD3/CD28 stimulated PBMCs from healthy donors were treated with or without IFN-α for 7 days. CD8⁺ T cells were purified using cell sorter. Oxidative and glycolytic capacities of purified CD8⁺ T cells were assessed using extracellular flux assay. (**A-B**) Representative graphs of (**A**) oxygen consumption rate (OCR) and (**B**) extracellular acidification rate (ECAR) in unstimulated (upper panel) and activated (lower panels) conditions. (**C-H)** Summary graphs of (**C**) basal respiration, (**D**) maximum respiration, (**E**) spare respiratory capacity (SRC), (**F**) %SRC (SRC/basal respiration ratio), (**G**) basal ECAR and (**H**) OCR/ECAR ratio. Each dot represents one donor. Data presented as mean ± S.E.M. * p<0.05, ** p<0.01. Wilcoxon test.

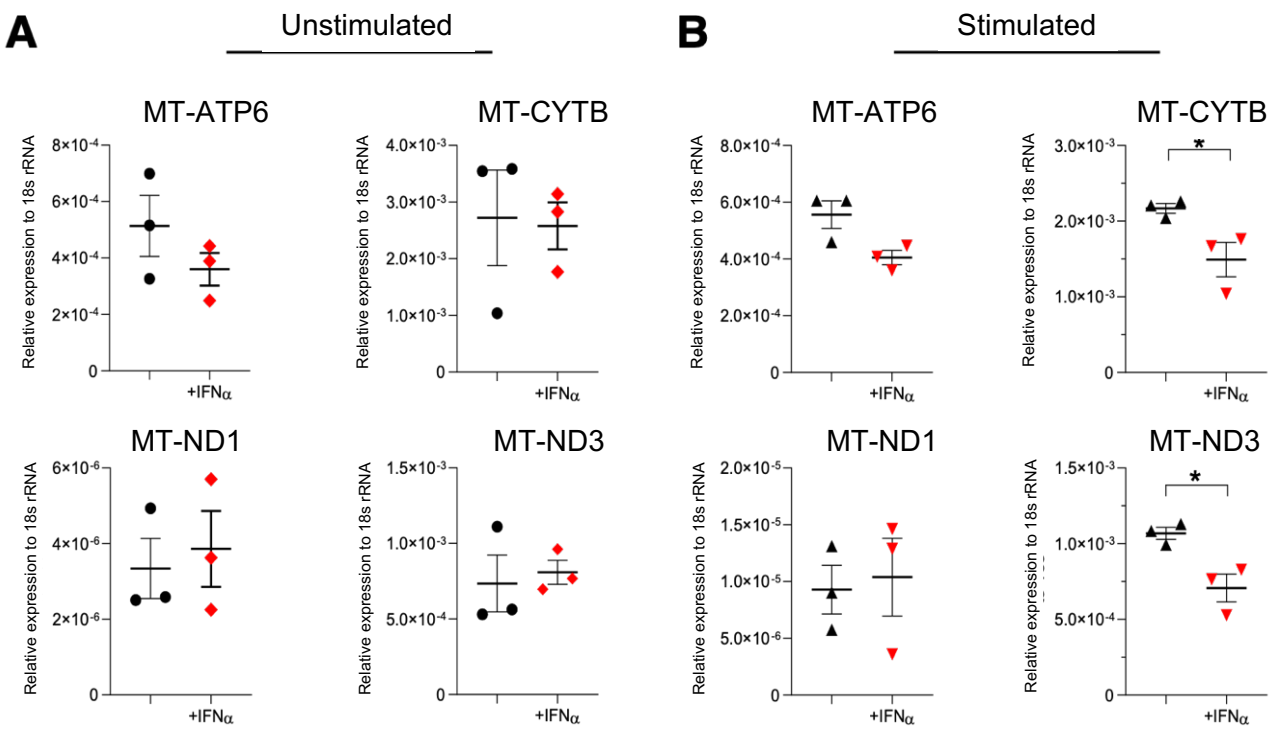

Figure 3.5. Mitochondria-derived gene expression in PBMCs.
Unstimulated and CD3/CD28 stimulated PBMCs from healthy donors were treated with or without IFN-α for 7 days. Relative expression of mitochondria-derived genes *MT-ATP6, MT-CYTB, MT-ND1* and *MT-ND3* was measured using qPCR in (**A**) unstimulated and (**B**) stimulated conditions. Each dot represents one donor. Data presented as mean ± S.E.M. * $p<0.05$. Wilcoxon test.

Impact of chronic IFN-I treatment on the mitochondria of purified CD8⁺ T cells

PBMCs contain several types of white blood cells including lymphocytes, monocytes, and dendritic cells. Therefore, analysing the gene expression from PBMCs was not adequate to pinpoint the direct effects of chronic IFN-I exposure on CD8⁺ T cells. To verify the direct impact of chronic IFN-α treatment on CD8⁺ T cell mitochondria, I isolated CD8⁺ T cells from healthy PBMCs. I then cultured them with or without 1000U/ml IFN-α as well as with or without CD3/CD28 stimulation for 7 days.

The mitochondrial phenotypes were assessed by flow cytometry as previously described. The data indicated that in the unstimulated conditions, chronic IFN-α exposure did not alter the mitochondrial mass of purified CD8⁺ T cells (**Fig.3.6A**). In contrast, following prolonged IFN-I treatment, there was a significant elevation in mitochondrial activity (**Fig.3.6B**) and a reduction in the population of mROS-positive cells (**Fig.3.6C**).

Regarding CD3/CD28-stimulated $CD8^+$ T cells, persistent IFN-α-treatment notably enhanced mitochondrial mass and activity (**Fig.3.6D** and **3.6E**), whereas the fraction of mROS positive cells was unaffected (**Fig.3.6F**). These findings displayed a comparable pattern to the results obtained from the PBMCs experiments.

Direct impact of chronic IFN-I treatment on the expression of MT-OXPHOS genes in $CD8^+$ T cells

Next, I investigated the expression of MT-OXPHOS genes, *MT-CYTB*, *MT-ND3* and *MT-ATP6*, in isolated $CD8^+$ T cells. I cultured the purified unstimulated and stimulated $CD8^+$ T cells with and without IFN-α for 7 days, collected the mRNA and performed qPCR analysis. I found that chronic IFN-α treatment alone significantly downregulated the expression of all three MT-OXPHOS genes (**Fig.3.7A**). In the stimulated $CD8^+$ T cells, *MT-CYTB* and *MT-ND3* genes were significantly downregulated upon IFN-I treatment (**Fig.3.7B**). A similar downward trend was also observed with *MT-ATP6* gene (**Fig.3.7B**). Importantly, these results replicated the data generated from the PBMC experiments, confirming the direct effect of IFN-I treatment on purified CD8+ T cells. These findings highlighted that PBMCs could be used as surrogate for CD8+ T cells in subsequent experiments.

In summary, the persistent treatment of IFN-I alone was able to rewire the metabolism of $CD8^+$ T cells. However, only the combination of chronic IFN-I exposure and TCR activation can mimic the mitochondrial and metabolic changes detected in $CD8^+$ T cells from SLE patients with high IFN signature[248]. These significant metabolic alterations comprised an elevation in mitochondrial mass and activity, a downregulation of mitochondria-derived-OXPHOS gene expression and SRC.

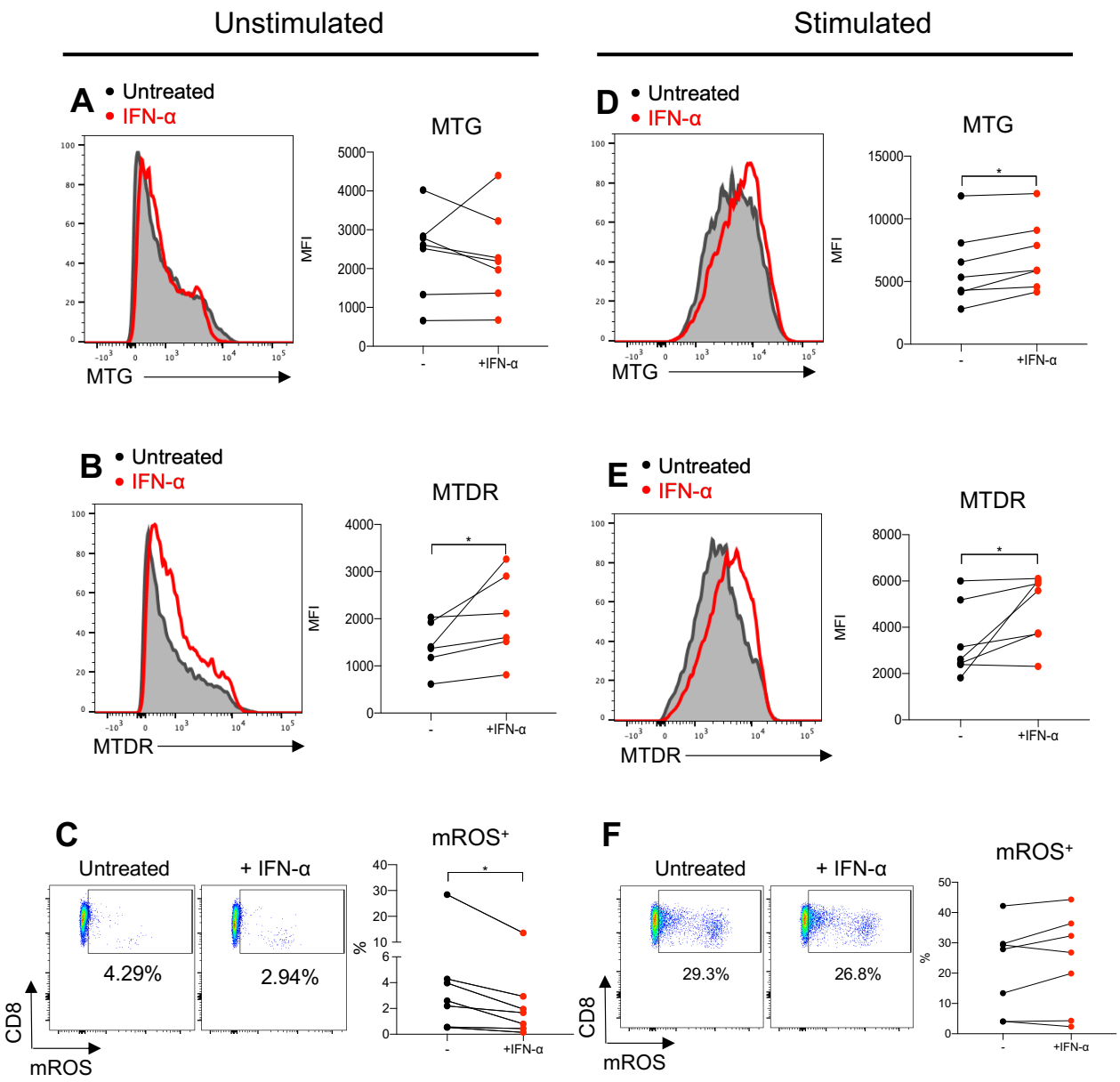

Figure 3.6. Mitochondria analysis of purified CD8⁺ T cells
Purified CD8⁺ T cells treated with or without 1000U/ml of IFN-α and stimulated with or without CD3/CD28 beads for 7 days. Mitochondria analysis was performed using flow cytometry. Unstimulated and stimulated CD8⁺ T cells were stained with (**A, D**) MTG, (**B, E**) MTDR, and (**C, F**) MitoSOX Red. (**A-D**) Representative histograms (**E**) representative flow cytometry plots of mROS⁺ population (left panels). Summary graphs of (**A-B, D-E**) MFI and (**C, F**) percentage of mROS⁺ cells (right panels) are presented. Each dot represents one donor. Data presented as mean ± S.E.M. * p<0.05. Wilcoxon test.

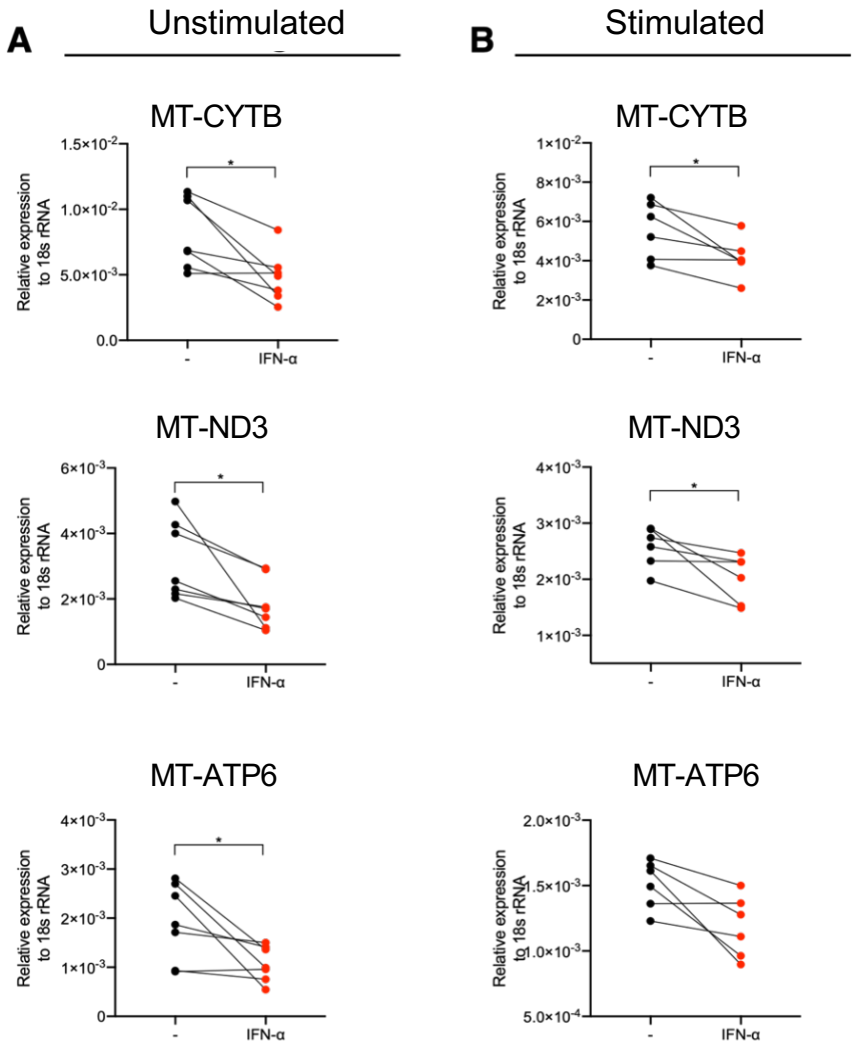

Figure 3.7. Mitochondria-derived gene expression of purified CD8⁺ T cells
Unstimulated and CD3/CD28 beads stimulated CD8⁺ T cells from healthy donors were treated with or without IFN-α for 7 days. Mitochondria-derived gene expression was measured using qPCR in (**A**) unstimulated and (**B**) stimulated purified CD8⁺ T cells. Each dot represents one donor. Data presented as mean ± S.E.M. * $p<0.05$. Wilcoxon test.

The downstream effect of IFN-I exposure and T-cell activation

Based on the findings highlighted previously, the stimulated $CD8^+$ T cells treated with prolonged IFN-α exposure were then called "SLE-like $CD8^+$ T cells". Next, I evaluated the downstream functional effects of the IFN-I-mediated metabolic changes in $CD8^+$ T cells and identified how these changes could contribute to SLE pathogenesis.

There is strong evidence in the literature that abnormalities in T cell activation are present in lupus patients[254] and that the $CD8^+$ T cells from lupus patients are impaired[255]. These abnormalities include diminished granzyme B and perforin production[255]. I, therefore, generated SLE-like $CD8^+$ T cells (PBMCs in 7-day culture with TCR stimulation in the presence or absence of IFN-α) and rested the cells by removing the stimuli overnight. I then re-stimulated them with anti-CD3/CD28 beads for 4 and 24 hours. Using flow cytometry, I quantified the surface expression of the early and late activation markers, (CD69 and CD25, respectively). The degranulation marker CD107a was also assessed. The results shown in **figure 3.8A** revealed that after 4-hour of re-stimulation, the expression of CD69, CD25 and CD107a was notably reduced in IFN-I-primed $CD8^+$ T cells. At 24 hour-timepoint, prolonged IFN-α treatment diminished the expression of CD25 but had no effect on CD69 and CD107a markers (**Fig.3.8A**). To further understand the effect of chronic IFN-I exposure on $CD8^+$ T cell effector functions, I collected the supernatant and measured the secretion of effector cytokines including granzyme B, TNF-α and IFN-γ using ELISA after 4 and 24 hours of re-stimulation. As shown in **figure 3.8B**, IFN-I priming did not impact the production of effector cytokines at 4 hours timepoint. However, there was a significant reduction in TNF-α secretion and a trend of reducing granzyme B and IFN-γ secretion at 24 hours (**Fig.3.8B**). To summarise, the combination of prolonged IFN-I exposure and TCR stimulation led to a defective acute response to further TCR activation.

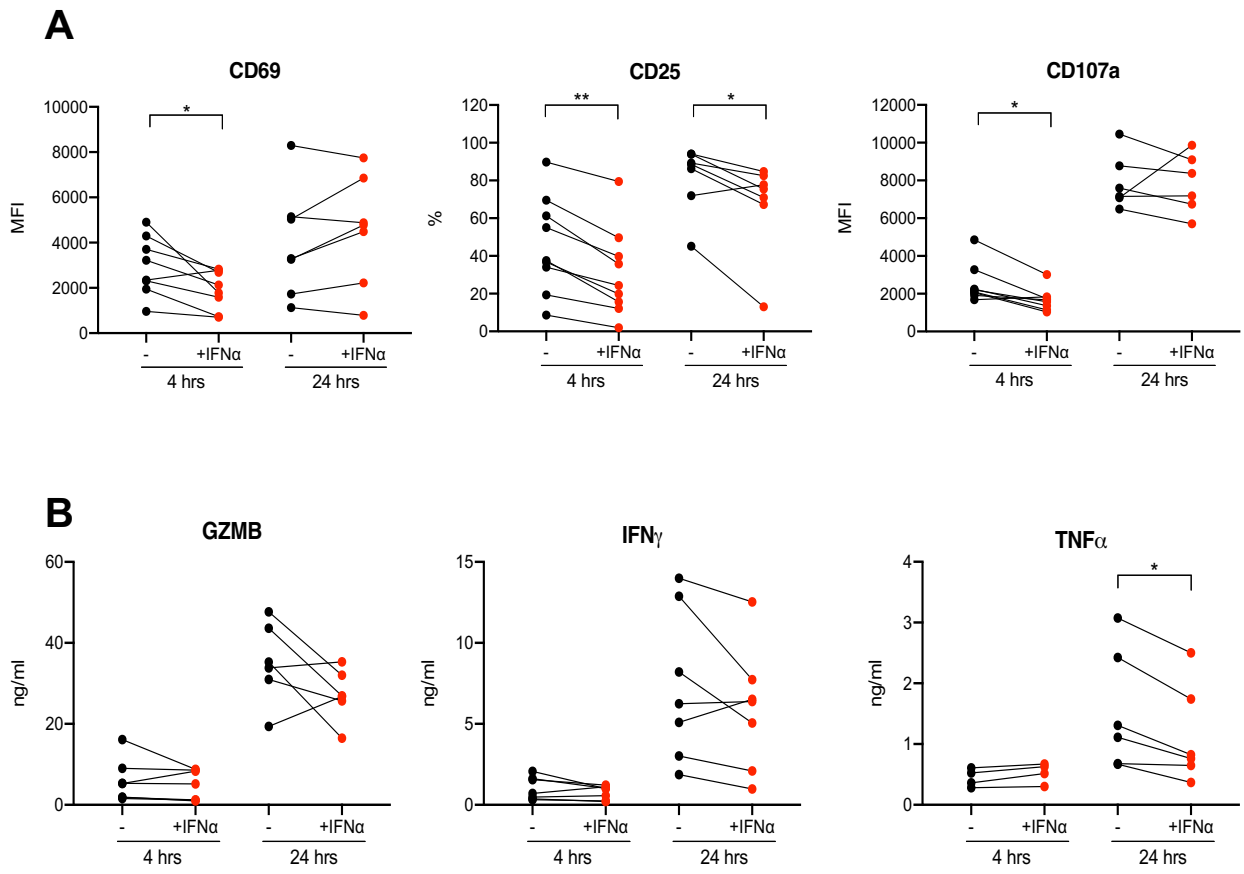

Figure 3.8. Activation status of SLE-like CD8⁺ T cells
CD3/CD28 beads stimulated CD8⁺ T cells from healthy donors were treated with or without IFN-α for 7 days. The cells then were re-stimulated with anti-CD3/CD28 beads for 4 and 24 hours. (**A**) Activation markers (CD69 and CD25) and degranulation (CD107a) markers were assessed using flow cytometry. (**B**) The secretion of Granzyme B (GZMB), IFN-γ and TNF-α was measured by ELISA. Each dot represents one donor. Data presented as mean ± S.E.M. * $p<0.05$. ** $p<0.01$. Wilcoxon test.

The downstream effect of IFN-I exposure on cell death

A considerable amount of literature has shown that PBMCs and T cells from SLE patients are prone to undergo apoptosis at a faster rate compared to the cells from healthy subjects[21,256]. I initially explored whether spontaneous apoptotic cell death of CD8⁺ T cells could be altered by IFN-α-induced mitochondrial changes. To address this, I created SLE-like CD8⁺ T cells by culturing PBMCs with 1000U/ml of IFN-α in the presence of TCR stimulation for 7 days. After that, PBMCs were washed and re-cultured again in medium alone for 24 or 48 hours. The spontaneous apoptosis rate was assessed using Annexin V and propidium iodide (PI) staining. Annexin V is a phospholipid-binding protein that can bind to exposed phospholipid

phosphatidylserine of apoptotic cells, whereas PI is a membrane impermeant dye that can intercalate DNA inside the cell. Therefore, viable cells with intact membranes can exclude PI. As shown in **figure 3.9A**, alive cells which have intact membranes are both Annexin V and PI negative. Cells that undergo early apoptosis are Annexin V positive and PI negative, whereas late apoptotic cells are positive for both Annexin V and PI staining.

After 24 hours of re-culture, the collected data from 7 donors revealed that IFN-α priming decreased cell viability of stimulated $CD8^+$ T cells compared to untreated conditions. Regarding apoptosis, the proportion of early apoptotic cells was significantly increased in the IFN-α priming condition. A similar increasing trend was also observed in that of late apoptotic cells, albeit not significantly (**Fig.3.9B**).

The data from the 48-hour time point are illustrated in **figure 3.9C**. Following IFN-α priming, the proportion of the alive cell population was significantly decreased. There was a trend towards an increased fraction of early apoptotic cells and the proportion of late apoptotic cells was increased.

I next explored whether chronic IFN-I treatment changed the cell death rate upon TCR re-stimulation. After removing dead cells from the 7-day-cell culture, I stained the cells with CFSE (Carboxyfluorescein succinimidyl ester). These $CD8^+$ T cells were then re-stimulated with anti-CD3/CD28 beads at different ratios of bead per cell (1:16, 1:8 and 1:4) for 3 days. I then stained the cells with Annexin V to observe cell proliferation and cell death at the same time. Using flow cytometry, I found that the percentage of proliferating $CD8^+$ T cells expressing annexin V (Annexin V+ CFSE low) was remarkably increased in the cells exposed to IFN-α, indicating that a great proportion of proliferating cells were dying by apoptosis (**Fig.3.10**). This increasing trend of cell death upon IFN-I treatment was observed across all different ratios of beads per cell (**Fig.3.10**).

Together, these results indicated that the combination of chronic IFN-I exposure and TCR activation triggered spontaneous cell death, and this is further increased if the cells are restimulated.

The findings in this chapter, demonstrating the link between chronic IFN-I and downstream mitochondrial and metabolic changes observed in the $CD8^+$ T cells, were a key component of a larger study that was published in Nature Communications[248].

In this paper, we showed that chronic IFN-I exposure enhanced the consumption of nicotinamide adenine dinucleotide (NAD) metabolic pathway, which is essential for energy metabolism, leading to abnormal mitochondrial function and increased $CD8^+$ T cell death.

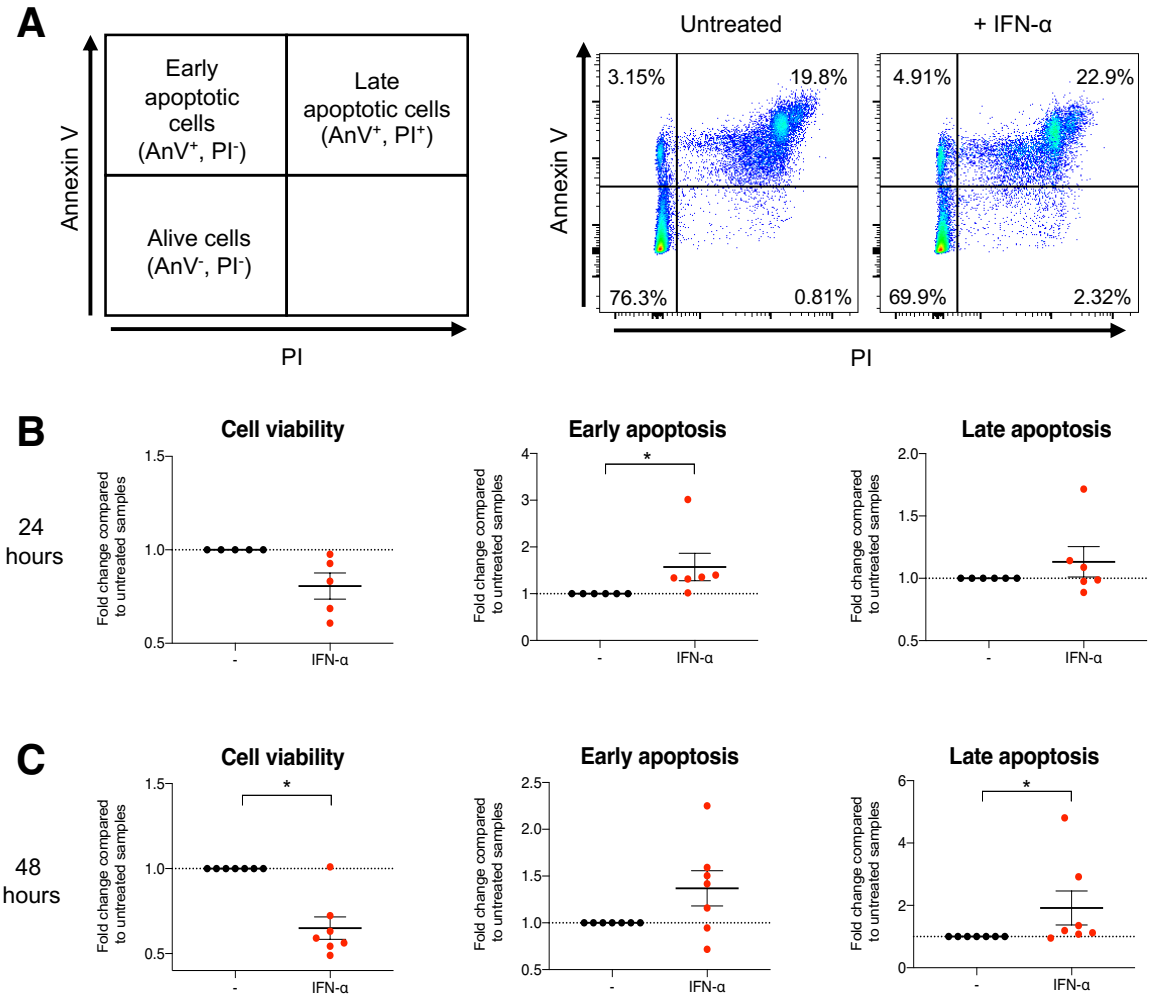

Figure 3.9. Spontaneous apoptosis in SLE-like $CD8^+$ T cells
CD3/CD28 bead stimulated $CD8^+$ T cells from healthy donors were treated with or without IFN-α for 7 days. Cells were washed and left in medium alone for 24 or 48 hours. Cells were then stained with Annexin V and PI and analysed by flow cytometry. (**A**) Representative flow cytometry plots of alive and apoptotic cells gated on $CD3^+CD8^+$ cell population. (**B-C**) Cell viability, early apoptosis and late apoptosis at (**B**) 24 and (**C**) 48 hours. Each dot represents one donor (n=7). Data presented as mean ± S.E.M. * $p<0.05$. Wilcoxon test.

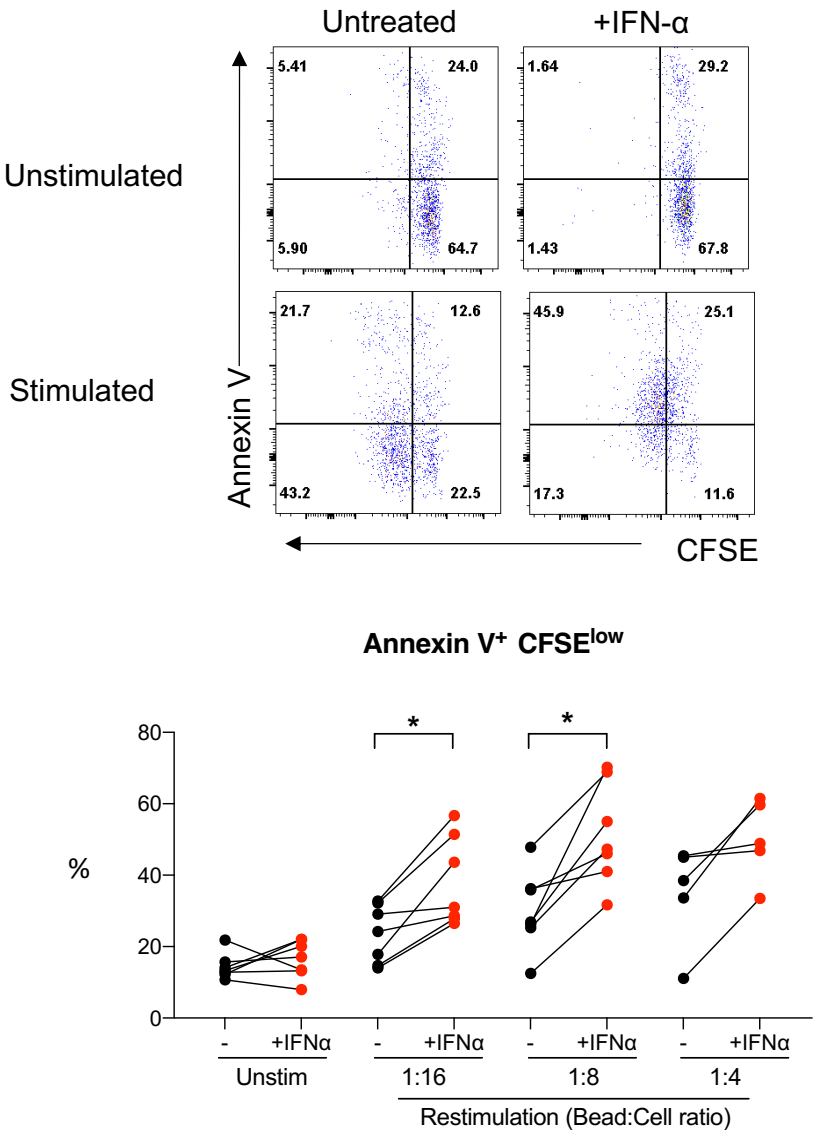

Figure 3.10. TCR-activation-induced apoptosis in SLE-like CD8⁺ T cells
CD3/CD28 bead stimulated CD8⁺ T cells from healthy donors were treated with or without IFN-α for 7 days. Anti-CD3/CD28 beads were removed from the culture and cells were rested overnight before labelling with CFSE and re-stimulation with anti-CD3/CD28 beads for 3 days. Representative flow plots of Annexin V staining and CFSE dilution ($CD3^+CD8^+$gated cells) at day 3 after re-stimulation (beads to cell ratio indicated) and percentage of AnV^+CFSE^{low}cells are shown. Each dot represents one donor. Data presented as mean ± S.E.M. * $p<0.05$. Wilcoxon test.

3.3. Discussion

I started by optimising the procedure to stimulate chronic IFN exposure *in vitro*. I established the appropriate IFN-α dosage (1000U/ml) and observed that a low amount of IL-2 was essential to improve T cell survival and proliferation[257-259]. I employed peripheral blood mononuclear cells (PBMCs) instead of purified $CD8^+$ T cells in all my initial investigations since PBMCs provided various advantages. These benefits include; i) simple separation from buffy coats or donor blood; ii) a greater number of cells available for all the planned analyses.; iii) increased lymphocyte viability in long-term cell culture[260]. Furthermore, because PBMCs comprise a variety of immune cell types, they may reproduce intercellular interactions more accurately. However, this could also be a disadvantage because other cellular components of PBMCs, including B cells, NK cells, and monocytes, can respond to IFN-α. Therefore, the observed effects may stem from extra mediators that IFN-α stimulates and may not represent the direct impact of IFN-α on $CD8^+$ T cells. As a result, after making the initial observations using PBMCs, I verified the data by culturing isolated $CD8^+$ T cells in the presence of IFN-α and analysing the same parameters. The results obtained from isolated $CD8^+$ T cell cultures were identical to those acquired from PBMCs, proving that the PBMCs could be used as a surrogate for $CD8^+$ T cells.

In SLE, abnormal mitochondrial metabolism has been reported largely in $CD4^+$ T cells[261,262]. These defects involve enlarged and hyperpolarised mitochondria, elevated ROS generation and ATP deficiency[238,239]. In addition, OXPHOS and glycolytic activity are elevated in $CD4^+$ T cells from lupus patients and SLE-prone mice[263]. Nevertheless, no study has yet investigated the relationship between these mitochondrial aberrations and long-term IFN-I exposure in SLE patients. Therefore, I questioned if chronic IFN-I treatment alone *in vitro* could affect the mitochondrial metabolism of $CD8^+$ T cells. After culturing the cells with IFN-I for 7 days, the data revealed that this cytokine can increase mitochondrial activity as evaluated by MTDR staining, without changing the mass or the MMP. More significantly, chronic IFN-I exposure induced the metabolic programming of $CD8^+$ T lymphocytes by augmenting OXPHOS and diminishing aerobic glycolysis, revealing a metabolic switch from glycolysis to OXPHOS. This IFN-I-mediated metabolic shift towards OXPHOS was formerly observed in a study in which IFN-I treatment increased OXPHOS and fatty acid oxidation in plasmacytoid dendritic cells[230]. With regards to the suppression of

glycolysis detected in this chapter, a study in rat lymphocytes has also demonstrated that IFN-Is diminish the metabolism of glycolysis and glutaminolysis by lowering gene expression levels[264]. In contrast, IFN-Is are found to boost glycolytic activity in dendritic cells and cancer cell lines according to studies in human and mouse models[226,265,266]. These conflicting results suggest that the control of glycolysis may vary depending on the cell type and the experimental setup. As a result, additional research is needed to fully demonstrate the influence of IFN-I on aerobic glycolysis in $CD8^+$ T cells.

In addition to ongoing exposure to IFN-I, SLE T cells frequently encounter self-antigens leading to TCR activation which can then promote B cells to produce autoantibodies[267,268]. When TCRs are activated, naive T cells undergo a metabolic rewiring from a catabolic state, in which they create ATP for cell viability, to an anabolic one, in which they synthesise complex molecules for cell growth[269]. The discrepancy in this metabolic shift can result in impaired T cell activation and, as a result, abnormal T cell responses[237]. However, it remains unclear whether persistent IFN-α exposure alters the metabolic response to TCR stimulation.

To address this, I treated PBMCs with IFN-α and CD3/CD28 beads concurrently for 7 days. I then evaluated the metabolic changes in these activated cells. In agreement with the literature[270], my data demonstrated a significant rise in glycolysis in response to TCR activation, indicating that these $CD8^+$ T cells altered their metabolic status to anabolic. However, IFN-α treatment had no effect on ECAR values on TCR-stimulated $CD8^+$ T cells. These unchanged ECAR values may be the result of the TCR-induced upregulation of glycolysis balancing the IFN-induced downregulation of glycolysis. Interestingly, the simultaneous activation of the TCR and IFN-α enhanced mitochondrial mass, activity, and OXPHOS. These findings point to preferential ATP generation from OXPHOS. However, after IFN-α treatment the SRC displayed a declining trend that became more apparent when the TCR stimulation was added. These results are in line with a prior study that reported lower SRC in PBMCs and total T cell populations from lupus patients[271]. The reduction of SRC reflects the impaired metabolic fitness of these IFN-I-primed $CD8^+$ T cells. The diminished SRC could be an indication of exhausted mitochondria, implying that their bioenergetic fitness to respond to further stress is compromised.

As observed in $CD8^+$ T cells from SLE patients with a IFN signature[248], I found a decrease of MT-OXPHOS gene expression after prolonged IFN-I exposure in both

unstimulated and activated $CD8^+$ T cells. It has been reported that in human lymphocyte cell lines the treatment of IFN-I suppresses the expression of 12 out of 13 MT-OXPHOS genes[235,272]. A reduction in the expression of mitochondrial genes could be due to IFN-I-activated RNase L which is an antiviral mechanism[236]. Overall, my data indicate that persistent IFN-I exposure diminishes MT-OXPHOS gene expression in $CD8^+$ T cells from healthy subjects. Notably, further analysis showed that there was no difference in MT-OXPHOS protein levels after prolonged IFN-I treatment[248], suggesting that the abnormal metabolism observed in this chapter was not due to the downregulation of MT-OXPHOS expression. More interestingly, my findings under stimulated conditions were comparable with the results from *ex vivo* $CD8^+$ T cells from IFN-high SLE patients, which showed reduced mitochondrial-derived OXPHOS gene expression, reduced SRC, enhanced mitochondrial mass and activity. Therefore, by exposing healthy $CD8^+$ T cells to chronic IFN-α treatment together with TCR stimulation I had successfully created the experimental settings that recapitulate the metabolic abnormalities seen in the patients and I called these cells: "SLE-like $CD8^+$ T cells". My data also showed that the mitochondrial defects seen in the patients are most likely the consequence of the combined effects of chronic IFN-I exposure and TCR stimulation.

The establishment of the appropriate *in vitro* experimental conditions allowed me to carry out further mechanistic studies. One of the important functions of $CD8^+$ T cells is their effector function to recognise and kill infected cells mainly through the secretion of granzyme B and perforin. I then investigated the effector functions of the SLE-like $CD8^+$ T cells. Here I demonstrated that chronic IFN-I exposure impaired $CD8^+$ T cell activation as evidenced by the reduction of activation markers. The expression of effector cytokines was also mildly impaired upon IFN-I treatment. This is consistent with a previous study whereby $CD8^+$ T cells from SLE patients displayed a reduction in effector functions, including diminished granzyme B production[255]. My data highlight the role of chronic IFN-I exposure in the abnormal functions of the SLE $CD8^+$ T cells. The cytolytic defect in $CD8^+$ T cells most likely contributes to the pathogenesis of autoimmunity as a result of failure of removing autoreactive B cells[273].

It is widely known that abnormal mitochondrial metabolism is associated with cell death pathways. Deficiency in metabolic substances, depletion in energy and imbalance in a redox reaction can induce excessive cell death leading to lymphopenia

in SLE[274] and to a rich source of self-antigens from the apoptotic debris[275]. Apoptosis, which is a type of programmed cell death pathway, has been implicated in SLE pathogenesis. Defects in apoptotic cell clearance have been reported in mouse models and patients[276]. I therefore investigated whether the abnormal mitochondrial metabolism induced by a prolonged IFN-α exposure could affect the degree of spontaneous cell death. I found that priming TCR-stimulated $CD8^+$ T cells with IFN-α significantly decreased their cell viability and increased the rate of early and late apoptosis. These results are consistent with several studies showing the effects of IFN-Is on apoptotic pathways. Tanaka and colleagues discovered that IFN-Is limit viral infection by the induction of apoptosis in infected cells[277]. IFN-Is are also known as apoptosis inducers in tumour cells[278,279]. This might occur through the JAK/STAT signalling and/or the NF-κB survival pathway, which are widely reported as the fundamental pathways for IFN-I-induced apoptotic signals [280]. Additionally, IFN-Is may also promote apoptosis through ISGs. Recent publications have shown that several ISGs have apoptotic functions[281,282]. For instance, *AIM2* gene shows a pro-apoptotic property[283,284], whereas *IF16 (6–16, G1P3)* is known to be an anti-apoptotic gene[285,286]. Further experiments need to be performed to uncover the underlying mechanism(s) of the cell death promoted by the chronic IFN-I stimulation.

My data and the findings from other laboratory members were published in Nature Communication[248]. From the transcriptomic analysis of $CD8^+$ T cells from SLE patients, we found that the NAD metabolic pathway correlated with type I IFN signalling. NAD-consuming enzymes, such as *CD38* and *PARP9*, *PARP10*, and *PARP12* were markedly upregulated in $CD8^+$ T cells from IFN-high SLE patients. I observed the same increased expression of CD38 in my *in vitro* conditions and this led to a decrease in NAD/NADH ratio. The IFN-I-mediated NAD reduction impaired mitochondrial respiration and reduced cell viability, both of which can be rectified by NAD+ supplementation. Taken together, the *in vitro* and the *ex vivo* findings suggest that chronic IFN-I exposure and TCR activation trigger mitochondrial changes via increasing NAD consumption that results in decreased energetic fitness. Upon increased energy demand, IFNα-exposed $CD8^+$ T cells are more prone to die, and this could perpetuate autoimmunity by increasing the autoantigen load. Importantly, this can be rectified by NAD supplementation with NMN.

Chapter 4

The effects of IFN-I on macrophages

4.1. Introduction

The findings described in chapter 3 have demonstrated that chronic IFN-I exposure alters NAD metabolism leading to abnormal mitochondrial metabolism and cell death in $CD8^+$ T cells. This work prompted me to investigate whether similar effects could be seen in other immune cell types.

Macrophages have been shown to play a central role in the development and progression of SLE. Several aberrations of macrophage phenotypes and functions have been widely reported and linked to disease pathogenesis. For example, the inability to eliminate immune complexes by defective macrophages contributes to immune complex accumulation in different tissues and eventually causes tissue damage and organ failure[287]. Evidence also suggests macrophages are highly activated and produce proinflammatory cytokines that can promote inflammation and tissue damage, leading to the development of lupus symptoms[33]. Furthermore, the activation of the IFN-I signalling in macrophages may mediate the development of the lupus nephritis[288].

The effects of the IFN-Is on macrophage metabolism have been recently reported, mostly in a short-term setup for viral infection context. Using publicly available transcriptional profiling datasets, Ahmed and their colleagues showed that 4 hours of IFN-α stimulation triggers metabolic changes in both mouse and human macrophage models[289]. These changes include increased expression of genes associated with OXPHOS such as genes from complexes I and V of the electron transport chain (*NDUFA9, NDUFS4,* and *ATP5G3*) in human macrophages, whilst in murine macrophages short-term IFN-I stimulation induced the expression of genes relevant to glycolysis such as *HK2, HK3* and *PGM2*[289]*.* Furthermore, Olsen and colleagues demonstrated that IFN-β controls macrophage metabolism during the infection of live, but not killed, *Mycobacterium tuberculosis* by diminishing glycolysis and inducing mitochondrial stress in activated bone marrow-derived macrophages[290]. However, little is known about how long-term IFN-I exposure modulates macrophage metabolism. Furthermore, the biological consequences of chronic IFN-I signature on

macrophage functions in SLE are poorly understood. Therefore, the aim of this chapter is to study how human macrophage metabolism changes over prolonged IFN-I stimulation and whether the changes affect macrophage functions.

4.2. Results

Prolonged IFN-I exposure increases the expression of NAD consumer enzymes leading to NAD reduction

I initially differentiated monocyte-derived macrophages (MDMs) from healthy PBMCs for 4 days and then treated them with 1000U/ml IFN-α or left them untreated for 3 days. The first parameter I explored was the NAD/NADH metabolic pathway. Using flow cytometry and qPCR techniques, I found that the expression of NAD consumer enzymes such as CD38 (**Fig.4.1A**), *SIRT1* (**Fig.4.1B**), *PARP1* (**Fig.4.1C**) was significantly increased in the IFN-α-treated samples. This prompted me to investigate the intracellular NAD+ and NADH levels using a colorimetric assay. As expected, the total NAD pool (**Fig.4.2C**) and NAD+ levels (**Fig.4.2A**) were depleted upon IFN-α treatment; however, NADH level (**Fig.4.2B**) and the ratio of NAD to NADH (**Fig.4.2D**) remained unchanged. Furthermore, IFN-α markedly increased the expression of *NAMPT* (*Nicotinamide phosphoribosyltransferase*) (**Fig.4.1D**), an enzyme in the NAD+ salvage pathway and *IDO1* (*Indoleamine 2,3-dioxygenase 1*) (**Fig.4.1E**), a key enzyme in the *de novo* NAD+ synthesis pathway (**Fig.4.2C**), suggesting that the cells are trying to compensate for the IFN-α-mediated reduction of cellular NAD+ level.

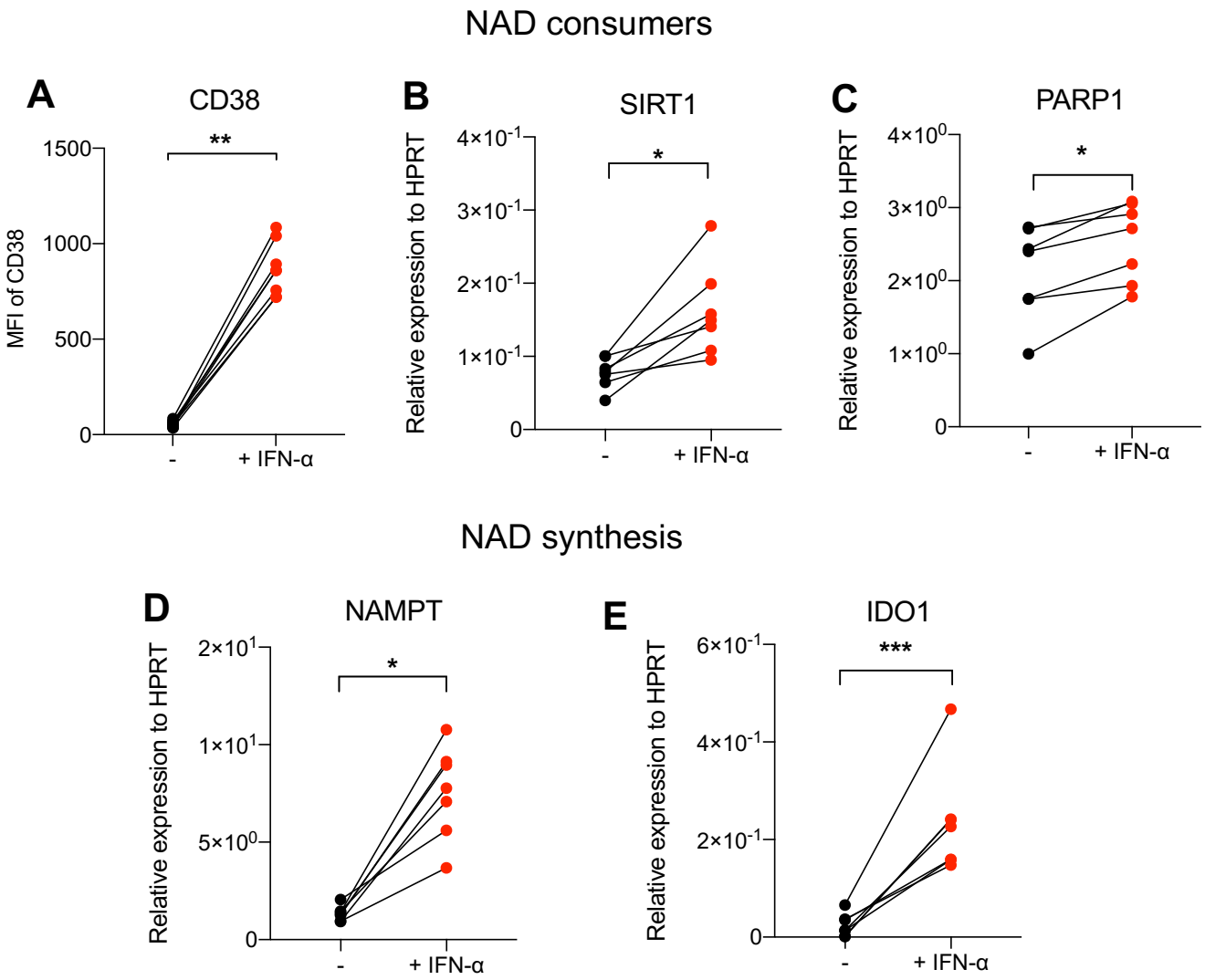

Figure 4.1. The expression of NAD consumer enzymes and genes related to NAD synthesis pathways. Human monocyte-derived macrophages were cultured with or without 1000U/ml IFN-α for 3 days. (**A**) Surface expression of NAD consumer CD38 was measured by flow cytometry. (**B-C**) Relative gene expression of NAD consumers SIRT1 (**B**) and PARP1 (**C**) was assessed by qPCR. (**D-E**) Relative expression of genes encoding key enzymes in NAD synthesis pathways including NAMPT from salvage pathway (**D**) and IDO1 from *de novo* pathway (E) was also assessed by qPCR. Each dot represents one donor. Data presented as mean ± S.E.M. * $p<0.05$, ** $p<0.01$, *** $p<0.001$. Wilcoxon test.

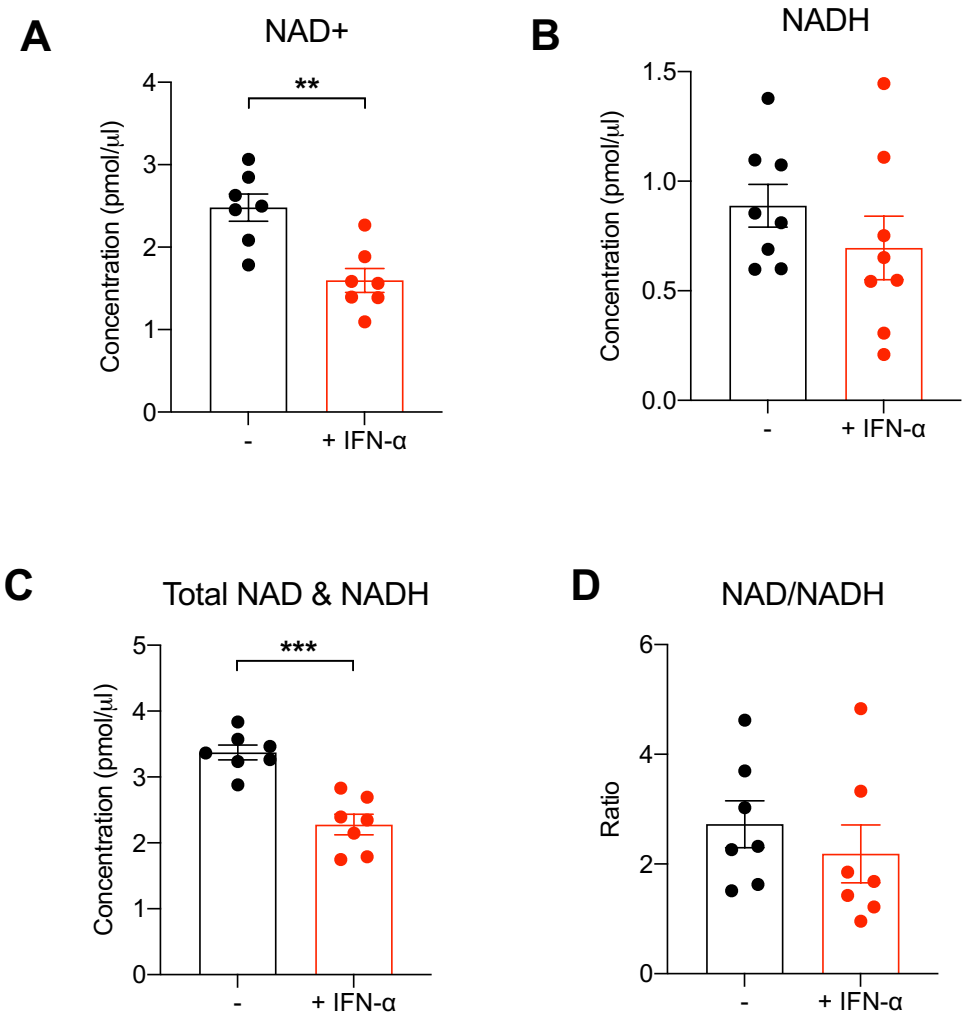

Figure 4.2. Intracellular NAD and NADH levels upon chronic IFN-I treatment
Human monocyte-derived macrophages were cultured with or without 1000U/ml IFN-α for 3 days. Cells then were collected and processed to measure NAD and NADH levels using a colourimetric assay. Summary graphs showing (**A)** NAD+ concentration, (**B)** NADH concentration, (**C)** the total amount of NAD and NADH and (**D**) the ratio of NAD and NADH. Each dot represents one donor. Data presented as mean ± S.E.M. ** p<0.01, *** p<0.001. Wilcoxon test.

Prolonged IFN-I exposure induces changes in macrophage transcriptome

To further understand the effects of prolonged IFN-I exposure in regulating the transcriptomic profile of MDMs, bulk RNA-sequencing analysis was performed to identify differential expression genes (DEGs) and important enriched signalling pathways in 3-day-IFN-I-treated macrophages.

The data from principal component analysis (PCA) showed that IFN-I-treated samples separated from untreated samples, indicating distinct transcriptomic profiles between the two groups (**Fig.4.3A**). Comparing the gene expression between the two groups, 3643 genes were identified with the absolute fold change (FC) of more or less than 1.5 and adjusted p value < 0.01. As shown in the volcano plot in **figure 4.3B**, 1840 genes were downregulated, whilst 1793 genes were upregulated in IFN-I-treated macrophages. Top upregulated DEGs were IFN-I-stimulated genes and pro-apoptotic genes (*HSH2D, TNFSF10, ZBP*), whereas top downregulated DEGs were genes involved in a negative regulator of the apoptotic process, cell proliferation and differentiation (*RPS3A* and *EIF3L*) (**Fig.4.3B**).

Further analysis by the Kyoto Encyclopedia of Genes and Genomes (KEGG) enriched pathways was then performed. As expected, IFN-I-related pathways including viral defence mechanisms were activated. Apoptosis pathways were also upregulated. In contrast, cell cycle pathways and metabolic pathways including glycolysis, OXPHOS and fatty acid metabolism were suppressed with IFN-I treatment (**Fig.4.3C**). These data suggested that chronic IFN-I treatment changed the activity of metabolic pathways at the transcriptomic level in human macrophages. However, from this analysis, I cannot conclude whether the treatment could affect the metabolic functions of the cells. Further analyses were then conducted.

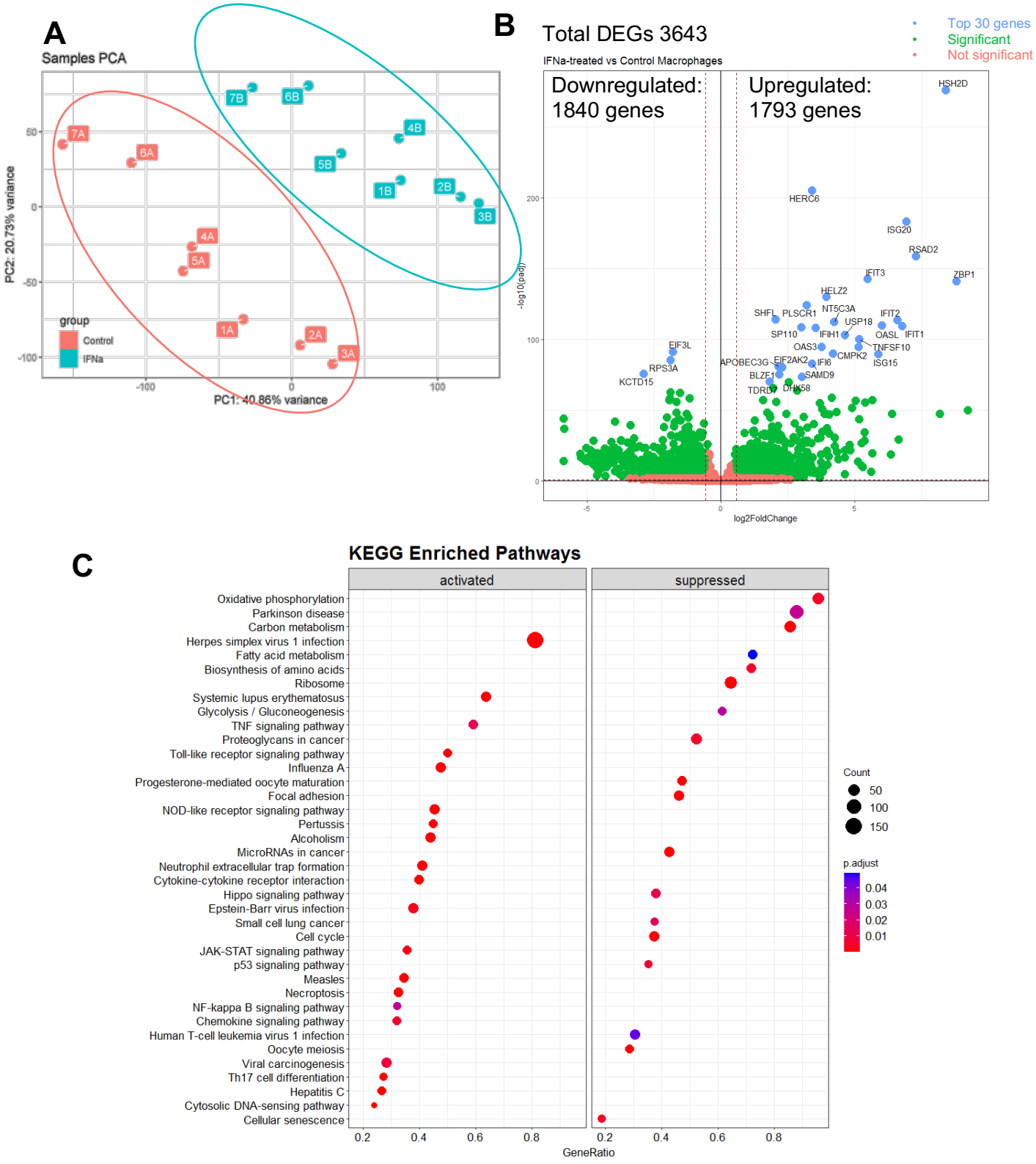

Figure 4.3. Transcriptomic analysis of IFN-I-treated macrophages
Human monocyte-derived macrophages were cultured with or without 1000U/ml IFN-α for 3 days. RNA-seq was performed to identify differential express genes (DEGs) and significantly enriched signalling pathways. (**A)** Unsupervised principal component analysis (PCA) plot for gene expression of untreated and IFN-I-treated cells. (**B)** Volcano plot showing upregulated and downregulated DEGs. (**C)** KEGG enriched pathway analysis. n = 7. The data generated from RNA-seq were kindly analysed and provided by Dr Norzawani Buang.

Changes in mitochondrial phenotypes upon chronic IFN-I exposure

To further understand how the metabolism of human macrophages changes upon the treatment, I next investigated the effects of prolonged IFN-I exposure on mitochondria metabolism. Firstly, to examine the effects of IFN-α on mitochondrial phenotypes, I stained the cells with mitochondrial-specific probes and assessed them by flow cytometry after 3 days of treatment. Mitochondrial mass, activity and membrane potential were observed using MTG, MTDR and TMRM dyes, respectively. The MFI of each staining is shown in **figure 4.4A**. IFN-α significantly decreased the MFI of MTG, suggesting reduced mitochondrial mass. No differences in mitochondrial activity and membrane potential were observed (**Fig.4.4A**). Next, I examined the mitochondrial ROS and cellular ROS production using MitoSox red and CellROS deep red dyes, respectively. The data demonstrated that mROS production was unchanged in IFN-I treated cells compared to the untreated group (**Fig.4.4B**). However, there was an increase in cROS production upon the treatment (**Fig.4.4B**).

I then examined the expression of mitochondrial DNA (mtDNA)-encoded genes *CYTB* and *ATP6*. These genes encode proteins involved in the electron transport complexes. Similar to the observations in $CD8^+$ T cells, IFN-I significantly decreased the gene expression level of *CYTB* and *ATP6* compared to untreated cells (**Fig.4.4C**).

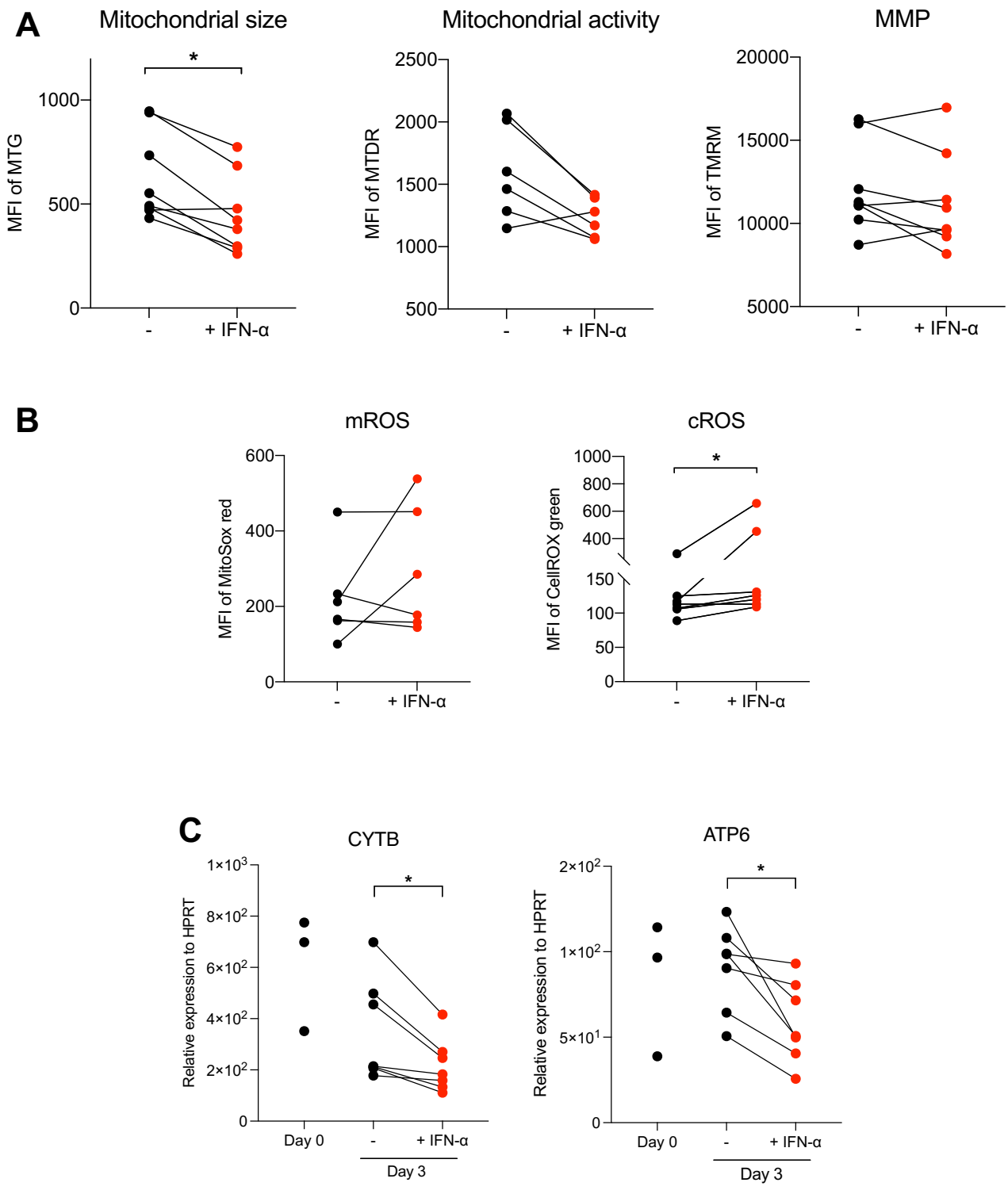

Figure 4.4. Mitochondrial phenotypes upon IFN-I treatment
Human monocyte-derived macrophages were cultured with or without 1000U/ml IFN-α for 3 days. (**A-B)** Cells were stained with specific mitochondrial probes and analysed by flow cytometry. (**A)** Summary graphs of MFI of MTG, MTDR and TMRM dyes showing mitochondrial mass, activity and membrane potential (MMP), respectively. (**B)** Summary graphs of MFI of MitoSox red and CellROX green dyes showing mitochondrial ROS and cellular ROS production, respectively. (**C**) Relative expression of mitochondria-derived OXPHOS genes CYTB and ATP6 was assessed using qPCR. Each dot represents one donor. Data presented as mean ± S.E.M. * $p<0.05$. Wilcoxon test.

Prolonged IFN-I exposure reduces glycolytic gene expression and glycolysis activity

It is known that the balance of NAD+ and NADH is crucial to sustaining metabolic events including OXPHOS and glycolysis pathways. Next, I investigated the alterations of mitochondrial functions in macrophages upon chronic IFN-I exposure. Firstly, I focused on the glycolysis pathway by measuring the expression of genes in glycolysis pathways using qPCR and determining ECAR value using Seahorse extracellular flux analyser.

Figure 4.5A illustrates the glycolysis pathway with the more relevant genes. I observed that IFN-I treatment did not change the expression of *HKII* (*Hexokinase II*), the first enzyme in the pathway (**Fig.4.5B**). Of note, the activity of the glycolysis enzyme *GAPDH* (*glyceraldehyde-3-phosphate dehydrogenase*) is dependent on NAD+ and NADH balance[291]. As expected, *GAPDH* expression was significantly reduced upon IFN-α exposure (**Fig.4.5C**). Interestingly, IFN-α treatment decreased the expression of *LDH* (*Lactate dehydrogenase*), the enzyme that converts pyruvate to lactate (**Fig.4.5D**), whereas the expression of *PDH* (*Pyruvate dehydrogenase*), the enzyme that converts pyruvate to acetyl-CoA, was significantly increased (**Fig.4.5E**). Furthermore, the expression of *PDK1* (*Pyruvate dehydrogenase kinase 1*), an inhibitor of *PDH*, was considerably reduced in IFN-α-treated MDMs (**Fig.4.5F**). The reduction of *LDH* expression prompted me to measure the production of lactate in the supernatant. Lactate is the initial by-product of aerobic glycolysis and is critical to maintaining glucose metabolism. As expected, I found that the production of lactate was reduced in IFN-α-treated HMDMs (**Fig.4.6C**). I then performed Seahorse extracellular flux analysis and measure ECAR, an indicator of glycolysis, at the basal state. Consistent with the decreased secretion of lactate, IFN-I significantly diminished basal ECAR, indicating the reduction of glycolysis (**Fig.4.6A** and **6B**). These data suggested that prolonged IFN-I exposure changed metabolism of macrophage by decreasing glycolytic gene expression and glycolysis activity.

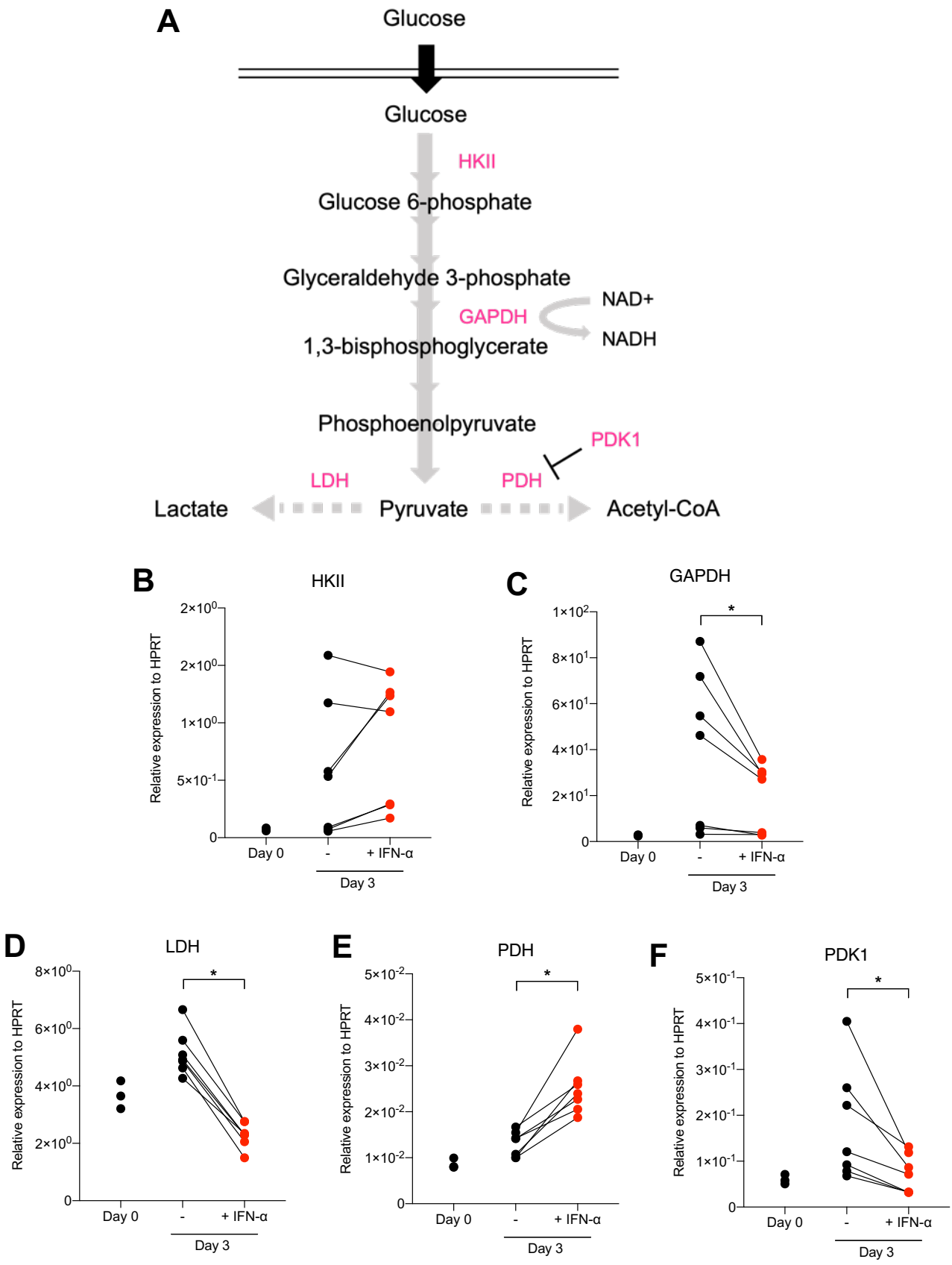

Figure 4.5. Changes in glycolysis gene expression upon IFN-I treatment
Human monocyte-derived macrophages were cultured with or without 1000U/ml IFN-α for 3 days. Relative expression of genes encoding enzymes in glycolysis pathway was measured by qPCR. (**A**) Schematic diagram of glycolysis pathway and key genes highlighted in pink. (**B-F**) Summary graphs of gene expression level of HKII **(B)**, GAPDH **(C)**, LDH **(D)**, PDH **(E)** and PDK1 **(F)**. Each dot represents one donor. Data presented as mean ± S.E.M. * $p<0.05$. Wilcoxon test.

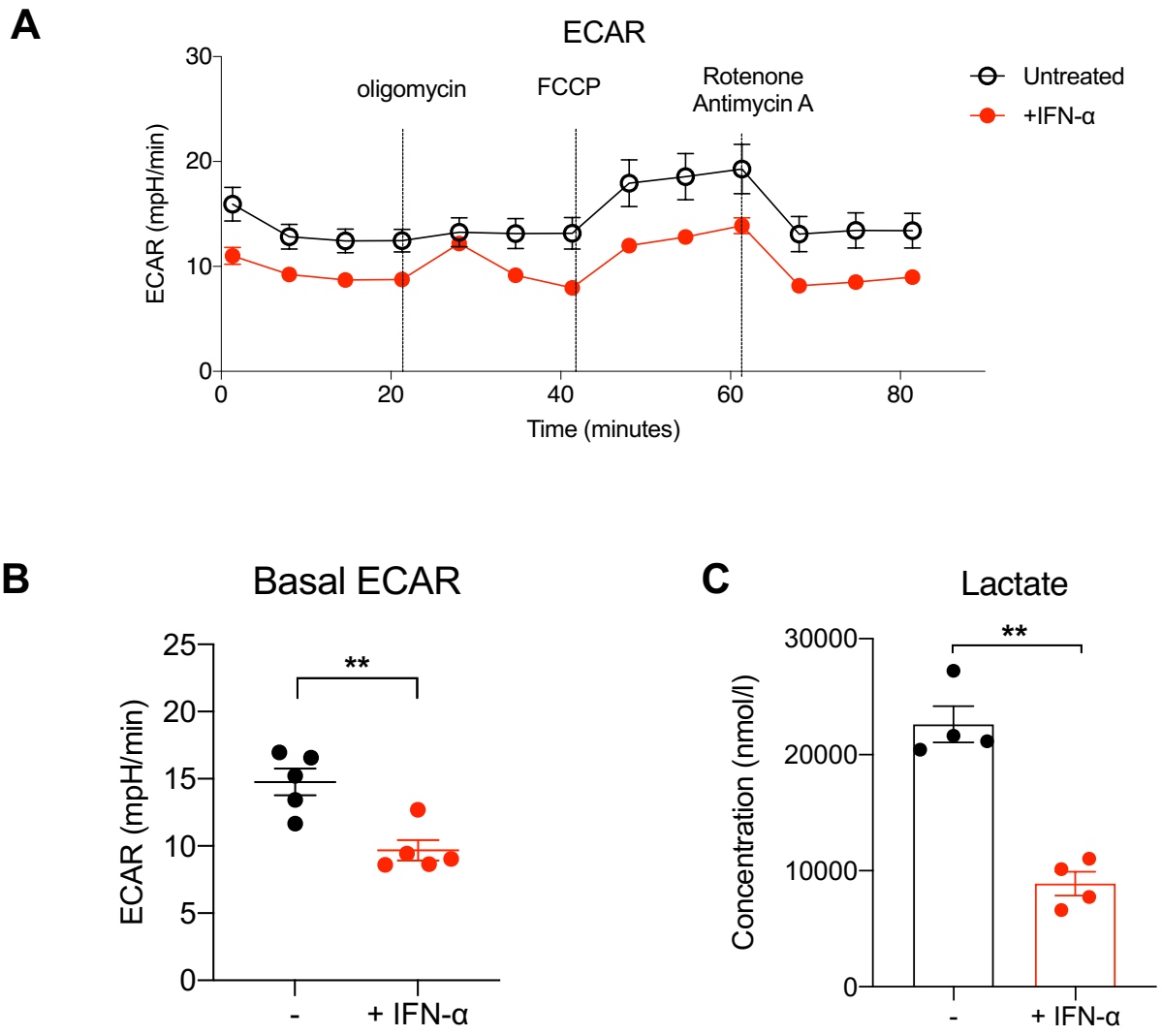

Figure 4.6. Changes in glycolysis activity upon IFN-I treatment
Human monocyte-derived macrophages were cultured with or without 1000U/ml IFN-α for 3 days. Glycolytic activity of macrophages was assessed using extracellular flux assay and lactate measurement. (**A**) Representative graph of extracellular acidification rate (ECAR) of untreated and IFN-I-treated macrophages (**B**) Summary graph of basal ECAR (**C**) Concentration of extracellular lactate. Each dot represents one donor. Data presented as mean ± S.E.M. ** $p<0.01$ Wilcoxon test.

Oxidative phosphorylation (OXPHOS) is not affected by prolonged IFN-I treatment

Next, I assessed the mitochondrial respiration upon IFN-I treatment by measuring OCR value, an indicator of OXPHOS activity at the basal state and in response to drugs that trigger mitochondrial stress. It allows me to determine the basal OCR, maximum OCR and SRC, which representing the capacity available in a cell to produce energy in response to increased metabolic demand. The data revealed that 3-day-IFN-α treatment had no effect on basal OCR (**Fig.4.7A** and **7B**), regardless of the reduction of glycolysis (**Fig.4.6B**). This metabolic shift led to a net increase in OCR/ECAR ratio (**Fig.4.7E**). Maximum OCR and SRC also remained unaffected by IFN-α (**Fig.4.7C** and **4.7D**). To determine whether IFN-I-induced metabolic reprogramming impacted the ability of macrophages to generate energy, ATP-linked respiration was calculated from this extracellular flux assay. No differences in ATP levels upon prolonged IFN-I treatment were noticed (**Fig.4.7F**). These data suggested that IFN-α treatment triggered a metabolic shift toward OXPHOS in human macrophages to maintain ATP levels for the cells.

So far data suggested that 3-day IFN-I-treatment induced metabolic reprogramming in human macrophages by inducing NAD consumption, reducing glycolysis, and increasing OXPHOS.

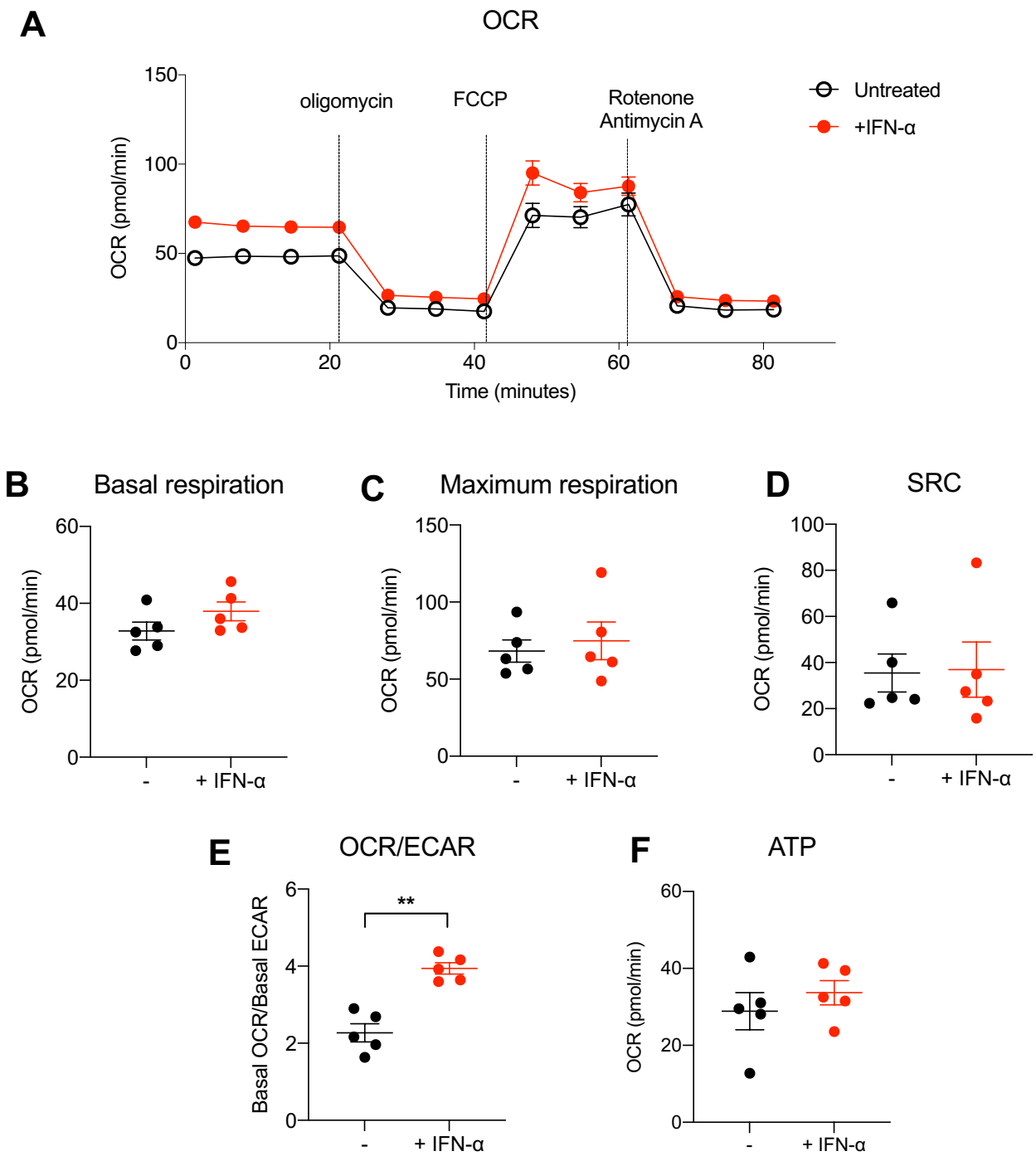

Figure 4.7. Changes in OXPHOS activity upon IFN-I treatment
Human monocyte-derived macrophages were cultured with or without 1000U/ml IFN-α for 3 days. Mitochondrial respiration of macrophages was then assessed using extracellular flux assay. (**A**) Representative graph of oxygen consumption rate (OCR) of untreated and IFN-I-treated macrophages. Oligomycin, carbonylcyanide p-trifluoromethoxyphenylhydrazone (FCCP), and Rotenone/antimycin A were added to the cells as indicated. Summary graphs of (**B**) basal respiration, (**C**) maximum respiration, (**D**) spare respiratory capacity, (**E**) ratio of basal OCR and basal ECAR and (**F**) ATP level**.** Each dot represents one donor. Data presented as mean ± S.E.M. ** p<0.01. Wilcoxon test.

Metabolomic analysis reveals that IFN-I treatment altered macrophage metabolomic profiles

To gain insights into the dynamic of metabolic changes in macrophages in response to IFN-I treatment, we next explored metabolite profiles of macrophages upon IFN-α treatment in a time-course manner. MDMs were treated with IFN-α for 8, 24 and 72 hours. Cells then were extracted and sent to collaborators to perform untargeted global metabolomic profiling using liquid chromatography-mass spectrometry (LC-MS). Since metabolites can be influenced by both biological and environmental factors, they provide great potential to bridge knowledge of genotype and phenotype[292]. This non-targeted approach will also offer an extensive list of identified small molecules that can be mapped to networks and pathways[292].

A comparison of relative intracellular metabolite abundance between untreated and IFN-I-treated cells at each time point was determined by differential metabolomic analysis (DMA). A total of 221 intracellular metabolites were found to be significantly different in the IFN-I-treated group by this analysis. For illustrative purposes, at each time point, the metabolites were highlighted in colour and the metabolic pathway that these metabolites belong to were also listed with the same colour as shown in **figure 4.8**.

At the 8-hour timepoint, IFN-I already influenced metabolites in NAD/NADH metabolism. For example, intracellular NAD was found to be reduced upon the treatment. Treatment of IFN-I also resulted in a reduction of an essential amino acid tryptophan and an increase in the downstream metabolites belonging to tryptophan degradation and kynurenine pathways such as formylkynurenine, kynurenine, picolinate and quinolinate (**Fig.4.8A**).

At the 24-hour timepoint, in addition to NAD/NADH metabolism and tryptophan degradation pathways, IFN-I treatment also affected metabolites associated with glycolysis and pentose phosphate pathway (**Fig.4.8B**). 24-hour IFN-I exposure increased short-chain and long-chain acylcarnitines (**Fig.4.8B**). Acylcarnitines act as carriers to transport activated short-chain or long-chain fatty acids into mitochondria for β-oxidation. Therefore, IFN-I-induced acylcarnitine accumulation possibly indicated incomplete fatty acid transportation or oxidation.

As shown in **figure 4.8C**, after 72 hours of the treatment, those previously mentioned pathways were still detected. Prolonged IFN-I exposure induced amino acid and vitamin catabolism pathways such as arginine metabolism and tyrosine and phenylalanine metabolism (**Fig.4.8C**).

Collectively, the overall results from differential metabolomic analysis confirmed that IFN-I treatment rewired metabolism in human macrophages. Furthermore, short-term and long-term IFN-I treatment induced different metabolomic profiles, highlighting the importance of the duration of the IFN-I exposure.

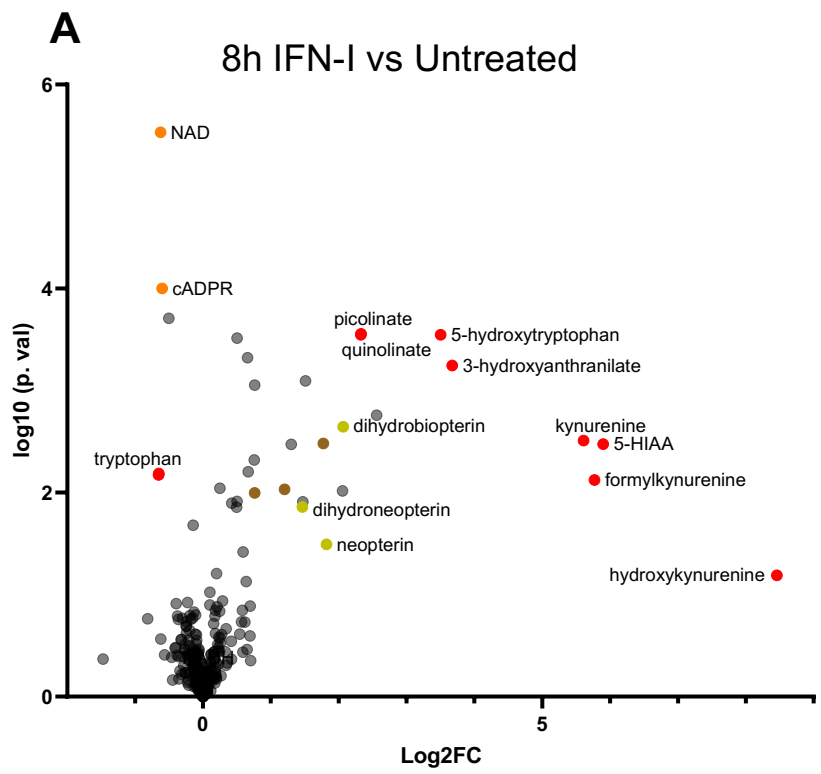

Tryptophan degradation and *de novo* NAD synthesis

NAD degradation

BH4 metabolism

Tyr/Phe degradation

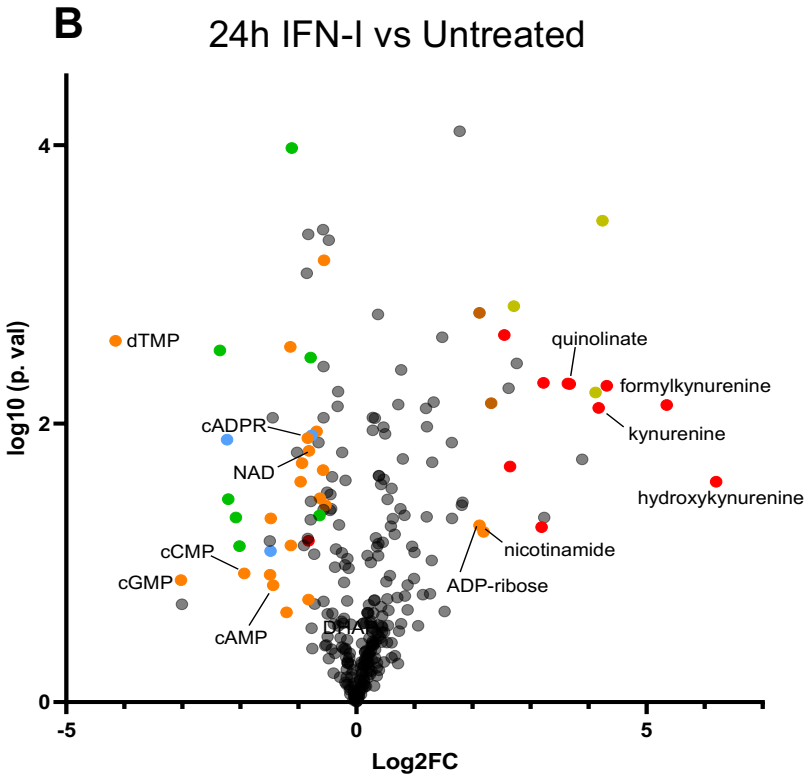

Tryptophan degradation and *de novo* NAD synthesis

NAD degradation

BH4 metabolism

Glycolysis and pentose phosphate pathway

SC- and LC-acylcarnitines

Tyr/Phe degradation

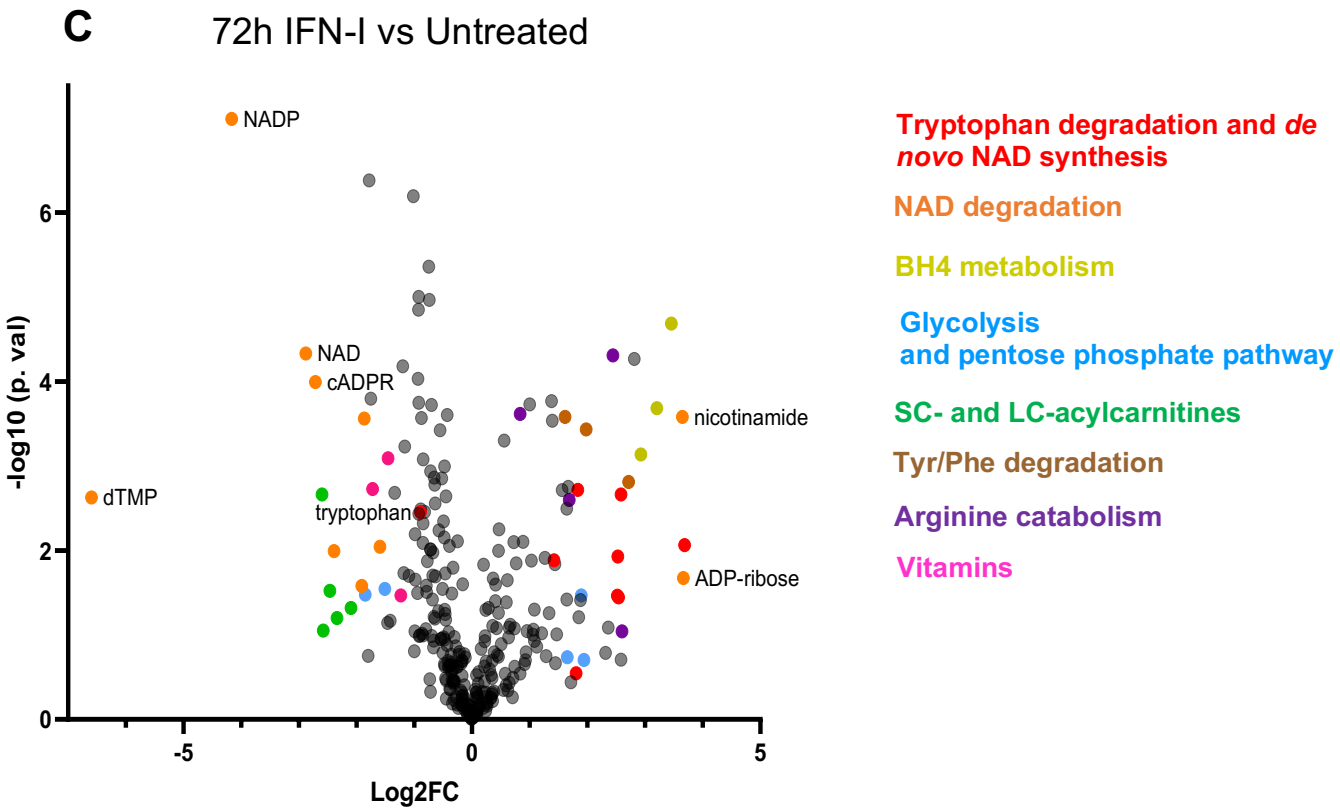

Figure 4.8. Effects of IFN-I treatment on metabolic profile of macrophages
Human monocyte-derived macrophages were cultured with or without 1000U/ml IFN-α for 8, 24 and 72 hours. Cells were extracted and global metabolomic profiling was performed using LC-MS. (**A-C)** Volcano plots showing the differentially abundant metabolites in untreated samples vs IFN-I-treated samples at different timepoints. The graphs show the relative abundance of each metabolite against its statistical significance, respectively reported as Log2FC and −log10 (*p*-value), at (**A**) 8 hours, (**B**) 24 hours, and (**C**) 72 hours after treatment. Each colour represents metabolites that belong to the metabolic pathway listed in the same colour. Log2FC = Log2-Fold change. The data generated from global metabolomic profiling were kindly analysed and provided by Dr Ming Yang.

Cellular NAD+ level is decreased in IFN-I-treated macrophages

Next, I further analysed prominent pathways that significantly changed over the time course of IFN-I treatment. The first pathway was NAD+ and NADH metabolism. Intermediates of NAD+ and NADH metabolism and the expression of gene-encoding enzymes involved in the NAD+ consumption and NAD+ synthesis pathway was assessed. As shown in **figure 4.9**, among NAD+ consumer enzymes, *CD38* was upregulated at the earlier time point (8 hours) when compared to *SIRT1* (at 24 hours) (**Fig.4.9B**). As a result, intracellular NAD+ was gradually downregulated upon the treatment in a time-dependent manner and was significantly reduced compared to the untreated group at the 72-hour timepoint (**Fig.4.9A**). A similar trend was also observed in the NADH level. However, the ratio of NAD to NADH remained unchanged over the time course of the experiment (**Fig.4.9A**).

The metabolomic analysis also showed that NAD synthesis pathways were activated with IFN-I treatment, indicating that human macrophages tried to compensate for the loss of NAD. The two NAD synthesis pathways affected by IFN-I were NAD salvage and *de novo* NAD synthesis. As demonstrated in **figure 4.10**, nicotinamide which is the precursor to generate NAD via the NAD salvage pathway was progressively accumulated with the treatment (**Fig.4.10A**). The gene expression of *NAMPT*, a rate-limiting step enzyme in the NAD salvage pathway, was also upregulated starting at 8-hour timepoint (**Fig.4.10B**). In addition, IFN-I exposure also increased the expression of *IDO1* which is a key enzyme in the *de novo* NAD synthesis pathway at the early time point before it gradually went down at 24 and 72-hour time points (**Fig.4.10D**). This enzyme catalyses tryptophan into the kynurenine pathway. As a result, intracellular tryptophan was decreased over the time course of IFN-I treatment and significantly reduced after 3-day of treatment (**Fig.4.10C**), possibly indicating that IFN-I-treated cells tried to synthesise the new NAD molecule through the degradation of tryptophan.

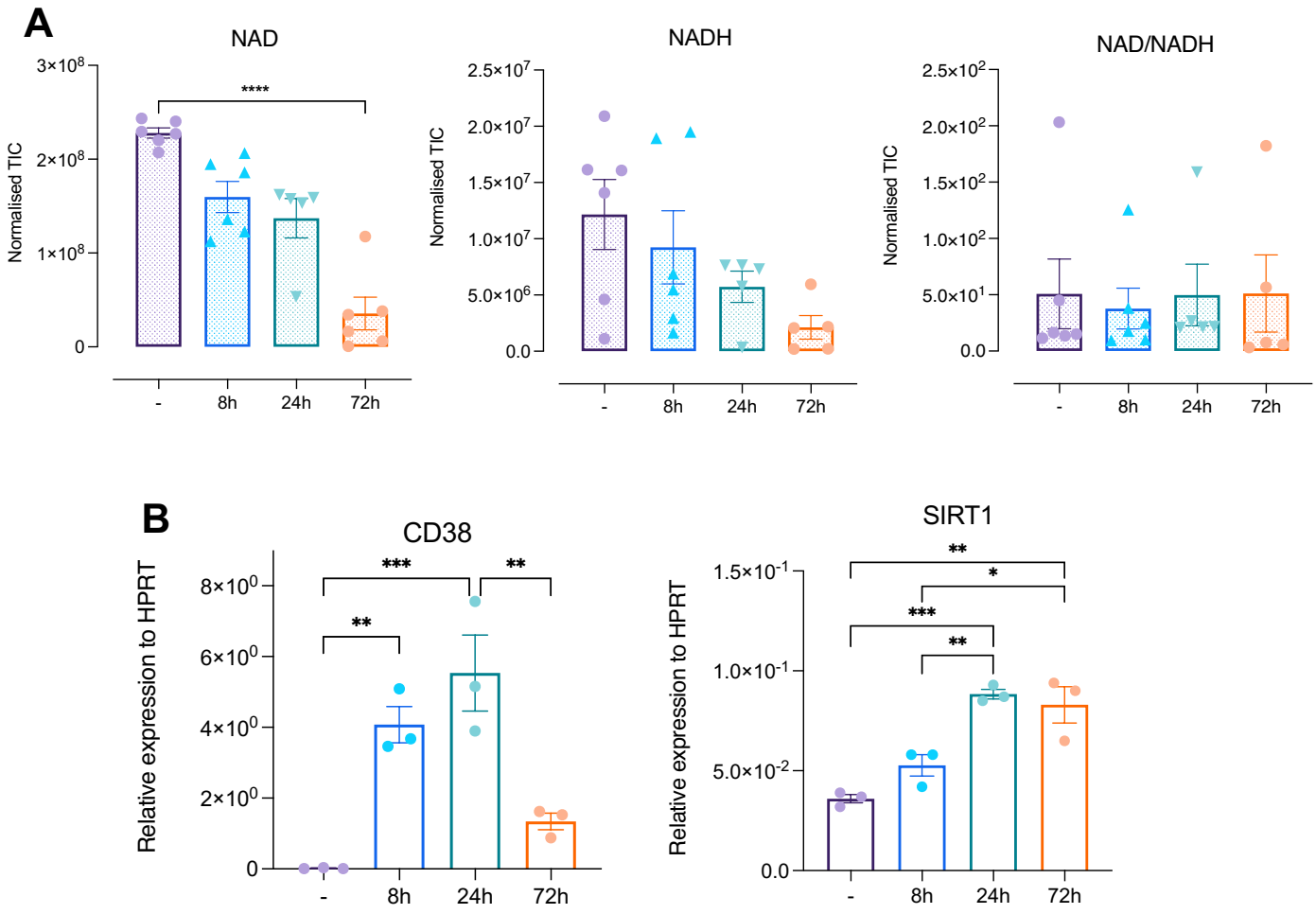

Figure 4.9. Analysis of metabolites and genes associated with the NAD metabolism
Human monocyte-derived macrophages were cultured with or without 1000U/ml IFN-α for 8, 24 and 72 hours. (**A**) Cells were extracted and global metabolomic profiling was performed using LC-MS. Summary graphs depicting level of intracellular NAD, NADH and the ratio of NAD to NADH are shown as normalised total ion count (TIC) (**B**) Relative expression of NAD consumer genes CD38 and SIRT1 at different timepoints was analysed using qPCR. Each dot represents one donor. Data presented as mean ± S.E.M. * p<0.05, ** p<0.01, *** p<0.001, **** p<0.0001. Kruskal-Wallis test for (**A**) and One-way ANOVA for (**B**).

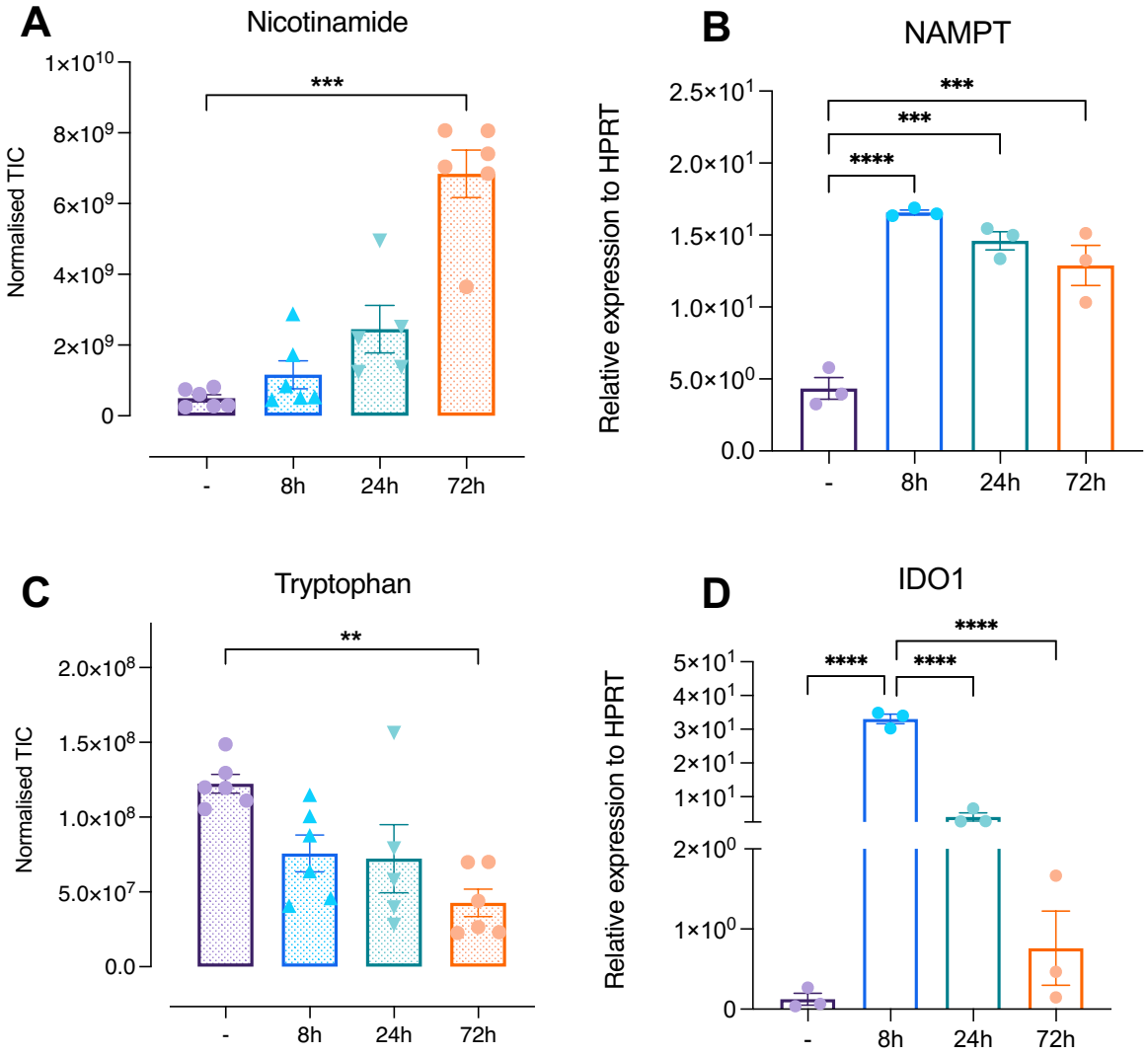

Figure 4.10. Analysis of metabolites and genes associated with the NAD synthesis pathway. Human monocyte-derived macrophages were cultured with or without 1000U/ml IFN-α for 8, 24 and 72 hours. Cells were extracted and global metabolomic profiling was performed using LC-MS. The gene expression was assessed using qPCR. (**A-B**) Summary graphs depicting intracellular nicotinamide (**A**) and gene expression of NAMPT enzyme (**B**). (**C-D**) Summary graphs of *de novo* NAD synthesis pathway, depicting intracellular tryptophan (**C**) and gene expression of IDO1 enzyme (**D**). Each dot represents one donor. Data presented as mean ± S.E.M. ** p<0.01, *** p<0.001, **** p<0.0001. Kruskal-Wallis test.

IFN-I exposure activates the tryptophan-kynurenine pathway to compensate for the reduction of NAD in macrophages

As previously demonstrated in **figure 4.10**, the reduction of tryptophan together with the increase of *IDO1* expression compelled me to further analyse metabolites involved in the tryptophan-kynurenine pathway. **Figure 4.11A** shows the simplified diagram demonstrating key metabolites and enzymes in the tryptophan and kynurenine pathways that were assessed in this analysis. As expected, I found that IFN-I-treated macrophages catabolised tryptophan toward the kynurenine pathway. The gene expression of *KYNU* was drastically increased after 8 hours of IFN-I treatment (**Fig.4.11F**). Consistently, there was a significant increase in kynurenine (**Fig.4.11B**) and 3-hydroxyanthranilic acid (**Fig.4.11C**) at the early time point. These metabolites were then gradually reduced later as they were used to generate the downstream metabolites including picolinic (**Fig.4.11D**) and quinolinic acid (**Fig.4.11E**). After 72 hours of IFN-I exposure, the level of quinolinic acid was reduced compared to 8 and 24-hour timepoint (**Fig.4.11E**) and the gene expression of *QPRT*, enzyme that converts quinolinic acid to NAD was significantly increased (**Fig.4.11G**). These data suggested that quinolinic acid was being used to generate NAD in IFN-I-treated macrophages.

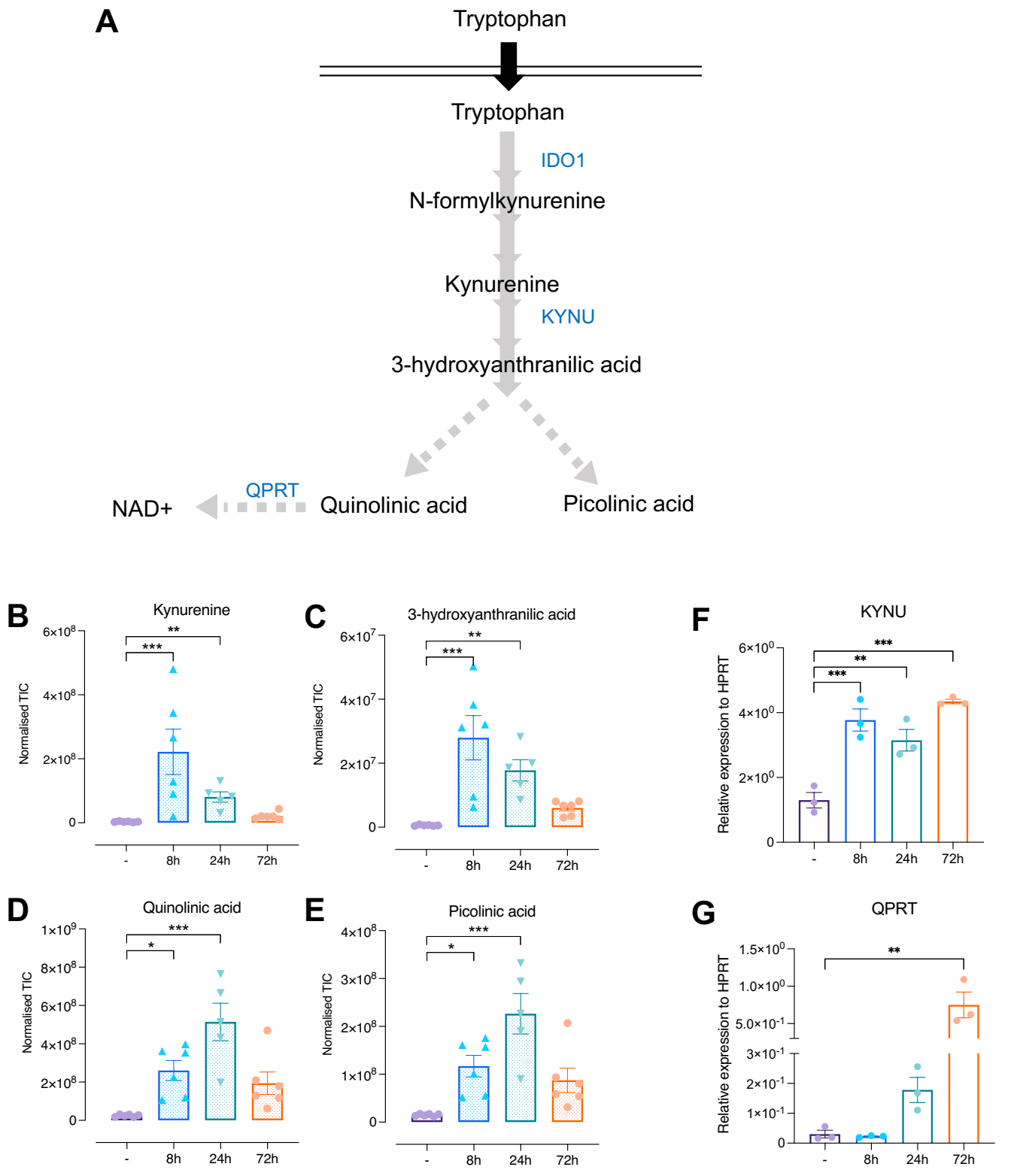

Figure 4.11. Analysis of metabolites and genes associated with the tryptophan degradation pathway. Human monocyte-derived macrophages were cultured with or without 1000U/ml IFN-α for 8, 24 and 72 hours. Cells were extracted and global metabolomic profiling was performed using LC-MS. Relative gene expression was assessed using qPCR. (**A**) Schematic diagram of tryptophan degradation pathway and key genes highlighted in blue (**B-E**) Summary graphs of metabolites kynurenine (**B**), 3-hydroxyanthranilic acid (**C**), quinolinic acid (**D**) and picolinic acid (**E**). (**F-G**) Summary graphs of relative expression of genes encoding KYNU (**F**) and QPRT (**G**). Each dot represents one donor. Data presented as mean ± S.E.M. * p<0.05, ** p<0.01, *** p<0.001. Kruskal-Wallis test.

IFN-I exposure does not change TCA cycle and ATP levels in macrophages

TCA cycle is known to be the preparation step for OXPHOS. It is a process whereby acetyl-CoA is modified to produce energy precursors which are then used to transport electron to generate ATP in ETC. It has been shown that macrophages treated with some cytokines such as IFN-γ together with LPS stimulation exhibit a broken TCA cycle leading to accumulation of citrate and succinate which can impact macrophage functions[293].

To further understand whether IFN-I treatment can affect the TCA cycle, I then examined changes in metabolites associated with the TCA cycle including acetyl-CoA, citrate, α-ketoglutarate, succinate, fumarate and malate. The results revealed that there was a reduction in the normalised total ion count of acetyl-CoA (**Fig.4.12A**) and no major difference in citrate (**Fig.4.12B**). Interestingly, an increase in α-ketoglutarate (**Fig.4.12C**) was detected, suggesting that cells utilised other metabolic pathways to supply a key substrate in TCA cycle. A similar trend was observed in the downstream metabolites including succinate (**Fig.4.12D**), fumarate (**Fig.4.12E**), and malate (**Fig.4.12F**). These findings suggested that the TCA cycle in IFN-I-treated cells remained intact and functioning. As expected, the ATP level was also unaffected by the treatment (**Fig.4.12G**). Of note, the metabolomic profiling was consistent with the observations from the seahorse extracellular flux assay.

Together, these results from global metabolomic profiling demonstrated that IFN-I induced metabolomic reprogramming by inducing NAD consumption. The depletion of NAD+ was then compensated with rapid and substantial *de novo* NAD synthesis via the tryptophan-kynurenine pathway. Furthermore, TCA cycle activity and ATP level remained unchanged.

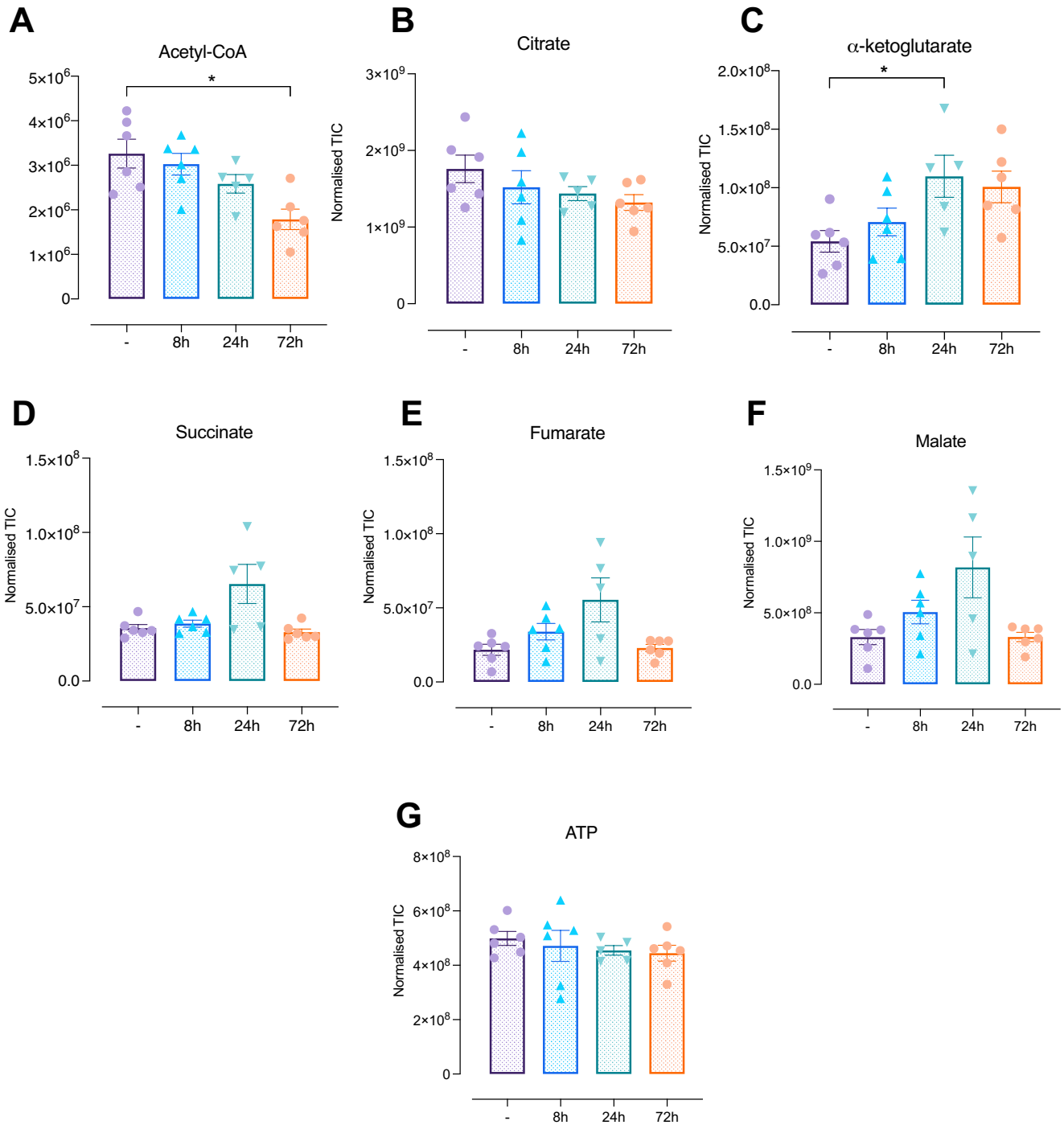

Figure 4.12. Analysis of metabolites associated with TCA cycle.
Human monocyte-derived macrophages were cultured with or without 1000U/ml IFN-α for 8, 24 and 72 hours. Cells were extracted and global metabolomic profiling was performed using LC-MS. Summary graphs showing normalised TIC of intracellular metabolites in TCA cycle (**A**) Acetyl-CoA (**B**) Citrate, (**C**) α-ketoglutarate, (**D**) Succinate, (**E**) Fumarate, (**F**) Malate, and (**G**) ATP. Each dot represents one donor. Data presented as mean ± S.E.M. * $p<0.05$. Kruskal-Wallis test.

Prolonged IFN-I exposure changes morphology, does not induce cell death but reduces cell proliferation of macrophages

The data so far suggested that prolonged IFN-I exposure induced changes in transcriptome and metabolome, including mitochondrial changes. Accumulating evidence indicates that metabolic reprogramming of immune cells is an important determinant of their functions[294]. Next step was to explore whether chronic IFN-I exposure influenced macrophage morphologies and functions.

After 3 days of IFN-α treatment, the first difference I noticed when monitoring the cells under a light microscope at 100X magnification was the cellular morphology. MDMs exhibited a round form and floated in IFN-I condition, whereas the untreated cells remained in elongated shape and attached to the cell culture plate (**Fig.4.13A**). Next, I investigated whether the floating cells were a sign for apoptotic cell death upon IFN-I exposure by staining the cells with Annexin V and PI solution. As shown in **figure 4.13B**, the percentages of Annexin V negative and PI negative cells which represented alive cells were similar across samples. These results suggested that 3-day IFN-I treatment did not induce cell death but possibly changed the adhesion properties of macrophages instead.

Studies have shown that IFN-I has an anti-proliferative effect on immune cells[295,296]. To understand whether prolonged IFN-I treatment affected cell proliferation, I then assessed the expression of proliferation marker Ki-67 using flow cytometer and RNA-sequencing analysis. As shown in **figure 4.13C**, there was a significant reduction of MFI of Ki-67 as well as a decrease in the normalised count of Ki-67 gene expression (**Fig.4.13C**). Consistent with the literature, prolonged IFN-I treatment diminished the cell proliferation of human macrophages.

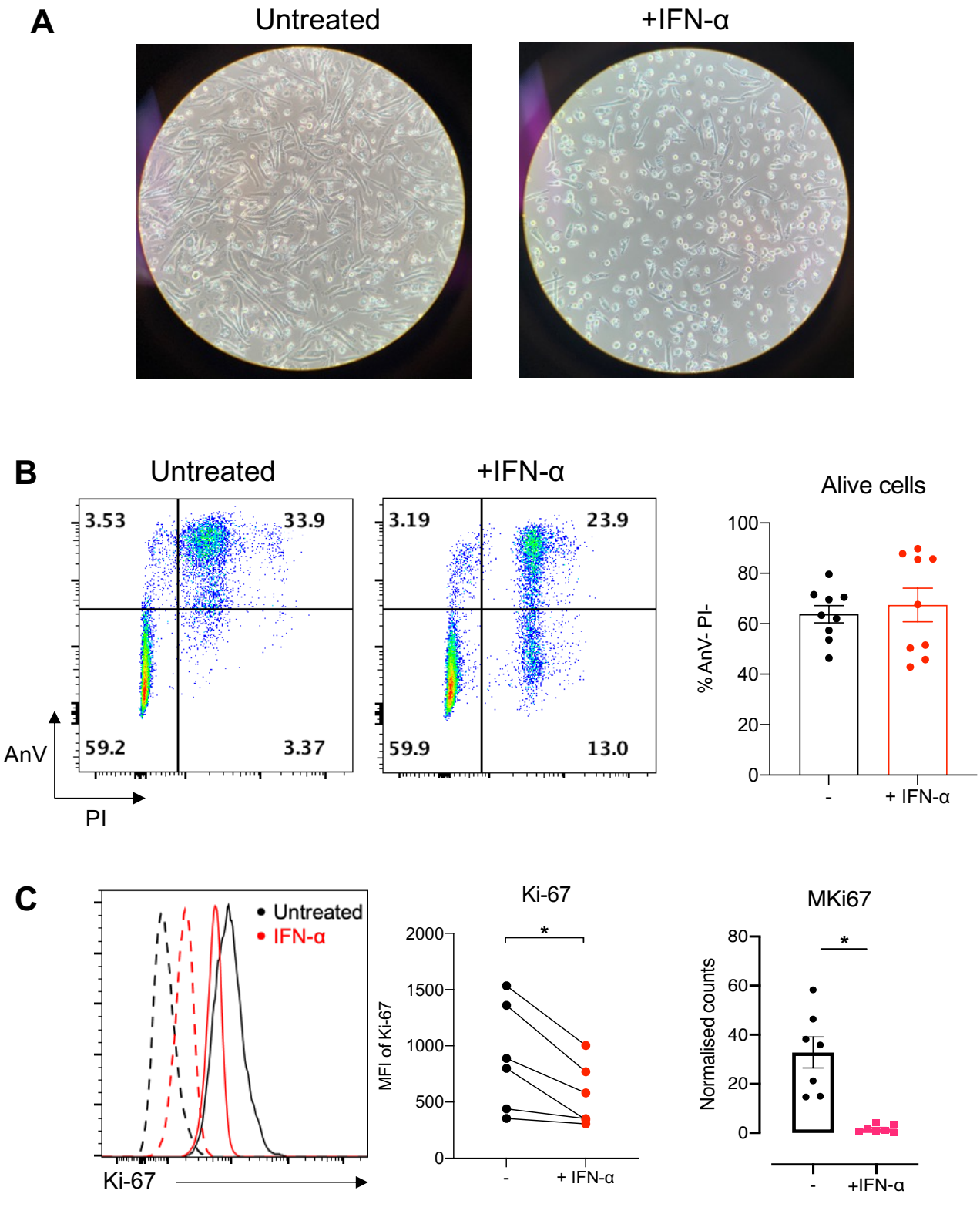

Figure 4.13. Morphology and cell viability of macrophages upon prolonged IFN-I exposure. Human monocyte-derived macrophages were cultured with or without 1000U/ml IFN-α for 3 days. (**A**) Macrophage morphology monitored under light microscope at 100X magnification. (**B**) Representative dot plots of AnV/PI staining and summary graph showing the percentage of alive cells ($AnV^{-}PI^{-}$). (**C**) Representative histogram of proliferation marker Ki-67 staining; dot line refers to fluorescent minus one control of each condition, summary graph showing MFI of Ki-67 and the normalised counts of Ki-67 gene from RNA-seq analysis. Each dot represents one donor. Data presented as mean ± S.E.M. * $p<0.05$. Wilcoxon test.

Prolonged IFN-I exposure induces a pro-inflammatory phenotype

Previous studies have shown that macrophages from SLE patients exhibit imbalanced polarisation and this can contribute to the development of SLE[297]. For example, the presence of macrophages with an M1 proinflammatory phenotype is correlated with disease activity[298]. However, whether chronic IFN-I exposure contributes to macrophage polarisation in SLE remains unclear.

To explore how long-term IFN-I treatment affects macrophage phenotypes, macrophage polarisation was assessed using bulk RNA sequencing, RT-qPCR, flow cytometry and ELISA. Heatmap analysis from RNA-sequencing revealed that prolonged IFN-α treatment induced a pro-inflammatory gene signature accompanied by a reduction in the expression of anti-inflammatory genes (**Fig.4.14A**). Consistently, I found that IFN-I treatment significantly increased the expression of pro-inflammatory surface markers such as CD80 and CD86 (**Fig.4.14B**). In addition, IL-6 secretion by IFN-I-treated macrophages was dramatically enhanced compared to the untreated group (**Fig.4.14D**). Though the amount of other pro-inflammatory cytokines such as IL-1β and TNF-α was undetectable by ELISA, the gene expression levels of both cytokines were significantly increased by IFN-I treatment (**Fig.4.14D**). In contrast, the protein expression of anti-inflammatory markers such as CD206 and CD163 was decreased upon the treatment (**Fig.4.14C**). Collectively, the data showed that prolonged IFN-I treatment polarised human macrophages toward a pro-inflammatory phenotype.

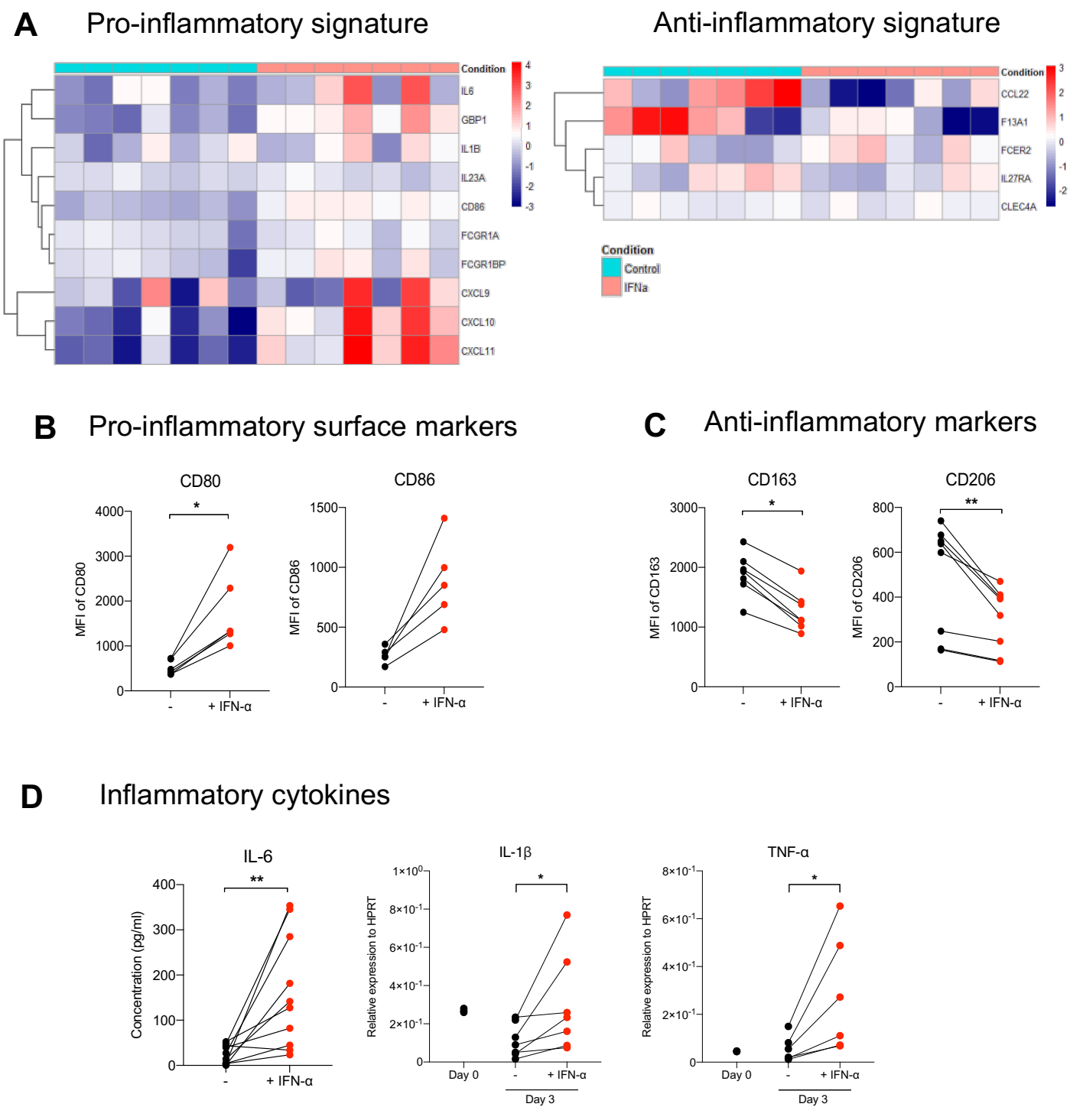

Figure 4.14. Macrophage polarisation upon prolonged IFN-I exposure
Human monocyte-derived macrophages were cultured with or without 1000U/ml IFN-α for 3 days. (**A**) Heatmap analysis of gene signature for macrophage polarisation from RNA-seq analysis. (**B-C**) Expression of polarisation surface markers was measured by flow cytometry. (**B**) Summary graphs showing MFI of pro-inflammatory markers CD80 and CD86. (**C**) Summary graphs showing MFI of anti-inflammatory markers CD163 and CD206. (**D**) Summary graphs showing the production of inflammatory cytokines IL-6, IL-1β and TNF-α. The concentration of IL-6 was measured by ELISA. The relative gene expression of IL-1β and TNF-α was assessed by qPCR. Each dot represents one donor. Data presented as mean ± S.E.M. * p<0.05, ** p<0.01. Wilcoxon Test. Heatmap analysis was kindly generated by Dr Norzawani Buang.

Prolonged IFN-I exposure compromises cell viability strictly upon TLR4 challenge

Several studies have shown defective phagocytosis in macrophages from SLE patients[33]. Therefore, I next explored the effects of chronic IFN-I exposure on macrophage phagocytosis. To assess this, after 3 days of IFN-I treatment MDMs were cultured with latex beads coated with FIT-C labelled IgG for 30 minutes. The uptake of fluorescent beads was detected using flow cytometry. As illustrated in **figure 4.15**, there was a downward trend in MFI of IgG-FIT-C in IFN-I-conditioned macrophages, albeit not significant (**Fig.4.15A** and **15B**).

Next, I wanted to understand how IFN-I-primed macrophages respond to further stimuli such as those triggered by pathogens. To begin with, after culturing MDMs with IFN-α for 3 days I then stimulated these cells with 1ng/ml LPS for 3 hours. The cell viability was first assessed using annexin V and PI staining. Surprisingly, the data revealed that IFN-I-conditioned macrophages showed a striking decrease in cell viability compared to the untreated and unstimulated cells (**Fig.4.15C**). This prompted me to determine whether this effect could be observed with other TLRs. I then stimulated the cells with poly I:C (TLR3 agonist) or R848 (TLR7/8 agonist) or CpG (TLR9 agonist). 3 hours after the challenge, the percentage of alive cells in IFN-I-primed condition remained the same as in the untreated and unstimulated cells (**Fig.4.15D**). I observed similar results after 8 hours (**Fig.4.15D**). In summary, these data suggest that chronic IFN-I treatment impairs the phagocytosis capacity of the macrophages and cell viability is compromised only upon TLR4 stimulation.

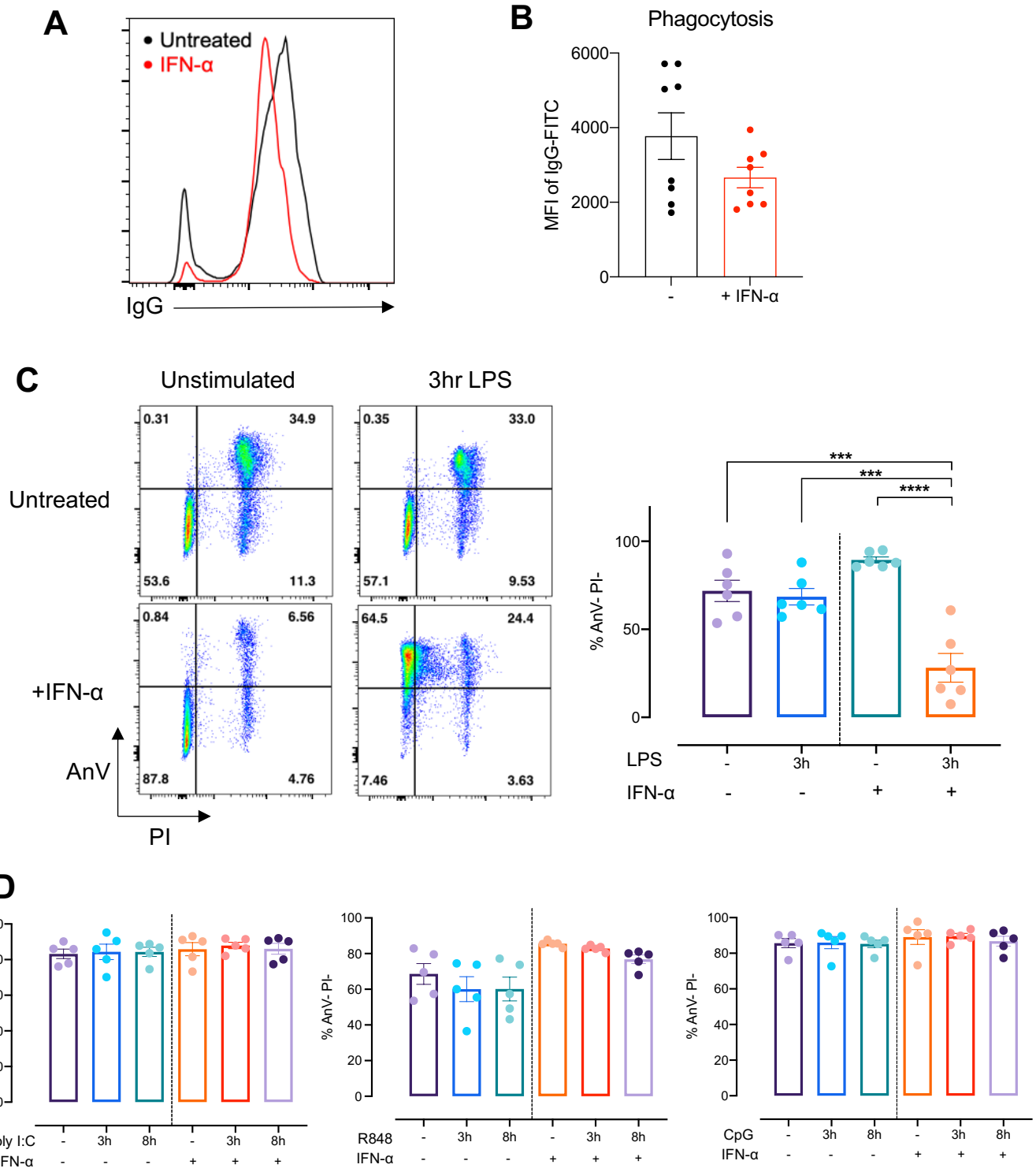

Figure 4.15. Macrophage functions upon prolonged IFN-I treatment
Human monocyte-derived macrophages were cultured with or without 1000U/ml IFN-α for 3 days. (**A-B**) Phagocytic capacity of macrophages was assessed by flow cytometry after incubating the cells with latex beads coated with IgG-FIT-C in 1:250 dilution for 30 minutes. (**A**) Representative histogram of IgG-FITC. (**B**) Summary graph of MFI of IgG-FITC. (**C-D**) After 3 days of IFN-α treatment, cells were stimulated with different TLR stimuli (1ng/ml LPS for TLR4, 10μg/ml Poly I:C for TLR3, 100ng/ml R848 for TLR7/8 and 7.5 μg/ml CpG for TLR9) for 3 or/and 8 hours. Cell viability was assessed by AnV/PI staining and flow cytometry. (**C**) Representative dot plots of AnV/PI and summary graph showing percentage of alive cells after 3 hours of LPS re-challenge. (**D**) Summary graphs of percentage of alive cells upon TLR3, TLR7/8 and TLR9 stimulation after 3 and 8 hours. Each dot represents one donor. Data presented as mean ± S.E.M. *** p<0.001, **** p<0.0001. One-way ANOVA.

4.3. Discussion

Macrophages are recognised to contribute to the pathophysiology of SLE and recent investigations have shown that the NAD pathway is essential for macrophage activity[299,300]. The relationship between IFN-I signalling and macrophage metabolism has primarily been studied in the setting of viral and bacterial infections and the outcomes of the IFN-I response are largely context specific[301]. However, most of the reported experimental setups have been carried using IFN-β and for a short period (less than 48 hours). Only one study in 2007 reported the long-term effects of IFN-I treatment (up to 14 days) on the tryptophan pathway[302]. Therefore, little is known about the effects of long-term IFN-I treatment on human macrophage metabolism. To explore this, I treated HMDMs from healthy buffy coats with 1000U/ml IFN-α for 72 hours (3 days) and used a wider range of techniques including RNA-sequencing, metabolomic profiling, extracellular flux analysis. Overall, I demonstrated that chronic IFN-I exposure (72 hours) triggered a metabolic reprogramming in HMDMs by increasing NAD consumption, increasing tryptophan catabolism, downregulating fatty acid metabolism and glycolysis but still maintaining OXPHOS and ATP. Furthermore, I found that chronic IFN-I treatment shifted macrophage phenotypes towards a pro-inflammatory-like phenotype, and compromised cell viability upon TLR4 re-challenge.

Recent research indicates that macrophage metabolic changes happen at the transcriptomic level relatively early in the process of activation and functional polarisation[303-305]. Literature has shown that short-term stimulation of IFN-I can alter the metabolic gene signature of macrophages[289]. Using microarray to assess transcriptomic profiles, Ahmed et al. have demonstrated that 4 hours of IFN-α stimulation induces an increase in the expression of genes associated with increased OXPHOS activity and antioxidant production and a decrease in the expression of genes related to branched-chain amino acid catabolism and fatty acid β-oxidation[289]. In this chapter, I have reported the effects of prolonged IFN-I exposure on the metabolic gene signature of human macrophages. Differently from the findings in short-term IFN-I conditions, using enriched pathway analysis from RNA-seq data, I observed the downregulation of the glycolysis, OXPHOS, and fatty acid metabolism pathways. Furthermore, apoptosis pathways were also upregulated with the treatment, suggesting a metabolic shutdown of the cells.

However, it is worth noting that the relationship between gene expression and function is complex. While transcriptomic data can provide valuable clues about the cellular processes and pathways that are affected, they should always be interpreted in the context of other types of data. Therefore, I employed functional and metabolic assays to better understand the metabolomic changes in response to prolonged IFN-I treatment. These assays included Seahorse extracellular flux assay, NAD and NADH colourimetric assay and global metabolomic profiling using LC-MS. With the global metabolomic profiling, I opted to treat HMDMs with IFN-I at different time points (8, 24 and 72 hours) to better understand the dynamic of how IFN-I affects macrophage metabolism.

My data showed a link between chronic IFN-I signalling and NAD metabolism in human macrophages. I demonstrated that prolonged IFN-I treatment increases the gene expression of NAD-consuming enzymes including *CD38* and *SIRT1* leading to a decrease in NAD levels. Although a trend of decrease in NAD could be seen at the earliest time point (8 hours), long-term IFN-I treatment was necessary to significantly lower NAD levels in macrophages. Furthermore, several NAD synthesis pathways, including the NAD salvage and the de novo pathway, were activated with the long-term IFN-I treatment, suggesting that macrophages were trying to compensate for the loss of NAD. Of note, the ratio of NAD to NADH was unaffected. The negative effect of IFN-I treatment on NAD level has been described previously in $CD8^+$ T cells from SLE patients[248]. The effects of IFN-I on NAD metabolism have also been reported in other diseases. In pancreatic ductal adenocarcinoma, Moore and their colleagues found that 24 hours of IFN-β treatment upregulated the expression of NAD-consuming enzymes PARP9, 10 and 14, but not CD38, leading to a reduction of NAD level in the pancreatic cancer cell lines and in a mouse model[306]. Similar to my results, this reduction of NAD was accompanied by an elevated expression of NAMPT, the key enzyme in the NAD salvage pathway, making these cells sensitised to the NAMPT inhibitor which stopped the proliferation of these pancreatic cancer cells[306]. Furthermore, it was recently discovered that COVID-19 infection caused an IFN response that negatively impacted the cellular NAD+ state by enhancing NAD consumption through the PARPs enzyme group[307]. These findings suggest that IFN-I signalling controls NAD metabolism through the upregulation of several NAD-consuming enzymes depending on the types of cells and the experimental conditions.

Declined NAD level has been linked to several diseases and researchers have proposed the use of NAD supplements to treat autoimmune diseases such as type 2 diabetes[308] and multiple sclerosis[309]. In SLE, dysregulation of NAD and NADH production was also reported. By measuring changes in NADH fluorescence, Bogaczewicz and their colleagues reported a reduction of NADH in the skin of SLE patients[310]. Analysis of NAD+ metabolic intermediates in monocytes from inactive lupus patients revealed increased levels of NAD+ and NMN together with signs of increased NAD+ consumption typified by increased levels of ADPR and elevated expression of NAD-consuming genes such as *CD38*, *PARP9* and *PARP10* when compared to monocytes from healthy individuals[311]. My findings underscore the role of chronic IFN-I in causing the decline in NAD that has been observed in SLE.

It is noted that the balance of NAD+ and NADH is important for maintaining metabolic events including OXPHOS and glycolysis pathway, especially the activity of the glycolysis enzyme GAPDH[291]. As expected, I found that chronic IFN-I exposure downregulated *GAPDH* gene expression while the expression of the gene encoding the upstream enzyme *HKII* was not affected. Interestingly, IFN-α treatment also decreased the expression of *LDHA*, the enzyme that converts pyruvate to lactate, whereas the expression of *PDH*, an enzyme that converts pyruvate to acetyl CoA, was significantly increased. Furthermore, the expression of *PDK1*, an inhibitor of PDH, was considerably reduced in IFN-α-treated HMDMs. These data suggest that pyruvate generated from glycolysis may enter the TCA cycle instead of being converted to lactate. I also found a decrease in glycolysis activity as demonstrated by a significant reduction of ECAR value and extracellular lactate concentration. This was consistent with IFN-I-mediated glycolysis reduction in $CD8^+$ T cells from the previous chapter. Furthermore, the downregulation of glycolysis in macrophages upon IFN-I has previously been described by Olson and their colleagues. They discovered that IFN-I signalling in mouse macrophages correlated with decreased glycolysis and mitochondrial damage during Mycobacterium tuberculosis (Mtb) infection[290]. Numerous investigations of extracellular metabolites present in the serum of SLE patients also seem to indicate that glycolysis is downregulated. However, more research is needed to determine if the IFN-I-induced downregulation of glycolysis was directly related to NAD metabolism.

Effects of IFN-Is on OXPHOS are known to vary and cell-specific. In pDCs, IFN-I was shown to upregulate OXPHOS and FAO activity leading to increased ATP and facilitating pDC activation[230]. On the other hand, the study conducted in B cell lines showed that IFN-I reduced OXPHOS activity leading to decreased cell proliferation[233]. Surprisingly, little is known about IFN-I signalling on the OXPHOS activity of macrophages. Olson and colleagues demonstrated that Mtb-induced IFN-I signalling decreased mitochondrial respiration in mouse bone marrow-derived macrophages (BMDMs). IFN-I was also shown to induce breaks in the TCA cycle, shifting innate immune cell metabolism from OXPHOS to aerobic glycolysis[228,312]. Furthermore, IFN-I has been reported to control the intracellular α-ketoglutarate and succinate ratio by inhibiting isocitrate dehydrogenase activity in LPS-stimulated BMDMs[313]. Differently from these reports, I found that regardless of the downregulation of glycolysis upon chronic IFN-I exposure, OXPHOS activity in human macrophages was not affected as indicated by similar OCR values to the untreated group. Metabolomic profile data revealed that α-ketoglutarate, which is a key substrate of the TCA cycle that can be obtained through the glutamine pathway, was increased upon IFN-I treatment. This suggests that IFN-I treatment may activate other pathways to maintain the TCA cycle and OXPHOS activity[314]. Furthermore, there was no major difference in the levels of other intracellular TCA intermediates upon IFN-I treatment, suggesting that the TCA cycle remained intact. As a result of intact TCA, there was also no difference in ATP production. Taken together, this may explain why IFN-I-treated cells maintained their cell viability as shown by Annexin V and PI staining (**Fig.4.13B**).

One of the pathways that could maintain the OXPHOS activity in response to chronic IFN-I is the tryptophan catabolism as part of the de novo NAD synthesis pathway. Tryptophan is an essential amino acid that has a significant role in maintaining immune function. Usually, it is used as a substrate for the synthesis of kynurenine, serotonin, and indoles[315]. Around 95% of ingested tryptophan in normal conditions is converted into NAD through the kynurenine pathway[316]. The IDO enzymes (IDO1 and IDO2) are the first rate-limiting enzyme of this pathway and have been shown to be more activated in response to IFN-I[317]. This is because the IDO1 promoter contains two IFN-I-stimulated response elements. Therefore, several reports have shown that IFN-I mediates a reduction of intracellular tryptophan through the induction of IDO1 activity in various cell types[318,319]. This is consistent with my findings. I found that the gene

expression of *IDO1* and *KYNU* was increased with IFN-I treatment starting at 8 hours. Metabolomic profiling data also showed a progressive decrease of intracellular tryptophan with a consistent increase in kynurenine and 3-hydroxyanthranilic acid. These metabolites gradually decreased as they were used to make downstream metabolites such as picolinic and quinolinic acid. The quinolinic acid was used for the generation of NAD as indicated by a reduction level of quinolinic acid at 72 hours together with an increase in gene expression of *QPRT* which converts quinolinic acid to NAD. Declining tryptophan levels have been observed in SLE murine models and in SLE patients. For example, the dysbiotic gut microbiota of lupus-prone mice charaterised by increased kynurenine levels in the faeces has been connected to the formation of autoantibodies [320]. In this study, the authors also showed that low dietary tryptophan inhibits the disease activity of these lupus-prone mice but high dietary tryptophan has the reverse effect[320]. SLE patients exhibit higher levels of extracellular kynurenine, kynurenine/tryptophan ratio and quinolinic acid compared to healthy individuals and these metabolites correlated with severe fatigue[321,322]. Furthermore, a recent metabolome study in the serum of SLE patients has shown that IFN-high SLE patients have increased ratios of serum kynurenine/tryptophan and quinolinic acid/kynurenic acid compared to healthy controls[323]. Based on these reports and my findings, I could speculate that chronic IFN-I regulates the tryptophan-kynurenine pathway, possibly in an effort to create NAD to compensate for IFN-I-mediated NAD depletion and this may supply NAD to maintain OXPHOS activity.

Cell metabolism is inextricably connected to macrophage growth, differentiation, and function[324,325] and my results indicated that chronic IFN-I exposure rewired metabolic pathways in human macrophages. The obvious next step was to investigate the phenotypes and functions of these IFN-I-treated macrophages. I found that prolonged IFN-I exposure induced change in macrophage morphology from being elongated to being rounder than that of untreated macrophages. Literature has shown that change in macrophage shape is associated with different functional state[326]. For example, anti-inflammatory macrophages exhibit a more elongated shape compared to the one of pro-inflammatory macrophages[326]. I also found that these round cells floated in the cell media; however, they were not dead cells, according to Annexin V and PI staining whereby these floating cells were analysed. The effect of IFN-I on the loss of adherence was reported in the DC maturation process whereby the authors found that

adherent monocytes changed into floating non-adherent cells within 3 days of IFN-I and GM-CSF treatment[327]. These results together suggest that IFN-I may influence adhesion molecules of monocyte-derived cells. Further experiments are required to address this hypothesis. In addition, I noticed that IFN-I-treated macrophages had decreased levels of the cell proliferation marker Ki-67. This finding is consistent with literature whereby IFN-I has been shown to have an anti-proliferative effect in many cell types including malignant cells due to their antimitogenic action[328], confirming that chronic IFN-I signalling plays a role in the regulation of cell cycle in human macrophages.

Though previous work has shown that IFN-I can induce cell death activity in macrophages[329], I did not find a difference in the cell viability of human macrophages upon 3-days after IFN-I exposure. Instead, I found that prolonged IFN-I treatment triggered macrophages to undergo rapid cell death when re-stimulated with a very loose amount of LPS (1ng/ml) for only 3 hours. Other TLR agonists did not have this impact. Of note, to my knowledge, little is known about the effects of other TLR stimulation on macrophage metabolism[330]. Studies in pDCs showed that TLR7 and TLR9 signalling can promote glycolysis and lipid metabolism in pDCs[230,331]. LPS is known to induce the activation of the cell surface receptor TLR4 leading to the activation of specific cytokine signalling pathways. Furthermore, LPS stimulation can reprogramme macrophage metabolism including increases in glycolysis and the pentose phosphate pathway[332]. These pathways are required to rapidly generate ATP to support cell proliferation and produce pro-inflammatory features[152]. Since I discovered that prolonged IFN-I exposure lowered the glycolysis in human macrophages, these cells may not have the ability to upregulate glycolysis upon LPS rechallenging which then resulted in rapid cell death. Another possible explanation could be related to the NAD metabolism. Literature has demonstrated that LPS treatment rapidly decreased NAD+ levels in macrophages through the activation of PARPs, a NAD-consuming enzyme, in response to mROS-induced DNA damage[299]. Moreover, a study by Minhas et al. also showed that LPS challenge can suppress de novo NAD+ synthesis leading to decreasing intracellular NAD+ concentration[300]. Therefore, one could speculate that as IFN-I-treated macrophages had low levels of NAD+ to begin with due to chronic IFN-I exposure; therefore, when they were exposed to LPS, too much NAD was lost for the cells to survive. However, further investigations

are required to pinpoint the underlying mechanism of LPS-induced cell death in IFN-I-treated macrophages.

It is well known that macrophages have diverse functional phenotypes in response to specific microenvironmental stimuli. For example, macrophages can be traditionally divided into two categories, either pro-inflammatory (M1) or anti-inflammatory (M2) phenotype. These macrophages differ in their cell surface markers, the secreted cytokines and biological functions. In response to 3-day-IFN-I exposure, human macrophages exhibited a pro-inflammatory-like phenotype. These features included an increase in surface pro-inflammatory markers such as CD80 and CD86 and a reduction of anti-inflammatory markers such as CD163 and CD206. Consistent with this, RNA-seq data showed an increased pro-inflammatory gene signature and a decreased anti-inflammatory gene signature in IFN-I-treated macrophages. Furthermore, pro-inflammatory cytokines including IL-6, TNF-α and IL-1β increased with the prolonged IFN-I treatment. However, from a metabolic perspective, these macrophages did not appear to be classical M1 macrophages that are typically generated *in vitro* by IFN-γ and LPS stimulation. In the conventional M1 macrophages, glycolysis is elevated and accompanied by a broken TCA cycle[170], whereas chronic IFN-I-treated cells showed downregulation in glycolysis and the OXPHOS and TCA cycle was unaffected. Therefore, my findings suggested that chronic IFN-I treatment induced a unique pro-inflammatory-like phenotype that differs from the conventional classification.

There are several mechanisms reported in the literature that could explain how IFN-I signalling contributes to the pro-inflammatory phenotype of macrophages. One of them is that IRF5, a transcription factor controlling gene expression of ISGs, can activate M1 genes such as IL-12p40, IL-6 and TNF-α and inhibit M2 genes such as IL-10 and TGF-β[333,334]. Another possible mechanism could be via the activation of the nuclear factor erythroid-related factor 2 (NRF2). A recent study conducted in a mouse model with mtDNA mutation has shown that chronic IFN-I signalling suppresses NRF2 activity, causing increased oxidative stress, glycolysis activity and pro-inflammatory cytokine secretion[335]. Interestingly, it has been shown that alterations in macrophage metabolism can also influence their polarisation [336]. Some of the observed metabolic changes in IFN-I-treated macrophages, such as NAD metabolism and tryptophan metabolism have been reported to be linked with pro-inflammatory

macrophages[299,300]. Minhas and colleagues demonstrated that resting macrophages primarily utilise the kynurenine pathway to generate NAD to maintain an anti-inflammatory response[300]. Inhibition of the kynurenine pathway by genetic mutation and pharmacological disruption in human and mouse macrophages resulted in a decrease in intracellular NAD concentration, a reduction in mitochondrial respiration, and an increase in glycolysis. This was accompanied by increased pro-inflammatory markers[299]. NAD salvage pathway has also been shown to regulate the inflammatory phenotype of macrophages. Cameron et al. showed that blocking the NAMPT, a key enzyme in the NAD salvage pathway, decreased inflammatory features in LPS-stimulated macrophages[299]. Moreover, secreted NAMPT can induce M1-shifted transcriptional expression independently from its extracellular enzymatic activity in IFN-γ-treated peritoneal macrophages[337].

Overall, I demonstrated that prolonged IFN-I exposure induced metabolomic reprogramming in macrophages by increasing NAD consumption, increasing the tryptophan-kynurenine pathway, and reducing glycolysis while maintaining TCA activity and ATP to allow cells to survive in a normal state. Chronic IFN-I exposure also promoted a pro-inflammatory phenotype and triggered cell death in response to TLR4 re-challenge in macrophages. However, it was still unclear whether and how IFN-I-induced metabolic changes lead to aberrant macrophage functions after prolonged IFN-I exposure. Therefore, further investigations were performed to address this question in the next chapter.

Chapter 5:

The role of CD38 in IFN-I-treated macrophages

5.1. Introduction

In the previous chapter, I have shown that chronic IFN-I exposure altered the phenotypes and functions of macrophages. This was also accompanied by changes in macrophage metabolism. However, it was not clear whether and how IFN-I-induced metabolic changes contribute to the abnormal functions of human macrophages upon persistent IFN-I exposure. Therefore, in this chapter, my overarching aim was to address that question.

As demonstrated in our publication[248], chronic IFN-I signalling upregulates the expression of NAD-consuming enzymes, CD38 and PARPs, causing aberrant NAD metabolism and impaired mitochondrial respiration. These IFN-I-induced metabolic alterations result in aberrant cell death and $CD8^+$ T cell activation state[248]. Similarly, one of the changes I observed in IFN-I-treated macrophages was an increased expression of NAD-consuming enzymes including *CD38* and *SIRT1* resulting in a reduction of NAD levels. CD38 has been shown to regulate NAD metabolism in macrophages[223] and the link between CD38 and inflammatory features has also been reported[220]. Amici *et al*. showed that: i) CD38 can be used as a marker for pro-inflammatory macrophages[203] ; ii) CD38 promoted inflammatory cytokine release in human macrophages; and III) pharmacological inhibition of CD38 reversed that effect[203]. The authors also showed a positive correlation of CD38 expression in non-classical monocytes with active SLE disease[203], suggesting a possible important role of CD38 in SLE pathogenesis.

Several reports have shown the ability of IFN-Is of upregulating CD38 in many cell types including B cells, T cells, and dendritic cells[248,338,339]. However, the relationship between chronic IFN-I signature and CD38 in human macrophages has not been fully explored. Considering the literature and our previous findings, I hypothesised that chronic IFN-I exposure increases CD38 expression leading to a decline in NAD levels and this process may subsequently trigger some NAD-related pathways, such as the tryptophan-kynurenine pathway, that could contribute to abnormal phenotypes and

functions. Therefore, in this chapter, I will focus on how CD38 contributes to IFN-I-induced changes in human macrophages.

5.2. Results

Expression of NAD-consuming enzymes upon IFN-I treatment

To identify the factor that potentially caused IFN-I-mediated NAD reduction and phenotypic changes in macrophages, I cultured MDMs with 1000U/ml of IFN-α for 8, 24 and 72 hours and then measured the expression of the genes encoding the main NAD-consuming enzymes *CD38* and *SIRT1* at each timepoint by RT-qPCR. As shown in the previous chapter, the expression of the CD38 gene was remarkably upregulated after 8 hours of treatment and continued increasing up to 24 hours. However, at the 72-hour timepoint, a downward trend of CD38 expression was observed but the expression level remained higher than in the untreated samples (more than 40-fold) (**Fig.5.1A**). For *SIRT1* expression, a gradual increase in expression level upon the treatment was detected. I found that the *SIRT1* gene was significantly upregulated after 24 hours of IFN-I exposure (**Fig.5.1B**). When comparing the fold change value of gene expression levels among these two NAD-consuming genes, the results revealed that upon IFN-I treatment the increase of *CD38* expression ranged from 40-fold to 400-fold, whereas *SIRT1* expression was increased up to only 3-fold (**Fig.5.1A and B**).

Considering that *CD38* was upregulated earlier, and the levels were much higher than those of *SIRT1*, I then further explored the enzymatic activity of CD38 by measuring global metabolomic profiling data and analysing the level of metabolites relevant to the CD38-mediated NAD consumption. Cyclic ADP ribose and ADP ribose are the by-products of CD38 enzymatic activity. I found that the normalised total ion count of the upstream metabolite cyclic ADP-ribose was significantly reduced (**Fig.5.1C**) whereas the downstream metabolite ADP-ribose ion count was increased with the treatment (**Fig.5.1D**). This highlighted that CD38 hydrolyze cyclic ADP-ribose to ADP-ribose upon IFN-I-treatment and the difference was more pronounced at the later time point (72 hours). Collectively, these findings suggest that CD38 is upregulated early and could be a key contributor to NAD reduction upon chronic IFN-I exposure.

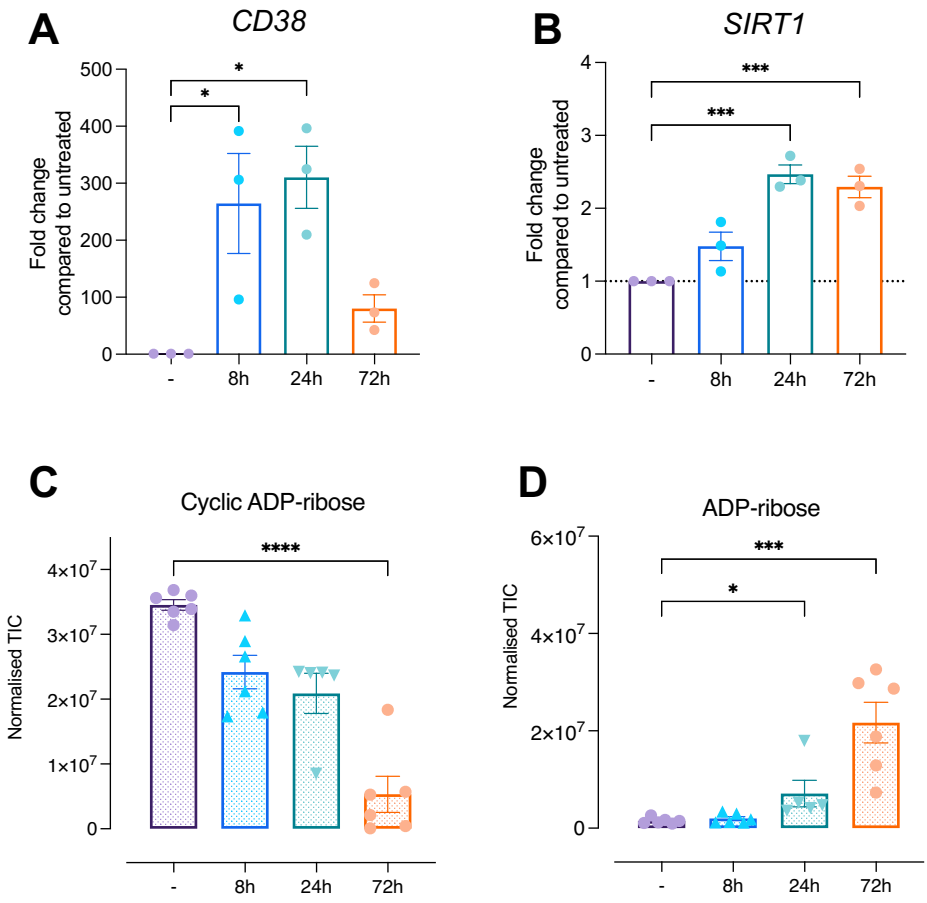

Figure 5.1. Analysis of genes and metabolites in CD38-NAD consuming pathway. Human monocyte-derived macrophages were cultured with or without 1000U/ml IFN-α for 8, 24 and 72 hours. (**A-B**) The gene expression was assessed using qPCR. Summary graphs depicting fold-change of gene expression of (**A**) *CD38* and (**B**) *SIRT1.* (**C-D**) Cells were extracted and global metabolomic profiling was performed using LC-MS. Summary graphs of CD38-NAD consuming pathway, depicting (**C**) intracellular cyclic ADP-ribose and (**D**) ADP-ribose. Each dot represents one donor. Data presented as mean ± S.E.M. * p<0.05, *** p<0.001, **** p<0.0001. One-way ANOVA for (**A**) and Kruskal-Wallis test for (**B**).

Identification of optimal concentration of CD38 inhibitor

Guided by these results, I confirmed the role of CD38 in initiating chronic IFN-I-mediated changes in macrophages using a well-established CD38 inhibitor: 78c. 78c or Thiazoloquin(az)olin(on)e is a small molecule that inhibits CD38 in a reversible and non-competitive manner. To identify the optimal dose of 78c, I cultured MDMs with 10, 20 and 50 μM of 78c together with 1000U/ml of IFN-α for 3 days. I then observed the toxicity of the drugs by assessing cell viability using annexin V and PI staining. As shown in **figure 5.2A**, on treating the cells with IFN-I combined with 10 or 20 μM of 78c, the percentage of alive cells was unchanged. However, after 3 days of incubation with 50μM of 78c and IFN-I, the percentage of alive cells decreased from around 90% in the control cells to 80%.

Furthermore, I tested the effect of different concentrations of 78c on the surface expression of CD38 and CD80 using flow cytometry. As previously shown, chronic IFN-I treatment alone upregulated the expression of CD38 and CD80 (**Fig.5.2B and C**). However, these IFN-I-mediated upregulations were dose-dependently reduced by 78c administration, as shown by shifts in the MFI histograms of CD38 and CD80 towards lower intensity (**Fig.5.2B and C**). The biggest shift was seen in the IFN-I-primed cells that were exposed to 20 and 50μM of 78c. Of note, the 50μM of 78c, the highest dose, had no additional effect on CD38 and CD80 expression. Taken together, the data on cell viability and surface expression prompted me to select the concentration of 20μM of 78c to suppress CD38 enzymatic activity in subsequent experiments.

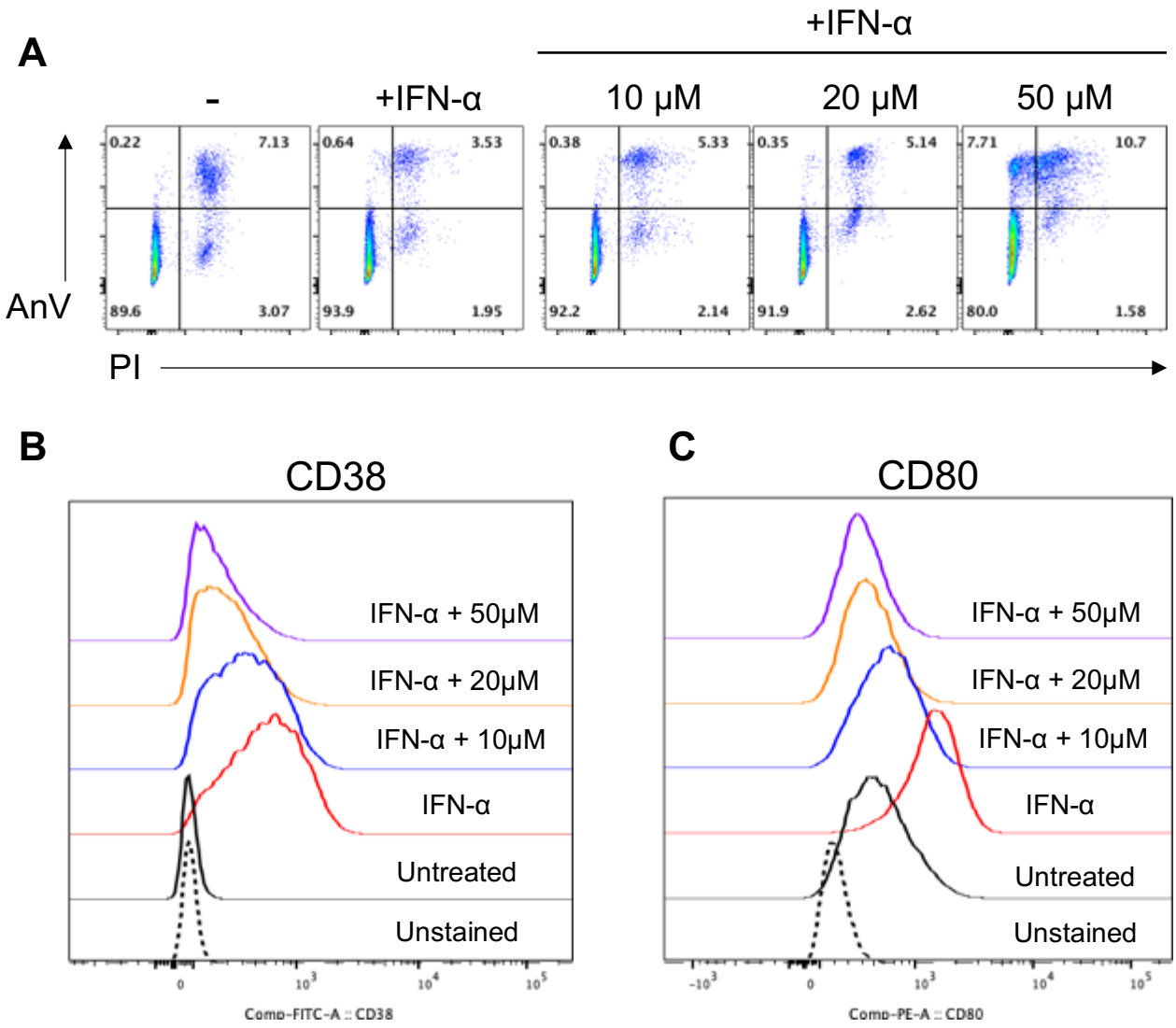

Figure 5.2. Identification of optimal concentration of CD38 inhibitor 78c
Human monocyte-derived macrophages were cultured with or without 1000U/ml IFN-α. IFN-α-treated cells were also cultured with 10, 20 and 50 μM of 78c for 3 days. (**A**) Representative dot plots showing cell viability across different treatments. (**B-C**) The expression of surface markers was measured by flow cytometry. Representative histogram graphs showing MFI of (**B**) CD38 and (**C**) the pro-inflammatory marker CD80. Each dot represents one donor. Data presented as mean ± S.E.M.

Intracellular NAD and NADH levels in IFN-I-treated macrophages upon CD38 inhibitor

To investigate whether CD38 inhibition could increase the level of NAD and NADH when combined with chronic IFN-I treatment, I extracted the cells and measured cellular NAD and NADH levels using a colorimetric assay. I then compared the levels of NAD and NADH in untreated cells, IFN-I-treated cells and IFN-I combined with 78c-treated cells. CD38 inhibitor 78c treatment showed a trend of increase in NAD+ level. Though there were no significant differences in the levels of NADH, total NAD and NADH and the ratio of NAD and NADH compared to IFN-I-treated condition (**Fig.5.3**).

Effects of inhibiting CD38 on macrophage phenotypes

I subsequently investigated the effect of CD38 inhibition on macrophage phenotypes and functions. MDMs were treated with or without 1000U/ml of IFN-α as well as 20μM of 78c for 3 days. Macrophage polarisation was assessed by measuring CD80 expression and IL-6 secretion by flow cytometry and ELISA, respectively. As previously shown, chronic IFN-I treatment enhanced the surface expression of CD80; however, 78c treatment reduced the elevation of CD80 MFI to a similar level seen in untreated cells (**Fig.5.4C**). Similarly, the increase of secreted IL-6 levels following IFN-I treatment was also reduced by the 78c treatment to levels comparable to untreated samples (**Fig.5.4D**). Of note, this cytokine suppressive effect was not due to increased cell death, as no differences in cell viability between the 78c-treated and untreated conditions were present after 3 days of culture (**Fig.5.4A**). Interestingly, though 78c is known to inhibit CD38 NADase activity, flow cytometry analysis revealed that the 78c treatment also decreased the upregulation of CD38 MFI upon IFN-I treatment by approximately 50% (**Fig.5.4B**.) The data so far suggested that inhibition of CD38 rescued the pro-inflammatory phenotypes observed in IFN-I-primed macrophages.

Next, I determined whether inhibition of CD38 could also rectify LPS-restimulation-induced cell death in IFN-I-treated cells. After culturing MDMs with IFN-I and/or 78c or left untreated for 3 days, these conditions were then stimulated with 1ng/ml LPS for 3 hours. Cell viability was assessed using annexin V and PI staining. Upon LPS stimulation, chronic IFN-I treatment significantly reduced the percentage of alive cells; however, this IFN-I mediated reduction of cell viability was improved by 78c treatment

as shown by an increase in the percentage of alive cells when compared to that of IFN-I treatment alone (**Fig.5.5**).

Collectively, these data highlighted the importance of CD38 in triggering pro-inflammatory phenotype and LPS-induced cell death in response to chronic IFN-I exposure.

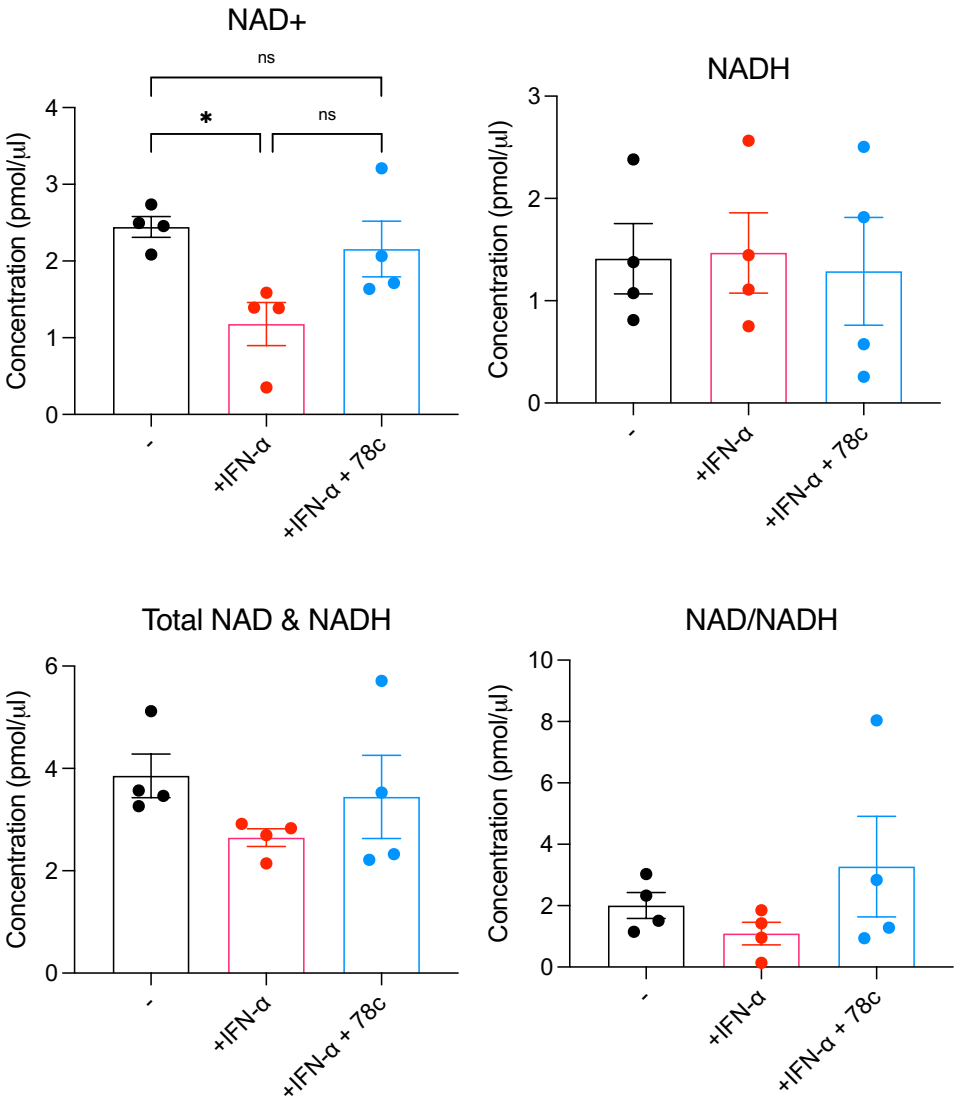

Figure 5.3. Intracellular NAD and NADH levels in IFN-I-treated macrophages upon CD38 inhibitor. Human monocyte-derived macrophages were cultured with or without 1000U/ml IFN-α or 20µM 78c for 3 days. Cells then were collected and processed to measure NAD and NADH levels using colorimetric assay. Summary graphs showing (A) NAD+ concentration, (B) NADH concentration, (C) total amount of NAD and NADH and (D) ratio of NAD and NADH. Each dot represents one donor. Data presented as mean ± S.E.M. *p<0.05. One-way ANOVA.

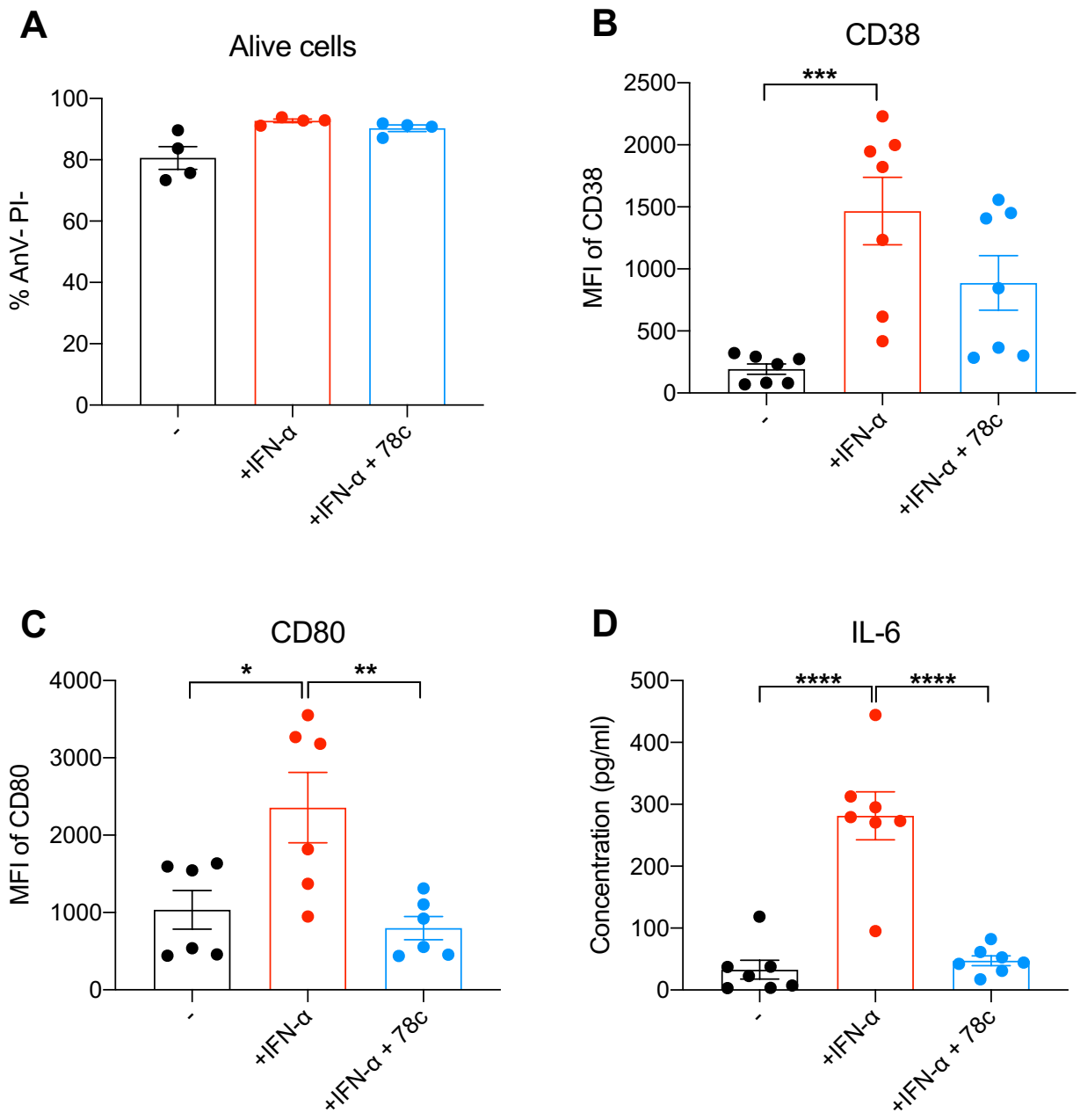

Figure 5.4. Effects of inhibiting CD38 on macrophage phenotypes
Human monocyte-derived macrophages were cultured with or without 1000U/ml IFN-α and 20μM 78c for 3 days. (**A**) Summary graphs showing percentage of alive cells across treatment. (**B-C**) Expression of surface markers was measured by flow cytometry. Summary graphs showing MFI of (**B**) CD38 and (**C**) the pro-inflammatory marker CD80. (**D**) Summary graphs showing the production of inflammatory cytokine IL-6 measured by ELISA. Each dot represents one donor. Data presented as mean ± S.E.M. * $p<0.05$, ** $p<0.01$, *** $p<0.001$, **** $p<0.0001$. Kruskal-Wallis test.

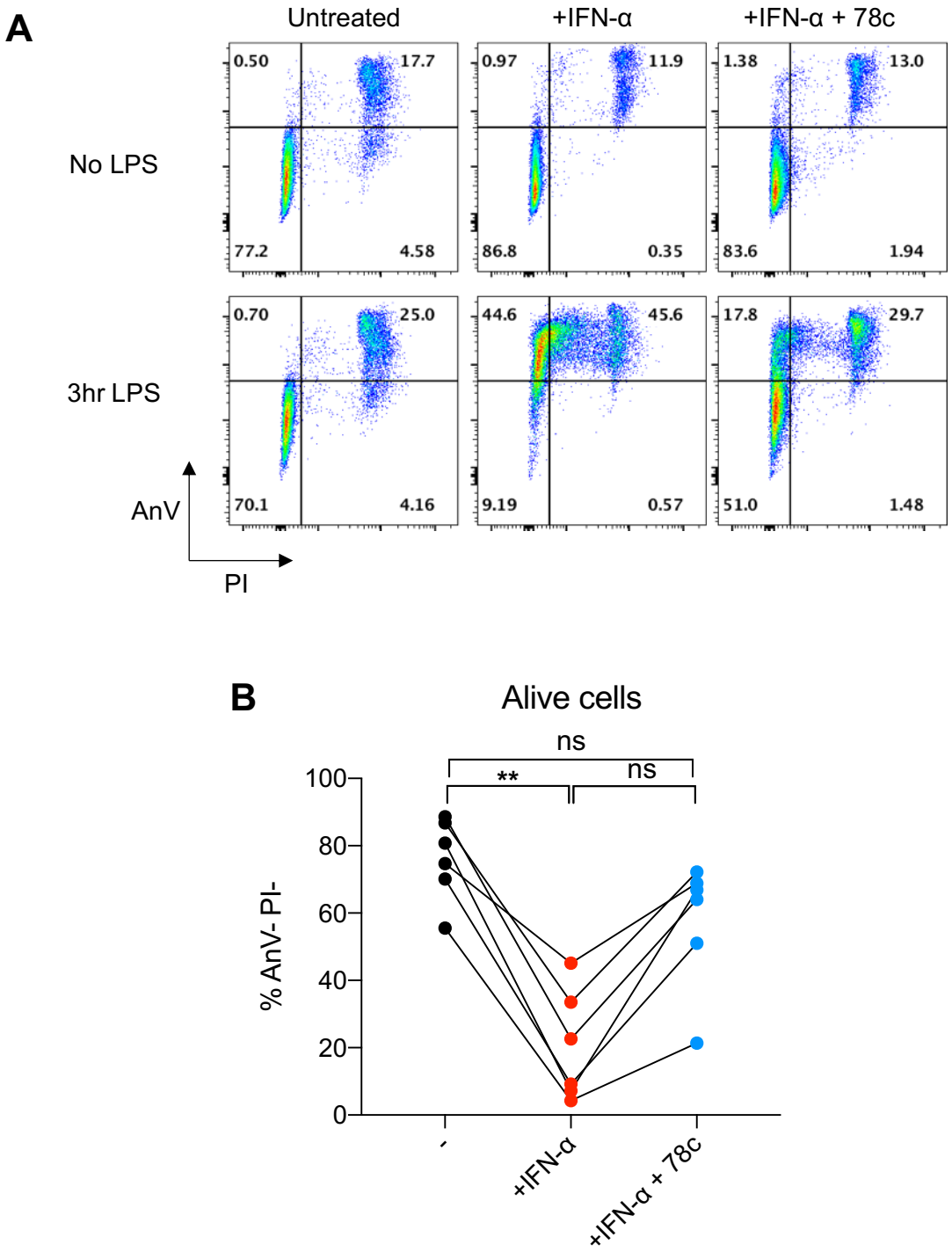

Figure 5.5. Effects of inhibiting CD38 on LPS-induced cell death
Human monocyte-derived macrophages were cultured with or without 1000U/ml IFN-α and 20μM 78c for 3 days. Cells then were stimulated with 1ng/ml LPS for 3 hours. Cell viability was assessed by flow cytometry. (**A**) Representative dot plots of AnV/PI staining across treatments. (**B**) Summary graph showing percentage of alive cells after 3 hours of LPS re-challenge. Each dot represents one donor. Data presented as mean ± S.E.M. ns=not significant, ** $p<0.01$. Kruskal-Wallis test.

Effects of NAD supplementation on LPS-induced cell death

So far, the data suggested that CD38 may be responsible for IFN-I-mediated NAD reduction and by blocking CD38, I managed to rescue the abnormal macrophage phenotype and function upon chronic IFN-I treatment. Therefore, I hypothesised that the decrease in NAD level contributed to changes observed in IFN-I-treated macrophages.

I subsequently tested whether an NAD+ supplementation could rectify the downstream effects of IFN-α stimulation. β-Nicotinamide mononucleotide (NMN) is a metabolite in NAD+ salvage pathway and studies have shown that supplementation with NMN can induce NAD+ synthesis leading to boosting NAD levels in several cell types[340]. I then cultured MDMs with IFN-α combined with 1 and 10 mM of NMN for 3 days. Next, I assessed the cell viability of macrophages at the baseline (on day 3 of culture) and upon restimulation with LPS for 3 hours. As shown in **figure 5.6A and 5.6B**, both concentrations of NAD+ supplementation NMN did not change the percentage of alive cells after 3 days of culturing with IFN-I. Importantly, NMN treatment also did not improve the cell viability of IFN-I-primed macrophages upon LPS stimulation (**Fig.5.6 A and C**), suggesting that the anti-inflammatory and pro-survival effects of CD38 inhibition were not mediated by changes in NAD levels in human macrophages. This assumption had to be verified experimentally, which I next set to investigate.

To confirm if the doses used of NMN supplement were effective in increasing the level of NAD and NADH when combined with chronic IFN-I treatment, I measured and compared the levels of NAD and NADH in untreated cells, IFN-I-treated cells, IFN-I combined with 78c-treated cells and NMN-treated cells using a colorimetric assay. Supplementation with 10 mM of NMN led to a significant increase in the levels of NAD+ and total NAD and NADH (**Fig.5.7A and 5.7C**). This was accompanied by an increasing trend of NADH and the ratio of NAD and NADH (**Fig.5.7B and 5.7D**). Collectively, these findings indicated that the rescue of macrophage phenotypes upon CD38 inhibition was not due to NAD level.

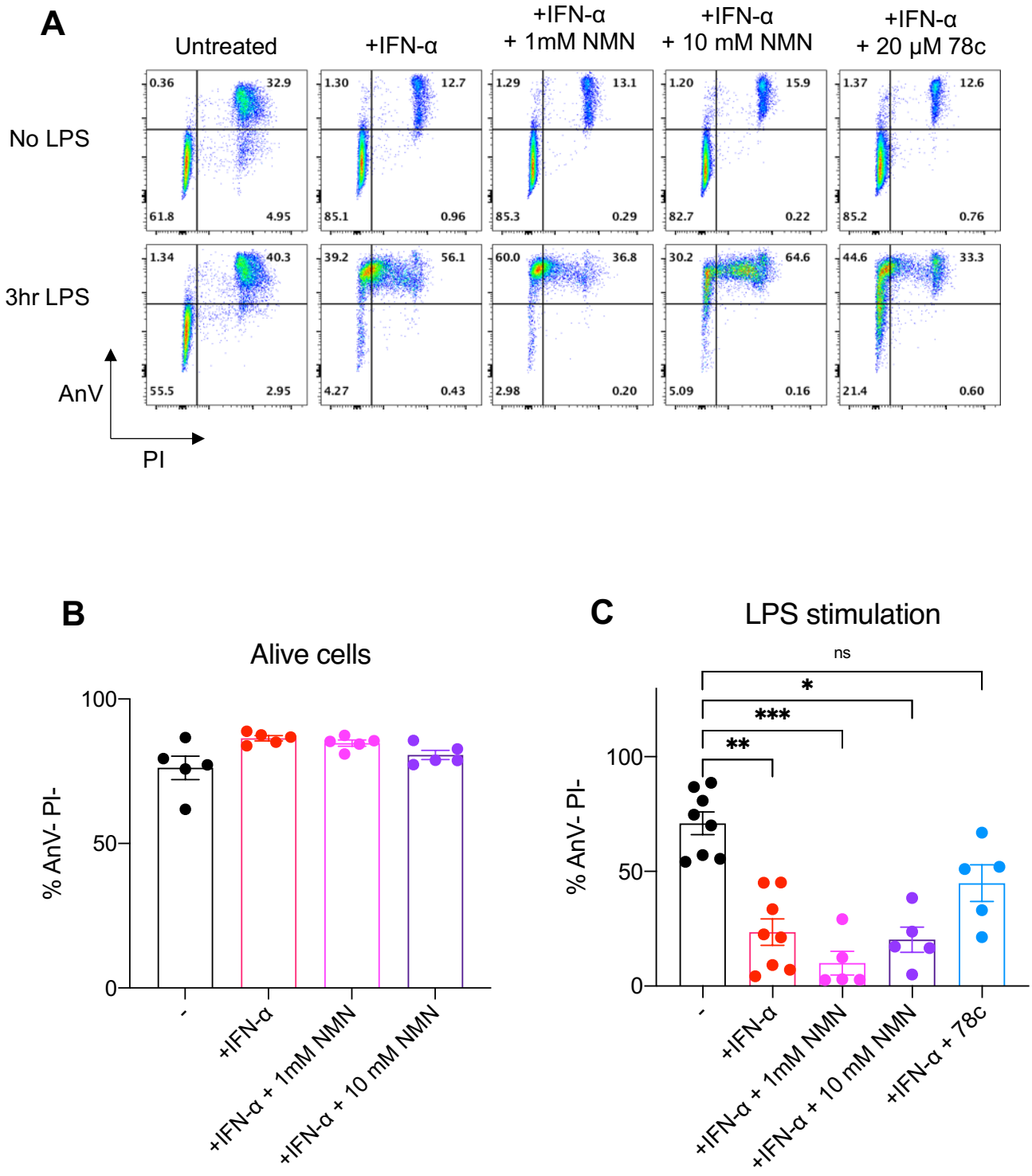

Figure 5.6. Effects of NAD supplementation on LPS-induced cell death
Human monocyte-derived macrophages were cultured with or without 1000U/ml IFN-α and 1 mM or 10mM NMN or 20μM 78c for 3 days. Cells then were stimulated with 1ng/ml LPS for 3 hours. Cell viability was assessed by flow cytometry. (**A**) Representative dot plots of AnV/PI staining across treatments. (**B**) Summary graph showing percentage of alive cells after 3 days of treatments **(C)** Summary graph showing percentage of alive cells after 3 hours of LPS re-challenge. Each dot represents one donor. Data presented as mean ± S.E.M. * $p<0.05$, ** $p<0.01$, *** $p<0.001$. Kruskal-Wallis test.

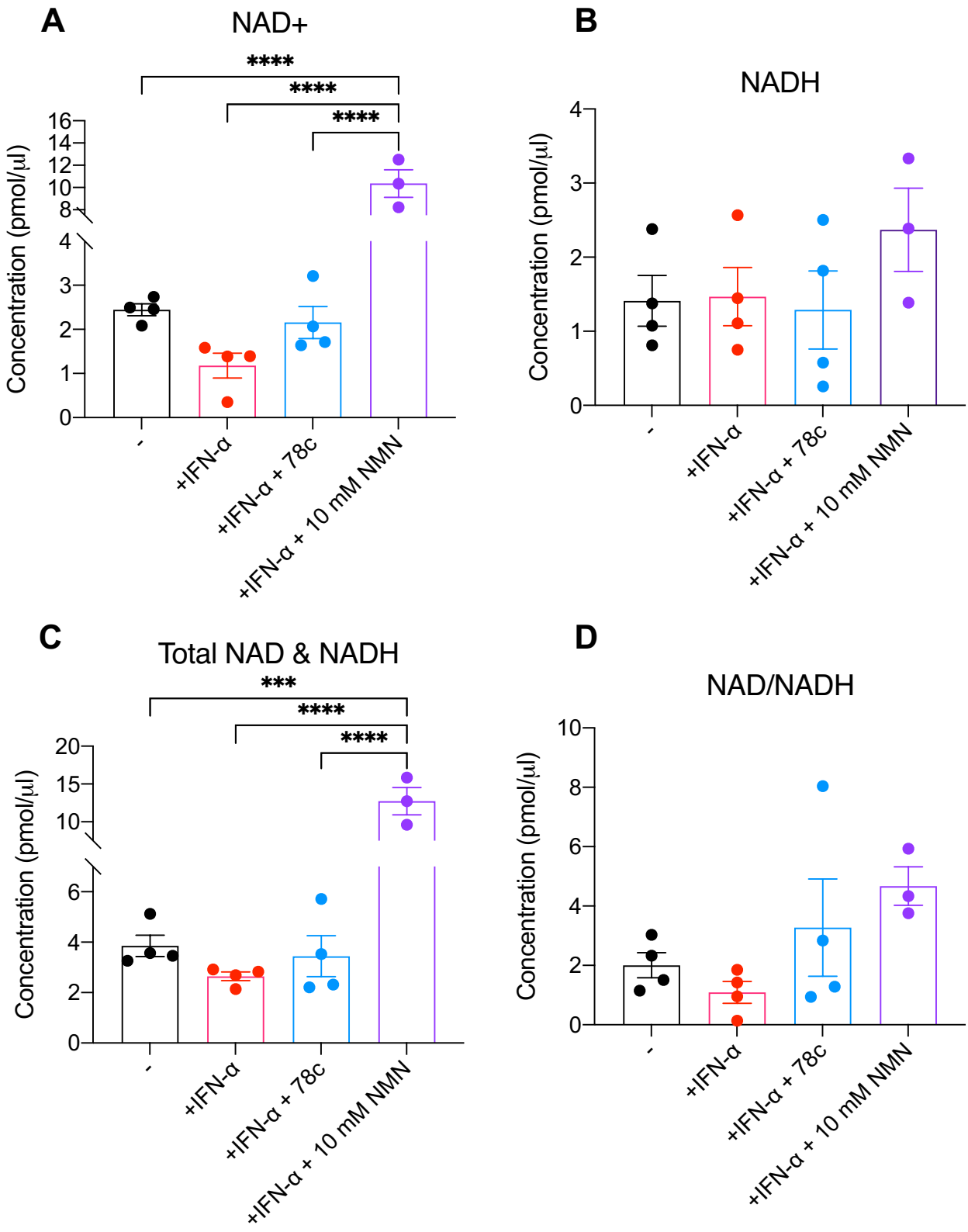

Figure 5.7. Intracellular NAD and NADH levels in IFN-I-treated macrophages upon CD38 inhibitor and NAD supplementation. Human monocyte-derived macrophages were cultured with or without 1000U/ml IFN-α and 10mM NMN or 20µM 78c for 3 days. Cells then were collected and processed to measure NAD and NADH levels using colorimetric assay. Summary graphs showing (**A**) NAD+ concentration, (**B**) NADH concentration, (**C**) total amount of NAD and NADH and (**D**) ratio of NAD and NADH. Each dot represents one donor. Data presented as mean ± S.E.M. *** $p<0.001$, **** $p<0.0001$. One-way ANOVA.

Effects of inhibiting CD38 on the metabolic profile of macrophages

To further understand the effects of CD38 inhibition on macrophage metabolism, I determined the metabolomic signature triggered by CD38 inhibition in IFN-I-treated macrophages. Therefore, I cultured MDMs with 1000 U/ml IFN-α in the presence or absence of 20 μM of 78c for 8 and 72 hours. Cells were processed and untargeted LC-MS-based metabolite profiling was then performed.

The metabolome between cells treated with the combination of IFN-I and 78c and cells treated with IFN-I alone was compared at each time point. Differential metabolomic analysis (DMA) was screened using a p-value less than 0.05 and a Log2-Fold change between -0.5 to 0.5. As shown in **figure 5.8**, a total of 305 differentially changed metabolites were identified in 78c-treated-IFN-I-primed macrophages compared to untreated IFN-I-primed macrophages.

As depicted in **figure 5.8A**, after 8 hours of treatment, several metabolites related to NAD and NADH metabolism were restored by 78c administration. These metabolites included NAD and cyclic ADP-ribose. Furthermore, the upregulation of tryptophan was detected following 78c treatment. This was accompanied by the downregulation of the downstream metabolites in tryptophan and kynurenine pathways including formylkynurenine, 3-hydroxyanthranilic acid and picolinic acid.

At the 72-hour-timepoint (**Fig.5.8B**), metabolites belonging to several different pathways were detected by this analysis. Amino acid catabolism pathways were detected as seen in the downregulation of several di-peptides including leucyl-valine, alanyl-isoleucine etc. Metabolites in the nucleotide synthesis pathway including deoxyguanosine were upregulated in IFN-I-treated macrophages following 78c treatment. Furthermore, vitamins including pantothenate (vitamin B5), and biotin (vitamin B7) were increased upon CD38 inhibition.

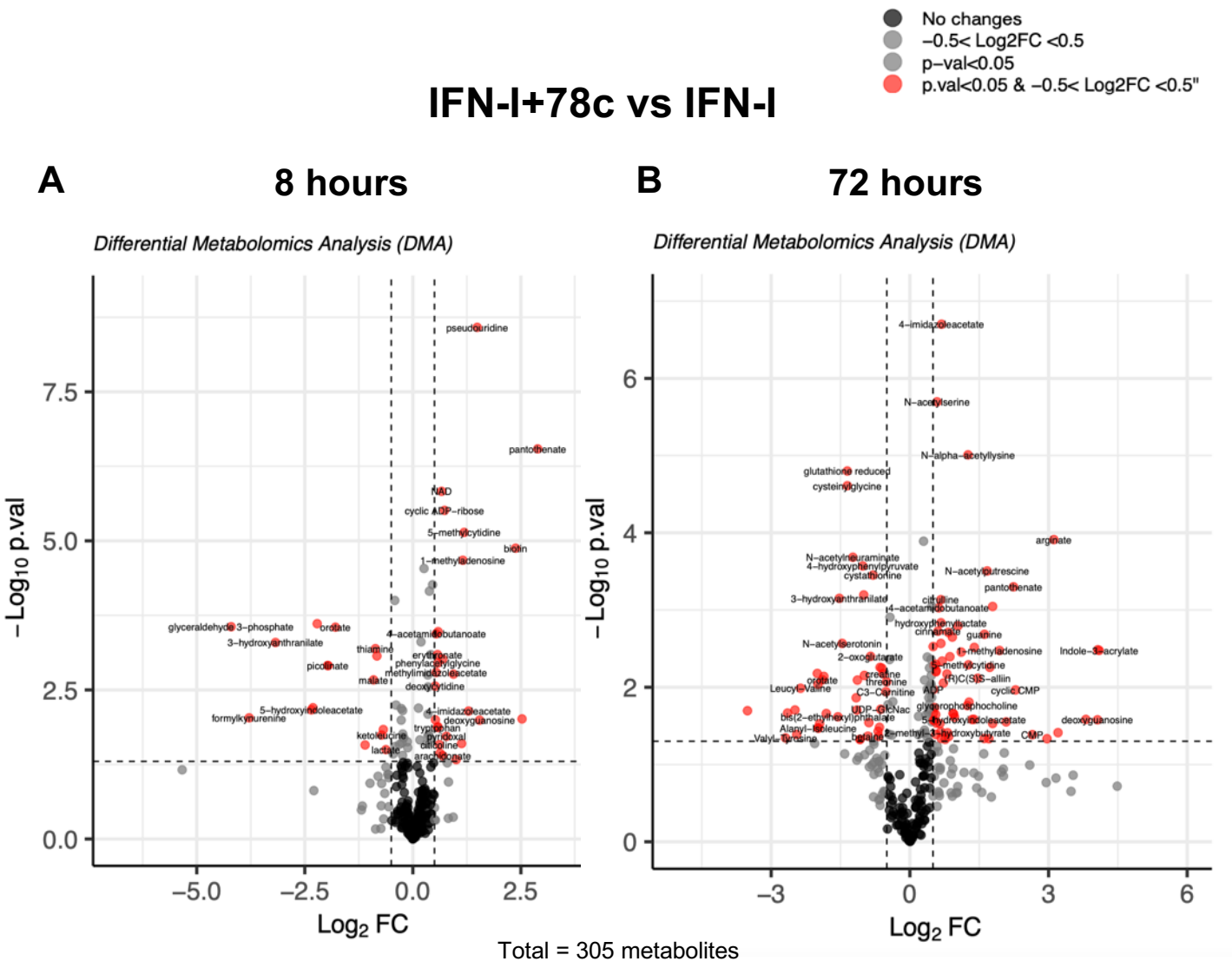

Figure 5.8. Effects of inhibiting CD38 on the metabolic profile of macrophages
Human monocyte-derived macrophages were cultured with 1000U/ml IFN-α and/or 20μM 78c for 8 and 72 hours. Cells were extracted and global metabolomic profiling was performed using LC-MS. (**A-B)** Volcano plots showing the differentially abundant metabolites in IFN-I-treated samples vs IFN-I-and-78c-treated samples at different time points. The graphs show the relative abundance of each metabolite against its statistical significance, respectively reported as Log2FC and −log10 (*p*-value), at (**A**) 8 hours and (**B**) 72 hours after treatment. Log2FC = Log2-Fold change. The data generated from global metabolomic profiling were kindly analysed and provided by Dr Ming Yang.

Effects of inhibiting CD38 on NAD metabolism

Next, I investigated whether the 78c treatment could rescue metabolomic changes triggered by IFN-I treatment in macrophages. The first pathway I assessed was the NAD and NADH metabolism. The normalised total ion counts of intracellular metabolites related to NAD and NAD metabolism are shown in **figure 5.9**. After 8 hours of treatment, the presence of 78c treatment restored the total ion count of NAD in IFN-I-treated macrophages to a similar level seen in the untreated cells (**Fig.5.9A**). However, the 78c treatment did not rescue the NAD level at the 72-hour time point. The levels of NADH remained largely unchanged, though, at both time points, an increasing trend was noticed in IFN-I-primed macrophages exposed to 78c treatment compared to the cells exposed to IFN-I treatment only. Nicotinamide levels were also measured. As shown in **figure 5.9C**, 78c treatment seemed to have a rescue effect on nicotinamide levels at the 8-hour timepoint but not at the 72-hour timepoint.

Effects of inhibiting CD38 on tryptophan metabolism

Moving on to the changes in intracellular metabolites of the tryptophan-kynurenine pathway, the normalized total ion counts of tryptophan, kynurenine, 3-hydroxyanthranilic acid, quinolinic acid and picolinic acid were plotted as shown in **figure 5.10**. Consistent with the previous metabolic experiment shown in chapter 4, tryptophan gradually decreased over the time course of IFN-I treatment (**Fig.5.10A**). Interestingly, this IFN-I-induced reduction of tryptophan was fully reversed with 78c treatment in both time points (**Fig.5.10A**), highlighting the importance of CD38 in triggering the tryptophan degradation pathway.

Following IFN-I treatment, the levels of kynurenine and 3-hydroxyanthranilic acid peaked at the 8-hour time point with a decrease at the 72-hour time point (**Fig.5.10B and 5.10C**). However, this IFN-I-mediated upregulation was reduced by 78c treatment (**Fig.5.10B and 5.10C**). A similar trend of rescue was also observed at the 72-hour time point. Quinolinic acid and picolinic acid levels were increased progressively over time with IFN-I treatment (**Fig.5.10D and 5.10E**). After 8 hours of 78c treatment, IFN-I-treated macrophages exhibited reduced levels of quinolinic acid and picolinic acid similar to the levels detected in untreated cells (**Fig.5.10D and 5.10E**). A similar reduction trend of these metabolites upon 78c treatment was also noticed at the 72-hour timepoint, albeit less pronounced (**Fig.5.10D and 5.10E**).

Taken together, these data suggested that CD38 inhibition by 78c rescued IFN-I-mediated NAD reduction at 8 hours but not at 72 hours. Overall, there was a significant rescue on tryptophan-kynurenine pathway upon CD38 inhibition. 78c treatment fully reversed the IFN-I-mediated increase in the tryptophan-kynurenine pathway at 8 hours and partially rescued at 72 hours.

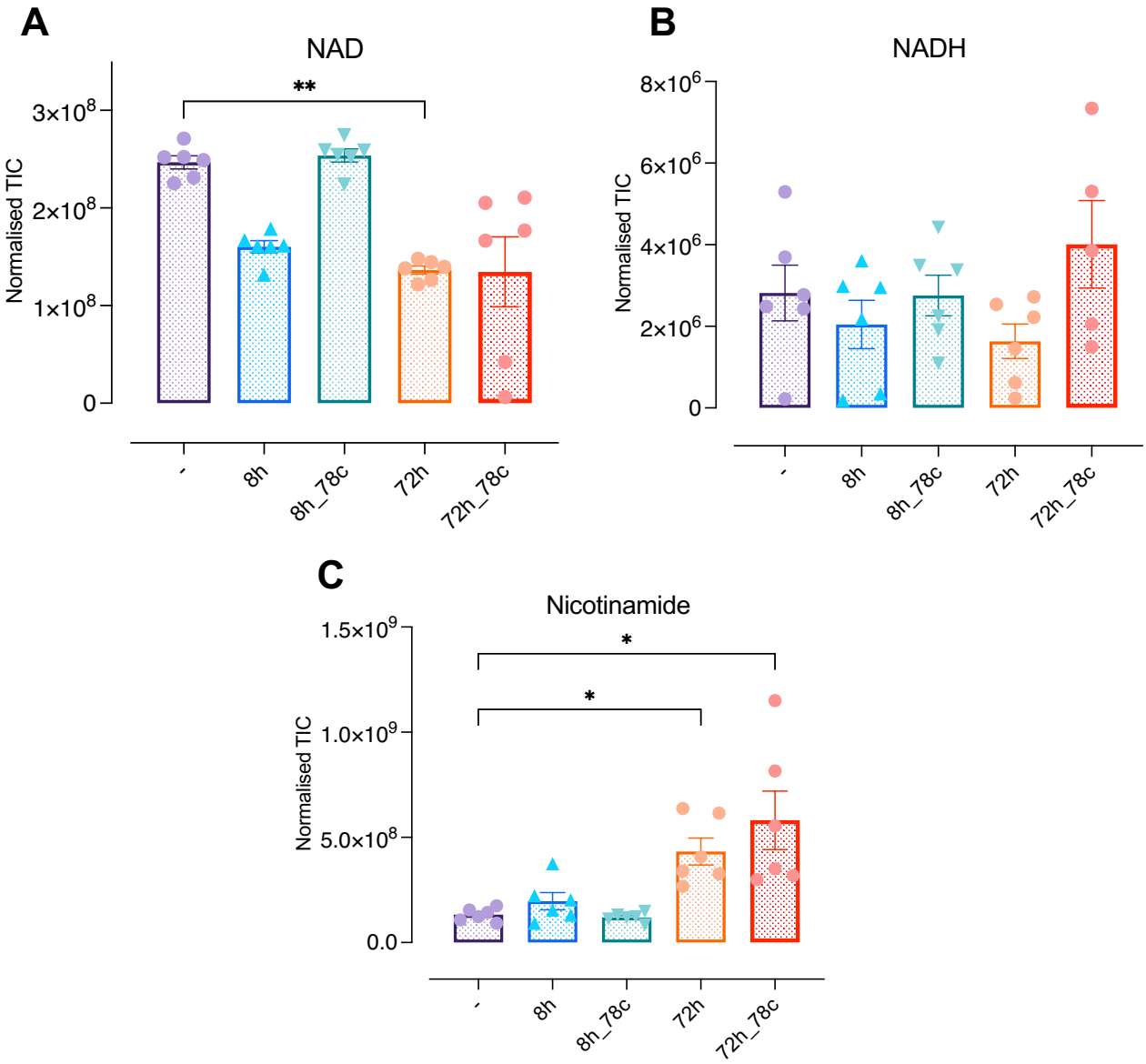

Figure 5.9. Analysis of metabolites associated with NAD metabolism upon CD38 inhibition. Human monocyte-derived macrophages were cultured with 1000U/ml IFN-α and/or 20μM 78c for 8 and 72 hours. Cells were extracted and global metabolomic profiling was performed using LC-MS. (**A-C**) Summary graphs depicting levels of intracellular (**A**) NAD, (**B**) NADH and (**C**) Nicotinamide are shown as normalised total ion count (TIC). Each dot represents one donor. Data presented as mean ± S.E.M. * $p<0.05$, ** $p<0.01$. Kruskal-Wallis test.

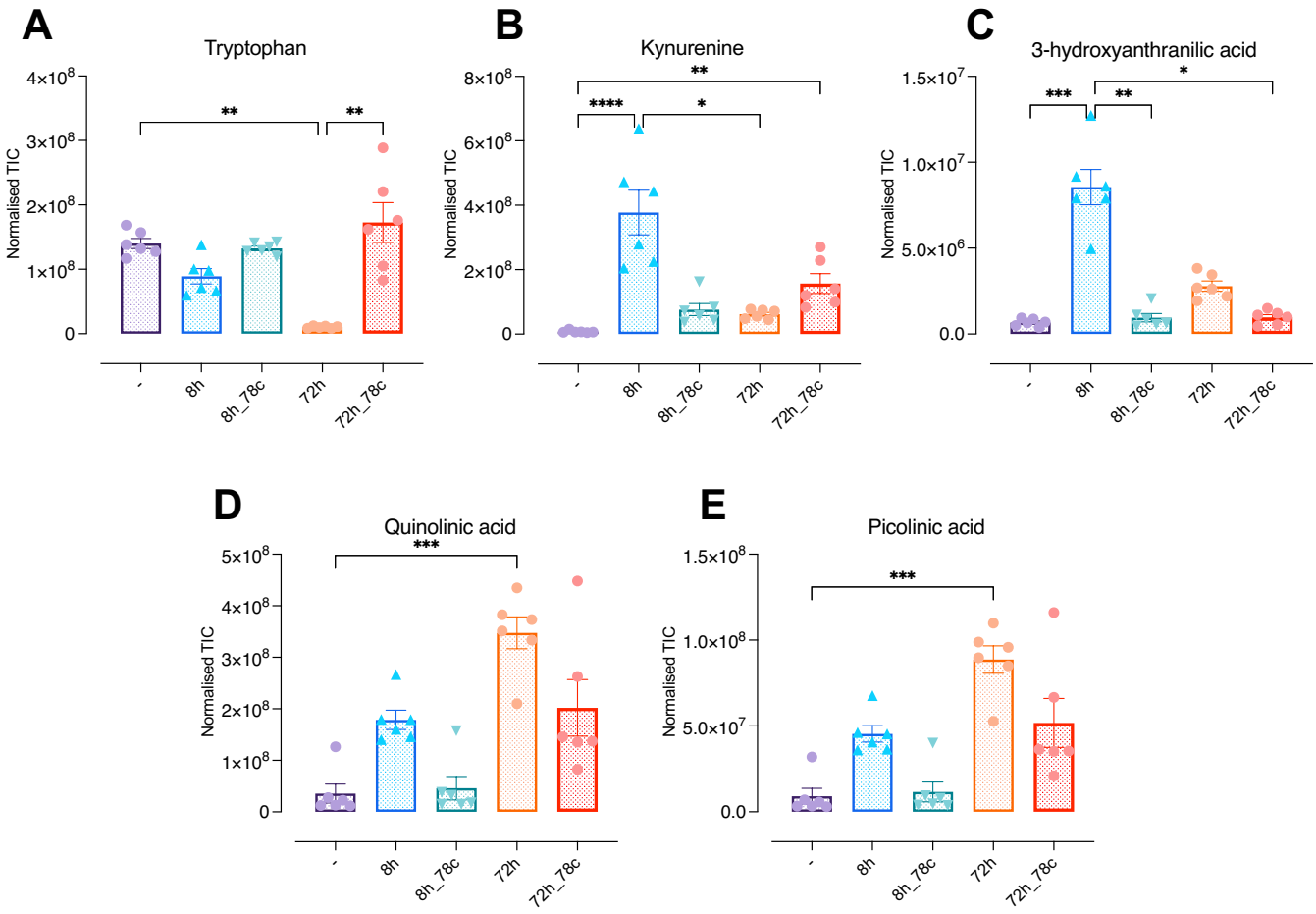

Figure 5.10. Analysis of intracellular metabolites associated with tryptophan degradation upon CD38 inhibition. Human monocyte-derived macrophages were cultured with 1000U/ml IFN-α and/or 20μM 78c for 8 and 72 hours. Cells were extracted and global metabolomic profiling was performed using LC-MS. (**A-E**) Summary graphs depicting levels of intracellular (**A**) tryptophan, (**B**) Kynurenine, (**C**) 3-hydroxyanthranilic acid, (**D**) quinolinic acid and (**E**) picolinic acid are shown as normalised total ion count (TIC). Each dot represents one donor. Data presented as mean ± S.E.M. * p<0.05, ** p<0.01, *** p<0.001. Kruskal-Wallis test.

Effects of tryptophan deficiency on macrophage phenotypes

So far, my findings combining cell assays and untargeted metabolomics showed that

(i) chronic IFN-I treatment reduced NAD levels via increasing the NAD-consuming enzyme CD38 and causing a pro-inflammatory macrophage state prone to cell death upon very short term and sub-optimal activation of TLR4 with only 1ng/ml of LPS.

(ii) the NAD reduction was not the primary cause of this weakened macrophage cell state.

(iii) instead, the macrophage metabolism was rewired toward tryptophan consumption as a result of CD38 upregulation, in order to activate the *de novo* NAD synthesis pathway.

Furthermore, there is evidence that dysregulation of the tryptophan degradation pathway leading to lower tryptophan and increased kynurenine is linked to disease severity in lupus patients and lupus-prone mice[321,341]. Furthermore, tryptophan and its downstream metabolites have been linked to inflammatory processes contributing to chronic inflammatory diseases[342]. Based on my findings and the current literature, I then checked whether the tryptophan pathway played a role in IFN-I-mediated changes in macrophage phenotype and function.

I first decided to elucidate the effects that the reduction of tryptophan or increase of downstream metabolites in the medium had on IFN-I-treated macrophages. I cultured MDMs in normal RPMI medium or tryptophan-free medium in the presence or absence of IFN-I for 3 days. Cell viability, pro-inflammatory phenotypes and LPS-induced cell death were assessed using the techniques previously mentioned.

The summary graphs of each parameter of untreated condition, IFN-I-treated cells cultured in normal RPMI medium and IFN-I-treated cells cultured in tryptophan-free medium (Trp free) are shown in **figure 5.11.** In the absence of tryptophan, IFN-I-mediated CD38 upregulation was reduced by around 50% compared to that of IFN-I-treated cells cultured in a medium that contained tryptophan (**Fig.5.11A**). Significant downregulations of CD80 expression and IL-6 secretion were also detected in IFN-I-treated cells cultured with the tryptophan-free medium (**Fig.5.11B and 5.11C**).

In terms of cell viability, the data revealed that the percentage of alive cells in IFN-I-treated cells cultured in the tryptophan-free medium did not significantly differ from

that of cells cultured in the normal RPMI medium (**Fig.5.11D**). In response to the short-term LPS rechallenge, I found that the percentage of alive cells in IFN-I treated macrophages was improved with the absence of tryptophan (**Fig.5.11E**). Overall, these data highlighted the involvement of tryptophan in initiating phenotypic changes in macrophages.

Overall, the results in this chapter suggested that CD38 and tryptophan were crucial in initiating changes in the metabolism, phenotypes and functions of human macrophages exposed to chronic IFN-I exposure.

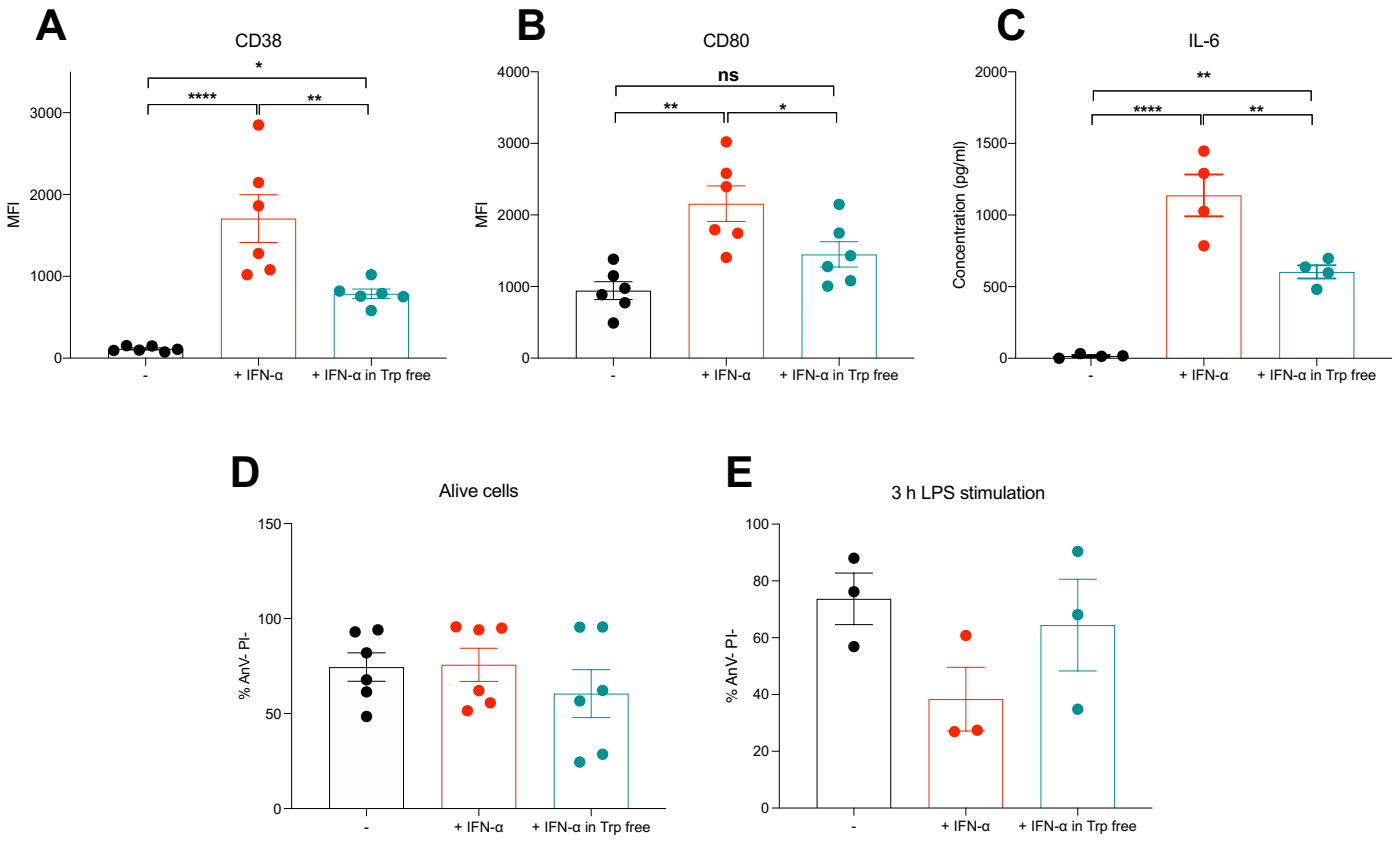

Figure 5.11. Effects of tryptophan deficiency on macrophage phenotypes
Human monocyte-derived macrophages were treated with 1000U/ml IFN-α in either RPMI medium or tryptophan-free RPMI medium for 3 days. (**A-B**) Expression of surface markers was measured by flow cytometry. Summary graphs showing MFI of (**A**) CD38 and (**B**) the pro-inflammatory marker CD80. (**C**) Summary graphs showing the production of inflammatory cytokine IL-6 measured by ELISA. (**D**) Summary graphs showing the percentage of alive cells across treatments. (**E**) After 3 days of culture, cells then were stimulated with 1ng/ml LPS for 3 hours. Cell viability was assessed by flow cytometry. Summary graph showing the percentage of alive cells after 3 hours of LPS re-challenge. Each dot represents one donor. Data presented as mean ± S.E.M. ns=not significant, * p<0.05, ** p<0.01, **** p<0.0001. Kruskal-Wallis test.

5.3. Discussion

The role of CD38 in lupus has been reported in both human and mouse models. In the early stages of SLE, there is an increase in the percentage CD38+ B cells, T cells and monocytes detected in the circulation of SLE patients[343-345]. However, it is still controversial whether CD38 has a protective or pathogenic role in SLE [203,346-348]. In our recent publication we reported that the IFN-I signature correlates with an increased CD38 expression in $CD8^+$ T cells from SLE patients[248]. Since I observed a similar IFN-I-induced upregulation of CD38 in human macrophages, I then investigated the impact of this on the metabolism and functions of the macrophages.

CD38 is a glycoprotein present mostly on the surface of numerous cell types such as immune cells and tumour cells. CD38 has several functions due to its multiple enzymatic activities. It can act as the main NAD catabolic enzyme or as a regulator of intracellular calcium homeostasis or as adhesion molecule interacting with CD31[349]. CD38 is considered to be a therapeutic target under many circumstances where metabolism is disturbed, such as infection, ageing, and cancer[202]. For instance, clinical trials have demonstrated that anti-CD38 antibodies like daratumumab and isatuximab are highly effective in treating multiple myeloma and other CD38+ malignancies[202]. There are several compounds that can block this enzyme and their effect is variable depending on the diverse roles played by CD38. These compounds can be classified as flavonoids or NAD+ analogue inhibitors or heterocyclic small molecules. They can establish covalent or non-covalent bonds with the amino acids in CD38's active site[202]. However, flavonoids and NAD+ analogue inhibitors lack selectivity and exhibit off-target effects[350-352]. In contrast, small molecule derivatives of 4-amino-quinoline including 78c have been shown to be highly potent and specific and to have potential beneficial effects in pre-clinical investigations comparable to NAD+-enhancing medications[353-355]. These small molecules can bind to site residues of CD38, leading to reduced glycohydrolase activity and increased cyclase activity of CD38[356]. Having reviewed the literature, I opted to employ 78c as a CD38 inhibitor to study the function of CD38 in the context of chronic IFN-I exposure in human macrophages. To achieve this, I administered IFN-α or the IFN-α and 78c combination to HMDMs and then used the same techniques as in the previous chapter to evaluate the phenotypes, functions and metabolomic profile of these macrophages.

In this chapter, I demonstrated the contribution of IFN-I-induced CD38 overexpression to macrophage changes including pro-inflammatory-like phenotype and LPS-induced cell death following chronic IFN-I exposure. Specifically, I found that blocking CD38 by 78c reduced the IFN-I-triggered upregulation of CD80 expression and IL-6 secretion back to similar levels to those of the untreated samples. This highlighted the significance of CD38 in the initiation of macrophage pro-inflammatory phenotypes in response to prolonged IFN-I exposure. These findings were consistent with the literature whereby the inflammatory role of CD38 in human macrophages and monocytes was reported. For instance, blocking CD38 using flavonoids such as Apigenin and Rhein reduced IL-6 and IL-12p expression in M1 macrophages[203]. In the pristane-induced mouse model of lupus[346], CD38 knockout mice developed less severe lupus-like autoimmunity compared to the wild-type mice. This was accompanied by the reduction of ISG expression and the numbers of $CCR2^{hi}Ly6C^{hi}$ inflammatory monocytes in the peritoneal cavity[346], suggesting a role of CD38 in promoting abnormal inflammation. Furthermore, I discovered that inhibiting CD38 greatly improved LPS-induced cell death in IFN-I-priming macrophages. This protective role of CD38 inhibition upon LPS stimulation was previously reported in LPS or LPS/IFN-γ-stimulated microglia[357,358]. Several reports have shown that LPS is a potent CD38 inducer[359,360] and that CD38 can mediate LPS-induced macrophage activation[361]. For example, Shu *et al.* reported that LPS increased CD38 expression in a time and dose-dependent manner and this CD38 upregulation contributed to M1 polarisation in LPS-activated macrophages through NF-κB signalling pathway[361]. In addition, CD38 knockout mice had significantly reduced NF-κB signalling in an autoimmune arthritic mouse model[362]. In contrast, Farahany *et al*. revealed that NF-κB activation was inhibited by CD38 activation[363]. The authors found increases in the expression of NF-κB target genes including inflammatory cytokines and NLRP3 inflammasome in CD38−/− macrophages compared with wild type cells[363]. They also suggested that CD38 activity suppressed TLR4 activation through inhibition of Btk (Bruton's tyrosine kinase) activation[363].

Even though CD38 is a major NAD consumer[211] and NAD imbalance can affect macrophage polarisation[200,300], the observed functional changes in IFN-I-treated macrophages were not caused by CD38-induced NAD depletion, but rather by alternative mechanisms. I found that increasing NAD levels by adding NMN, an NAD+

precursor of the NAD salvage pathway did not rectify IFN-I-induced changes in macrophages. Furthermore, data from global metabolomic profiling revealed that inhibiting CD38 with 78c restored intracellular NAD levels completely at the 8-hour time point but only partially at the 72-hour time point. This could be due to the upregulation of other NAD-consuming enzymes such as SIRT1 and PARPs at later time points. Future work of combining 78c with other NAD-consuming enzyme inhibitors like Ex-527 (a SIRT1 inhibitor) may improve our understanding of the pathways involved.

Like the NAD metabolism, 78c treatment corrected the levels of tryptophan completely at the 72-hour time point. 78c treatment also rescued the level of various metabolites in the tryptophan-kynurenine pathway fully at the early time point and partially at the latter time points. These findings indicated that the activation of tryptophan-kynurenine was indeed dependent on NAD decline which was triggered by CD38 at the early time point following IFN-I treatment. Literature has recently suggested a link between the activation of the tryptophan pathway and IFN-I signature[323]. Anderson *et al*. reported the correlation of high ISG expression analysed from whole blood with the increase in the ratios of kynurenine and tryptophan in the serum of SLE patients[323]. They also suggested that this activation of the tryptophan-kynurenine pathway may be especially significant in monocytes[323]. Taken together, my findings suggested that the IFN-I-mediate tryptophan metabolism seen in SLE patients may be regulated through CD38 overexpression and reduction of NAD.

The roles of the tryptophan-kynurenine pathway in inflammatory conditions are controversial. Kynurenine was discovered to reduce hyperinflammation by acting as a ligand of the aryl hydrocarbon receptor (AhR), a transcription factor that regulates both local and systemic immune responses[364]. This pathway was also associated with the differentiation of Treg cells and the immune regulation of DC phenotypes, inducing prolonged immune tolerance[365-367]. On the other hand, using multi-omics approaches, Bustamante and colleagues found that the tryptophan-kynurenine pathway may act as a central regulator of genes associated with increased inflammation in COVID-19 and inflammatory bowel disease[368]. Furthermore, the increased ratios of kynurenine to tryptophan are considered to be an indication of the rate of inflammation in ageing[364,369,370]. As one of the chronic IFN-I-induced changes in macrophages was the pro-inflammatory phenotypes, I then tried to identify whether IFN-I-induced

tryptophan-kynurenine activation contributed to changes in macrophages. To achieve this, I cultured IFN-I-treated macrophages in the medium lacking tryptophan. Of note, the medium used in this project was RPMI 1640 supplemented with 10% FBS. It is known that RPMI 1640 normally contains 25 μM tryptophan and adding 10% FBS elevated tryptophan concentration to 26 μM[371]. Therefore, to completely remove tryptophan from the cell culture, I opted to use the tryptophan-free RPMI medium without FBS. FBS was also excluded from the normal RPMI medium in this experiment. I found that tryptophan deficiency could reverse IFN-I-mediated pro-inflammatory phenotypes and LPS-induced cell death, like those treated with 78c. These results demonstrated that chronic IFN-I treatment could induce alterations in macrophage activity through the tryptophan pathways. One may speculate that there might be certain metabolites in the tryptophan pathways that are produced by IFN-I-treated macrophages that cause pro-inflammatory features or could be harmful to the cells when LPS was present. Of note, Fallarino *et al.* demonstrated that 24 hours of 3-hydroxyanthranilic or quinolinic acids could induce apoptosis in thymocytes, T helper cells and macrophages[372]. Therefore, other metabolites related to tryptophan pathways such as 3-hydroxyanthranilic or quinolinic acids may be involved in the harmful effect mediated by LPS in IFN-I-treated cells.

Another intriguing observation from inhibiting CD38 by 78c in IFN-I-treated macrophages was that it caused the macrophages' metabolic status to transition from exhausted to revitalised. After 72 hours of treatment, the metabolomic profiling data revealed that the usage of 78c induced nucleotide synthesis and several vitamins including vitamin B5 and vitamin B7, and amino acid catabolism. These pathways in human macrophages were not affected by chronic IFN-I treatment. This suggested that the effects of blocking CD38 by 78c were beyond the correction of the phenotypes observed by prolonged IFN treatment. Further experiments are required to pinpoint the underlying mechanism of these changes and to determine whether this effect contributes to IFN-I-mediated changes.

Overall, in this chapter, I reported that CD38 was indeed important in initiating changes in the metabolism, phenotypes and functions of human macrophages exposed to chronic IFN-I exposure. My results demonstrate that CD38-induced NAD reduction triggered the activation of the tryptophan-kynurenine pathway. As a result, this tryptophan pathway contributed to the IFN-I-mediated changes including pro-

inflammatory phenotypes and increased LPS-induced cell death. Blocking CD38 or limiting tryptophan in cell culture could reverse chronic IFN-I-mediated effects in human macrophages, suggesting that these may be therapeutic targets for SLE treatment.

Chapter 6: Overall discussion

6.1. Summary and conclusions

SLE is a chronic autoimmune disease in which autoantibodies attack healthy cells and tissues, causing extensive inflammation and tissue destruction in organs such as the skin, joints, kidneys, brain, and blood vessels. This condition is complex, and the aetiology is assumed to be the combination of several factors, making the cure for SLE difficult to find. Because of its complexity, further research is needed to better understand its aetiopathogenesis and eventually to develop effective novel treatments.

The majority of SLE patients exhibit an IFN signature[373] and thus IFN-Is are considered one of the key mediators of SLE pathogenesis[374]. Bulk transcriptomic analyses have shown that hallmarks of this disease include enhanced IFN-I signalling, abnormal T cell activation and inability to remove apoptotic cells[249]. However, how IFN-Is affect these immune pathways remain poorly understood and the primary objective of my PhD study was to fill this knowledge gap.

Ex vivo analysis of PBMCs from SLE patients previously performed in the group suggested a possible link between the chronic IFN-I signature and an aberrant mitochondrial metabolism in $CD8^+$ T cells[248]. However, due to the technical limitation that relates to maintaining the IFN signature in cultured $CD8^+$ T cells from SLE patients, it was technically challenging to further determine the long-term biological consequences of IFN-induced mitochondrial changes in $CD8^+$ T cells from SLE patients. Guided by these preliminary data and other literature reports, I firstly hypothesised that the chronic IFN-I exposure was the cause of the mitochondrial alterations present in the SLE $CD8^+$ T cells. I tested the hypothesis by establishing the *in vitro* experimental conditions able of recapitulating the mitochondrial abnormalities seen in $CD8^+$ T cells from IFN-high SLE patients and by assessing downstream $CD8^+$ T cell activation and cell death. The following key findings of the first part of my thesis (Chapter 3) contribute to existing knowledge:

1. Mitochondrial defects seen in IFN-high SLE patients are most likely the consequence of the combined effects of prolonged IFN-I exposure and TCR stimulation.
2. The combination of chronic IFN-I exposure and TCR activation triggers mitochondrial changes including an increase in mitochondrial mass and activity, a reduction in OXPHOS-related gene expression and SRC.
3. The combination of chronic IFN-I exposure and TCR activation can lead to a defective acute response to TCR activation and increased cell death upon antigen rechallenge.

Further investigations conducted by my supervisors' laboratory discovered that chronic IFN-I exposure mediated mitochondrial changes in $CD8^+$ T cells through the regulation of NAD metabolism[248]. As illustrated in **figure 6.1**[248], we propose that in SLE patients with high IFN signatures, the combination of chronic IFN-I exposure and TCR activation enhances the expression of NAD-consuming enzymes such as CD38, resulting in lower NAD/NADH ratios[248]. This IFN-I-mediated NAD reduction impairs mitochondrial respiration and decreases the energetic fitness of the cells. As a result, these IFN-exposed $CD8^+$ T cells are more likely to die in situations of high energy demand such as antigen stimulation. These events may promote autoimmunity by increasing autoantigen loads[248]. Of note, these IFN-I-mediated abnormalities in $CD8^+$ T cells can be rescued by NMN supplementation[248].

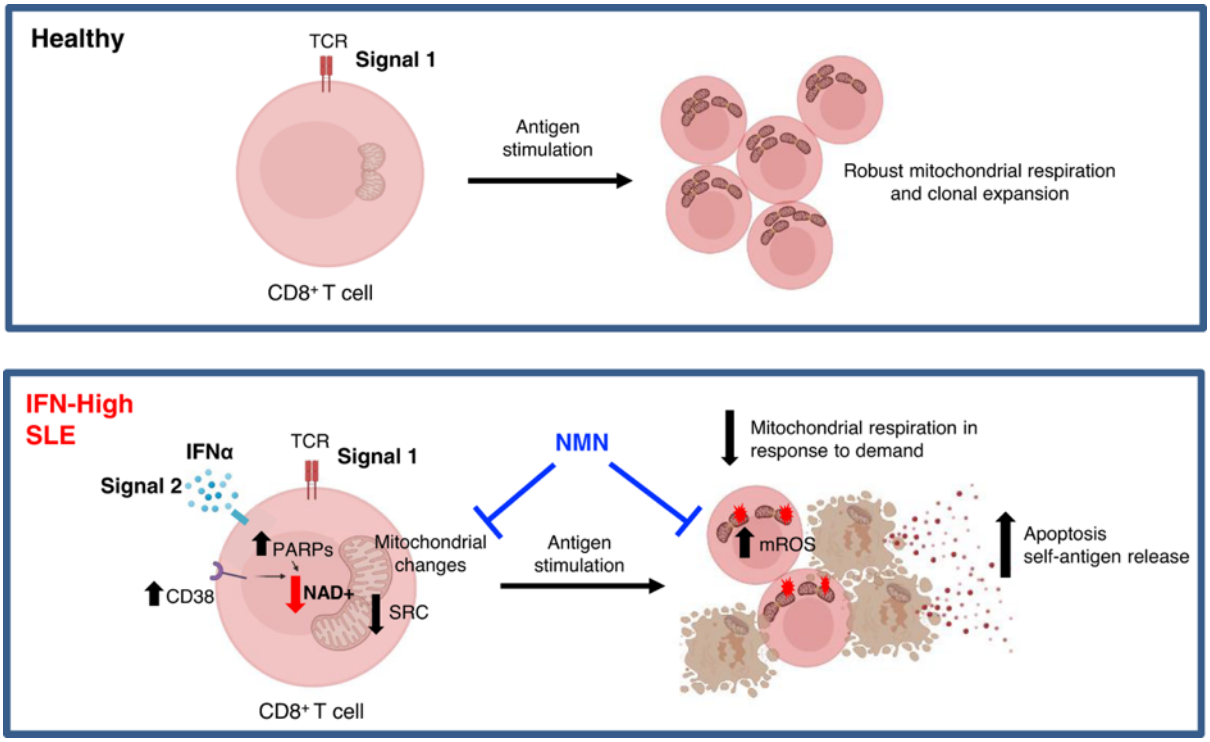

Figure 6.1. Chronic IFN-I exposure influences the metabolic fitness of CD8⁺ T cells in SLE patients. The figure is taken from Buang et al.[248]

This discovery in CD8⁺ T cells inspired me to explore whether similar effects could be observed in other immune cell types. It is known that macrophages play a crucial part in the onset and progression of SLE[33,287]. Recent research has shown that IFN-Is affect macrophage metabolism, but these data were primarily obtained in short-term settings for viral infection applications. Therefore, there is still a limited understanding of how long-term IFN-I exposure modulates macrophage metabolism and the impact of macrophage metabolism on lupus pathogenesis. My subsequent objective was to examine how human macrophage metabolism changes in response to prolonged IFN-I exposure and whether the changes influence macrophage functions. I achieved this aim integrating the transcriptomic and, metabolomic profiling with phenotypes and functions of IFN-I-treated macrophages and investigating the role of NAD-consuming enzyme CD38 in IFN-I-treated macrophages. My following key findings of the second part of the thesis (Chapter 4 and Chapter 5) contribute to existing knowledge as follows:

1. Chronic IFN-I exposure increases the expression of NAD-consuming enzymes such as CD38, resulting in decreased NAD concentrations in macrophages.
2. This IFN-I-mediated NAD+ decline is compensated by rapid and substantial *de novo* NAD synthesis through the tryptophan-kynurenine pathway, which may subsequently maintain TCA cycle activity and ATP levels.
3. Chronic IFN-I exposure promotes a pro-inflammatory phenotype in macrophages and induces cell death in response to TLR4 re-challenge
4. These IFN-I-induced changes in macrophages are mediated by CD38 and possibly via activation of the tryptophan pathway.

It has been widely accepted that macrophages play important roles in the development of SLE. For example, dysregulated activation and polarisation of macrophages towards pro-inflammatory or M1 phenotype in SLE can result in tissue damage[33]. My research highlighted that chronic IFN-I exposure could be one of the factors contributing to the pro-inflammatory phenotype observed in macrophages from SLE patients. Interestingly, though IFN-I-treated macrophages showed an M1-like phenotype, the metabolomics changes in these macrophages are distinct from those observed in classical M1 LPS-treated macrophages[375]. I found that chronic IFN-I exposure induced NAD+-dependent metabolic reprogramming, allowing the cell to survive. These cells, however, appeared to be vulnerable to bacterial infection and this seems to be specific to LPS/TLR4 pathway.

Mechanistically, my data suggest that in SLE patients with high IFN signatures, IFN-I exposure enhances CD38 expression together with other NAD-consuming enzymes in macrophages. This increased CD38 expression treatment could be because the CD38 promoter contains potential IRF binding sites, and IRF-1 has been found to boost CD38 mRNA and protein levels[376-378]. CD38-mediated NAD decline subsequently triggers the activation of the tryptophan-kynurenine pathway as part of the *de novo* NAD synthesis pathway to compensate for the loss of NAD. As a result, this tryptophan-kynurenine pathway contributes to promoting pro-inflammatory phenotypes and increased LPS-induced cell death. Tryptophan itself or other metabolites in the tryptophan-kynurenine pathways produced by IFN-I-treated macrophages may be responsible for these chronic IFN-I-mediated changes.

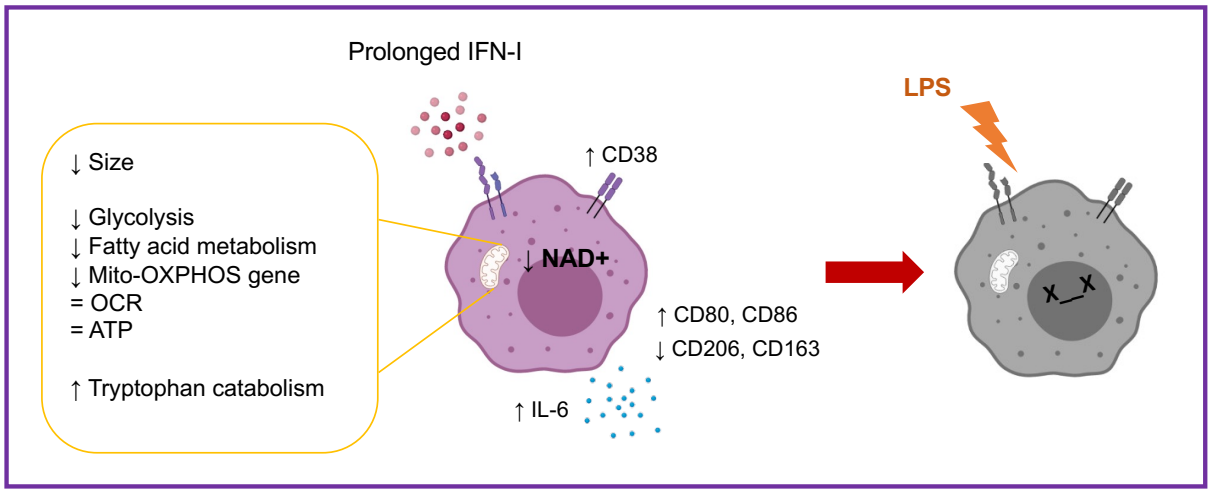

Figure 6.2. Summary of how chronic IFN-I exposure affects human macrophages. Chronic IFN-I exposure in human macrophages induces an NAD+-dependent metabolic reprogramming that allows cell survival but increases their vulnerability to bacterial infection.

Overall, my findings contribute to increasing the existing knowledge about the role of IFN-Is in SLE. I demonstrated that one of the ways IFN-Is impact mitochondrial function in SLE is through the regulation of the NAD metabolism[248]. My thesis also describes the complex relationship between chronic IFN-I exposure and the metabolic reprogramming in $CD8^+$ T cells and macrophages. It also reveals the immune and metabolic consequences of prolonged IFN-I stimulation in human macrophages. This is an area of research with limited resources as most of the studies did not exceed the 24-hour-stimulation period, which I believe does not mimic the chronic exposure that characterizes the “SLE-like macrophages”. This implies that investigating metabolic pathways may be a useful therapeutic strategy for treating SLE. In addition, my findings suggest that patient classification based on IFN signature should be taken into consideration when treating SLE patients, as the fundamental pathological processes between IFN-high and IFN-neg SLE patients may be distinct[248].

6.2. Future works

The data reported in this thesis have, to a certain extent, addressed my initial hypothesis, by showing how chronic IFN-I exposure affects $CD8^+$ T cell and macrophage metabolism and their immune functions. Future studies are required to validate the findings in SLE patients and to further pinpoint the underlying mechanisms. This could be investigated by doing the following:

1. Validating the *in vitro* observations by staining kidney biopsies from IFN-high SLE patients for CD38. My host laboratory already has a collection of paraffin-embedded kidney biopsies from IFN-high and IFN-neg SLE patients. Immunohistochemical staining will be performed to assess CD68+CD38+ macrophages in the tissue. This is to assess whether macrophages of IFN-high SLE patients exhibit higher CD38 expression compared to IFN-neg SLE patients and healthy controls. These findings will be also correlated with clinical and histological data.
2. Assessing the global metabolomic profile of plasma from IFN-high SLE patients and comparing it with that of IFN-neg SLE patients and healthy controls. Plasma from 265 SLE patients and 18 healthy controls have already been collected and will be analysed by our collaborator at the CECAD Research Centre, University of Cologne, Germany using LC-MS. The metabolomic profiling will be correlated with the ISG expression.
3. Identifying the metabolites in tryptophan pathways that contribute to IFN-I-mediated phenotypic changes and induce rapid cell death upon LPS stimulation. Literature has highlighted the potential role of tryptophan catabolites such as 3-hydroxyanthranilic or quinolinic acids[372]. Therefore, future experiments should consider supplementation with these metabolites to assess whether they are responsible for the macrophage pro-inflammatory phenotype and LPS-induced cell death.

Bibliography

1 Crow, M. K. Type I Interferon in the Pathogenesis of Lupus. *The Journal of Immunology* **192**, 5459, doi:10.4049/jimmunol.1002795 (2014).

2 Cancro, M. P. Age-Associated B Cells. *Annu Rev Immunol* **38**, 315-340, doi:10.1146/annurev-immunol-092419-031130 (2020).

3 Pyfrom, S. *et al.* The dynamic epigenetic regulation of the inactive X chromosome in healthy human B cells is dysregulated in lupus patients. *Proc Natl Acad Sci U S A* **118**, doi:10.1073/pnas.2024624118 (2021).

4 Yu, B. *et al.* B cell-specific XIST complex enforces X-inactivation and restrains atypical B cells. *Cell* **184**, 1790-1803.e1717, doi:10.1016/j.cell.2021.02.015 (2021).

5 Aringer, M. *et al.* 2019 European League Against Rheumatism/American College of Rheumatology Classification Criteria for Systemic Lupus Erythematosus. *Arthritis Rheumatol* **71**, 1400-1412, doi:10.1002/art.40930 (2019).

6 Bultink, I. E. M., de Vries, F., van Vollenhoven, R. F. & Lalmohamed, A. Mortality, causes of death and influence of medication use in patients with systemic lupus erythematosus vs matched controls. *Rheumatology (Oxford)* **60**, 207-216, doi:10.1093/rheumatology/keaa267 (2021).

7 Block, S. R. A brief history of twins. *Lupus* **15**, 61-64, doi:10.1191/0961203306lu2263ed (2006).

8 Deapen, D. *et al.* A revised estimate of twin concordance in systemic lupus erythematosus. *Arthritis Rheum* **35**, 311-318, doi:10.1002/art.1780350310 (1992).

9 Hochberg, M. C. The application of genetic epidemiology to systemic lupus erythematosus. *J Rheumatol* **14**, 867-869 (1987).

10 Alarcón-Segovia, D. *et al.* Familial aggregation of systemic lupus erythematosus, rheumatoid arthritis, and other autoimmune diseases in 1,177 lupus patients from the GLADEL cohort. *Arthritis Rheum* **52**, 1138-1147, doi:10.1002/art.20999 (2005).

11 Kaul, A. *et al.* Systemic lupus erythematosus. *Nature Reviews Disease Primers* **2**, 16039, doi:10.1038/nrdp.2016.39 (2016).

12 Mak, A. & Tay, S. H. Environmental factors, toxicants and systemic lupus erythematosus. *International journal of molecular sciences* **15**, 16043-16056, doi:10.3390/ijms150916043 (2014).

13 Gulati, G. & Brunner, H. I. Environmental triggers in systemic lupus erythematosus. *Semin Arthritis Rheum* **47**, 710-717, doi:10.1016/j.semarthrit.2017.10.001 (2018).

14 Lossius, A., Johansen, J. N., Torkildsen, Ø., Vartdal, F. & Holmøy, T. Epstein-Barr virus in systemic lupus erythematosus, rheumatoid arthritis and multiple sclerosis—association and causation. *Viruses* **4**, 3701-3730, doi:10.3390/v4123701 (2012).

15 Van Vollenhoven, R. F. *et al.* Treat-to-target in systemic lupus erythematosus: recommendations from an international task force. *Annals of the rheumatic diseases* **73**, 958-967 (2014).

16 Tanaka, Y. State-of-the-art treatment of systemic lupus erythematosus. *International journal of rheumatic diseases* **23**, 465-471, doi:10.1111/1756-185X.13817 (2020).

17 Furie, R. *et al.* A phase III, randomized, placebo-controlled study of belimumab, a monoclonal antibody that inhibits B lymphocyte stimulator, in patients with systemic lupus erythematosus. *Arthritis and rheumatism* **63**, 3918-3930, doi:10.1002/art.30613 (2011).

18 Navarra, S. V. *et al.* Efficacy and safety of belimumab in patients with active systemic lupus erythematosus: a randomised, placebo-controlled, phase 3 trial. *The Lancet* **377**, 721-731, doi:10.1016/S0140-6736(10)61354-2 (2011).

19 Arbuckle, M. R. *et al.* Development of autoantibodies before the clinical onset of systemic lupus erythematosus. *N Engl J Med* **349**, 1526-1533, doi:10.1056/NEJMoa021933 (2003).

20 Walport, M. J. Complement and systemic lupus erythematosus. *Arthritis Res* **4 Suppl 3**, S279-293, doi:10.1186/ar586 (2002).

21 Emlen, W., Niebur, J. & Kadera, R. Accelerated in vitro apoptosis of lymphocytes from patients with systemic lupus erythematosus. *The Journal of Immunology* **152**, 3685 (1994).

22 Jin, O. *et al.* Lymphocyte apoptosis and macrophage function: correlation with disease activity in systemic lupus erythematosus. *Clinical Rheumatology* **24**, 107-110, doi:10.1007/s10067-004-0972-x (2005).

23 Perniok, A., Wedekind, F., Herrmann, M., Specker, C. & Schneider, M. High levels of circulating early apoptic peripheral blood mononuclear cells in systemic lupus erythematosus. *Lupus* **7**, 113-118, doi:10.1191/096120398678919804 (1998).

24 Ren, Y. *et al.* Increased apoptotic neutrophils and macrophages and impaired macrophage phagocytic clearance of apoptotic neutrophils in systemic lupus erythematosus. *Arthritis & Rheumatism* **48**, 2888-2897, doi:10.1002/art.11237 (2003).

25 Tas, S. W., Quartier, P., Botto, M. & Fossati-Jimack, L. Macrophages from patients with SLE and rheumatoid arthritis have defective adhesion in vitro, while only SLE macrophages have impaired uptake of apoptotic cells. *Annals of the rheumatic diseases* **65**, 216-221, doi:10.1136/ard.2005.037143 (2006).

26 Muñoz, L. E., Lauber, K., Schiller, M., Manfredi, A. A. & Herrmann, M. The role of defective clearance of apoptotic cells in systemic autoimmunity. *Nature Reviews Rheumatology* **6**, 280-289, doi:10.1038/nrrheum.2010.46 (2010).

27 Jørgensen, M. H., Rekvig, O. P., Jacobsen, R. S., Jacobsen, S. & Fenton, K. A. Circulating levels of chromatin fragments are inversely correlated with anti-dsDNA antibody levels in human and murine systemic lupus erythematosus. *Immunology Letters* **138**, 179-186, doi:https://doi.org/10.1016/j.imlet.2011.04.006 (2011).

28 Füllgrabe, J., Hajji, N. & Joseph, B. Cracking the death code: apoptosis-related histone modifications. *Cell Death & Differentiation* **17**, 1238-1243, doi:10.1038/cdd.2010.58 (2010).

29 van Bavel, C. C. *et al.* Apoptosis-induced histone H3 methylation is targeted by autoantibodies in systemic lupus erythematosus. *Annals of the Rheumatic Diseases* **70**, 201, doi:10.1136/ard.2010.129320 (2011).

30 van Bavel, C. C., Dieker, J. W., Tamboer, W. P., van der Vlag, J. & Berden, J. H. Lupus-derived monoclonal autoantibodies against apoptotic chromatin recognize acetylated conformational epitopes. *Molecular Immunology* **48**, 248-256, doi:https://doi.org/10.1016/j.molimm.2010.08.003 (2010).

31 Zhang, J., Jacobi, A. M., Wang, T. & Diamond, B. Pathogenic autoantibodies in systemic lupus erythematosus are derived from both self-reactive and non-self-reactive B cells. *Molecular medicine (Cambridge, Mass.)* **14**, 675-681, doi:10.2119/2008-00066.Zhang (2008).

32 Kalaaji, M. *et al.* Glomerular apoptotic nucleosomes are central target structures for nephritogenic antibodies in human SLE nephritis. *Kidney International* **71**, 664-672, doi:https://doi.org/10.1038/sj.ki.5002133 (2007).

33 Ma, C., Xia, Y., Yang, Q. & Zhao, Y. The contribution of macrophages to systemic lupus erythematosus. *Clin Immunol* **207**, 1-9, doi:10.1016/j.clim.2019.06.009 (2019).

34 Hakkim, A. *et al.* Impairment of neutrophil extracellular trap degradation is associated with lupus nephritis. *Proceedings of the National Academy of Sciences of the United States of America* **107**, 9813-9818, doi:10.1073/pnas.0909927107 (2010).

35 Yang, F., He, Y., Zhai, Z. & Sun, E. Programmed Cell Death Pathways in the Pathogenesis of Systemic Lupus Erythematosus. *Journal of Immunology Research* **2019**, 3638562, doi:10.1155/2019/3638562 (2019).

36 Brinkmann, V. *et al.* Neutrophil Extracellular Traps Kill Bacteria. *Science* **303**, 1532, doi:10.1126/science.1092385 (2004).

37 Caielli, S. *et al.* A CD4+ T cell population expanded in lupus blood provides B cell help through interleukin-10 and succinate. *Nature Medicine* **25**, 75-81, doi:10.1038/s41591-018-0254-9 (2019).

38 Bijl, M., Reefman, E., Horst, G., Limburg, P. C. & Kallenberg, C. G. M. Reduced uptake of apoptotic cells by macrophages in systemic lupus erythematosus: correlates with decreased serum levels of complement. *Annals of the rheumatic diseases* **65**, 57-63, doi:10.1136/ard.2005.035733 (2006).

39 Bijl, M., Reefman, E., Horst, G., Limburg, P. C. & Kallenberg, C. G. Reduced uptake of apoptotic cells by macrophages in systemic lupus erythematosus: correlates with decreased serum levels of complement. *Ann Rheum Dis* **65**, 57-63, doi:10.1136/ard.2005.035733 (2006).

40 Katsiari, C. G., Liossis, S.-N. C. & Sfikakis, P. P. The Pathophysiologic Role of Monocytes and Macrophages in Systemic Lupus Erythematosus: A Reappraisal. *Seminars in Arthritis and Rheumatism* **39**, 491-503, doi:https://doi.org/10.1016/j.semarthrit.2008.11.002 (2010).

41 Korman, B. D. *et al.* Inflammatory expression profiles in monocyte-to-macrophage differentiation in patients with systemic lupus erythematosus and relationship with atherosclerosis. *Arthritis Res Ther* **16**, R147, doi:10.1186/ar4609 (2014).

42 Manderson, A. P., Botto, M. & Walport, M. J. The Role of Complement in the Development of Systemic Lupus Erythematosus. *Annual Review of Immunology* **22**, 431-456, doi:10.1146/annurev.immunol.22.012703.104549 (2004).

43 Chan, V. S.-F. *et al.* Distinct roles of myeloid and plasmacytoid dendritic cells in systemic lupus erythematosus. *Autoimmunity Reviews* **11**, 890-897, doi:https://doi.org/10.1016/j.autrev.2012.03.004 (2012).

44 Banchereau, J. & Steinman, R. M. Dendritic cells and the control of immunity. *Nature* **392**, 245-252, doi:10.1038/32588 (1998).

45 Blanco, P., Palucka, A. K., Pascual, V. & Banchereau, J. Dendritic cells and cytokines in human inflammatory and autoimmune diseases. *Cytokine & growth factor reviews* **19**, 41-52, doi:10.1016/j.cytogfr.2007.10.004 (2008).

46 Klarquist, J., Zhou, Z., Shen, N. & Janssen, E. M. Dendritic Cells in Systemic Lupus Erythematosus: From Pathogenic Players to Therapeutic Tools. *Mediators of Inflammation* **2016**, 5045248, doi:10.1155/2016/5045248 (2016).

47 Mozaffarian, N., Wiedeman, A. & Stevens, A. Active systemic lupus erythematosus is associated with failure of antigen-presenting cells to express programmed death ligand-1. *Rheumatology* **47**, 1335-1341 (2008).

48 Crow, M. K., Olferiev, M. & Kirou, K. A. Targeting of type I interferon in systemic autoimmune diseases. *Translational research : the journal of laboratory and clinical medicine* **165**, 296-305, doi:10.1016/j.trsl.2014.10.005 (2015).

49 Stetson, D. B. Endogenous retroelements and autoimmune disease. *Current opinion in immunology* **24**, 692-697, doi:10.1016/j.coi.2012.09.007 (2012).

50 Fritzler, M. J. Clinical relevance of autoantibodies in systemic rheumatic diseases. *Molecular Biology Reports* **23**, 133-145, doi:10.1007/BF00351161 (1996).

51 Akahoshi, M. *et al.* Th1/Th2 balance of peripheral T helper cells in systemic lupus erythematosus. *Arthritis & Rheumatism* **42**, 1644-1648, doi:10.1002/1529-0131(199908)42:8<1644::AID-ANR12>3.0.CO;2-L (1999).

52 Kunman, D. M. & Steinberg, A. D. Inquiry into Murine and Human Lupus. *Immunological Reviews* **144**, 157-193, doi:10.1111/j.1600-065X.1995.tb00069.x (1995).

53 Katsuyama, T., Tsokos, G. C. & Moulton, V. R. Aberrant T Cell Signaling and Subsets in Systemic Lupus Erythematosus. *Frontiers in Immunology* **9**, doi:10.3389/fimmu.2018.01088 (2018).

54 Brundula, V. *et al.* Diminished levels of T cell receptor ζ chains in peripheral blood T lymphocytes from patients with systemic lupus erythematosus. *Arthritis & Rheumatism* **42**, 1908-1916, doi:10.1002/1529-0131(199909)42:9<1908::AID-ANR17>3.0.CO;2-7 (1999).

55 Liossis, S. N., Ding, X. Z., Dennis, G. J. & Tsokos, G. C. Altered pattern of TCR/CD3-mediated protein-tyrosyl phosphorylation in T cells from patients with systemic lupus erythematosus. Deficient expression of the T cell receptor zeta chain. *The Journal of Clinical Investigation* **101**, 1448-1457, doi:10.1172/JCI1457 (1998).

56 Pang, M. *et al.* Defective expression and tyrosine phosphorylation of the T cell receptor zeta chain in peripheral blood T cells from systemic lupus erythematosus patients. *Clinical & Experimental Immunology* **129**, 160-168, doi:10.1046/j.1365-2249.2002.01833.x (2002).

57 Juang, Y.-T. *et al.* PP2A Dephosphorylates Elf-1 and Determines the Expression of CD3ζ and FcRγ in Human Systemic Lupus Erythematosus T Cells. *The Journal of Immunology* **181**, 3658, doi:10.4049/jimmunol.181.5.3658 (2008).

58 Shlomchik, M. J., Craft, J. E. & Mamula, M. J. From T to B and back again: positive feedback in systemic autoimmune disease. *Nature Reviews Immunology* **1**, 147, doi:10.1038/35100573 (2001).

59 Koshy, M., Berger, D. & Crow, M. K. Increased expression of CD40 ligand on systemic lupus erythematosus lymphocytes. *The Journal of clinical investigation* **98**, 826-837, doi:10.1172/JCI118855 (1996).

60 Vakkalanka, R. K. *et al.* Elevated levels and functional capacity of soluble CD40 ligand in systemic lupus erythematosus sera. *Arthritis & Rheumatism* **42**, 871-881, doi:10.1002/1529-0131(199905)42:5<871::AID-ANR5>3.0.CO;2-J (1999).

61 Crispín, J. C., Kyttaris, V. C., Juang, Y.-T. & Tsokos, G. C. How signaling and gene transcription aberrations dictate the systemic lupus erythematosus T cell phenotype. *Trends in Immunology* **29**, 110-115, doi:https://doi.org/10.1016/j.it.2007.12.003 (2008).

62 Kong, P. L. *et al.* Intrinsic T cell defects in systemic autoimmunity. *Ann N Y Acad Sci* **987**, 60-67, doi:10.1111/j.1749-6632.2003.tb06033.x (2003).

63 Vratsanos, G. S., Jung, S., Park, Y. M. & Craft, J. CD4(+) T cells from lupus-prone mice are hyperresponsive to T cell receptor engagement with low and high affinity peptide antigens: a model to explain spontaneous T cell activation in lupus. *The Journal of experimental medicine* **193**, 329-337, doi:10.1084/jem.193.3.329 (2001).

64 Suárez-Fueyo, A., Barber, D. F., Martínez-Ara, J., Zea-Mendoza, A. C. & Carrera, A. C. Enhanced Phosphoinositide 3-Kinase δ Activity Is a Frequent Event in Systemic Lupus Erythematosus That Confers Resistance to Activation-Induced T Cell Death. *The Journal of Immunology* **187**, 2376, doi:10.4049/jimmunol.1101602 (2011).

65 Talaat, R. M., Mohamed, S. F., Bassyouni, I. H. & Raouf, A. A. Th1/Th2/Th17/Treg cytokine imbalance in systemic lupus erythematosus (SLE) patients: Correlation with disease activity. *Cytokine* **72**, 146-153, doi:https://doi.org/10.1016/j.cyto.2014.12.027 (2015).

66 Collier, J. L., Weiss, S. A., Pauken, K. E., Sen, D. R. & Sharpe, A. H. Not-so-opposite ends of the spectrum: CD8+ T cell dysfunction across chronic infection, cancer and autoimmunity. *Nature Immunology* **22**, 809-819, doi:10.1038/s41590-021-00949-7 (2021).

67 Gravano, D. M. & Hoyer, K. K. Promotion and prevention of autoimmune disease by CD8+ T cells. *Journal of Autoimmunity* **45**, 68-79, doi:https://doi.org/10.1016/j.jaut.2013.06.004 (2013).

68 Gravano, D. M. & Hoyer, K. K. Promotion and prevention of autoimmune disease by CD8+ T cells. *J Autoimmun* **45**, 68-79, doi:10.1016/j.jaut.2013.06.004 (2013).

69 Suárez-Fueyo, A., Bradley, S. J. & Tsokos, G. C. T cells in Systemic Lupus Erythematosus. *Current opinion in immunology* **43**, 32-38, doi:10.1016/j.coi.2016.09.001 (2016).

70 Kis-Toth, K. *et al.* Selective Loss of Signaling Lymphocytic Activation Molecule Family Member 4–Positive CD8+ T Cells Contributes to the Decreased Cytotoxic Cell Activity in Systemic Lupus Erythematosus. *Arthritis & Rheumatology* **68**, 164-173, doi:10.1002/art.39410 (2015).

71 Blanco, P. *et al.* Increase in activated CD8+ T lymphocytes expressing perforin and granzyme B correlates with disease activity in patients with systemic lupus erythematosus. *Arthritis & Rheumatism* **52**, 201-211, doi:10.1002/art.20745 (2005).

72 Dolff, S. *et al.* Urinary CD8+ T-cell counts discriminate between active and inactive lupus nephritis. *Arthritis Research & Therapy* **15**, R36, doi:10.1186/ar4189 (2013).

73 Couzi, L. *et al.* Predominance of CD8+ T lymphocytes among periglomerular infiltrating cells and link to the prognosis of class III and class IV lupus nephritis. *Arthritis & Rheumatism* **56**, 2362-2370, doi:10.1002/art.22654 (2007).

74 Nowling, T. K. & Gilkeson, G. S. Mechanisms of tissue injury in lupus nephritis. *Arthritis research & therapy* **13**, 250-250, doi:10.1186/ar3528 (2011).

75 Klarquist, J. & Janssen, E. M. The bm12 Inducible Model of Systemic Lupus Erythematosus (SLE) in C57BL/6 Mice. *Journal of Visualized Experiments : JoVE*, 53319, doi:10.3791/53319 (2015).

76 Ling, G. S. *et al.* C1q restrains autoimmunity and viral infection by regulating CD8⁺ T cell metabolism. *Science* **360**, 558-563, doi:10.1126/science.aao4555 (2018).

77 McKinney, E. F., Lee, J. C., Jayne, D. R. W., Lyons, P. A. & Smith, K. G. C. T-cell exhaustion, co-stimulation and clinical outcome in autoimmunity and infection. *Nature* **523**, 612, doi:10.1038/nature14468

https://www.nature.com/articles/nature14468#supplementary-information (2015).

78 Yi, J. S., Cox, M. A. & Zajac, A. J. T-cell exhaustion: characteristics, causes and conversion. *Immunology* **129**, 474-481, doi:10.1111/j.1365-2567.2010.03255.x (2010).

79 Chen, Y. *et al.* CXCR5+PD-1+ follicular helper CD8 T cells control B cell tolerance. *Nature Communications* **10**, 4415, doi:10.1038/s41467-019-12446-5 (2019).

80 Isaacs, A. & Lindenmann, J. Virus interference. I. The interferon. *Proc R Soc Lond B Biol Sci* **147**, 258-267, doi:10.1098/rspb.1957.0048 (1957).

81 Odorizzi, P. M. & Wherry, E. J. An Interferon Paradox. *Science* **340**, 155-156, doi:10.1126/science.1237568 (2013).

82 Smith, M. A. *et al.* Using the circulating proteome to assess type I interferon activity in systemic lupus erythematosus. *Scientific Reports* **10**, 4462, doi:10.1038/s41598-020-60563-9 (2020).

83 Fried, M. W. *et al.* Peginterferon Alfa-2a plus Ribavirin for Chronic Hepatitis C Virus Infection. *New England Journal of Medicine* **347**, 975-982, doi:10.1056/NEJMoa020047 (2002).

84 Golomb, H. M. *et al.* Alpha-2 interferon therapy of hairy-cell leukemia: a multicenter study of 64 patients. *Journal of Clinical Oncology* **4**, 900-905, doi:10.1200/JCO.1986.4.6.900 (1986).

85 Lau, G. K. K. *et al.* Peginterferon Alfa-2a, Lamivudine, and the Combination for HBeAg-Positive Chronic Hepatitis B. *New England Journal of Medicine* **352**, 2682-2695, doi:10.1056/NEJMoa043470 (2005).

86 Furie, R. *et al.* Anifrolumab, an Anti–Interferon-α Receptor Monoclonal Antibody, in Moderate-to-Severe Systemic Lupus Erythematosus. *Arthritis & Rheumatology* **69**, 376-386, doi:10.1002/art.39962 (2017).

87 Higgs, B. W. *et al.* Patients with systemic lupus erythematosus, myositis, rheumatoid arthritis and scleroderma share activation of a common type I interferon pathway. *Annals of the Rheumatic Diseases* **70**, 2029, doi:10.1136/ard.2011.150326 (2011).

88 Higgs, B. W. *et al.* A phase 1b clinical trial evaluating sifalimumab, an anti-IFN-α monoclonal antibody, shows target neutralisation of a type I IFN signature in blood of dermatomyositis and polymyositis patients. *Annals of the Rheumatic Diseases* **73**, 256, doi:10.1136/annrheumdis-2012-202794 (2014).

89 Hervas-Stubbs, S. *et al.* Direct Effects of Type I Interferons on Cells of the Immune System. *Clinical Cancer Research* **17**, 2619 (2011).

90 Swiecki, M. & Colonna, M. Unraveling the functions of plasmacytoid dendritic cells during viral infections, autoimmunity, and tolerance. *Immunological Reviews* **234**, 142-162, doi:10.1111/j.0105-2896.2009.00881.x (2010).

91 Ito, T., Wang, Y.-H. & Liu, Y.-J. Plasmacytoid dendritic cell precursors/type I interferon-producing cells sense viral infection by Toll-like receptor (TLR) 7 and TLR9. *Springer Seminars in Immunopathology* **26**, 221-229, doi:10.1007/s00281-004-0180-4 (2005).

92 Swiecki, M. *et al.* Type I interferon negatively controls plasmacytoid dendritic cell numbers in vivo. *The Journal of Experimental Medicine* **208**, 2367 (2011).

93 Mostafavi, S. *et al.* Parsing the Interferon Transcriptional Network and Its Disease Associations. *Cell* **164**, 564-578, doi:https://doi.org/10.1016/j.cell.2015.12.032 (2016).

94 Schneider, W. M., Chevillotte, M. D. & Rice, C. M. Interferon-Stimulated Genes: A Complex Web of Host Defenses. *Annual Review of Immunology* **32**, 513-545, doi:10.1146/annurev-immunol-032713-120231 (2014).

95 de Veer, M. J. *et al.* Functional classification of interferon-stimulated genes identified using microarrays. *Journal of Leukocyte Biology* **69**, 912-920, doi:10.1189/jlb.69.6.912 (2001).

96 Katze, M. G., He, Y. & Gale, M. Viruses and interferon: a fight for supremacy. *Nature Reviews Immunology* **2**, 675-687, doi:10.1038/nri888 (2002).

97 Ng, Cherie T., Mendoza, Juan L., Garcia, K. C. & Oldstone, Michael B. A. Alpha and Beta Type 1 Interferon Signaling: Passage for Diverse Biologic Outcomes. *Cell* **164**, 349-352, doi:https://doi.org/10.1016/j.cell.2015.12.027 (2016).

98 Mesev, E. V., LeDesma, R. A. & Ploss, A. Decoding type I and III interferon signalling during viral infection. *Nature Microbiology* **4**, 914-924, doi:10.1038/s41564-019-0421-x (2019).

99 Prchal, M. *et al.* Type I interferons as mediators of immune adjuvants for T- and B cell-dependent acquired immunity. *Vaccine* **27**, G17-G20, doi:https://doi.org/10.1016/j.vaccine.2009.10.016 (2009).

100 Muller, U. *et al.* Functional role of type I and type II interferons in antiviral defense. *Science* **264**, 1918, doi:10.1126/science.8009221 (1994).

101 Snell, L. M., McGaha, T. L. & Brooks, D. G. Type I Interferon in Chronic Virus Infection and Cancer. *Trends in Immunology* **38**, 542-557, doi:https://doi.org/10.1016/j.it.2017.05.005 (2017).

102 Kurche, J. S., Haluszczak, C., McWilliams, J. A., Sanchez, P. J. & Kedl, R. M. Type I IFN-Dependent T Cell Activation Is Mediated by IFN-Dependent Dendritic Cell OX40 Ligand Expression and Is Independent of T Cell IFNR Expression. *The Journal of Immunology* **188**, 585, doi:10.4049/jimmunol.1102550 (2012).

103 Montoya, M. *et al.* Type I interferons produced by dendritic cells promote their phenotypic and functional activation. *Blood* **99**, 3263-3271, doi:10.1182/blood.V99.9.3263 (2002).

104 Lee, A. J. *et al.* Inflammatory monocytes require type I interferon receptor signaling to activate NK cells via IL-18 during a mucosal viral infection. *Journal of Experimental Medicine* **214**, 1153-1167, doi:10.1084/jem.20160880 (2017).

105 Martinez, J., Huang, X. & Yang, Y. Direct Action of Type I IFN on NK Cells Is Required for Their Activation in Response to Vaccinia Viral Infection In Vivo. *The Journal of Immunology* **180**, 1592, doi:10.4049/jimmunol.180.3.1592 (2008).

106 Teijaro, J. R. Type I interferons in viral control and immune regulation. *Current Opinion in Virology* **16**, 31-40, doi:https://doi.org/10.1016/j.coviro.2016.01.001 (2016).

107 Sandler, N. G. *et al.* Type I interferon responses in rhesus macaques prevent SIV infection and slow disease progression. *Nature* **511**, 601-605, doi:10.1038/nature13554 (2014).

108 Teijaro, J. R. *et al.* Persistent LCMV Infection Is Controlled by Blockade of Type I Interferon Signaling. *Science* **340**, 207-211, doi:10.1126/science.1235214 (2013).

109 Ng, C. T. & Oldstone, M. B. A. Infected CD8α[−] dendritic cells are the predominant source of IL-10 during establishment of persistent viral infection. *Proceedings of the National Academy of Sciences* **109**, 14116, doi:10.1073/pnas.1211910109 (2012).

110 Wilson, E. B. *et al.* Emergence of distinct multiarmed immunoregulatory antigen-presenting cells during persistent viral infection. *Cell host & microbe* **11**, 481-491, doi:10.1016/j.chom.2012.03.009 (2012).

111 Rönnblom, L. & Elkon, K. B. Cytokines as therapeutic targets in SLE. *Nat Rev Rheumatol* **6**, 339-347, doi:10.1038/nrrheum.2010.64 (2010).

112 Hooks, J. J. *et al.* Immune Interferon in the Circulation of Patients with Autoimmune Disease. *New England Journal of Medicine* **301**, 5-8, doi:10.1056/NEJM197907053010102 (1979).

113 Ytterberg, S. R. & Schnitzer, T. J. Serum interferon levels in patients with systemic lupus erythematosus. *Arthritis & Rheumatism* **25**, 401-406, doi:10.1002/art.1780250407 (1982).

114 Rönnblom, L. E., Alm, G. V. & Öberg, K. E. Autoimmunity after Alpha-Interferon Therapy for Malignant Carcinoid Tumors. *Annals of Internal Medicine* **115**, 178-183, doi:10.7326/0003-4819-115-3-178 (1991).

115 RÖNnblom, L. E., Alm, G. V. & ÖBerg, K. E. Possible induction of systemic lupus erythematosus by interferon-α treatment in a patient with a malignant carcinoid tumour. *Journal of Internal Medicine* **227**, 207-210, doi:10.1111/j.1365-2796.1990.tb00144.x (1990).

116 Baechler, E. C. *et al.* Interferon-inducible gene expression signature in peripheral blood cells of patients with severe lupus. *Proceedings of the National Academy of Sciences* **100**, 2610-2615, doi:10.1073/pnas.0337679100 (2003).

117 Bennett, L. *et al.* Interferon and Granulopoiesis Signatures in Systemic Lupus Erythematosus Blood. *Journal of Experimental Medicine* **197**, 711-723, doi:10.1084/jem.20021553 (2003).

118 Crow, M. K., Kirou, K. A. & Wohlgemuth, J. Microarray Analysis of Interferon-regulated Genes in SLE. *Autoimmunity* **36**, 481-490, doi:10.1080/08916930310001625952 (2003).

119 Han, G. M. *et al.* Analysis of gene expression profiles in human systemic lupus erythematosus using oligonucleotide microarray. *Genes & Immunity* **4**, 177-186, doi:10.1038/sj.gene.6363966 (2003).

120 Absher, D. M. *et al.* Genome-Wide DNA Methylation Analysis of Systemic Lupus Erythematosus Reveals Persistent Hypomethylation of Interferon Genes and Compositional Changes to CD4+ T-cell Populations. *PLoS Genetics* **9**, e1003678, doi:10.1371/journal.pgen.1003678 (2013).

121 Coit, P. *et al.* Genome-wide DNA methylation study suggests epigenetic accessibility and transcriptional poising of interferon-regulated genes in naïve CD4+ T cells from lupus patients. *Journal of Autoimmunity* **43**, 78-84, doi:https://doi.org/10.1016/j.jaut.2013.04.003 (2013).

122 Berry, M. P. R. *et al.* An interferon-inducible neutrophil-driven blood transcriptional signature in human tuberculosis. *Nature* **466**, 973-977, doi:10.1038/nature09247 (2010).

123 Kennedy, W. P. *et al.* Association of the interferon signature metric with serological disease manifestations but not global activity scores in multiple cohorts of patients with SLE. *Lupus science & medicine* **2**, e000080-e000080, doi:10.1136/lupus-2014-000080 (2015).

124 Linsley, P. S., Speake, C., Whalen, E. & Chaussabel, D. Copy Number Loss of the Interferon Gene Cluster in Melanomas Is Linked to Reduced T Cell Infiltrate

and Poor Patient Prognosis. *PLOS ONE* **9**, e109760, doi:10.1371/journal.pone.0109760 (2014).

125 Zak, D. E. *et al.* A blood RNA signature for tuberculosis disease risk: a prospective cohort study. *The Lancet* **387**, 2312-2322, doi:10.1016/S0140-6736(15)01316-1 (2016).

126 Feng, D. *et al.* Genetic variants and disease-associated factors contribute to enhanced interferon regulatory factor 5 expression in blood cells of patients with systemic lupus erythematosus. *Arthritis & Rheumatism* **62**, 562-573, doi:10.1002/art.27223 (2010).

127 Landolt-Marticorena, C. *et al.* Lack of association between the interferon-α signature and longitudinal changes in disease activity in systemic lupus erythematosus. *Annals of the Rheumatic Diseases* **68**, 1440 (2009).

128 Chiche, L. *et al.* Modular Transcriptional Repertoire Analyses of Adults With Systemic Lupus Erythematosus Reveal Distinct Type I and Type II Interferon Signatures. *Arthritis & Rheumatology* **66**, 1583-1595, doi:10.1002/art.38628 (2014).

129 Rönnblom, L. & Leonard, D. Interferon pathway in SLE: one key to unlocking the mystery of the disease. *Lupus science & medicine* **6**, e000270-e000270, doi:10.1136/lupus-2018-000270 (2019).

130 Hertzog, P., Forster, S. & Samarajiwa, S. Systems Biology of Interferon Responses. *Journal of Interferon & Cytokine Research* **31**, 5-11, doi:10.1089/jir.2010.0126 (2011).

131 Rönnblom, L. & Eloranta, M.-L. The interferon signature in autoimmune diseases. *Current Opinion in Rheumatology* **25**, 248-253, doi:10.1097/BOR.0b013e32835c7e32 (2013).

132 Forster, S. Interferon signatures in immune disorders and disease. *Immunology and Cell Biology* **90**, 520-527, doi:10.1038/icb.2012.12 (2012).

133 Rönnblom, L., Alm, G. V. & Eloranta, M.-L. The type I interferon system in the development of lupus. *Seminars in Immunology* **23**, 113-121, doi:https://doi.org/10.1016/j.smim.2011.01.009 (2011).

134 Bronson, P. G., Chaivorapol, C., Ortmann, W., Behrens, T. W. & Graham, R. R. The genetics of type I interferon in systemic lupus erythematosus. *Current Opinion in Immunology* **24**, 530-537, doi:https://doi.org/10.1016/j.coi.2012.07.008 (2012).

135 Niewold, T. B. *et al.* IRF5 haplotypes demonstrate diverse serological associations which predict serum interferon alpha activity and explain the majority of the genetic association with systemic lupus erythematosus. *Annals of the Rheumatic Diseases* **71**, 463 (2012).

136 Yuan, Y. J., Luo, X. B. & Shen, N. Current advances in lupus genetic and genomic studies in Asia. *Lupus* **19**, 1374-1383, doi:10.1177/0961203310376639 (2010).

137 Lood, C. *et al.* C1q inhibits immune complex–induced interferon-α production in plasmacytoid dendritic cells: A novel link between C1q deficiency and systemic lupus erythematosus pathogenesis. *Arthritis & Rheumatism* **60**, 3081-3090, doi:10.1002/art.24852 (2009).

138 Santer, D. M. *et al.* C1q Deficiency Leads to the Defective Suppression of IFN-α in Response to Nucleoprotein Containing Immune Complexes. *The Journal of Immunology* **185**, 4738 (2010).

139 Clancy, R. M. *et al.* Targeting downstream transcription factors and epigenetic modifications following Toll-like receptor 7/8 ligation to forestall tissue injury in anti-Ro60 associated heart block. *Journal of Autoimmunity* **67**, 36-45, doi:https://doi.org/10.1016/j.jaut.2015.09.003 (2016).

140 Catalina, M. D., Bachali, P., Geraci, N. S., Grammer, A. C. & Lipsky, P. E. Gene expression analysis delineates the potential roles of multiple interferons in systemic lupus erythematosus. *Communications Biology* **2**, 140, doi:10.1038/s42003-019-0382-x (2019).

141 Jin, Z. *et al.* Single-cell gene expression patterns in lupus monocytes independently indicate disease activity, interferon and therapy. *Lupus Science & Medicine* **4**, e000202, doi:10.1136/lupus-2016-000202 (2017).

142 Perez, R. K. *et al.* Single-cell RNA-seq reveals cell type-specific molecular and genetic associations to lupus. *Science* **376**, eabf1970, doi:10.1126/science.abf1970 (2022).

143 Psarras, A., Wittmann, M. & Vital, E. M. Emerging concepts of type I interferons in SLE pathogenesis and therapy. *Nature Reviews Rheumatology* **18**, 575-590, doi:10.1038/s41584-022-00826-z (2022).

144 Akiyama, C. *et al.* Conditional Upregulation of IFN-α Alone Is Sufficient to Induce Systemic Lupus Erythematosus. *The Journal of Immunology* **203**, 835, doi:10.4049/jimmunol.1801617 (2019).

145 Pylaeva, E., Lang, S. & Jablonska, J. The Essential Role of Type I Interferons in Differentiation and Activation of Tumor-Associated Neutrophils. *Frontiers in Immunology* **7**, doi:10.3389/fimmu.2016.00629 (2016).

146 Kiefer, K., Oropallo, M. A., Cancro, M. P. & Marshak-Rothstein, A. Role of type I interferons in the activation of autoreactive B cells. *Immunology and Cell Biology* **90**, 498-504, doi:10.1038/icb.2012.10 (2012).

147 Brinkmann, V., Geiger, T., Alkan, S. & Heusser, C. H. Interferon alpha increases the frequency of interferon gamma-producing human CD4+ T cells. *The Journal of Experimental Medicine* **178**, 1655 (1993).

148 Tough, D. F. Modulation of T-cell function by type I interferon. *Immunology & Cell Biology* **90**, 492-497, doi:10.1038/icb.2012.7 (2012).

149 Cucak, H., Yrlid, U., Reizis, B., Kalinke, U. & Johansson-Lindbom, B. Type I Interferon Signaling in Dendritic Cells Stimulates the Development of Lymph-Node-Resident T Follicular Helper Cells. *Immunity* **31**, 491-501, doi:10.1016/j.immuni.2009.07.005 (2009).

150 Kolumam, G. A., Thomas, S., Thompson, L. J., Sprent, J. & Murali-Krishna, K. Type I interferons act directly on CD8 T cells to allow clonal expansion and memory formation in response to viral infection. *The Journal of Experimental Medicine* **202**, 637 (2005).

151 Deeks, E. D. Anifrolumab: First Approval. *Drugs* **81**, 1795-1802, doi:10.1007/s40265-021-01604-z (2021).

152 O'Neill, L. A. J., Kishton, R. J. & Rathmell, J. A guide to immunometabolism for immunologists. *Nature Reviews Immunology* **16**, 553-565, doi:10.1038/nri.2016.70 (2016).

153 Kolliniati, O., Ieronymaki, E., Vergadi, E. & Tsatsanis, C. Metabolic Regulation of Macrophage Activation. *J Innate Immun* **14**, 51-68, doi:10.1159/000516780 (2022).

154 Ratnayake, D. *et al.* Macrophages provide a transient muscle stem cell niche via NAMPT secretion. *Nature* **591**, 281-287, doi:10.1038/s41586-021-03199-7 (2021).

155 Chen, L. B. Mitochondrial Membrane Potential in Living Cells. *Annual Review of Cell Biology* **4**, 155-181, doi:10.1146/annurev.cb.04.110188.001103 (1988).

156 Skulachev, V. P. Transmembrane electrochemical H+-potential as a convertible energy source for the living cell. *FEBS Letters* **74**, 1-9, doi:10.1016/0014-5793(77)80739-4 (1977).

157 Li, X. *et al.* Targeting mitochondrial reactive oxygen species as novel therapy for inflammatory diseases and cancers. *Journal of Hematology & Oncology* **6**, 19, doi:10.1186/1756-8722-6-19 (2013).

158 Cross, C. E., Halliwell, B., Borish, E. T. & et al. OXygen radicals and human disease. *Annals of Internal Medicine* **107**, 526-545, doi:10.7326/0003-4819-107-4-526 (1987).

159 Basso, P. J., Andrade-Oliveira, V. & Câmara, N. O. S. Targeting immune cell metabolism in kidney diseases. *Nature Reviews Nephrology* **17**, 465-480, doi:10.1038/s41581-021-00413-7 (2021).

160 Osellame, L. D., Blacker, T. S. & Duchen, M. R. Cellular and molecular mechanisms of mitochondrial function. *Best Practice & Research Clinical Endocrinology & Metabolism* **26**, 711-723, doi:10.1016/j.beem.2012.05.003 (2012).

161 Sharabi, A. & Tsokos, G. C. T cell metabolism: new insights in systemic lupus erythematosus pathogenesis and therapy. *Nature Reviews Rheumatology* **16**, 100-112, doi:10.1038/s41584-019-0356-x (2020).

162 Almeida, L., Lochner, M., Berod, L. & Sparwasser, T. Metabolic pathways in T cell activation and lineage differentiation. *Seminars in Immunology* **28**, 514-524, doi:https://doi.org/10.1016/j.smim.2016.10.009 (2016).

163 Michalek, R. D. *et al.* Cutting Edge: Distinct Glycolytic and Lipid Oxidative Metabolic Programs Are Essential for Effector and Regulatory CD4⁺ T Cell Subsets. *The Journal of Immunology* **186**, 3299, doi:10.4049/jimmunol.1003613 (2011).

164 Lai, Z.-W. *et al.* N-acetylcysteine reduces disease activity by blocking mammalian target of rapamycin in T cells from systemic lupus erythematosus patients: A randomized, double-blind, placebo-controlled trial. *Arthritis & Rheumatism* **64**, 2937-2946, doi:10.1002/art.34502 (2012).

165 Yin, Y. *et al.* Normalization of CD4⁺ T cell metabolism reverses lupus. *Science Translational Medicine* **7**, 274ra218-274ra218, doi:10.1126/scitranslmed.aaa0835 (2015).

166 Delgoffe, G. M. *et al.* The kinase mTOR regulates the differentiation of helper T cells through the selective activation of signaling by mTORC1 and mTORC2. *Nature immunology* **12**, 295-303, doi:10.1038/ni.2005 (2011).

167 Finlay, D. & Cantrell, D. A. Metabolism, migration and memory in cytotoxic T cells. *Nature reviews. Immunology* **11**, 109-117, doi:10.1038/nri2888 (2011).

168 van der Windt, Gerritje J. W. *et al.* Mitochondrial Respiratory Capacity Is a Critical Regulator of CD8+ T Cell Memory Development. *Immunity* **36**, 68-78, doi:https://doi.org/10.1016/j.immuni.2011.12.007 (2012).

169 van der Windt, G. J. W. *et al.* CD8 memory T cells have a bioenergetic advantage that underlies their rapid recall ability. *Proceedings of the National Academy of Sciences* **110**, 14336, doi:10.1073/pnas.1221740110 (2013).

170 Viola, A., Munari, F., Sánchez-Rodríguez, R., Scolaro, T. & Castegna, A. The Metabolic Signature of Macrophage Responses. *Frontiers in Immunology* **10**, doi:10.3389/fimmu.2019.01462 (2019).

171 Nathan, C. F., Murray, H. W., Wiebe, M. E. & Rubin, B. Y. Identification of interferon-gamma as the lymphokine that activates human macrophage oxidative metabolism and antimicrobial activity. *The Journal of experimental medicine* **158**, 670-689 (1983).

172 Pace, J. L., Russell, S. W., Schreiber, R. D., Altman, A. & Katz, D. H. Macrophage activation: priming activity from a T-cell hybridoma is attributable to interferon-gamma. *Proceedings of the National Academy of Sciences* **80**, 3782-3786 (1983).

173 Stein, M., Keshav, S., Harris, N. & Gordon, S. Interleukin 4 potently enhances murine macrophage mannose receptor activity: a marker of alternative immunologic macrophage activation. *The Journal of experimental medicine* **176**, 287-292 (1992).

174 Doyle, A. G. *et al.* Interleukin-13 alters the activation state of murine macrophages in vitro: Comparison with interleukin-4 and interferon-γ. *European journal of immunology* **24**, 1441-1445 (1994).

175 Martinez, F. O. & Gordon, S. The M1 and M2 paradigm of macrophage activation: time for reassessment. *F1000prime reports* **6** (2014).

176 Caielli, S. *et al.* Oxidized mitochondrial nucleoids released by neutrophils drive type I interferon production in human lupus. *J Exp Med* **213**, 697-713, doi:10.1084/jem.20151876 (2016).

177 Mantovani, A., Biswas, S. K., Galdiero, M. R., Sica, A. & Locati, M. Macrophage plasticity and polarization in tissue repair and remodelling. *The Journal of pathology* **229**, 176-185 (2013).

178 Viola, A., Munari, F., Sánchez-Rodríguez, R., Scolaro, T. & Castegna, A. The Metabolic Signature of Macrophage Responses. *Front Immunol* **10**, 1462, doi:10.3389/fimmu.2019.01462 (2019).

179 Hard, G. Some biochemical aspects of the immune macrophage. *British journal of experimental pathology* **51**, 97 (1970).

180 Freemerman, A. J. *et al.* Metabolic reprogramming of macrophages: glucose transporter 1 (GLUT1)-mediated glucose metabolism drives a proinflammatory phenotype. *Journal of Biological Chemistry* **289**, 7884-7896 (2014).

181 Jha, A. K. *et al.* Network integration of parallel metabolic and transcriptional data reveals metabolic modules that regulate macrophage polarization. *Immunity* **42**, 419-430 (2015).

182 Tannahill, G. *et al.* Succinate is an inflammatory signal that induces IL-1β through HIF-1α. *Nature* **496**, 238-242 (2013).

183 Rius, J. *et al.* NF-κB links innate immunity to the hypoxic response through transcriptional regulation of HIF-1α. *Nature* **453**, 807-811 (2008).

184 Van Uden, P., Kenneth, N. S. & Rocha, S. Regulation of hypoxia-inducible factor-1α by NF-κB. *Biochemical Journal* **412**, 477-484 (2008).

185 Wang, T. *et al.* HIF1α-induced glycolysis metabolism is essential to the activation of inflammatory macrophages. *Mediators of inflammation* **2017** (2017).

186 Huang, S. C.-C. *et al.* Metabolic reprogramming mediated by the mTORC2-IRF4 signaling axis is essential for macrophage alternative activation. *Immunity* **45**, 817-830 (2016).

187 Tan, Z. *et al.* Pyruvate dehydrogenase kinase 1 participates in macrophage polarization via regulating glucose metabolism. *The Journal of immunology* **194**, 6082-6089 (2015).

188 Wang, F. *et al.* Glycolytic stimulation is not a requirement for M2 macrophage differentiation. *Cell metabolism* **28**, 463-475. e464 (2018).

189 Vats, D. *et al.* Oxidative metabolism and PGC-1β attenuate macrophage-mediated inflammation. *Cell metabolism* **4**, 13-24 (2006).

190 Rath, M., Müller, I., Kropf, P., Closs, E. I. & Munder, M. Metabolism via Arginase or Nitric Oxide Synthase: Two Competing Arginine Pathways in Macrophages. *Frontiers in Immunology* **5**, doi:10.3389/fimmu.2014.00532 (2014).

191 Griess, B., Mir, S., Datta, K. & Teoh-Fitzgerald, M. Scavenging reactive oxygen species selectively inhibits M2 macrophage polarization and their pro-tumorigenic function in part, via Stat3 suppression. *Free Radic Biol Med* **147**, 48-60, doi:10.1016/j.freeradbiomed.2019.12.018 (2020).

192 Harden, A., Young, W. J. & Martin, C. J. The alcoholic ferment of yeast-juice. Part II.—The coferment of yeast-juice. *Proceedings of the Royal Society of London. Series B, Containing Papers of a Biological Character* **78**, 369-375, doi:10.1098/rspb.1906.0070 (1906).

193 Warburg, O. & Christian, W. Pyridin, the hydrogen-transferring component of the fermentation enzymes (pyridine nucleotide). *Biochem. Z* **287** (1936).

194 Xie, N. *et al.* NAD+ metabolism: pathophysiologic mechanisms and therapeutic potential. *Signal Transduction and Targeted Therapy* **5**, 227, doi:10.1038/s41392-020-00311-7 (2020).

195 Haigis, M. C. & Sinclair, D. A. Mammalian sirtuins: biological insights and disease relevance. *Annual review of pathology* **5**, 253 (2010).

196 Chang, H.-C. & Guarente, L. SIRT1 and other sirtuins in metabolism. *Trends in Endocrinology & Metabolism* **25**, 138-145 (2014).

197 Murata, M. M. *et al.* NAD+ consumption by PARP1 in response to DNA damage triggers metabolic shift critical for damaged cell survival. *Mol Biol Cell* **30**, 2584-2597, doi:10.1091/mbc.E18-10-0650 (2019).

198 Altmeyer, M. & Hottiger, M. O. Poly (ADP-ribose) polymerase 1 at the crossroad of metabolic stress and inflammation in aging. *Aging* **1**, 458 (2009).

199 Fukunaga, M. *et al.* Studies on tissue and cellular distribution of indoleamine 2,3-dioxygenase 2: the absence of IDO1 upregulates IDO2 expression in the epididymis. *J Histochem Cytochem* **60**, 854-860, doi:10.1369/0022155412458926 (2012).

200 Covarrubias, A. J., Perrone, R., Grozio, A. & Verdin, E. NAD+ metabolism and its roles in cellular processes during ageing. *Nature Reviews Molecular Cell Biology* **22**, 119-141, doi:10.1038/s41580-020-00313-x (2021).

201 Dwivedi, S., Rendón-Huerta, E. P., Ortiz-Navarrete, V. & Montaño, L. F. CD38 and regulation of the immune response cells in cancer. *Journal of Oncology* **2021** (2021).

202 Hogan, K. A., Chini, C. C. S. & Chini, E. N. The Multi-faceted Ecto-enzyme CD38: Roles in Immunomodulation, Cancer, Aging, and Metabolic Diseases. *Frontiers in Immunology* **10**, doi:10.3389/fimmu.2019.01187 (2019).

203 Amici, S. A. *et al.* CD38 Is Robustly Induced in Human Macrophages and Monocytes in Inflammatory Conditions. *Frontiers in Immunology* **9**, doi:10.3389/fimmu.2018.01593 (2018).

204 Glaría, E. & Valledor, A. F. Roles of CD38 in the Immune Response to Infection. *Cells* **9**, 228 (2020).

205 Liu, J. *et al.* Cytosolic interaction of type III human CD38 with CIB1 modulates cellular cyclic ADP-ribose levels. *Proceedings of the National Academy of Sciences* **114**, 8283-8288 (2017).

206 Shrimp, J. H. *et al.* Revealing CD38 cellular localization using a cell permeable, mechanism-based fluorescent small-molecule probe. *Journal of the American Chemical Society* **136**, 5656-5663 (2014).

207 Zhao, Y. J., Lam, C. M. C. & Lee, H. C. The membrane-bound enzyme CD38 exists in two opposing orientations. *Science signaling* **5**, ra67-ra67 (2012).

208 Muñoz, P. *et al.* Antigen-induced clustering of surface CD38 and recruitment of intracellular CD38 to the immunologic synapse. *Blood, The Journal of the American Society of Hematology* **111**, 3653-3664 (2008).

209 van de Donk, N. W., Richardson, P. G. & Malavasi, F. CD38 antibodies in multiple myeloma: back to the future. *Blood, The Journal of the American Society of Hematology* **131**, 13-29 (2018).

210 Camacho-Pereira, J. *et al.* CD38 dictates age-related NAD decline and mitochondrial dysfunction through an SIRT3-dependent mechanism. *Cell metabolism* **23**, 1127-1139 (2016).

211 Chini, E. N. CD38 as a regulator of cellular NAD: a novel potential pharmacological target for metabolic conditions. *Current pharmaceutical design* **15**, 57-63 (2009).

212 Palmer, A. K. *et al.* Targeting senescent cells alleviates obesity-induced metabolic dysfunction. *Aging cell* **18**, e12950 (2019).

213 Van Beek, A. A., Van den Bossche, J., Mastroberardino, P. G., De Winther, M. P. & Leenen, P. J. Metabolic alterations in aging macrophages: ingredients for inflammaging? *Trends in Immunology* **40**, 113-127 (2019).

214 Garten, A. *et al.* Physiological and pathophysiological roles of NAMPT and NAD metabolism. *Nature Reviews Endocrinology* **11**, 535-546 (2015).

215 Imai, S.-i. The NAD World 2.0: the importance of the inter-tissue communication mediated by NAMPT/NAD+/SIRT1 in mammalian aging and longevity control. *NPJ systems biology and applications* **2**, 1-9 (2016).

216 Imai, S.-i. & Guarente, L. NAD+ and sirtuins in aging and disease. *Trends in cell biology* **24**, 464-471 (2014).

217 Scheibye-Knudsen, M. *et al.* A high-fat diet and NAD+ activate Sirt1 to rescue premature aging in cockayne syndrome. *Cell metabolism* **20**, 840-855 (2014).

218 Salminen, A., Kauppinen, A. & Kaarniranta, K. Emerging role of NF-κB signaling in the induction of senescence-associated secretory phenotype (SASP). *Cellular signalling* **24**, 835-845 (2012).

219 Lopes-Paciencia, S. *et al.* The senescence-associated secretory phenotype and its regulation. *Cytokine* **117**, 15-22 (2019).

220 Jablonski, K. A. *et al.* Novel markers to delineate murine M1 and M2 macrophages. *PloS one* **10**, e0145342 (2015).

221 Lee, C.-U., Song, E.-K., Yoo, C.-H., Kwak, Y.-K. & Han, M.-K. Lipopolysaccharide induces CD38 expression and solubilization in J774 macrophage cells. *Molecules and cells* **34**, 573-576 (2012).

222 Matalonga, J. *et al.* The nuclear receptor LXR limits bacterial infection of host macrophages through a mechanism that impacts cellular NAD metabolism. *Cell reports* **18**, 1241-1255 (2017).

223 Li, W. *et al.* CD38: A Significant Regulator of Macrophage Function. *Front Oncol* **12**, 775649, doi:10.3389/fonc.2022.775649 (2022).

224 O'Neill, L. A. J. & Pearce, E. J. Immunometabolism governs dendritic cell and macrophage function. *The Journal of Experimental Medicine* **213**, 15 (2016).

225 Fritsch, S. D. & Weichhart, T. Effects of Interferons and Viruses on Metabolism. *Frontiers in immunology* **7**, 630-630, doi:10.3389/fimmu.2016.00630 (2016).

226 Burke, J. D., Platanias, L. C. & Fish, E. N. Beta interferon regulation of glucose metabolism is PI3K/Akt dependent and important for antiviral activity against

coxsackievirus B3. *Journal of virology* **88**, 3485-3495, doi:10.1128/JVI.02649-13 (2014).

227 MacIver, N. J., Michalek, R. D. & Rathmell, J. C. Metabolic Regulation of T Lymphocytes. *Annual Review of Immunology* **31**, 259-283, doi:10.1146/annurev-immunol-032712-095956 (2013).

228 Pantel, A. *et al.* Direct type I IFN but not MDA5/TLR3 activation of dendritic cells is required for maturation and metabolic shift to glycolysis after poly IC stimulation. *PLoS biology* **12**, e1001759 (2014).

229 Grunert, T. *et al.* A comparative proteome analysis links tyrosine kinase 2 (Tyk2) to the regulation of cellular glucose and lipid metabolism in response to poly(I:C). *Journal of Proteomics* **74**, 2866-2880, doi:https://doi.org/10.1016/j.jprot.2011.07.006 (2011).

230 Wu, D. *et al.* Type 1 Interferons Induce Changes in Core Metabolism that Are Critical for Immune Function. *Immunity* **44**, 1325-1336, doi:10.1016/j.immuni.2016.06.006 (2016).

231 Yim, H. Y. *et al.* The mitochondrial pathway and reactive oxygen species are critical contributors to interferon-α/β-mediated apoptosis in Ubp43-deficient hematopoietic cells. *Biochemical and Biophysical Research Communications* **423**, 436-440 (2012).

232 Gkirtzimanaki, K. *et al.* IFNα Impairs Autophagic Degradation of mtDNA Promoting Autoreactivity of SLE Monocytes in a STING-Dependent Fashion. *Cell reports* **25**, 921-933.e925, doi:10.1016/j.celrep.2018.09.001 (2018).

233 Hsu, Y.-A. *et al.* The anti-proliferative effects of type I IFN involve STAT6-mediated regulation of SP1 and BCL6. *Cancer Letters* **375**, 303-312, doi:https://doi.org/10.1016/j.canlet.2016.02.047 (2016).

234 Lewis, J. A., Huq, A. & Najarro, P. Inhibition of Mitochondrial Function by Interferon. *Journal of Biological Chemistry* **271**, 13184-13190, doi:10.1074/jbc.271.22.13184 (1996).

235 Shan, B., Vazquez, E. & Lewis, J. A. Interferon selectively inhibits the expression of mitochondrial genes: a novel pathway for interferon-mediated responses. *The EMBO Journal* **9**, 4307-4314 (1990).

236 Le Roy, F. *et al.* The 2–5A/RNase L/RNase L Inhibitor (RNI) Pathway Regulates Mitochondrial mRNAs Stability in Interferon α-treated H9 Cells. *Journal of Biological Chemistry* **276**, 48473-48482, doi:10.1074/jbc.M107482200 (2001).

237 Perl, A. Oxidative stress in the pathology and treatment of systemic lupus erythematosus. *Nature Reviews Rheumatology* **9**, 674, doi:10.1038/nrrheum.2013.147

https://www.nature.com/articles/nrrheum.2013.147#supplementary-information (2013).

238 Gergely, P. *et al.* Mitochondrial Hyperpolarization and ATP Depletion in Patients With Systemic Lupus Erythematosus. *Arthritis and rheumatism* **46**, 175-190, doi:10.1002/1529-0131(200201)46:1<175::AID-ART10015>3.0.CO;2-H (2002).

239 Caza, T. N., Talaber, G. & Perl, A. Metabolic regulation of organelle homeostasis in lupus T cells. *Clinical Immunology* **144**, 200-213, doi:https://doi.org/10.1016/j.clim.2012.07.001 (2012).

240 Shah, D., Kiran, R., Wanchu, A. & Bhatnagar, A. Oxidative stress in systemic lupus erythematosus: Relationship to Th1 cytokine and disease activity. *Immunology Letters* **129**, 7-12, doi:https://doi.org/10.1016/j.imlet.2010.01.005 (2010).

241 Fernandez, D. & Perl, A. mTOR Signaling: A Central Pathway to Pathogenesis in Systemic Lupus Erythematosus? *Discovery medicine* **9**, 173-178 (2010).

242 Lui, S. L. *et al.* Rapamycin attenuates the severity of established nephritis in lupus-prone NZB/W F 1 mice. *Nephrology Dialysis Transplantation* **23**, 2768-2776, doi:10.1093/ndt/gfn216 (2008).

243 Lee, S.-Y. *et al.* Metformin Suppresses Systemic Autoimmunity in Roquin(san/san) Mice through Inhibiting B Cell Differentiation into Plasma Cells via Regulation of AMPK/mTOR/STAT3. *Journal of immunology (Baltimore, Md. : 1950)* **198**, 2661-2670, doi:10.4049/jimmunol.1403088 (2017).

244 Wahl, D. R. *et al.* Characterization of the metabolic phenotype of chronically activated lymphocytes. *Lupus* **19**, 1492-1501, doi:10.1177/0961203310373109 (2010).

245 Morel, L. Immunometabolism in systemic lupus erythematosus. *Nature Reviews Rheumatology* **13**, 280, doi:10.1038/nrrheum.2017.43 (2017).

246 Yin, Y. *et al.* Glucose Oxidation Is Critical for CD4+ T Cell Activation in a Mouse Model of Systemic Lupus Erythematosus. *J Immunol* **196**, 80-90, doi:10.4049/jimmunol.1501537 (2016).

247 Jing, C. *et al.* Macrophage metabolic reprogramming presents a therapeutic target in lupus nephritis. *Proceedings of the National Academy of Sciences* **117**, 15160, doi:10.1073/pnas.2000943117 (2020).

248 Buang, N. *et al.* Type I interferons affect the metabolic fitness of CD8+ T cells from patients with systemic lupus erythematosus. *Nature Communications* **12**, 1980, doi:10.1038/s41467-021-22312-y (2021).

249 Banchereau, R. *et al.* Personalized immunomonitoring uncovers molecular networks that stratify lupus patients. *Cell* **165**, 551-565 (2016).

250 Gubser, P. M. *et al.* Rapid effector function of memory CD8+ T cells requires an immediate-early glycolytic switch. *Nature immunology* **14**, 1064-1072, doi:10.1038/ni.2687 (2013).

251 Nicholas, D. *et al.* Advances in the quantification of mitochondrial function in primary human immune cells through extracellular flux analysis. *PLoS One* **12**, e0170975, doi:10.1371/journal.pone.0170975 (2017).

252 Kennedy, W. P. *et al.* Association of the interferon signature metric with serological disease manifestations but not global activity scores in multiple cohorts of patients with SLE. *Lupus Sci Med* **2**, e000080, doi:10.1136/lupus-2014-000080 (2015).

253 D'Souza, A. D., Parikh, N., Kaech, S. M. & Shadel, G. S. Convergence of multiple signaling pathways is required to coordinately up-regulate mtDNA and mitochondrial biogenesis during T cell activation. *Mitochondrion* **7**, 374-385, doi:10.1016/j.mito.2007.08.001 (2007).

254 Portales-Pérez, D., González-Amaro, R., Abud-Mendoza, C. & Sánchez-Armáss, S. Abnormalities in CD69 expression, cytosolic pH and Ca2+ during activation of lymphocytes from patients with systemic lupus erythematosus. *Lupus* **6**, 48-56, doi:10.1177/096120339700600107 (1997).

255 Comte, D. *et al.* Signaling Lymphocytic Activation Molecule Family Member 7 Engagement Restores Defective Effector CD8+ T Cell Function in Systemic Lupus Erythematosus. *Arthritis Rheumatol* **69**, 1035-1044, doi:10.1002/art.40038 (2017).

256 Dhir, V., Singh, A. P., Aggarwal, A., Naik, S. & Misra, R. Increased T-lymphocyte apoptosis in lupus correlates with disease activity and may be responsible for reduced T-cell frequency: a cross-sectional and longitudinal study. *Lupus* **18**, 785-791, doi:10.1177/0961203309103152 (2009).

257 Baker, P. E., Gillis, S., Ferm, M. M. & Smith, K. A. The Effect of T Cell Growth Factor on the Generation of Cytolytic T Cells. *The Journal of Immunology* **121**, 2168 (1978).

258 Kelly, E., Won, A., Refaeli, Y. & Van Parijs, L. IL-2 and Related Cytokines Can Promote T Cell Survival by Activating AKT. *The Journal of Immunology* **168**, 597, doi:10.4049/jimmunol.168.2.597 (2002).

259 Mier, J. W. & Gallo, R. C. Purification and some characteristics of human T-cell growth factor from phytohemagglutinin-stimulated lymphocyte-conditioned media. *Proceedings of the National Academy of Sciences of the United States of America* **77**, 6134-6138, doi:10.1073/pnas.77.10.6134 (1980).

260 Belmonte, L. *et al.* Increased lymphocyte viability after non-stimulated peripheral blood mononuclear cell (PBMC) culture in patients with X-linked lymphoproliferative disease (XLP). *Clinical Immunology* **133**, 86-94, doi:https://doi.org/10.1016/j.clim.2009.05.015 (2009).

261 Gergely, P. *et al.* Mitochondrial hyperpolarization and ATP depletion in patients with systemic lupus erythematosus. *Arthritis & Rheumatism* **46**, 175-190, doi:doi:10.1002/1529-0131(200201)46:1<175::AID-ART10015>3.0.CO;2-H (2002).

262 Perl, A., Gergely, P. & Banki, K. MITOCHONDRIAL DYSFUNCTION IN T CELLS OF PATIENTS WITH SYSTEMIC LUPUS ERYTHEMATOSUS. *International Reviews of Immunology* **23**, 293-313, doi:10.1080/08830180490452576 (2004).

263 Li, W., Sivakumar, R., Titov, A. A., Choi, S.-C. & Morel, L. Metabolic Factors that Contribute to Lupus Pathogenesis. *Critical reviews in immunology* **36**, 75-98, doi:10.1615/CritRevImmunol.2016017164 (2016).

264 Navarro, F. *et al.* Changes in glucose and glutamine lymphocyte metabolisms induced by type I interferon α. *Mediators of inflammation* **2010**, 364290-364290, doi:10.1155/2010/364290 (2010).

265 Pantel, A. *et al.* Direct type I IFN but not MDA5/TLR3 activation of dendritic cells is required for maturation and metabolic shift to glycolysis after poly IC stimulation. *PLoS Biol* **12**, e1001759-e1001759, doi:10.1371/journal.pbio.1001759 (2014).

266 Pitroda, S. P. *et al.* STAT1-dependent expression of energy metabolic pathways links tumour growth and radioresistance to the Warburg effect. *BMC medicine* **7**, 68-68, doi:10.1186/1741-7015-7-68 (2009).

267 Desai-Mehta, A., Mao, C., Rajagopalan, S., Robinson, T. & Datta, S. K. Structure and specificity of T cell receptors expressed by potentially pathogenic anti-DNA autoantibody-inducing T cells in human lupus. *The Journal of Clinical Investigation* **95**, 531-541, doi:10.1172/JCI117695 (1995).

268 Rajagopalan, S., Zordan, T., Tsokos, G. C. & Datta, S. K. Pathogenic anti-DNA autoantibody-inducing T helper cell lines from patients with active lupus nephritis: isolation of CD4-8- T helper cell lines that express the gamma delta T-cell antigen receptor. *Proceedings of the National Academy of Sciences* **87**, 7020-7024, doi:10.1073/pnas.87.18.7020 (1990).

269 Weinberg, S. E., Sena, L. A. & Chandel, N. S. Mitochondria in the regulation of innate and adaptive immunity. *Immunity* **42**, 406-417, doi:10.1016/j.immuni.2015.02.002 (2015).

270 Menk, A. V. *et al.* Early TCR Signaling Induces Rapid Aerobic Glycolysis Enabling Distinct Acute T Cell Effector Functions. *Cell Reports* **22**, 1509-1521, doi:https://doi.org/10.1016/j.celrep.2018.01.040 (2018).

271 Buskiewicz, I. A. *et al.* Reactive oxygen species induce virus-independent MAVS oligomerization in systemic lupus erythematosus. *Sci Signal* **9**, ra115, doi:10.1126/scisignal.aaf1933 (2016).

272 Lewis, J. A., Huq, A. & Najarro, P. Inhibition of mitochondrial function by interferon. *J Biol Chem* **271**, 13184-13190 (1996).

273 Stohl, W. Impaired polyclonal T cell cytolytic activity. A possible risk factor for systemic lupus erythematosus. *Arthritis Rheum* **38**, 506-516, doi:10.1002/art.1780380408 (1995).

274 Perl, A., Gergely, P., Puskas, F. & Banki, K. Metabolic Switches of T-Cell Activation and Apoptosis. *Antioxidants & Redox Signaling* **4**, 427-443, doi:10.1089/15230860260196227 (2002).

275 Fernandez, D. & Perl, A. Metabolic control of T cell activation and death in SLE. *Autoimmunity reviews* **8**, 184-189, doi:10.1016/j.autrev.2008.07.041 (2009).

276 Muñoz, L. E. *et al.* Autoimmunity and chronic inflammation — Two clearance-related steps in the etiopathogenesis of SLE. *Autoimmunity Reviews* **10**, 38-42, doi:https://doi.org/10.1016/j.autrev.2010.08.015 (2010).

277 Tanaka, N. *et al.* Type I interferons are essential mediators of apoptotic death in virally infected cells. *Genes to Cells* **3**, 29-37, doi:10.1046/j.1365-2443.1998.00164.x (1998).

278 Chawla-Sarkar, M., Leaman, D. W. & Borden, E. C. Preferential Induction of Apoptosis by Interferon (IFN)-β Compared with IFN-α2. *Clinical Cancer Research* **7**, 1821 (2001).

279 Lokshin, A., Mayotte, J. E. & Levitt, M. L. Mechanism of Interferon Beta-Induced Squamous Differentiation and Programmed Cell Death in Human Non—Small—Cell Lung Cancer Cell Lines. *JNCI: Journal of the National Cancer Institute* **87**, 206-212, doi:10.1093/jnci/87.3.206 (1995).

280 Kotredes, K. P. & Gamero, A. M. Interferons as inducers of apoptosis in malignant cells. *Journal of interferon & cytokine research : the official journal of the International Society for Interferon and Cytokine Research* **33**, 162-170, doi:10.1089/jir.2012.0110 (2013).

281 Clemens, M. J. Interferons and Apoptosis. *Journal of Interferon & Cytokine Research* **23**, 277-292, doi:10.1089/107999003766628124 (2003).

282 Pokrovskaja, K., Panaretakis, T. & Grandér, D. Alternative Signaling Pathways Regulating Type I Interferon-Induced Apoptosis. *Journal of Interferon & Cytokine Research* **25**, 799-810, doi:10.1089/jir.2005.25.799 (2005).

283 Chen, I. F. *et al.* AIM2 suppresses human breast cancer cell proliferation in vitro and mammary tumor growth in a mouse model. *Molecular Cancer Therapeutics* **5**, 1, doi:10.1158/1535-7163.MCT-05-0310 (2006).

284 Luan, Y., Lengyel, P. & Liu, C.-J. p204, a p200 family protein, as a multifunctional regulator of cell proliferation and differentiation. *Cytokine & growth factor reviews* **19**, 357-369, doi:10.1016/j.cytogfr.2008.11.002 (2008).

285 Gugliesi, F. *et al.* The proapoptotic activity of the Interferon-inducible gene IFI16 provides new insights into its etiopathogenetic role in autoimmunity. *Journal of Autoimmunity* **35**, 114-123, doi:https://doi.org/10.1016/j.jaut.2010.04.001 (2010).

286 Tahara, E. *et al.* G1P3, an interferon inducible gene 6-16, is expressed in gastric cancers and inhibits mitochondrial-mediated apoptosis in gastric cancer cell line TMK-1 cell. *Cancer Immunology, Immunotherapy* **54**, 729-740, doi:10.1007/s00262-004-0645-2 (2005).

287 Katsiari, C. G., Liossis, S. N. & Sfikakis, P. P. The pathophysiologic role of monocytes and macrophages in systemic lupus erythematosus: a reappraisal. *Semin Arthritis Rheum* **39**, 491-503, doi:10.1016/j.semarthrit.2008.11.002 (2010).

288 Han, S. *et al.* NF-E2-Related Factor 2 Regulates Interferon Receptor Expression and Alters Macrophage Polarization in Lupus. *Arthritis Rheumatol* **72**, 1707-1720, doi:10.1002/art.41383 (2020).

289 Ahmed, D. *et al.* Transcriptional Profiling Suggests Extensive Metabolic Rewiring of Human and Mouse Macrophages during Early Interferon Alpha Responses. *Mediators of Inflammation* **2018**, 5906819, doi:10.1155/2018/5906819 (2018).

290 Olson, G. S. *et al.* Type I interferon decreases macrophage energy metabolism during mycobacterial infection. *Cell Rep* **35**, 109195, doi:10.1016/j.celrep.2021.109195 (2021).

291 Arutyunova, E. I., Danshina, P. V., Domnina, L. V., Pleten, A. P. & Muronetz, V. I. Oxidation of glyceraldehyde-3-phosphate dehydrogenase enhances its binding to nucleic acids. *Biochem Biophys Res Commun* **307**, 547-552, doi:10.1016/s0006-291x(03)01222-1 (2003).

292 Schrimpe-Rutledge, A. C., Codreanu, S. G., Sherrod, S. D. & McLean, J. A. Untargeted Metabolomics Strategies—Challenges and Emerging Directions. *Journal of the American Society for Mass Spectrometry* **27**, 1897-1905, doi:10.1007/s13361-016-1469-y (2016).

293 O'Neill, Luke A. J. A Broken Krebs Cycle in Macrophages. *Immunity* **42**, 393-394, doi:https://doi.org/10.1016/j.immuni.2015.02.017 (2015).

294 Ganeshan, K. & Chawla, A. Metabolic regulation of immune responses. *Annu Rev Immunol* **32**, 609-634, doi:10.1146/annurev-immunol-032713-120236 (2014).

295 Paucker, K., Cantell, K. & Henle, W. Quantitative studies on viral interference in suspended L cells. III. Effect of interfering viruses and interferon on the growth rate of cells. *Virology* **17**, 324-334, doi:10.1016/0042-6822(62)90123-x (1962).

296 Welsh, R. M., Bahl, K., Marshall, H. D. & Urban, S. L. Type 1 interferons and antiviral CD8 T-cell responses. *PLoS Pathog* **8**, e1002352, doi:10.1371/journal.ppat.1002352 (2012).

297 Li, F., Yang, Y., Zhu, X., Huang, L. & Xu, J. Macrophage Polarization Modulates Development of Systemic Lupus Erythematosus. *Cell Physiol Biochem* **37**, 1279-1288, doi:10.1159/000430251 (2015).

298 Labonte, A. C. *et al.* Identification of alterations in macrophage activation associated with disease activity in systemic lupus erythematosus. *PLOS ONE* **13**, e0208132, doi:10.1371/journal.pone.0208132 (2018).

299 Cameron, A. M. *et al.* Inflammatory macrophage dependence on NAD+ salvage is a consequence of reactive oxygen species–mediated DNA damage. *Nature Immunology* **20**, 420-432, doi:10.1038/s41590-019-0336-y (2019).

300 Minhas, P. S. *et al.* Macrophage de novo NAD+ synthesis specifies immune function in aging and inflammation. *Nature Immunology* **20**, 50-63, doi:10.1038/s41590-018-0255-3 (2019).

301 McNab, F., Mayer-Barber, K., Sher, A., Wack, A. & O'garra, A. Type I interferons in infectious disease. *Nature Reviews Immunology* **15**, 87-103 (2015).

302 Maneglier, B. *et al.* Comparative effects of two type I interferons, human IFN-α and ovine IFN-τ on indoleamine-2, 3-dioxygenase in primary cultures of human macrophages. *Fundamental & clinical pharmacology* **21**, 29-34 (2007).

303 Nagy, C. & Haschemi, A. Time and demand are two critical dimensions of immunometabolism: the process of macrophage activation and the pentose phosphate pathway. *Frontiers in immunology* **6**, 164 (2015).

304 O'Neill, L. A. & Pearce, E. J. Immunometabolism governs dendritic cell and macrophage function. *Journal of Experimental Medicine* **213**, 15-23 (2016).

305 Kelly, B. & O'neill, L. A. Metabolic reprogramming in macrophages and dendritic cells in innate immunity. *Cell research* **25**, 771-784 (2015).

306 Moore, A. M. *et al.* NAD(+) depletion by type I interferon signaling sensitizes pancreatic cancer cells to NAMPT inhibition. *Proc Natl Acad Sci U S A* **118**, doi:10.1073/pnas.2012469118 (2021).

307 Heer, C. D. *et al.* Coronavirus infection and PARP expression dysregulate the NAD metabolome: An actionable component of innate immunity. *J Biol Chem* **295**, 17986-17996, doi:10.1074/jbc.RA120.015138 (2020).

308 Yoshino, J., Mills, Kathryn F., Yoon, Myeong J. & Imai, S.-i. Nicotinamide Mononucleotide, a Key NAD+ Intermediate, Treats the Pathophysiology of Diet-

and Age-Induced Diabetes in Mice. *Cell Metabolism* **14**, 528-536, doi:https://doi.org/10.1016/j.cmet.2011.08.014 (2011).

309 Wang, J. *et al.* Treatment with NAD(+) inhibited experimental autoimmune encephalomyelitis by activating AMPK/SIRT1 signaling pathway and modulating Th1/Th17 immune responses in mice. *Int Immunopharmacol* **39**, 287-294, doi:10.1016/j.intimp.2016.07.036 (2016).

310 Bogaczewicz, J., Tokarska, K. & Wozniacka, A. Changes of NADH Fluorescence from the Skin of Patients with Systemic Lupus Erythematosus. *BioMed Research International* **2019**, 5897487, doi:10.1155/2019/5897487 (2019).

311 Wu, J. *et al.* Boosting NAD+ blunts TLR4-induced type I IFN in control and systemic lupus erythematosus monocytes. *The Journal of clinical investigation* **132**, e139828, doi:10.1172/JCI139828 (2022).

312 De Souza, D. P. *et al.* Autocrine IFN-I inhibits isocitrate dehydrogenase in the TCA cycle of LPS-stimulated macrophages. *The Journal of clinical investigation* **129**, 4239-4244 (2019).

313 Ming-Chin Lee, K. *et al.* Type I interferon antagonism of the JMJD3-IRF4 pathway modulates macrophage activation and polarization. *Cell Reports* **39**, 110719, doi:https://doi.org/10.1016/j.celrep.2022.110719 (2022).

314 Hsu, Y. A. *et al.* The anti-proliferative effects of type I IFN involve STAT6-mediated regulation of SP1 and BCL6. *Cancer Lett* **375**, 303-312, doi:10.1016/j.canlet.2016.02.047 (2016).

315 Bender, D. A. Biochemistry of tryptophan in health and disease. *Molecular aspects of medicine* **6**, 101-197 (1983).

316 Muneer, A. Kynurenine Pathway of Tryptophan Metabolism in Neuropsychiatric Disorders: Pathophysiologic and Therapeutic Considerations. *Clin Psychopharmacol Neurosci* **18**, 507-526, doi:10.9758/cpn.2020.18.4.507 (2020).

317 Capuron, L. *et al.* Interferon-alpha-induced changes in tryptophan metabolism. relationship to depression and paroxetine treatment. *Biol Psychiatry* **54**, 906-914, doi:10.1016/s0006-3223(03)00173-2 (2003).

318 Raniga, K. & Liang, C. Interferons: Reprogramming the Metabolic Network against Viral Infection. *Viruses* **10**, doi:10.3390/v10010036 (2018).

319 Rothhammer, V. *et al.* Type I interferons and microbial metabolites of tryptophan modulate astrocyte activity and central nervous system inflammation via the aryl hydrocarbon receptor. *Nat Med* **22**, 586-597, doi:10.1038/nm.4106 (2016).

320 Roy, D. G. *et al.* Methionine metabolism shapes T helper cell responses through regulation of epigenetic reprogramming. *Cell metabolism* **31**, 250-266. e259 (2020).

321 Åkesson, K. *et al.* Kynurenine pathway is altered in patients with SLE and associated with severe fatigue. *Lupus Science & Medicine* **5**, e000254, doi:10.1136/lupus-2017-000254 (2018).

322 Widner, B. *et al.* in *Tryptophan, Serotonin, and Melatonin: Basic Aspects and Applications* (eds Gerald Huether, Walter Kochen, Thomas J. Simat, & Hans Steinhart) 571-577 (Springer US, 1999).

323 Anderson, E. W. *et al.* Associations between circulating interferon and kynurenine/tryptophan pathway metabolites: support for a novel potential mechanism for cognitive dysfunction in SLE. *Lupus Sci Med* **9**, doi:10.1136/lupus-2022-000808 (2022).

324 Liu, G., Xia, X. P., Gong, S. L. & Zhao, Y. The macrophage heterogeneity: difference between mouse peritoneal exudate and splenic F4/80+ macrophages. *Journal of cellular physiology* **209**, 341-352 (2006).

325 Zhu, L. *et al.* TSC1 controls macrophage polarization to prevent inflammatory disease. *Nature communications* **5**, 1-13 (2014).

326 McWhorter, F. Y., Wang, T., Nguyen, P., Chung, T. & Liu, W. F. Modulation of macrophage phenotype by cell shape. *Proceedings of the National Academy of Sciences* **110**, 17253-17258 (2013).

327 Santini, S. M. *et al.* Type I interferon as a powerful adjuvant for monocyte-derived dendritic cell development and activity in vitro and in Hu-PBL-SCID mice. *J Exp Med* **191**, 1777-1788, doi:10.1084/jem.191.10.1777 (2000).

328 Sangfelt, O., Erickson, S. & Grander, D. Mechanisms of interferon-induced cell cycle arrest. *Front Biosci* **5**, D479-487, doi:10.2741/sangfelt (2000).

329 Adler, B. & Adler, H. Type I interferon signaling and macrophages: a double-edged sword? *Cellular & Molecular Immunology* **19**, 967-968, doi:10.1038/s41423-020-00609-0 (2022).

330 Huang, L., Xu, H. & Peng, G. TLR-mediated metabolic reprogramming in the tumor microenvironment: potential novel strategies for cancer immunotherapy. *Cell Mol Immunol* **15**, 428-437, doi:10.1038/cmi.2018.4 (2018).

331 Saas, P., Varin, A., Perruche, S. & Ceroi, A. Recent insights into the implications of metabolism in plasmacytoid dendritic cell innate functions: Potential ways to control these functions. *F1000Research* **6**, 456 (2017).

332 Erlich, J. R. *et al.* Glycolysis and the Pentose Phosphate Pathway Promote LPS-Induced NOX2 Oxidase- and IFN-β-Dependent Inflammation in Macrophages. *Antioxidants* **11**, 1488 (2022).

333 Dalmas, E. *et al.* Irf5 deficiency in macrophages promotes beneficial adipose tissue expansion and insulin sensitivity during obesity. *Nature medicine* **21**, 610-618 (2015).

334 Krausgruber, T. *et al.* IRF5 promotes inflammatory macrophage polarization and TH1-TH17 responses. *Nature immunology* **12**, 231-238 (2011).

335 Lei, Y. *et al.* Elevated type I interferon responses potentiate metabolic dysfunction, inflammation, and accelerated aging in mtDNA mutator mice. *Science Advances* **7**, eabe7548, doi:doi:10.1126/sciadv.abe7548 (2021).

336 Thapa, B. & Lee, K. Metabolic influence on macrophage polarization and pathogenesis. *BMB Rep* **52**, 360-372, doi:10.5483/BMBRep.2019.52.6.140 (2019).

337 Colombo, G., Travelli, C., Porta, C. & Genazzani, A. A. Extracellular nicotinamide phosphoribosyltransferase boosts IFNγ-induced macrophage polarization independently of TLR4. *iScience* **25**, 104147, doi:https://doi.org/10.1016/j.isci.2022.104147 (2022).

338 Nguyen-Pham, T.-N. *et al.* Type I and II interferons enhance dendritic cell maturation and migration capacity by regulating CD38 and CD74 that have synergistic effects with TLR agonists. *Cellular & Molecular Immunology* **8**, 341-347, doi:10.1038/cmi.2011.7 (2011).

339 Bauvois, B. *et al.* Upregulation of CD38 gene expression in leukemic B cells by interferon types I and II. *J Interferon Cytokine Res* **19**, 1059-1066, doi:10.1089/107999099313299 (1999).

340 Shade, C. The Science Behind NMN-A Stable, Reliable NAD+Activator and Anti-Aging Molecule. *Integr Med (Encinitas)* **19**, 12-14 (2020).

341 Choi, S.-C. *et al.* Gut microbiota dysbiosis and altered tryptophan catabolism contribute to autoimmunity in lupus-susceptible mice. *Science Translational Medicine* **12**, eaax2220, doi:10.1126/scitranslmed.aax2220 (2020).

342 Ramprasath, T., Han, Y.-M., Zhang, D., Yu, C.-J. & Zou, M.-H. Tryptophan Catabolism and Inflammation: A Novel Therapeutic Target For Aortic Diseases. *Frontiers in Immunology* **12**, doi:10.3389/fimmu.2021.731701 (2021).

343 al-Janadi, M. & Raziuddin, S. B cell hyperactivity is a function of T cell derived cytokines in systemic lupus erythematosus. *The Journal of Rheumatology* **20**, 1885-1891 (1993).

344 Katsuyama, E. *et al.* The CD38/NAD/SIRTUIN1/EZH2 axis mitigates cytotoxic CD8 T cell function and identifies patients with SLE prone to infections. *Cell reports* **30**, 112-123. e114 (2020).

345 Wardowska, A. *et al.* Alterations in peripheral blood B cells in systemic lupus erythematosus patients with renal insufficiency. *International Immunopharmacology* **83**, 106451 (2020).

346 García-Rodríguez, S. *et al.* CD38 promotes pristane-induced chronic inflammation and increases susceptibility to experimental lupus by an apoptosis-driven and TRPM2-dependent mechanism. *Scientific reports* **8**, 1-19 (2018).

347 Domínguez-Pantoja, M. *et al.* CD38 protein deficiency induces autoimmune characteristics and its activation enhances IL-10 production by regulatory B cells. *Scandinavian Journal of Immunology* **87**, e12664, doi:https://doi.org/10.1111/sji.12664 (2018).

348 Viegas, M. S., Silva, T., Monteiro, M. M., do Carmo, A. & Martins, T. C. Knocking out of CD38 accelerates development of a lupus-like disease in lpr mice. *Rheumatology* **50**, 1569-1577, doi:10.1093/rheumatology/ker178 (2011).

349 Costa, F., Dalla Palma, B. & Giuliani, N. CD38 Expression by Myeloma Cells and Its Role in the Context of Bone Marrow Microenvironment: Modulation by Therapeutic Agents. *Cells* **8**, doi:10.3390/cells8121632 (2019).

350 Chatterjee, S. *et al.* CD38-NAD+ axis regulates immunotherapeutic anti-tumor T cell response. *Cell metabolism* **27**, 85-100. e108 (2018).

351 Escande, C. *et al.* Flavonoid apigenin is an inhibitor of the NAD+ ase CD38: implications for cellular NAD+ metabolism, protein acetylation, and treatment of metabolic syndrome. *Diabetes* **62**, 1084-1093 (2013).

352 Kellenberger, E., Kuhn, I., Schuber, F. & Muller-Steffner, H. Flavonoids as inhibitors of human CD38. *Bioorganic & medicinal chemistry letters* **21**, 3939-3942 (2011).

353 Becherer, J. D. *et al.* Discovery of 4-amino-8-quinoline carboxamides as novel, submicromolar inhibitors of NAD-hydrolyzing enzyme CD38. *Journal of medicinal chemistry* **58**, 7021-7056 (2015).

354 Haffner, C. D. *et al.* Discovery, synthesis, and biological evaluation of thiazoloquin (az) olin (on) es as potent CD38 inhibitors. *Journal of medicinal chemistry* **58**, 3548-3571 (2015).

355 Tarragó, M. G. *et al.* A Potent and Specific CD38 Inhibitor Ameliorates Age-Related Metabolic Dysfunction by Reversing Tissue NAD(+) Decline. *Cell Metab* **27**, 1081-1095.e1010, doi:10.1016/j.cmet.2018.03.016 (2018).

356 Zhang, S., Xue, X., Zhang, L., Zhang, L. & Liu, Z. Comparative Analysis of Pharmacophore Features and Quantitative Structure–Activity Relationships for CD 38 Covalent and Non-covalent Inhibitors. *Chemical Biology & Drug Design* **86**, 1411-1424 (2015).

357 Mayo, L. *et al.* Dual role of CD38 in microglial activation and activation-induced cell death. *The Journal of Immunology* **181**, 92-103 (2008).

358 Wang, Y.-M. *et al.* Blocking the CD38/cADPR pathway plays a double-edged role in LPS stimulated microglia. *Neuroscience* **361**, 34-42, doi:https://doi.org/10.1016/j.neuroscience.2017.08.010 (2017).

359 Barata, H. *et al.* The role of cyclic-ADP-ribose-signaling pathway in oxytocin-induced Ca2+ transients in human myometrium cells. *Endocrinology* **145**, 881-889 (2004).

360 Lee, C.-U., Song, E.-K., Yoo, C.-H., Kwak, Y.-K. & Han, M.-K. Lipopolysaccharide induces CD38 expression and solubilization in J774 macrophage cells. *Molecules and cells* **34**, 573-576 (2012).

361 Shu, B. *et al.* Blockade of CD38 diminishes lipopolysaccharide-induced macrophage classical activation and acute kidney injury involving NF-κB signaling suppression. *Cell Signal* **42**, 249-258, doi:10.1016/j.cellsig.2017.10.014 (2018).

362 Du, Y. *et al.* CD38 deficiency downregulates the onset and pathogenesis of collagen-induced arthritis through the NF-κB Pathway. *Journal of Immunology Research* **2019** (2019).

363 Farahany, J. *et al.* CD38-mediated Inhibition of Bruton's Tyrosine Kinase in Macrophages Prevents Endotoxemic Lung Injury. *Am J Respir Cell Mol Biol* **66**, 183-195, doi:10.1165/rcmb.2021-0272OC (2022).

364 Sorgdrager, F. J. H., Naudé, P. J. W., Kema, I. P., Nollen, E. A. & Deyn, P. P. D. Tryptophan Metabolism in Inflammaging: From Biomarker to Therapeutic Target. *Frontiers in Immunology* **10**, doi:10.3389/fimmu.2019.02565 (2019).

365 Mezrich, J. D. *et al.* An interaction between kynurenine and the aryl hydrocarbon receptor can generate regulatory T cells. *The Journal of Immunology* **185**, 3190-3198 (2010).

366 Nguyen, N. T. *et al.* Aryl hydrocarbon receptor negatively regulates dendritic cell immunogenicity via a kynurenine-dependent mechanism. *Proceedings of the National Academy of Sciences* **107**, 19961-19966 (2010).

367 Vogel, C. F., Goth, S. R., Dong, B., Pessah, I. N. & Matsumura, F. Aryl hydrocarbon receptor signaling mediates expression of indoleamine 2, 3-dioxygenase. *Biochemical and biophysical research communications* **375**, 331-335 (2008).

368 Bustamante, S. *et al.* Tryptophan Metabolism ‘Hub’ Gene Expression Associates with Increased Inflammation and Severe Disease Outcomes in COVID-19 Infection and Inflammatory Bowel Disease. *International Journal of Molecular Sciences* **23**, 14776 (2022).

369 Solvang, S.-E. H. *et al.* The kynurenine pathway and cognitive performance in community-dwelling older adults. The Hordaland Health Study. *Brain, Behavior, and Immunity* **75**, 155-162 (2019).

370 Schröcksnadel, K., Wirleitner, B., Winkler, C. & Fuchs, D. Monitoring tryptophan metabolism in chronic immune activation. *Clinica chimica acta* **364**, 82-90 (2006).

371 Frumento, G. *et al.* Tryptophan-derived catabolites are responsible for inhibition of T and natural killer cell proliferation induced by indoleamine 2,3-dioxygenase. *J Exp Med* **196**, 459-468, doi:10.1084/jem.20020121 (2002).

372 Fallarino, F. *et al.* T cell apoptosis by tryptophan catabolism. *Cell Death & Differentiation* **9**, 1069-1077, doi:10.1038/sj.cdd.4401073 (2002).

373 Becker, A. M. *et al.* SLE Peripheral Blood B Cell, T Cell and Myeloid Cell Transcriptomes Display Unique Profiles and Each Subset Contributes to the

Interferon Signature. *PLoS ONE* **8**, e67003, doi:10.1371/journal.pone.0067003 (2013).

374 Elkon, K. B. & Stone, V. V. Type I interferon and systemic lupus erythematosus. *J Interferon Cytokine Res* **31**, 803-812, doi:10.1089/jir.2011.0045 (2011).

375 Rattigan, K. M. *et al.* Metabolomic profiling of macrophages determines the discrete metabolomic signature and metabolomic interactome triggered by polarising immune stimuli. *PloS one* **13**, e0194126 (2018).

376 Bauvois, B. *et al.* Upregulation of CD38 gene expression in leukemic B cells by interferon types I and II. *Journal of interferon & cytokine research* **19**, 1059-1066 (1999).

377 Shen, M. *et al.* Interferon regulatory factor-1 binds c-Cbl, enhances mitogen activated protein kinase signaling and promotes retinoic acid-induced differentiation of HL-60 human myelo-monoblastic leukemia cells. *Leuk Lymphoma* **52**, 2372-2379, doi:10.3109/10428194.2011.603449 (2011).

378 Tliba, O. *et al.* Cytokines induce an early steroid resistance in airway smooth muscle cells: novel role of interferon regulatory factor-1. *American journal of respiratory cell and molecular biology* **38**, 463-472 (2008).